

ELECTRON MICROSCOPE STUDIES OF SOLIDS PRODUCED
BY α -RADIOLYSIS OF CARBON MONOXIDE

by

Thomas Baird

Department of Chemistry, University of Glasgow.

Thesis submitted for the degree of Doctor of
Philosophy.

June, 1969.

ProQuest Number: 11011880

All rights reserved

INFORMATION TO ALL USERS

The quality of this reproduction is dependent upon the quality of the copy submitted.

In the unlikely event that the author did not send a complete manuscript and there are missing pages, these will be noted. Also, if material had to be removed, a note will indicate the deletion.



ProQuest 11011880

Published by ProQuest LLC (2018). Copyright of the Dissertation is held by the Author.

All rights reserved.

This work is protected against unauthorized copying under Title 17, United States Code
Microform Edition © ProQuest LLC.

ProQuest LLC.
789 East Eisenhower Parkway
P.O. Box 1346
Ann Arbor, MI 48106 – 1346

ACKNOWLEDGEMENTS

This work was carried out in the Physical Chemistry Department which is under the direction of Professor J.M. Robertson.

I wish to thank Dr. I.M. Dawson for supervision of the work and Dr. S.J. Thomson for helpful advice and discussion during the writing of this thesis.

I am most grateful to the U.K.A.E.A. and many members of staff of the U.K.A.E.A. for providing facilities for certain aspects of the work, notably; Mr. R. Paris for manufacturing the α -sources; Dr. F.S. Feates and Mr. A.G. Poole for dosimetry measurements; Mr. J.V.F. Best for collaboration in the proton Van de Graaff experiments.

I am indebted to Mr. P. Wright, G.E.C.-A.E.I. Ltd., for providing electron probe microanalysis data, and to Mr. G.H. Mills, National Engineering Laboratory, East Kilbride, for co-operation in electron probe work. I thank Siemens (U.K.) Ltd., and Fulmer Research Institute for making the spectrometer attachment to the Elmiskop 1A available for use.

Finally, I wish to thank my colleagues in the electron microscope group for their help throughout the course of this work.

SUMMARY

A study has been made of the solids produced by radiolysis of carbon monoxide gas at room temperature using principally 5 MeV α -particles from plutonium -240. The solids were produced in situ within a Siemens Elmiskop I electron microscope and were examined directly. The morphological nature of the solid particles has been studied and the effect of subsequent exposure of the particles to the atmosphere has been investigated using transmission electron microscopy and electron diffraction techniques. It has been established that the particles grow in the gas phase and are of an amorphous nature.

The effect on the radiolysis of varying the gas composition has been investigated. Metallic carbonyl impurities in the carbon monoxide have been found to influence the nature and composition of the solids produced. Two distinct types of solid particles can be obtained. Initially these have a similar appearance but they behave differently on subsequent exposure to water vapour. Solids from carbon monoxide containing nickel tetracarbonyl impurity are hygroscopic and they become fluid on absorption of water vapour. Electron diffraction

and electron probe microanalysis studies reveal the presence of several per cent of nickel in these solids. The presence of iron pentacarbonyl impurity in the carbon monoxide yields solids which are inert towards water vapour; these solids contain several per cent of iron. Higher yields of solid are obtained with the iron pentacarbonyl impurity. When both iron and nickel carbonyls are present in the carbon monoxide the influence exerted by the iron carbonyl predominates and the solids produced have all the characteristics of the material formed when iron carbonyl alone is present. A possible explanation to account for this phenomenon is proposed.

Infrared spectroscopy studies of the α -radiolytic solids and of the solid from complementary proton radiolysis experiments provide evidence which suggests that the solids are composed of linear polymeric carbon suboxide units. The nature of the bonding between the basic polymer units and the iron and nickel is discussed.

The α -radiolysis of carbon monoxide in the presence of graphite has been studied. It has been found that in addition to the gas-phase deposits which are produced there is a solid which grows on the surface of the graphite. This solid has similar characteristics to the nickel-containing gas-phase material.

GENERAL CONTENTS

	<u>Page</u>
I N T R O D U C T I O N	1
E X P E R I M E N T A L	42
R E S U L T S	76
D I S C U S S I O N	189
R E F E R E N C E S	225

I N T R O D U C T I O N

INTRODUCTION

Contents

	<u>Page</u>
1. <u>The Absorption of Radiation by Gases</u>	3
(a) Ultraviolet Radiation	3
(b) High Energy Radiation	4
(c) Methods of Expressing Yield	7
2. <u>α-Radiolysis of Hydrocarbons</u>	7
3. <u>The Effect of Radiation on Carbon Dioxide</u>	11
4. <u>The Effect of Radiation on Carbon Monoxide</u>	13
(a) Introduction	13
(b) Formation of Solids by α -Radiation	14
(c) Formation of Solids by Other Radiations	16
(d) Composition of Solids from CO Radiolysis	18
(e) The Effect of Various Parameters on the Radiolysis of CO	21
5. <u>Nature of Solids from CO Decomposition</u>	25
6. <u>Electron Microscopy of Solids from CO Radiolysis</u>	29
7. <u>Aim of Present Work</u>	32
8. <u>Electron Microscopy</u>	34
(a) Introduction	34
(b) Resolution	34
(c) Specimen Contrast	36
(d) Electron Diffraction	37
9. <u>Electron Probe Microanalysis</u>	38

1. The Absorption of Radiation by Gases

This thesis is concerned principally with the results of studies of the effect of α -radiation on carbon monoxide gas, particular reference being made to the nature of the solid decomposition products. Previous work in the literature on the effect of ultraviolet light, reactor, proton, α - and γ -radiation on CO and various gaseous mixtures has been mainly concerned with the gaseous products of the reactions. Each of the radiations mentioned above is known to bring about decomposition of CO into carbon dioxide and a carbon-rich solid and various mechanisms have been postulated for the reactions.

(a) Ultraviolet Radiation

The absorption of ultraviolet radiation by a gaseous system results in the production of electronically excited species which may dissociate and lead to chemical reaction. The energy of a photon can be chosen to be about the same order of magnitude as the excitation energy of atoms and molecules (a few electron volts) and each quantum of radiation is absorbed completely by one atom or molecule. The energy E (in eV) of a quantum of radiation is related to the wavelength λ (in \AA) by $E = hc/\lambda = 12,395/\lambda$ and by examining spectroscopic data it is often possible to select a wavelength which will produce a desired excited state.

If the wavelengths are sufficiently short, ionisation can occur, but in general photolytic reactions involve electronically excited species.

(b) High Energy Radiations

γ -rays and heavy charged particles such as α -particles and protons, and other high energy radiations, have in common, the ability to produce ions in their path through a medium and are thus termed ionising radiations. Most chemical effects produced by high energy radiations result from the stopping of high velocity charged particles which lose their energy by electrostatic interaction with the electrons of the stopping medium.

Alpha-particles, (He^{++}), differ from each other in velocity according to their origins. When different high velocity α -particles are slowed down to identical velocities then they have identical properties in the same medium. The energy possessed by α -particles (and other heavy charged particles) can greatly exceed that required to excite or ionise atoms or molecules ($\sim 5 - 25$ eV) and on passing through a medium a range of electronically excited species and ions is produced. The amount of energy transferred to the electrons of the stopping medium on collision with an α -particle depends on the distance of approach and velocity of the particle. The energy loss per collision is small relative

to the energy of the particle - unlike the absorption of photons - and deceleration occurs by a large number of events, each involving usually a few electron volts. The total energy required to produce an ion pair in CO (i.e. $\text{CO} \rightarrow \text{CO}^+ + e$) is 34 eV (Lind, 1961). This value exceeds the ionisation potential of CO by about 20 eV. The extra energy absorbed is used in producing electronically excited molecules and ions and some of this may be subsequently lost as heat on collision with other molecules, or may lead to dissociation of the CO molecules. The electrons produced by ion pair formation may also cause excitation and dissociation. Collisions between α -particles and electrons of the stopping medium do not deflect the particle from its path, which is approximately straight. In the event of a collision with a nucleus the particle is deflected, but these collisions are elastic - except for low energy particles - and do not contribute to the deceleration of the particles.

The rate at which energy is lost per unit distance travelled is termed the stopping power or linear energy transfer and is given by the formula (Bethe and Ashkin, 1952):

$$-dE/dx = \frac{4\pi z^2 e^4 N Z}{m v^2} \ln \frac{2m v^2}{I}$$

E , z and v are the energy, charge and velocity of the particles; e and m are the charge and mass of an electron; N is the number of atoms of atomic number Z per cm^3 of the stopping medium and I is a value called the mean excitation potential of the medium and is characteristic for each medium. The formula does not hold for very high velocity particles where the energy loss is greater than predicted by the equation or for particles of very low energy (< 2.5 MeV for α 's). From the above formula it is evident that the stopping power increases as the particle velocity decreases and this is illustrated in Fig. 1 by a Bragg curve for an α -particle from RaC' .

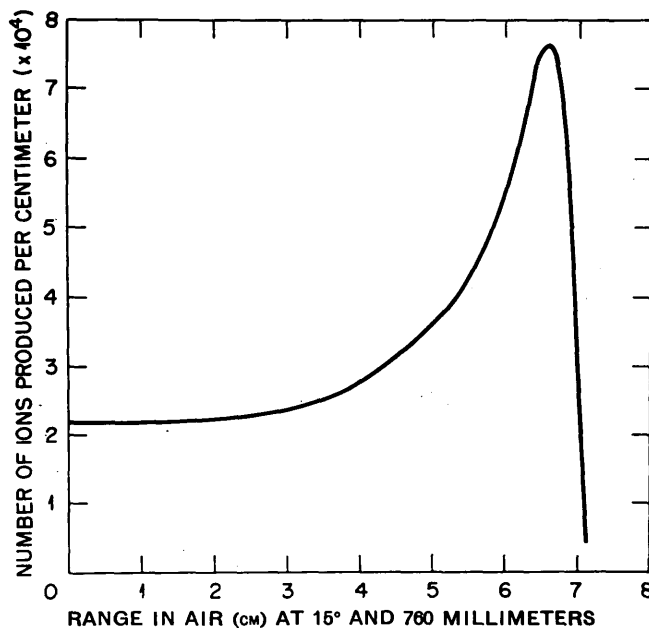


Fig. 1: Bragg curve for an α -particle from RaC' (Lind, 1961)

The area under the curve represents the number of ion pairs produced by a single α -particle from RaC' and in this case is 2.37×10^5 . The rapid fall to zero after the maximum is reached is a result of the decelerated particles becoming neutralised, for part of the time, by electron capture; the neutral particles lose energy less rapidly than the corresponding charged particles.

(c) Methods of Expressing Yield

The yield of a reaction in a gaseous system can be expressed in terms of the number of molecules changed (M) per ion pair formed (N). The ratio M/N is known as the ion pair yield. Another method commonly used is to relate the number of species changing (G) with every 100 eV of energy absorbed. Since the energy (W) required to produce an ion pair in a gaseous reaction is about 33 eV, then $G \approx 3\left(\frac{M}{N}\right)$. Accurately for a gaseous reaction,

$$G = \frac{100}{W} \times \frac{M}{N}$$

G values usually lie between 1 and 10, unless a reaction proceeds by a chain mechanism, when values of thousands can be attained.

2. α -Radiolysis of Hydrocarbons

Many organic gases are decomposed by α -radiation to give liquid or solid polymers together with gaseous products. Most studies have been made with radon as the source of

α -radiation and reaction was effected by mixing the gas under examination with radon contained in small glass spheres. By analysing the mixtures after reaction and calculating the total number of ion pairs produced in the gas, the ion pair yields ($\frac{M}{N}$) for many reactions were obtained. The ease with which liquid or solid polymers are formed in these reactions has been found to depend mainly on the degree of unsaturation of the gas (Lind, 1961). Saturated gases such as methane, ethane and propane, form polymers less readily than the corresponding unsaturated gases, and evolve larger quantities of gaseous products during radiolysis. Highly unsaturated gases, for example cyanogen, C_2N_2 , form solid polymers in high yield with very little gas evolution.

The α -radiolysis of saturated hydrocarbons was first studied by Lind and Bardwell (1924, 1925, 1926) and independently by Mund and Koch (1925). Hydrogen, methane and other hydrocarbons were evolved and a liquid of formula $(C_nH_{2n})_x$ was produced. The fraction of gaseous hydrocarbons which reacted under similar conditions increased with the higher members of the series on account of their greater stopping power and consequently more intense ionisation. However, the ion pair yields for the lower hydrocarbons were similar with a value of $\frac{M}{N} \approx 2$. The

empirical formula of the liquid, $C_n H_{2n}$, infers some degree of unsaturation and a careful examination was made of the gas phase for unsaturated compounds, but none was found and the authors concluded that unsaturated gaseous products must rapidly polymerise to liquid. It was demonstrated (Lind and Bardwell, 1926) that further irradiation of the liquid phase could cause transformation to the solid state. Honig and Sheppard (1946) using α -particles and deuterons confirmed the results of the above authors and showed further that the liquid from butane radiolysis was olefinic in character and was possibly partly aromatic. Back and Miller (1959) studied the α -radiolysis of pentane using ^{242}Cm α -particles and unlike Lind and Bardwell (1926), obtained high yields of hydrogen and unsaturated compounds but no liquid or solid polymers. This discrepancy was attributed to the lower doses and much larger volumes used by the later workers which would require much more product to be formed before condensation to liquid could occur. The decomposition of some six-membered hydrocarbons was investigated by Henri, Maxwell, White and Petersen (1952). The gaseous products, analysed by mass spectrometry, were similar to those from lower hydrocarbons and the appearance of a liquid product was again noted.

Mund and Koch (1926) subjected acetylene, C_2H_2 , to α -radiation and obtained a powdery, yellow solid (cuprene) in high yield ($\frac{-M}{N} = 20.2$). This value was confirmed by Lind, Bardwell and Perry (1926) who found that further irradiation of the solid resulted in the evolution of hydrogen. Rosenblum (1937, 1948) and Mund and Rosenblum (1937) claimed that α -irradiation of acetylene produced both cuprene and benzene and this was confirmed by Dorfman and Wahl (1959). Solid polymers have been obtained from the α -radiolysis of cyanogen, C_2N_2 , and hydrogen cyanide, HCN (Lind, Bardwell and Perry, 1926), and it was found that further irradiation of the black polymer from cyanogen caused nitrogen to be evolved.

The effect of α -radiation on a number of unsaturated compounds was investigated by Heisig (1931, 1932a, 1932b, 1933, 1935, 1939). He found a general relationship between the ion pair yields and the heats of formation of the hydrocarbons. Gases with positive heats of formation (saturated hydrocarbons) gave low yields whereas those with negative heats of formation (unsaturated gases) gave higher yields. Shortly after mixing the hydrocarbon with the radon, a fog formed inside the reaction vessel and after several hours colourless liquid collected at the bottom of the vessel. Cyclobutane and cyclobutene formed a liquid which increased

in viscosity and colour with irradiation time. Many other gases studied gave coloured liquid or solid products. Vinyl acetylene, for example, gave a high yield of a solid which was white when first formed and which gradually changed through a cream colour to orange. As with acetylene and other triple bonded compounds the evolution of gaseous products was low.

The above studies show that the absorption of α -radiation by gases containing carbon can result in the formation of solid or liquid products. Further irradiation of the primary product can obviously effect physical and chemical changes in the product.

3. The Effect of Radiation on Carbon Dioxide

The use of carbon dioxide as the heat transfer medium in graphite-moderated reactors stimulated many studies of the effect of high energy radiations on this gas. It has been established that pure gaseous carbon dioxide is relatively stable to radiation due to the rapid recombination of the oxygen atoms and the carbon monoxide initially formed (Harteck and Dondes, 1955, 1957; Davidge and Marsh, 1955). Reaction can be promoted, however, if a substance is present with which the oxygen atoms will combine preferentially. Indeed, the first study of the effect of radiation on carbon dioxide, made by Cameron and Ramsay

(1908) who used α -particles from radon, showed that carbon dioxide was decomposed to give free carbon. Wourtzell (1919) later showed that the formation of carbon was due to the reduction of carbon dioxide by mercury impurity and that carbon dioxide in the absence of a reducing agent was stable to ionising radiation. This was later confirmed by Lind and Bardwell (1925). Substances capable of promoting reaction include carbon, mercury, phosphorus and hydrogen. Harteck and Dondes (1955, 1957) showed that nitrogen dioxide also inhibited the recombination of the oxygen atoms with the carbon monoxide. In some of their experiments they found that heating the quartz reaction vessel led to the production of carbon monoxide and this was attributed to the decomposition of a carbon suboxide polymer formed during the irradiations. Feates and Sach (1965) when investigating the vacuum ultraviolet photolysis of carbon dioxide in the presence of graphite found a dark deposit on the transmission window of their apparatus after a long experimental run and attributed this to the secondary photolysis of CO formed in the system. Baird and Dawson (1963) made a preliminary electron microscopic study of the oxidation of graphite by irradiated CO₂ and found, in addition to the oxidation of graphite, that a deposit appeared on the graphite surfaces after reaction. This

work was subsequently undertaken and reported by Adamson (1966) who suggests that the deposits are formed from the secondary irradiation of the CO produced during reaction.

4. The Effect of Radiation on Carbon Monoxide

(a) Introduction

Carbon monoxide - unlike carbon dioxide - can be readily decomposed by various radiations to yield carbon dioxide and a solid product consisting chiefly of carbon and oxygen. The effect of radiation on carbon monoxide has received increased attention in recent years as this process is of relevance to certain reactor systems where carbon monoxide is present.

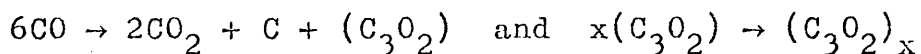
The chemical relationship between graphite, CO₂ and CO is important in graphite-moderated, CO₂-cooled reactor systems where the radiation induced reactions represented by $C + CO_2 \xrightarrow{\gamma} 2CO$ and $CO \xrightarrow{\gamma} \text{solids}$, occur simultaneously. The thermal reaction between graphite and CO₂ is not appreciable below 625°C (Copestake, Davidson and Tonge, 1959) and in present day reactors is of minor importance relative to the radiation induced reaction. It has already been shown that pure CO₂ is stable to ionising radiation. However, graphite fulfils a similar function to that of NO₂ in the decomposition of CO₂ as demonstrated by Hardeck and Dondes (1955, 1957) and in a reactor, decomposition of CO₂

is appreciable at low temperatures (Davidge and Marsh, 1955; Woodley, 1955). The CO formed by this reaction is subsequently decomposed by reactor radiation and results in the formation of carbonaceous solids which are deposited unevenly throughout the system (Lind and Wright, 1963). In addition there is usually a few per cent of carbon monoxide added deliberately to the coolant (CO_2) to suppress the gasification reaction, and this too leads to deposition. Literature on the radiolysis of CO is less extensive than that of the forward gasification reaction, $\text{C} + \text{CO}_2 \xrightarrow{\text{radiation}} 2\text{CO}$, but the general features of the reaction are well established; CO is decomposed by radiation to give CO_2 and carbon-rich solids of variable composition (Lind, 1961).

(b) Formation of Solids by α -Radiation

Cameron and Ramsay (1908) reported their results on the decomposition of CO using α -particles from radon; they found that carbon, oxygen and carbon dioxide were the products of the irradiations. Lind and Bardwell (1925), however, did not find any free oxygen in similar experiments, but reported carbon dioxide, carbon and a third product suspected of being a suboxide of carbon $(\text{C}_3\text{O}_2)_n$. The decompositions were performed in glass spheres at room temperature and from time to time a brownish film was observed

on the vessel walls. This was shown to be distinct from the bluish or brown colour which often occurs in glass by the action of α -particles and the film could be stripped off and examined. The film was inert to most reagents and was believed to be a suboxide polymer. The free carbon collected in a loose fluffy condition at the bottom of the vessel and on the walls. The results indicated an overall stoichiometry of



$$\text{with} \quad \frac{-\Delta\text{CO}}{+\Delta\text{CO}_2} \approx 3.$$

The ion pair yield was reported to diminish from 1.85 to 1.2 as the reaction continued and this was attributed to back reaction between the carbon dioxide formed and the solid products. Another explanation put forward to account for the decrease was that charge transfer was possibly occurring between the CO^+ and the CO_2 i.e., $\text{CO}^+ + \text{CO}_2 \rightarrow \text{CO} + \text{CO}_2^+$; this is feasible since the ionisation potentials of CO and CO_2 are respectively 14.01 eV and 13.79 eV. Cameron and Ramsay's results suggested that the decomposition of CO occurred in the gas phase with the carbon settling to the bottom of the vessel and the suboxide diffusing to and polymerising at the vessel walls.

CO decomposition initiated by α -particles from radon was studied by Rudolph and Lind (1960a). The reaction appeared to occur in the gas phase and a Tyndall effect was observed on focusing a beam of light through the reaction sphere. Solid products settled to the bottom of the vessel and these were partially soluble in water. The soluble portion was carefully dehydrated and the white crystalline solid obtained was found to be very similar to malonic acid, $C_3H_4O_4$. The authors concluded that the solids consisted of partially polymerised C_3O_2 (malonic anhydride) and carbon.

Stewart and Bowlden (1960) in a study of the effect on radiolysis of addition of inert gases to CO, found very finely divided carbon at the bottom of the reaction vessel. This work, however, was essentially a kinetic study and no further information about the solid was given.

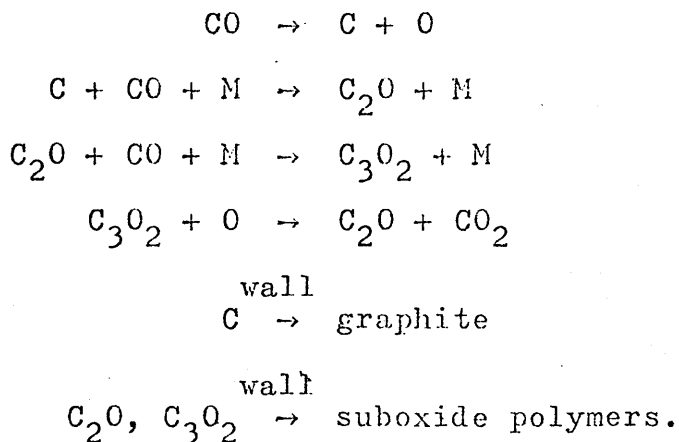
An electron microscope study of the solid from the α -radiolysis of carbon monoxide was made by Watson, Vanpee and Lind (1950) who showed that the solid was formed by a gas-phase process. This work is discussed later together with other electron microscope studies of solids produced by different radiations.

(c) Formation of Solids by Other Radiations

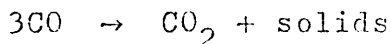
Several workers have used reactor radiation to

investigate the radiolytic decomposition of carbon monoxide. The complexity of the radiations involved in these experiments, the range of temperatures employed and the presence of other gases in the system have led to the formation of solids of variable composition and properties.

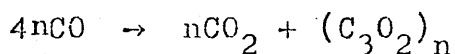
Woodley (1955) decomposed carbon monoxide in sealed quartz ampoules using pile radiation at low temperatures and obtained carbon dioxide, a powdery brown solid consisting of polymerised carbon suboxides and possibly free carbon. The mechanism proposed for the reaction was similar to that suggested by Harteck and Dondes (1955):



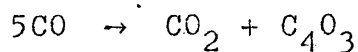
Corney and Copestake (1962) using the reactor DIDO obtained brown or black deposits from carbon monoxide and found, in agreement with Rudolph and Lind (1960a), the stoichiometry to be



Marsh and Wright (1964) also used reactor radiation to decompose carbon monoxide and obtained carbon dioxide and a dark brown solid. Some information about the structure of this solid was obtained and this is discussed later. A very careful study of the gamma and proton radiolysis of carbon monoxide was made by Anderson, Best and Willett (1966). Their results clearly showed that the products of the radiolyses were carbon dioxide and a dark brown solid, $(C_3O_2)_n$, which formed in the gas phase. The stoichiometry derived was



The gamma-radiolysis of liquid carbon monoxide at 77° K, investigated by Briggs and Clay (1968), also produced carbon dioxide and a brown solid, $(C_3O_2)_n$. The overall stoichiometry was shown to be identical with that proposed by Anderson, Best and Willett (1966). Woodley (1954) using gamma-radiation (~50° C) found the stoichiometry was



and again a brown solid was obtained.

(d) Composition of Solids from CO Radiolysis

Detailed analysis of deposits from a number of different reactor systems have been carried out at the Reactor Materials Laboratories, Culcheth. The deposits

were shown to be composed of carbon, oxygen and often of appreciable amounts of hydrogen and small amounts of inorganic substances (Lind, 1966). Anderson, Best and Willett (1966) found the empirical composition of the solid from proton-radiolysis and γ -radiolysis was $\sim C_{1.5}O$ when formed at room temperature and $C_{3.0}O$ at $300^{\circ}C$ and tended towards pure carbon at $>450^{\circ}C$. Increased temperature reduced the yields of solid and increased the yields of CO_2 but this effect was shown to be due to the subsequent thermal decomposition of the solid and was not a genuine temperature effect. Marsh and Wright (1964) found the reactor polymer formed at $\sim 130^{\circ}C$ to have an intermediate value of $C_{1.9}O$ which is consistent with the proton results of Anderson, Best and Willett. Woodley (1954) found the granular brown solid from high intensity γ -radiation (at $\sim 50^{\circ}C$) to be $(C_4O_3)_n$; this solid decomposed thermally to give CO and CO_2 and eventually left a residue of carbon. Anderson et al (1958) found, on reactor surfaces, carbonaceous deposits which contained at least 0.8 per cent iron and suggested that iron carbonyls in the system were being decomposed by the reactor radiation. Lind and Wright (1963) listed a number of properties of deposits formed in an experimental reactor loop. These are summarised in Table I.

Table I

Summary of properties of carbonaceous deposits produced by radiolysis of CO/CO₂ mixtures in the DMTR 7H2 loop

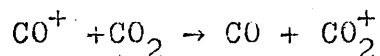
<u>Rig Characteristics</u>	7 ^v /o CO/CO ₂ at 210 lb/sq. in. g. and mass flow 0.15 lb CO ₂ /sec, is irradiated at 350-400°C, passed through a cooler to 250°C, a 5 μ filter, an impeller, and finally over a bank of heaters before returning to the in-pile section.
<u>Physical Properties</u>	
Appearance	Deposits were dark-brown to black, fluffy and non-adherent.
Electron Microscopy	Spherical particles from 100 to 2000 Å dia. (typically 1000 Å) joined by a continuous outer membrane into long filaments which aggregate into intertwined clusters up to 10 μ in dia.
Helium Density	≈ 1.45 g/cm ³ .
Tap Density	≈ 0.05 g/cm ³ .
Specific Surface Area	86-140 in ² /g.
<u>Chemical Properties</u>	
Composition	60-70% carbon, 2.5 to 4% hydrogen, 28 to 33% oxygen and up to 4% residue after combustion. Not identified to date.
Solubility	Insoluble in non-polar solvents partially soluble in polar solvents - best to date di-methyl formamide.
Infra-red absorption	Some similarities with laboratory preparations of β-propiolactone polymers.
X-ray Examination	Two broad bands of no analytical significance.
U.V. Fluorescence	Green/yellow fluorescence in solution
Thermal Degradation	Liberates CO and CO ₂ on heating.
Oxidation in 7 ^v /o CO/CO ₂	650°C - 5.8 mg/g.h.
Oxidation in air	300°C and 400°C - 28 and 293 mg./g.h. respectively.

The presence of hydrogen in the analysis suggests that the deposits had reacted with moisture at some stage in the interval between formation and analysis. Further observations made by Lind (1966) on deposits from various reactor sources showed that the radiolysis of CO/CO₂ and CH₄/CO/CO₂ coolant mixtures resulted in carbonaceous deposits which often contained appreciable amounts of inorganic substances including iron and nickel oxides.

(e) The Effect of Various Parameters on the Radiolysis of CO.

Marsh and Wright (1964) used reactor (DIDO) radiation to study the effects of pressure and gas composition on the radiolysis of CO irradiated in sealed silica tubes. The products were CO₂ and a black or dark brown solid which usually settled out in the bottom of the tube. After exposure to air for a few days the solids became reddish-brown and had probably reacted with water vapour. The amount of CO decomposed increased rapidly with irradiation time (dose) but at high doses a levelling-off of the decomposition was observed and was attributed to a back reaction between CO₂ and the solid products to reform CO. A value of $G(-CO) \approx 6$ was obtained up to high doses. The initial high $\frac{-M_{CO}}{N}$ values found by Rudolph and Lind (1966a) and Lind (1961) were observed also to decrease with

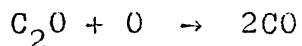
accumulation of reaction products and to account for this inhibition Rudolph and Lind suggested that a charge transfer process was operating thus:



By this process, shown by mass spectrometry to be very efficient, the CO would become deactivated by transferring energy to CO₂ which has a lower ionisation potential than CO. However, the same authors (1960b) found no inhibition by xenon - which also has a lower ionisation potential than CO - as would be expected by the proposed deactivation process, and the authors suggest that compensating processes operate involving excited states. Dondes, Harteck and Weyssenhoff (1964) also propose that the principal energy transfer processes involve excited states and that the decomposition of CO occurs mainly by excitation processes.

Marsh and Wright (1964) found that N₂ (up to 25%) did not appear to affect the radiolysis of CO. CO/CO₂ mixtures with < 10% CO gave little evidence of deposits. With higher CO concentrations (~16%) deposits were clearly visible and were of variable nature. Anderson, Best and Willett (1966) made an elegant study of the effect of radiation on CO using ⁶⁰Co γ-radiation and low energy protons from a Van de Graaff accelerator. Emphasis was

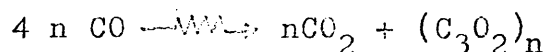
placed on studying the effects of dose rate, temperature and small amounts of additives (CO_2 and C_2) on the radiolyses. In order to avoid a significant build-up of products during irradiation the γ -radiations were restricted to $< 0.1\%$ conversion of CO and a specially designed gas-flow system was employed in the proton work. The reaction products of the room temperature experiments were CO_2 and a dark brown solid which was formed in the gas phase. The yields of both of these decreased with increasing dose rate over the range $6.5 \times 10^{15} - 1.3 \times 10^{18} \text{ eV cm}^3 \text{ sec}^{-1}$. This decrease was shown to be a true dose rate inhibition effect and was not a consequence of the accumulation of reaction products. The inhibition at high dose rates was believed to be due to reactions involving intermediate species such as C_2O which could reform CO by reaction with oxygen atoms thus:



Low concentrations of CO_2 ($\sim 0.5\%$) did not affect the yields of products but initial yields were extremely sensitive to traces of oxygen especially at the lower dose rates. In the presence of oxygen (a few p.p.m.) the yield of solid dropped and the amount of CO_2 formed increased. Lind and Bardwell (1925) showed that when CO/O_2 mixtures were irradiated the yield of CO_2 was higher than in the absence

of oxygen and no solid polymer was obtained. The γ -radiolytic oxidation of CO was studied by Clay, Johnson and Warman (1963) who found an ionic chain mechanism was in operation and $G(\text{CO}_2)$ values as high as 8000 were obtained, thus implying that the radiolysis of CO is markedly affected by the presence of small amounts of oxygen.

Anderson, Best and Willett using protons and γ -rays obtained values of $G(\text{C}) \sim 6$ and $G(\text{CO})_2 \sim 2$ in the absence of oxygen. The constancy of the ratio $G(\text{C})/G(\text{CO}_2) \sim 3$ found for a range of dose rates suggested that the stoichiometry was best represented by



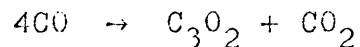
The yield of $G(-\text{CO}) \sim 8$ thus obtained from this stoichiometry for the γ and proton irradiations is in good agreement with the initial values found by Rudolph and Lind (1960a) for α -radiation in the absence of CO_2 , $G(-\text{CO}) = 8.4 - 9.6$, and with that of Marsh and Wright (1964) for reactor radiation ($G(-\text{CO}) \approx 6$) to high total doses.

Assuming the above stoichiometry, values of $G(-\text{CO}) \sim 9$ are derived from the work of Clay, Johnson and Warman (1963) for γ -radiation and from Dondes, Harteck and Weyssenhoff (1964) for α -radiation. These values indicate that the type of radiation used does not appear to affect the initial decomposition process.

5. Nature of Solids from CO Decomposition

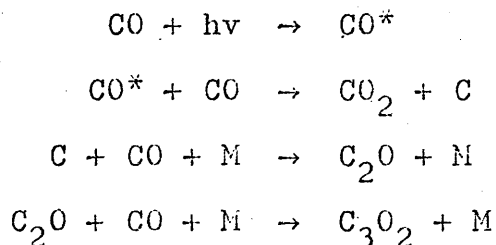
Most of the early work on the decomposition of CO was concerned principally with the gaseous reaction products and detailed studies of the solids were not made. Evidence that the solid produced was a carbon suboxide polymer was usually derived from material balance studies rather than from actual analyses of the solids. The discovery of carbon-rich solids on reactor surfaces has led to more recent investigations and analytical data have now been acquired. The results of most investigations indicate that CO₂ and a solid suboxide of carbon are formed.

As early as 1873, Brodie reported the formation of a red-brown solid carbon suboxide from the decomposition of CO by an electric discharge. The solid dissolved in water to give an acidic solution. Crespi and Lunt (1925) obtained a solid suboxide the composition of which was dependent upon the pressure of CO during discharge. When CO was passed through an ozoniser, Ott (1925) claimed that carbon suboxide monomer and CO₂ were formed by the reaction:



Faltings, Groth and Harteck (1938) made a study of the photolysis of CO under the action of Xe $\lambda 1295 \overset{\circ}{\text{A}}$ radiation and found carbon dioxide and carbon suboxide,

C_3O_2 , as products. Groth, Passara and Rommel (1962), using similar radiation, also obtained CO_2 and suboxide and explained their formation by a reaction involving excited CO molecules thus:



The thermal polymerisation of C_3O_2 was studied by Klemenc and Wagner (1938) who reported that the products were dicarbon gas, C_2 , and solids of composition C_3O_4 and C_3O_6 , but later work disagrees with these findings. The chemistry of carbon suboxide has been reviewed by Reyerson and Kobe (1930) and Hudswell (1961). The photolysis of carbon suboxide gas in the presence of hydrogen was investigated by Forchioni and Willis (1968). These authors were primarily interested in the various gaseous products and the yellow-brown solid which they obtained as one of the products was not examined in detail; the solid was believed to be a carbon suboxide polymer. Schmidt, Boehm and Hofmann (1955, 1959) thermally polymerised carefully purified C_3O_2 monomer and obtained a solid $(C_3O_2)_n$ which took up water irreversibly. On heating,

the solid lost CO or CO₂ and became darker in colour and richer in carbon content. The proposed structure for the solid - known as "red carbon" - is given in Fig. 2.

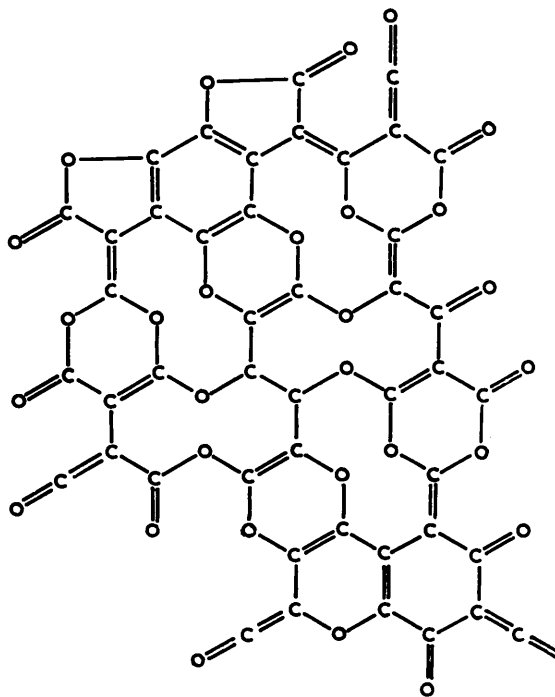


FIG. 2: Structure of "red carbon" suggested by Schmidt, Boehm and Hofmann (1955, 1959).

Smith, Young, Smith and Carter (1963) and Blake, Eeles and Jennings (1964) made detailed studies of the thermal polymer by infrared and X-ray diffraction techniques and agreed that the basic structure is a polycyclic

six-membered lactone ring (Fig. 3) rather than the complex structure suggested by Schmidt, Boehm and Hofmann.

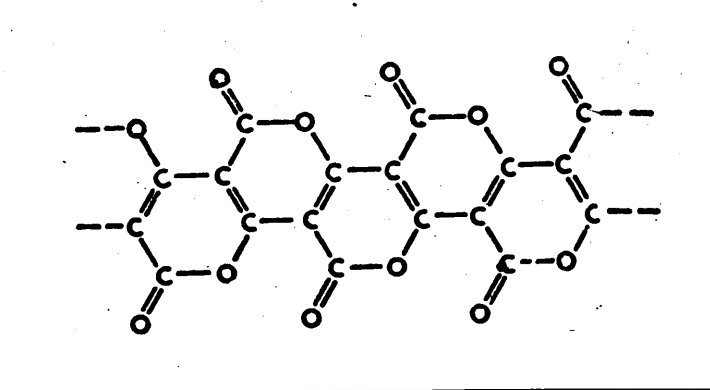


FIG. 3: Structure of the thermal polymer after Smith, Young, Smith and Carter (1963) and Blake, Eeles and Jennings (1964).

Unsaturated linear terminal end groups such as $=C=C=O$ were postulated to account for some of the infrared data. The dark brown solid obtained by Anderson, Best and Willett (1966) showed only a characteristic infrared absorption band at 5.6μ for $>C=O$ which shifted to 5.8μ on hydration and these authors concluded that the radio-polymer does not have the closed ring structure of the thermal polymer but suggested a linear structure cross-linked by C-C bonds. Marsh and Wright (1963) had the solids from reactor radiation examined by infrared techniques and established that they were structurally different

from thermal polymers produced from C_3O_2 monomer but had similar features to those which may be produced by the pyrolysis of lactones.

6. Electron Microscopy of Solids from CO Radiolysis

Several workers have used electron microscopy to investigate the structure of the solid deposit obtained by decomposing carbon monoxide both alone and in the presence of other gases. The results of these studies are obviously influenced by the geometry of the deposition system and the techniques used in preparing specimens suitable for electron microscopy, and in all cases the specimens were exposed to the atmosphere prior to examination in the electron microscope.

The effect of irradiating various $CO/CO_2/CH_4$ gas mixtures by vacuum ultraviolet light in the presence of graphite was studied by Adamson, Dawson, Feates and Sach (1966). Electron micrographs of the same areas of graphite specimens before and after reaction showed - in addition to oxidation of the graphite - that deposits were formed at localised sites on the graphite surfaces during the period of irradiation. Electron diffraction studies gave no information about the structure of the deposits due to the strong reflections from the underlying graphite. Further irradiation of the specimens did not appear to affect the deposits.

Clark (1969) decomposed carbon monoxide in the presence of graphite in a quartz reaction vessel using a low pressure microwave glow discharge. Brown and black deposits were obtained together on the graphite and on the quartz surroundings. An electron microscope study revealed little information about these solid materials. The brown solid was thought to be a carbon suboxide polymer. It was noted that the growth patterns of the black material appeared to be influenced by the quartz surface.

Two reports issued by the General Electric Company, Limited, (1962, 1963) describe electron micrographs of solid obtained from the neutron irradiation of carbon monoxide in sealed glass or silica bulbs and from pure carbon dioxide in the presence of graphite. Fern-like structures about 50 microns across were observed in the latter irradiations, together with rough spheres approximately 0.3 microns in diameter. It was reported that some of the spheres were covered with a structure that appeared to be the early stages of the fern-like growth. No electron diffraction patterns were detected. As these samples had been dispersed in benzene in preparation for microscopy it is possible that the fern-like growth reported was due to recrystallisation of a soluble component of the solid and was not a genuine product of the irradiation.

Watson, Vanpee and Lind (1950) made a most detailed electron microscope study of the solids produced by the α -radiolysis of CO using 5.6 MeV α -particles from radon. Dark brown solids were obtained, mounted dry on specimen grids and examined by bright and dark field transmission microscopy. Studies revealed that the solid consisted of irregularly shaped particles with a small proportion of approximately hexagonal clumps present. The particles were often joined by short necks of a material which appeared to be different from the bulk matter. This was believed to be suboxide polymer. The particles were about 0.4 - 0.5 μ in diameter and were shown by the shadow-casting technique to be about the same in height. On heating in the electron beam (by increasing the beam intensity) the particles were observed to shrink by about ten to twenty per cent but they did not sublime completely even under prolonged intense bombardment. X-ray diffraction studies on the solid were made and a considerable number of lines were observed, indicating a crystalline nature for the solid. Some of these corresponded with graphite and it was concluded that graphite was present in the solid. The extra lines were attributed to the suboxide polymer for which no data are available. The X-ray diffraction patterns, however,

were not always reproducible and sometimes no lines at all were present. Re-examination of deposit particles after exposure to the atmosphere for sixteen days showed a slight decrease (~ 5 per cent) in particle size but this was not significant since the authors stated the decrease to be within the order of accuracy of their particle size measurements. The results of this study showed clearly that the particles formed in the gas phase.

Ryan (1963) made an electron microscope study of his reactor deposits (formed at 360-675°C) and those obtained by Tingey from γ -radiolysis (35°C). The appearance of the particles was rather similar to those depicted in the electron micrographs of Watson, Vanpee and Lind (1950) for α -radiolytic deposits. The particles were approximately spherical, resembled carbon blacks and were often linked together by short necks of an amorphous material to form chain-like networks. Baird, Dawson and Wood (1964) illustrated the chain-like features of deposits from proton Van de Graaff experiments and found that varying the nature of the collecting substrate did not appear to influence the morphology of the particles.

7. Aim of the Present Work

There have been few detailed electron microscope

studies of the solids produced by the radiolysis of carbon monoxide gas. Most of the previous studies necessitated some mechanical treatment of the solids before viewing in the microscope and in all cases the solids which have been shown to be of an hygroscopic nature, were exposed to the atmosphere before examination. The electron micrographs depicted in previous studies therefore may not be a true representation of the morphological nature of the solid as formed.

The main aim of the present work was to decompose carbon monoxide in a system which would allow direct examination to be made of the solid product. It was intended subsequently to investigate the effect of exposing the solid to the atmosphere and to observe structural changes in the solid after heating. Subsequent studies depended upon the ability to obtain reproducible results and it was intended to investigate the effect on the radiolysis of varying the gas composition. The radiolyses were to be performed within a commercial electron microscope and the relative techniques of electron diffraction and electron probe microanalysis were intended to supplement the microscopy studies in order to gain information about the crystalline nature and composition of the solid.

8. Electron Microscopy

(a) Introduction

The principles and applications of electron microscopy have been extensively reviewed (Cosslett, 1951; Hall, 1953; Heidenrich, 1964; Kay, 1965 and Hirsch, Howie, Nicholson, Pashley and Whelan, 1965) and specific features of various instruments have been described. A Siemens Elmiskop I electron microscope was used in the present work. Specimen magnifications from 200 to 160,000 times are obtainable with this instrument which can operate at an accelerating voltage of 40, 60, 80 or 100 KV. The specimen can be illuminated by either a single or double condenser lens system with subsequent three-stage magnification by objective, intermediate and projector lenses (Fig. 4(a)).

(b) Resolution

The unaided human eye is incapable of resolving points closer together than about 0.1 to 0.2 mm. In optical and electron microscopy the theoretical resolution (d) is dependent mainly upon the wavelength (λ) of the medium used to form the image and the half aperture angle (α) of the cone of light leaving the specimen and entering the objective lens and is given by the Abbé equation as $d = \frac{\lambda}{\sin \alpha}$; thus the resolution will improve when λ

is small and α is large. The wavelength of a moving stream of electrons is several orders of magnitude shorter than that of visible light and may be calculated from the de Broglie equation, $\lambda = \frac{12.3}{\sqrt{V}}$ where V is the accelerating voltage. The Siemens Elmiskop I will therefore provide values of λ from 0.062 Å to 0.039 Å. The actual resolution which can be achieved, however, is about 8 Å for the Elmiskop I and this is limited mainly by the inherent spherical aberration of the objective lens where refraction effects occur; the further the distance from the optical axis of the lens then the worse is the aberration effect. The Abbé equation favours a high value of α for high resolution, i.e. a cone of illumination containing a large amount of "information" about the specimen, but the optimum value is a compromise between this and that which minimises spherical aberration by diminishing the cone of illumination from the specimen. Objective apertures of about 50 μ diameter are usually inserted to give optimum resolution.

Astigmatism of the whole system and in particular of the objective lens is a factor which causes deterioration in the resolution as it leads to a deformation of the focusing field from rotational symmetry. In the Elmiskop I use is made of a stigmator control, at the objective

lens, which provides an elliptical correcting field. Astigmatism arises from manufacturing defects and inhomogeneities in the soft iron pole-piece systems and from dirt which becomes electrically charged on objective apertures and other parts of the microscope interior. A number of other factors, e.g. chromatic aberration, influence the ultimate resolution obtainable but most of these have been overcome by modern instrument design and specimen preparation techniques.

The single condenser illuminating system (Fig. 5) gives an illuminated specimen area of about 50 μ . By using the double condenser system - also illustrated in Fig. 5 - a demagnified image of the electron source is obtained and this is projected by the second condenser lens on to the specimen to give an illuminated area of about 2 μ minimum thus confining the heating effect of the electron beam to a smaller area. This system also produces a more coherent beam of electrons and reduces the scattering angle of the electrons leaving the specimen so that for high resolution work, where increased brightness is required at high magnifications, the double condenser system is favoured.

(c) Specimen contrast

The contrast in an electron microscope image arises

from the differential scattering of electrons in the object. A dense region of the object will scatter more electrons out of the beam than a less dense region and will appear darker in the final image viewing screen. The contrast can be improved by reducing the size of the objective aperture or by operating the microscope at a lower accelerating voltage thus causing more interaction between the beam and the object which consequently increases the electron scatter. The change in the wavelength of the electron beam caused by altering the voltage does not significantly affect the resolution and for most applications the choice of voltage depends on the contrast required and the thickness of the specimen under examination.

(d) Electron Diffraction

The Siemens Elmiskop I can be used to obtain electron diffraction patterns from crystalline objects. The technique used in the present work was that of selected area diffraction which allows an observed diffraction pattern to be correlated to a small defined area of the specimen. The diffracted beams which emerge from a crystalline specimen at angles characteristic of the specimen are focused on to the back focal plane of the objective lens (Fig. 4 (b)) together with the

undeviated beam and are subsequently magnified to form the final image. The various lattice spacings (d) of the specimen can be determined by $d = \frac{K}{R}$, where K is a constant for the instrument and R is the radius of reflection in the observed pattern. It is necessary to determine K for each pattern (Hirsch, Howie, Nicholson, Pashley and Whelan, 1965) and this is achieved by making measurements of diffraction patterns of a substance of known d -spacings. The accuracy of this technique is of the order of 1 per cent and this is usually good enough to allow identification of an unknown crystal.

9. Electron Probe Microanalysis

This technique is used to analyse very small specimens or specific areas ($0.1 - 3.07\mu\text{m}$ in diameter) of a specimen, and was used in the present work to supplement the microscopy. Birks (1963) has discussed various instrumental features and techniques in X-ray microanalysis and a number of papers on X-ray optics and detectors have been compiled by the American Society for Testing and Materials (1964). X-rays are generated by bombarding the specimen with a probe of electrons, the wavelengths of the emitted X-rays being characteristic for each specific element (Moseley, 1913). The X-rays are then passed into a spectrometer consisting of an analysing

crystal and a detector. The crystal separates the characteristic wavelengths (λ) according to the Bragg law, $n\lambda = 2d\sin\theta$, where n is the order of reflection, d is the crystal lattice spacing and θ is the Bragg angle of diffraction, so that by changing the value of θ a particular wavelength can be selected. The diffracted X-rays are then directed into a detector which converts X-ray quanta to voltage pulses and measures the intensity of the X-rays thus allowing an estimate to be made of the concentration of an element within a very small area. The range of elements which a spectrometer can detect depends on the type of detector used and the operative d-spacing of the analysing crystal. Most instruments incorporate a range of crystals with different d-spacings allowing the detection of elements from atomic number 11-94. Elements of lower atomic number emit low energy X-rays of long wavelength and special techniques are required for their detection; these include the use of analysing crystals with large d-spacings, e.g., lead stearate and a method of preventing contamination build-up on the specimen surface which would otherwise absorb the low energy X-rays.

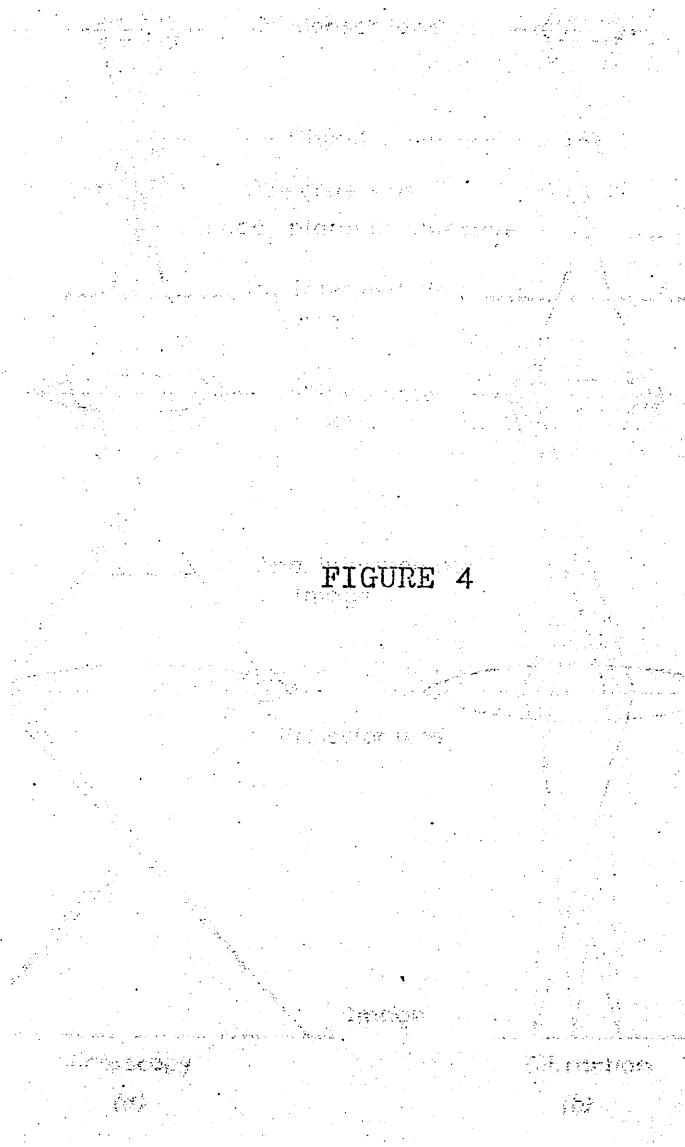


FIGURE 4

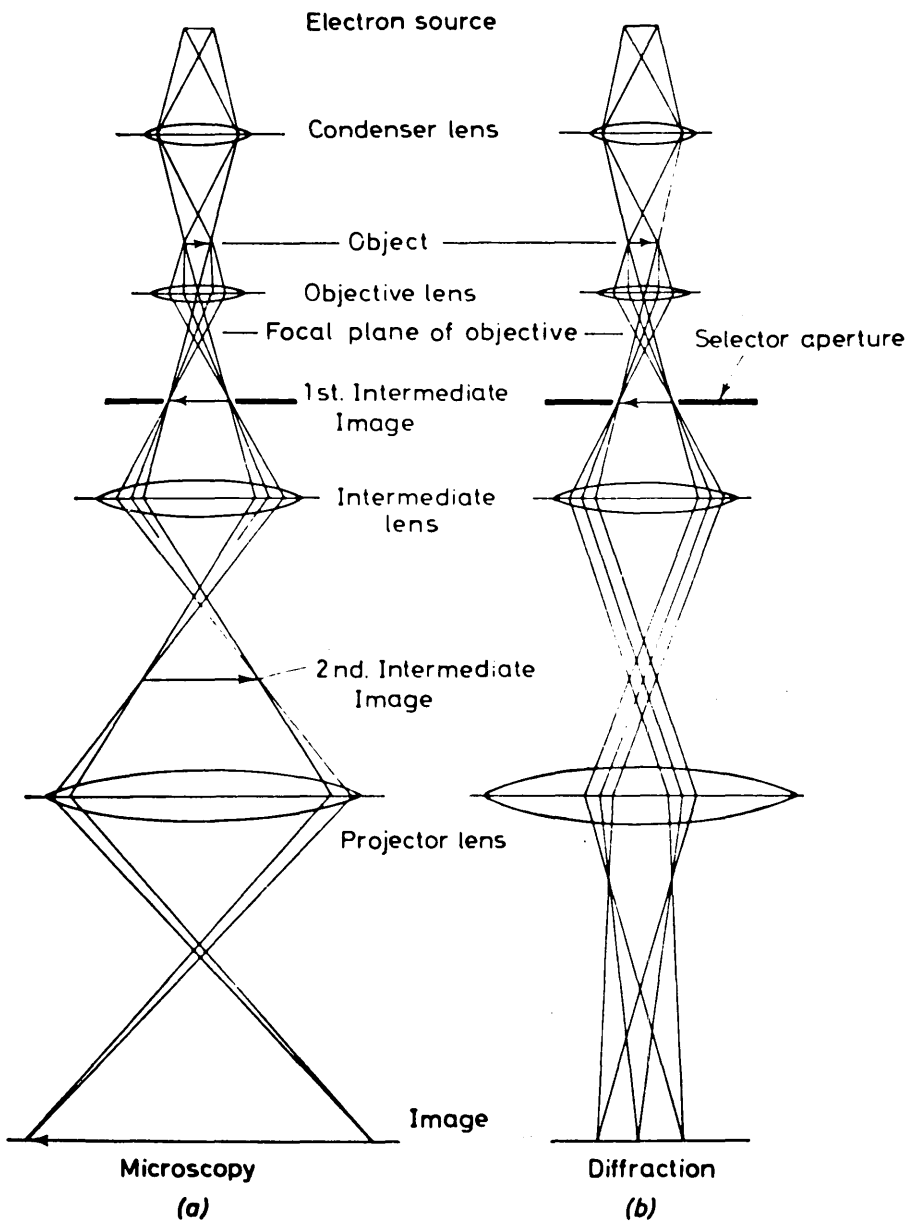


FIG. 4. Ray Diagrams for (a) Transmission Microscopy and (b) Selected Area Diffraction. (From Hirsch, Howie, Nicholson, Pashley and Whelan, 1965).

FIGURE 5



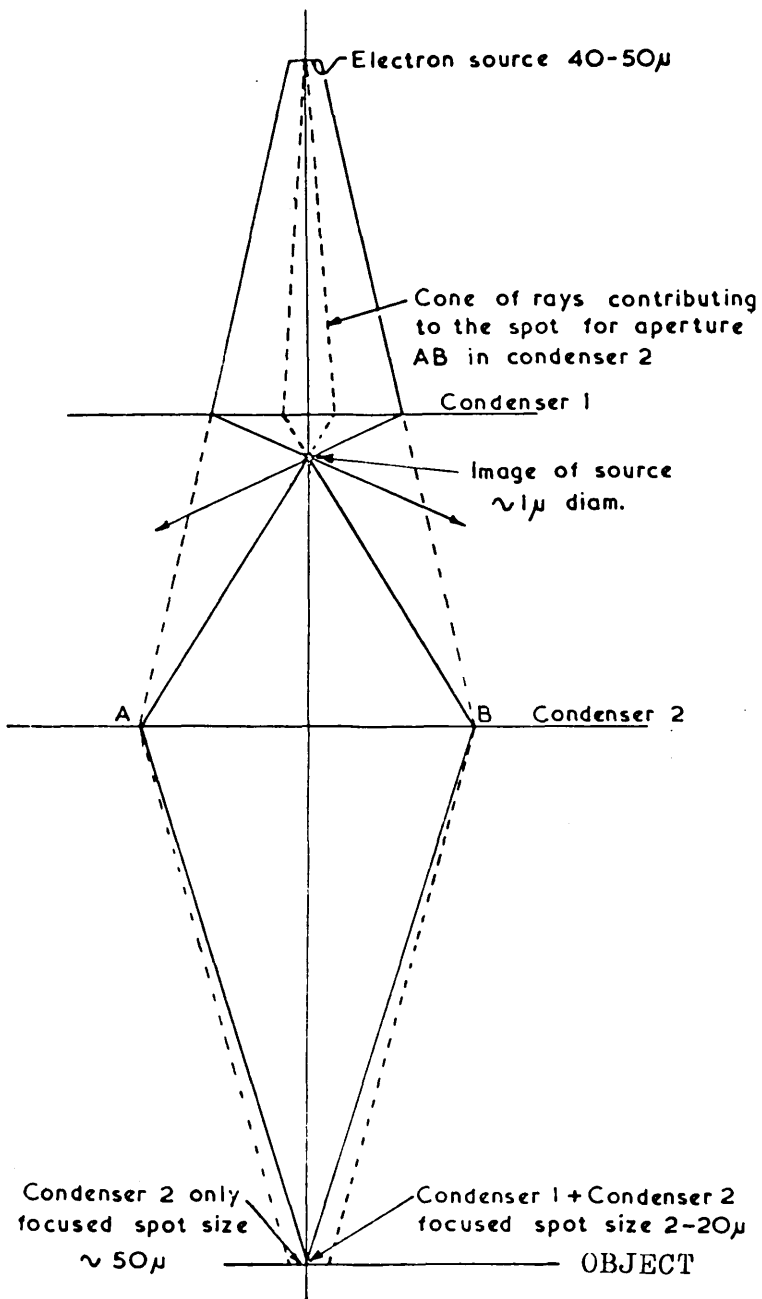


FIG. 5. Ray Paths for Single and Double Condenser Illumination. (After Agar in Kay, 1965).

EXPERIMENTAL

EXPERIMENTAL

Contents

	Page
1. <u>α-Sources</u>	44
2. <u>Safety Preacutions</u>	45
3. <u>Procedure for Deposition in situ</u>	47
4. <u>Experiments using Cylinder CO</u>	48
5. <u>Experiments using Spectroscopically Pure CO</u>	53
6. <u>Materials</u>	53
(a) Gases	53
(b) Substrates	55
(c) Graphites	56
7. <u>Post-treatment of Specimens</u>	56
(a) Shadowing	58
(b) Vacuum Heating	58
(c) Oxidation of Deposits	59
8. <u>Deposition within the Irradiation Zone of the α-Source</u>	60
9. <u>Decoration</u>	60
10. <u>External Deposition</u>	63
11. <u>Proton Van de Graaff Experiments</u>	66
12. <u>Electron Microscopy</u>	68
13. <u>Microanalytical Techniques</u>	68
(a) Electron Diffraction	68
(b) Electron Probe Microanalysis	69
(i) Siemens X-Ray Spectrometer Attachment	69
(ii) G.E.C. - A.E.I. S.E.M.2	71
(c) Infrared Analysis	72
(i) Solids from Van de Graaff Experiments	72
(ii) Solid from α -Radiolytic Experiment	72
14. <u>Dosimetry</u>	74

1. α -Sources

The α -sources used in this work were made at A.E.R.E. Harwell and utilised the α -radiation from plutonium-240. The long half-life of this isotope ($\sim 6,600$ years) means that the source strength remains effectively constant throughout the course of this work. Four sources of about 10 millicuries were manufactured within a three-year period and for convenience are designated A, B, C and D. A, B and C were designed for use in a Siemens Elmiskop I electron microscope and D for use in the Philips EM 100 B. Source D was found to be technically difficult to handle without the risk of becoming readily unsealed and was scrapped. The Siemens prototype A, was not used extensively and was subsequently replaced by B and C with which most of the results were obtained.

The three Siemens-type sources were of similar design and consisted of a phosphor bronze ring of 6.0 mm internal diameter coated on the interior surface with plutonium/3.5% aluminium alloy sealed in by Araldite to prevent radio-active contamination. The thickness of the Araldite coating varied from source to source as did the amount of alloy used, which was about 200 mg. The literature on the α -radiolysis of organic gases showed that secondary irradiation of the primary products often effected changes

in the properties of the solids, thus the present sources, designed to fit inside the object cartridge of the Siemens Elmiskop I, were so arranged that the gas phase was irradiated and any solid material which settled out on to the specimen grid was shielded from further irradiation. Fig. 6 shows the incorporation of the α -source into the cartridge.

Sources A and B were not fixed permanently into the object cartridge and had to be manipulated carefully into position before each experiment. Source C, however, was sealed to the walls of the cartridge by Araldite so that the source plus cartridge was essentially a single unit which could be handled more easily.

2. Safety Precautions

In dry air at room temperature the oxidation of plutonium is slow, but when moisture is present the attack is relatively rapid. The oxidation product is usually the dioxide PuO_2 which forms as small loose particles on the metal surfaces; these tend to break off and spread out from the parent body of material thus contaminating the surroundings with extremely hazardous plutonium. It is therefore imperative to minimise the oxidation and spread of the corrosion products. By alloying the plutonium with aluminium, stabilisation of the delta-phase

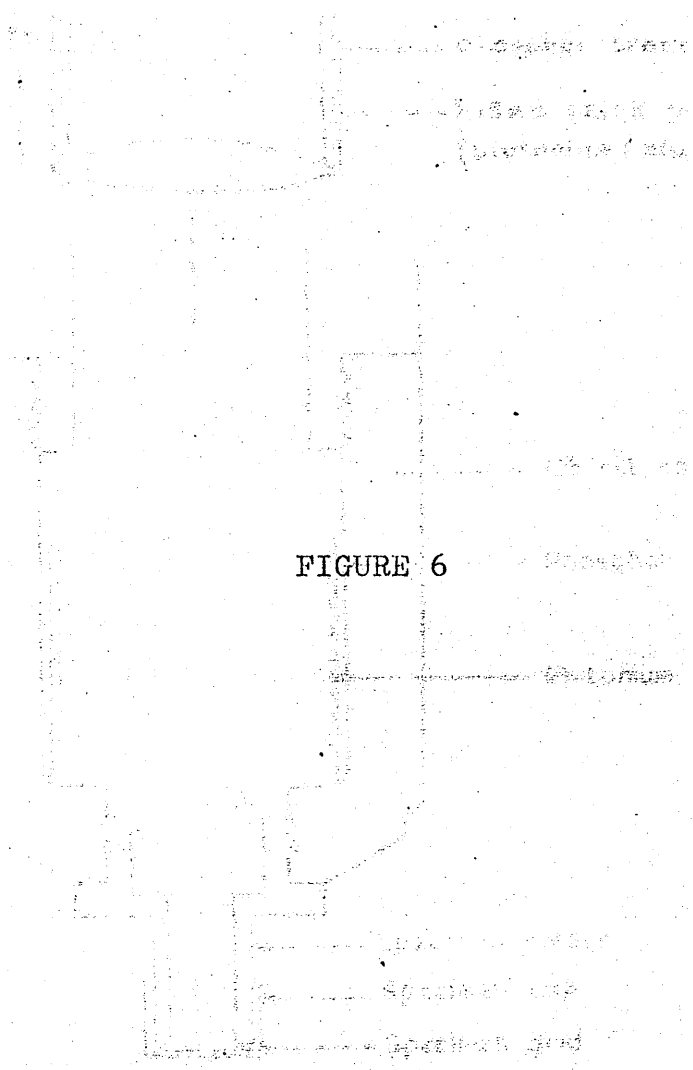


FIGURE 6

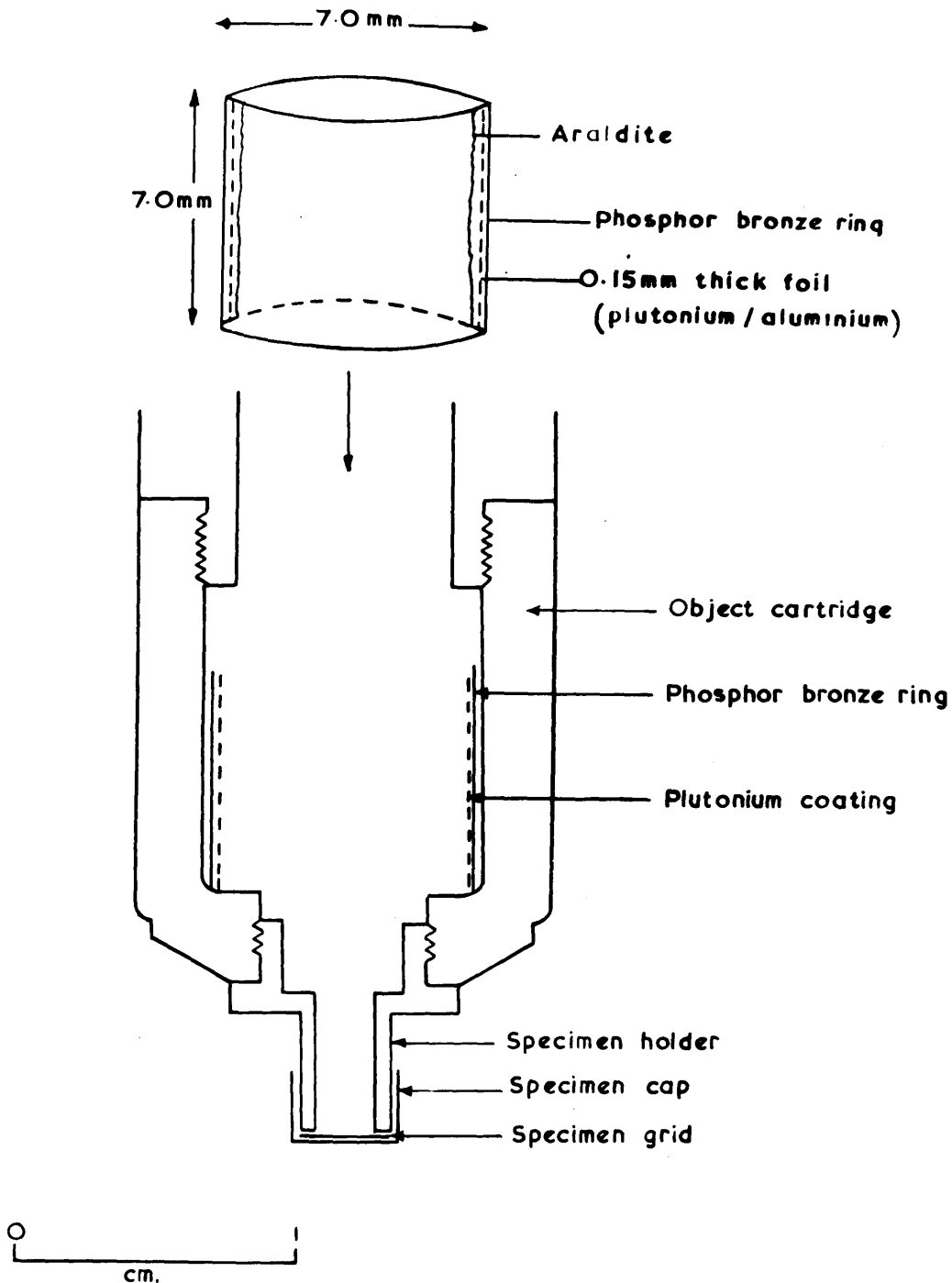


FIG. 6. CROSS SECTION OF THE ELECTRON MICROSCOPE
OBJECT CARTRIDGE SHOWING THE INCORPORATION
OF THE α -SOURCE ABOVE THE SPECIMEN GRID.

of plutonium occurs (Waber and Wright, 1961) and considerable corrosion resistance is conferred to the plutonium.

Strict handling and monitoring routines were maintained throughout the course of the work. A laboratory coat, gloves and overshoes were worn and the α -source and surroundings were monitored before and after each experiment. The acceptable level of contamination on the skin is $10^{-5} \mu\text{c}/\text{cm}^2$ for α -radiation (Holliday, 1963). The monitor used for checking was a Type 1320 probe manufactured by Ericsson Telephones Limited. The area of this probe and its efficiency are such that $10^{-5} \mu\text{c}/\text{cm}^2$ corresponds to a reading of three counts per second. If this reading was exceeded decontamination of the surface became necessary. The first α -source in regular use (B) was detected to be unsealed after about two years and decontamination of the microscope was necessary. To reduce the risk of a further leak, source C was used for one year only. In addition, this source had two 0.015" thick rings inserted, one above and one below the bronze cylinder, to provide ledges which would tend to collect corrosion products should a leak occur.

3. Procedure for Deposition in Situ

The specimen holder with a suitable grid was inserted

into the object cartridge and the microscope was evacuated to $3-5 \times 10^{-5}$ torr as for normal use. The electron beam was then switched on momentarily to check and dry the substrate. A modification of the air inlet vent on the specimen chamber allowed gas to be transferred from a vacuum line into the whole microscope column. The column was flushed out with gas, the whole system re-evacuated and then filled to a predetermined pressure not greater than atmospheric. Experiments were usually conducted at pressures between 0.2 and one atmosphere. Beyond one atmosphere, losses occur through the various vacuum gaskets of the electron microscope which become ineffective seals. The radiolysis was then allowed to proceed for a set time, normally between 17 and 67 hours, after which the system was carefully pumped out and the specimen grid examined for deposition products. Since the specimen occupied the normal position for viewing (Fig. 7), the deposits could be examined directly, without exposure to the atmosphere. Due to the geometry of the system the deposits were not irradiated once they had settled on to the substrate.

4. Experiments Using Cylinder CO.

The vacuum line employed to supply gas to the microscope is shown in Fig. 8. The furnace, used in a

FIGURE 7

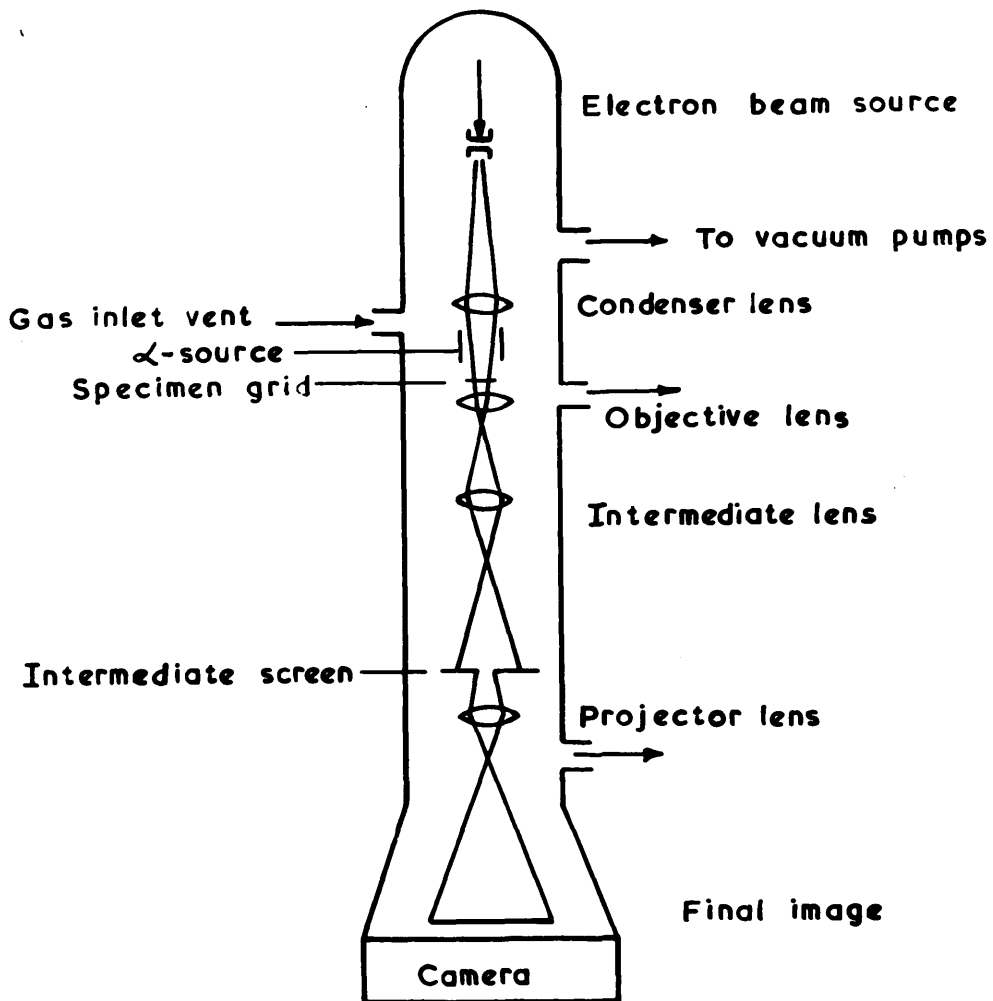


FIG. 7. SCHEMATIC DIAGRAM SHOWING POSITION OF X-SOURCE WITHIN THE SIEMENS ELMISKOP I.

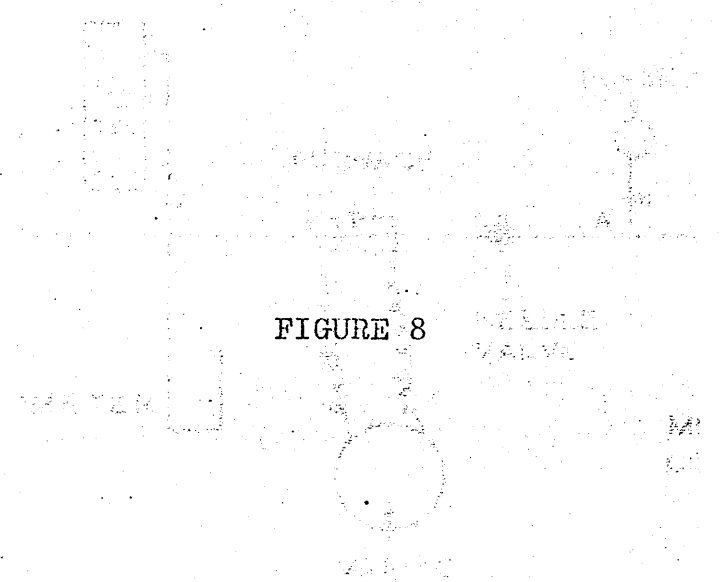


FIGURE 8

BLOCK DIAGRAM OF FACILITY

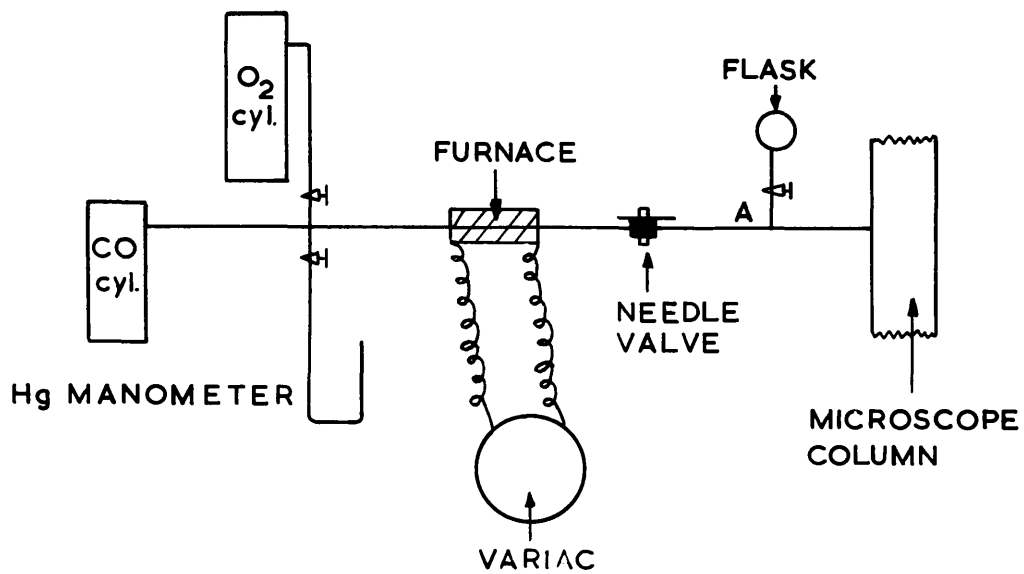


FIG. 8 BLOCK DIAGRAM OF VACUUM LINE.

purification process, consisted of a silica tube wound with Nichrome wire and asbestos paper impregnated with sodium silicate to act as a sealant. Calibration of the furnace Variac was achieved by means of a platinum/rhodium thermocouple and a temperature indicator (Standard Portable Indicator manufactured by Cambridge Instrument Company Limited). The flow of gas to the microscope was controlled by the needle valve (OS Series, Edwards High Vacuum Limited), 20 minutes being about the average time allowed for the gas to leak in. The volume of gas required to fill the microscope column and adjacent voids was found experimentally (by a water suck-back technique) to be 10.2 litres.

In some experiments the CO was purified of oxygen by passing it over copper turnings at 450°C held in a Pyrex glass tube packed at each end with glass beads to prevent loss of small copper particles during operation (Fig. 9). Glass wool was used initially as packing but microscopic glass wool fibres were found to have been blown through the system on to the specimen grid and its use was discontinued.

Deliberate addition of impurity to the CO was often made, either from a cylinder of gas connected to the gas line or from a flask at A, Fig. 8. The additives were,

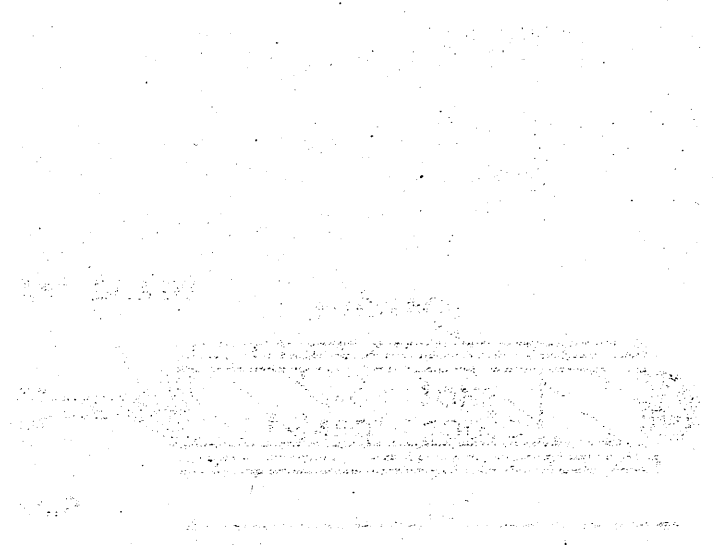


FIGURE 9

ENTER TOWN

DETERMINATION 1984 US

INVESTIGATION PROCESS

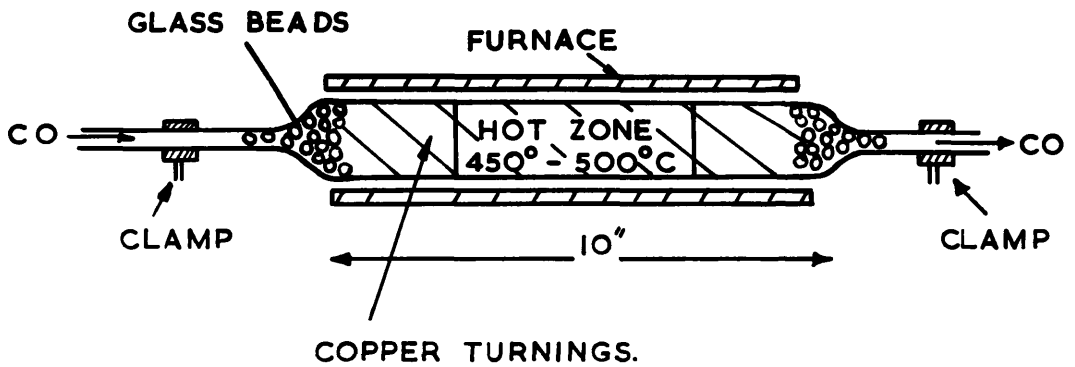


FIG. 9. DECOMPOSITION TUBE USED IN
PURIFICATION PROCESS.

oxygen, methane, iron pentacarbonyl, nickel tetracarbonyl or water vapour.

5. Experiments Using Spectroscopically Pure CO

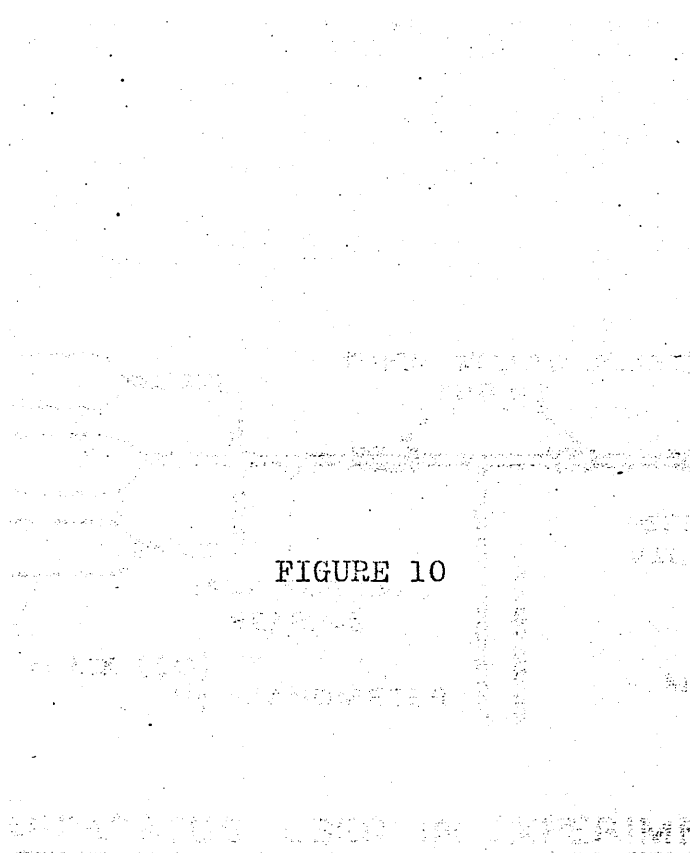
Spectroscopically pure CO supplied in 2½ litre glass flasks (British Oxygen Company Limited) at one atmosphere pressure, was used in the first set of experiments. The flasks were connected either singly or three in parallel to the microscope column (Fig. 10). After evacuation, the seals were broken by the usual method using a plunger and magnet.

6. Materials

(a) Gases

Three 2½ litre flasks of CO (B.O.C. Limited) gave a gas pressure of 0.4 atm. within the total volume of the system. A single flask gave a pressure of only 0.2 atm.. The results from these experiments indicated that a higher gas pressure was desirable and much of the work was subsequently done using I.C.I. cylinder CO. This was quoted as better than 99% pure with nitrogen, oxygen and carbon dioxide as the other major constituents. Parts per million of hydrocarbons (mainly methane) were also quoted as constituents.

Two aluminium cylinders of CO (at ~700 p.s.i.) from A.E.R.E., Harwell, were also utilised. This gas had been



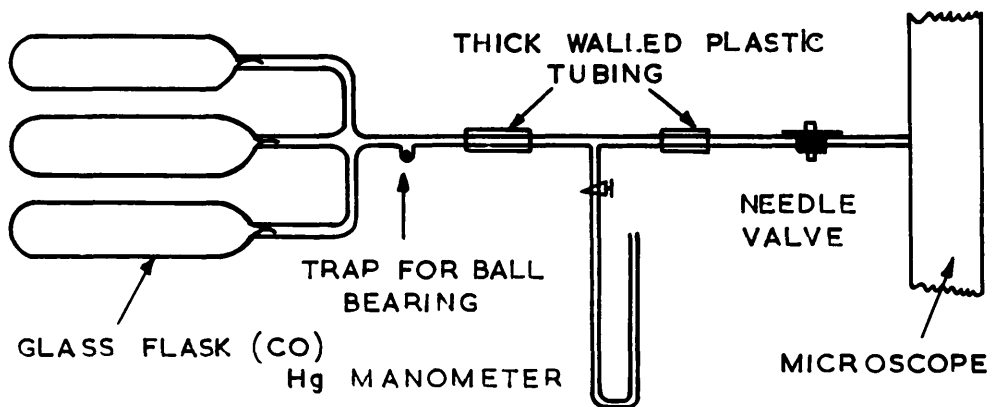


FIG. 10 APPARATUS USED IN EXPERIMENTS 1-5

purified by passing it through a bed of finely divided reduced copper oxide at 120°C to remove oxygen, then through magnesium perchlorate to dry it. Analysis figures for the particular cylinders used were not available but the gas was representative of that used at Harwell which usually contained about 50 vpm oxygen and 3,600 vpm nitrogen as the main impurities.

Cylinder oxygen (B.O.C. Limited), methane (Matheson Co. Inc.) and helium (B.O.C. Limited) were used without further purification. Liquid iron pentacarbonyl and nickel tetracarbonyl (α -Inorganics Inc.) were also used as supplied.

(b) Substrates

Carbon films were prepared in a manner similar to that described by Bradley (1954), by evaporating carbon under a vacuum of about 10^{-5} torr on to cleaved mica, floating the film off on to water and picking it up with copper grids or platinum-iridium mounts. Carbon films of 100-200 Å thick were used.

Silicon monoxide substrates of about 200 Å thick were made after Bradley's (1954) technique, by evaporating a mixture of silicon and silicon dioxide (Barcote Q, manufactured by British American Research Limited) from a molybdenum boat on to Formvar - filmed platinum-iridium

mounts. By heating the mounts to dull red heat, clean, Formvar-free mounts were obtained.

(c) Graphites

Three types of graphite were irradiated by α -particles in the presence of CO. These were (a), a polycrystalline synthetic graphite (P.G.A.) of the type used in British nuclear reactors, (b), a highly purified natural graphite (SPI) and (c), pile grade A (P.G.A.) graphite which had been previously neutron-irradiated ($4 \times 10^{20} \text{ n/cm}^2$) in DIDO at A.E.R.E. Harwell. The impurity contents of the P.G.A. and SPI graphites are shown in the table overleaf (Labaton 1965).

Graphite specimens were prepared by placing a small quantity of the powdered graphite in distilled water in a test tube and subjecting the sample to ultrasonics (80 K cycles/sec) for about one minute. In this way a suspension of thin flakes suitable for microscopy was obtained. A drop of the suspension was then allowed to dry down in a cool oven ($\sim 30^\circ\text{C}$) on to the required substrate.

7. Post-treatment of Specimens

In many experiments it was desirable to relocate specific areas of the specimen after further treatment had been effected. The platinum specimen mounts were found to be useful in this capacity as they could be marked with

Typical Analysis for Impurity (p.p.m.)

	<u>SPL. Maximum</u>	<u>P.G.A. Range</u>
Ash	-	.005 -- .025
Aluminium	.015	.25 -- 2.5
Barium	.015	.3 -- 15
Beryllium	.015	.02 -- .03
Bismuth	.06	.06 -- .15
Boron	.02	.03 -- .16
Calcium	.15	7 -- 60
Chromium	.015	.1 -- .7
Cobalt	.015	.01 -- .03
Copper	.04	.01 -- .5
Hydrogen	-	15 -- 40
Indium	.04	.04 -- .08
Iron	.05	2 -- 16
Lead	.025	.04 -- 2.5
Lithium	.005	.04 -- .15
Magnesium	.025	.03 -- 1.5
Manganese	.015	.01 -- .06
Nickel	.025	.03 -- 8
Phosphorous	-	.1 -- .2
Silicon	.15	15 -- 60
Sodium	.1	1 -- 2
Tungsten	.08	.08 -- 2
Vanadium	.02	.4 -- 30
Zinc	.08	.08 -- .2
Others	.045	.1 -- 1.64

a fine needle and oriented in a holder (also marked) so that visual comparison of a specific area was possible before and after reaction.

(a) Shadowing

By using this technique it is possible to gain information about the morphology of a material. A shadow can be produced by evaporating a suitable electron-dense metal or alloy from a source on to the required material tilted at a known angle to the source. Shadows will then appear as areas of greater intensity than the surroundings and by studying the shape and size of the shadow produced useful information is often revealed. In these experiments specimens were shadowed in an Edwards Coating Unit (Type 12 E6) using nickel/palladium alloy (70/30) or platinum/carbon (40/60) when finer detail was required. The thickness of the shadowing film was about 100 Å.

(b) Vacuum Heating

Deposits obtained from the radiolysis of CO were heated in a vacuum of 10^{-5} torr for 15 minutes at 500°C in order to observe any gasification reaction. Heating was effected externally in an Edwards Coating Unit (type 12 E6) or, alternatively, in the microscope itself by using a Siemens Object Heating Device which could be

fitted in place of the normal object cartridge. By using the latter technique it was possible to observe reaction progressing as the temperature was raised from 20°C to about 1000°C. The device was designed to operate with batteries but a 1.5 A/ 16 V stabiliser fitted between the mains and the power control unit was found to be more satisfactory.

(c) Oxidation of Deposits

Deposits were heated in a stream of oxygen in a 1,800°C Pyrocore Furnace (Metals Research Limited). This is a molybdenum-wound, water-cooled furnace in which a flow of hydrogen protects the windings. The specimen mounts were placed in a long handled silica boat and inserted into a silica U-tube within the furnace work zone. The temperature was registered by means of a tungsten/rhenium thermocouple and an indicator (Foster Instrument Company Limited). When the mounts were re-examined in the electron microscope they showed very little contamination after oxidation in this apparatus.

A muffle furnace similar to the one described earlier also gave clean oxidations and was more convenient to use. As above, the mounts were placed in a silica boat and inserted into a long silica tube placed

within the furnace. All silica components were cleaned and fired before use in order to reduce contamination of the mounts.

8. Deposition within the Irradiation Zone of the α -Source

In order to study the effect of radiolysing CO in the presence of graphite a number of experiments were conducted in which the specimen substrates were placed into the irradiation zone of the α -source. The intention was to observe any change in the deposit particle size and to note if growth occurred on the graphite surfaces. Carbon films, and carbon films with graphite deposited on them were irradiated in CO within the active zone.

The specimens were held by a small, tapered brass tube fitted into the back of a normal specimen holder (Fig. 11). It was necessary in these experiments to move the specimen from the centre of the source back to the normal position before viewing, thus exposing the specimen to the atmosphere for a short period (about two minutes).

9. Decoration

When certain metals are evaporated on to heated surfaces and then examined in the electron microscope it is often observed that the metal particles are arranged on

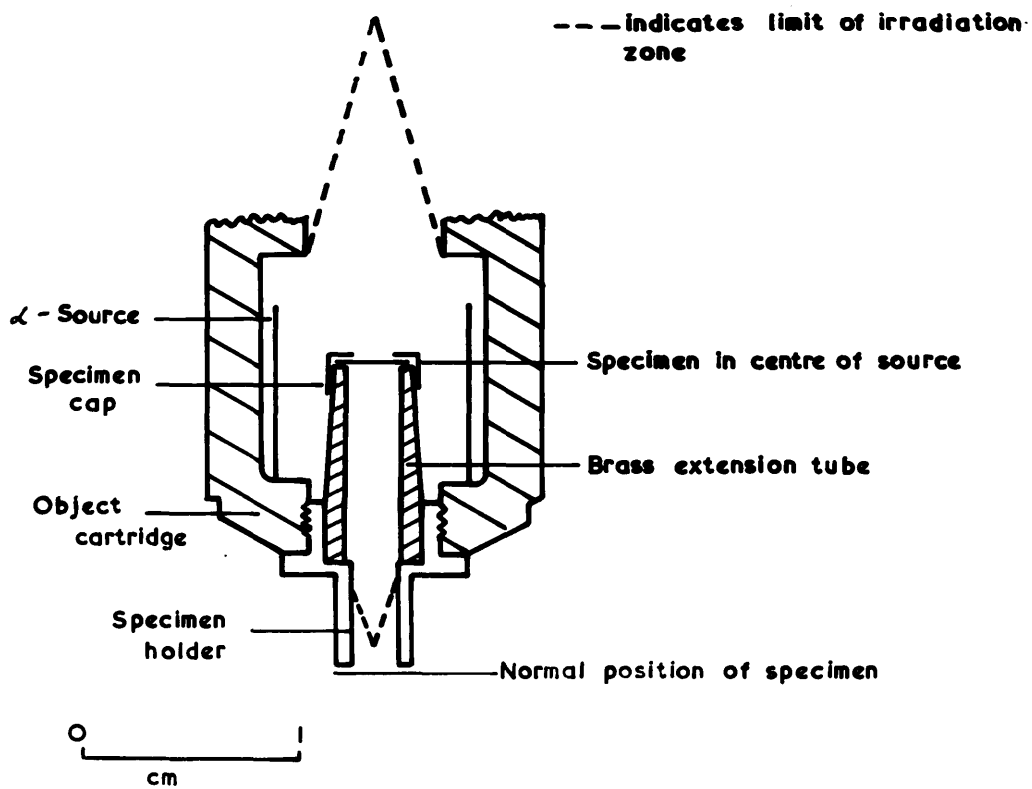


FIG. II. ILLUSTRATES THE POSITION OF SPECIMENS IN EXPERIMENTS WITHIN THE IRRADIATION ZONE OF THE SOURCE.

the specimen surface and are not distributed completely at random. The specimen is said to be "decorated" by the metal which is located at specific sites on the surfaces. The decoration technique was developed by Bassett (1958, 1960) and Bassett, Menter and Pashley (1959) who studied the decoration of rock-salt by silver and gold. Hennig (1964, 1965, 1966) applied the technique to graphite to reveal surface irregularities such as steps, dislocations and other defects.

In the present work a decoration effect was observed on the graphite specimens which were irradiated within the active zone of the α -source in an atmosphere of CO. A comparison was made between the radiation decorated graphites and similar graphites decorated with silver in the following manner. Samples of SP1, P.G.A. and neutron irradiated graphite ($4 \times 10^{20} \text{ n/cm}^2$) were prepared on silicon monoxide - coated platinum mounts as described earlier and placed on a flat surface filed on a carbon rod connected between electrodes in the Edwards coating unit. The mounts were located around a hole in the centre of the rod into which a thermocouple was placed. The specimens were heated under vacuum ($\sim 10^{-4}$ torr) to 300-350°C and then about 0.004 g of silver was evaporated from a hot tungsten wire held at 10 cm from the specimens.

From the formula $t = \frac{m}{4\pi r^2 \rho}$ (Kay 1965) where ρ = metal density, m the weight of metal and r the specimen to source distance, it was calculated that this would give a film thickness (t) of about 35 Å. After evaporation the temperature was maintained for one minute to allow decoration to occur. Prior to decoration the tungsten wire was cleaned being heated to white heat, and the carbon rod was degassed for one half hour at 500°C.

10. External Deposition

During the course of this work it became apparent that metallic carbonyls were playing an important role in the radiolysis of CO and it was decided to produce deposits in a system free from iron and nickel surfaces. The essentially all-glass vacuum system employed for this purpose is shown schematically in Fig. 12.

The most successful reaction vessel was one of design shown in Fig. 13. The metallic components were either of brass (cartridge and holder), phosphor bronze (source) or copper (glass - metal seal). Iron and nickel are possibly present in small amounts as alloying constituents or impurities. The Kovar seal was threaded to take the α -source unit, thus allowing the reaction vessel to be assembled easily.

Other vessels designed with much larger voids

FIGURE 12

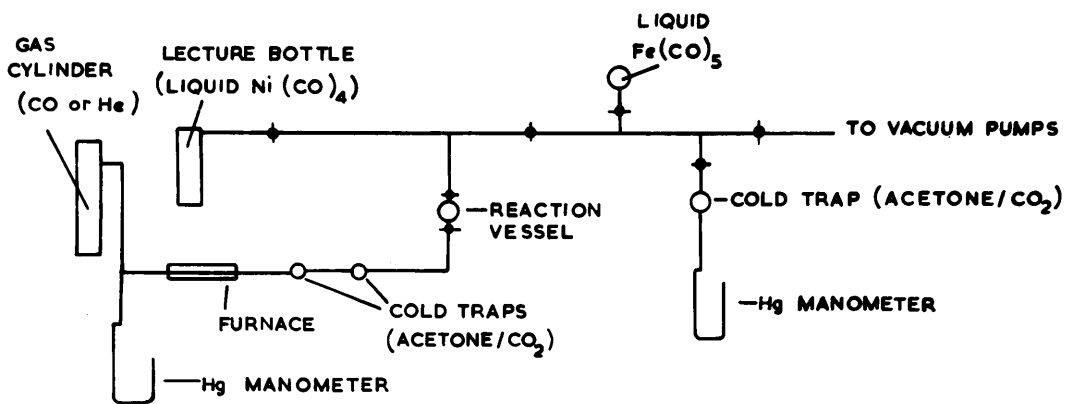
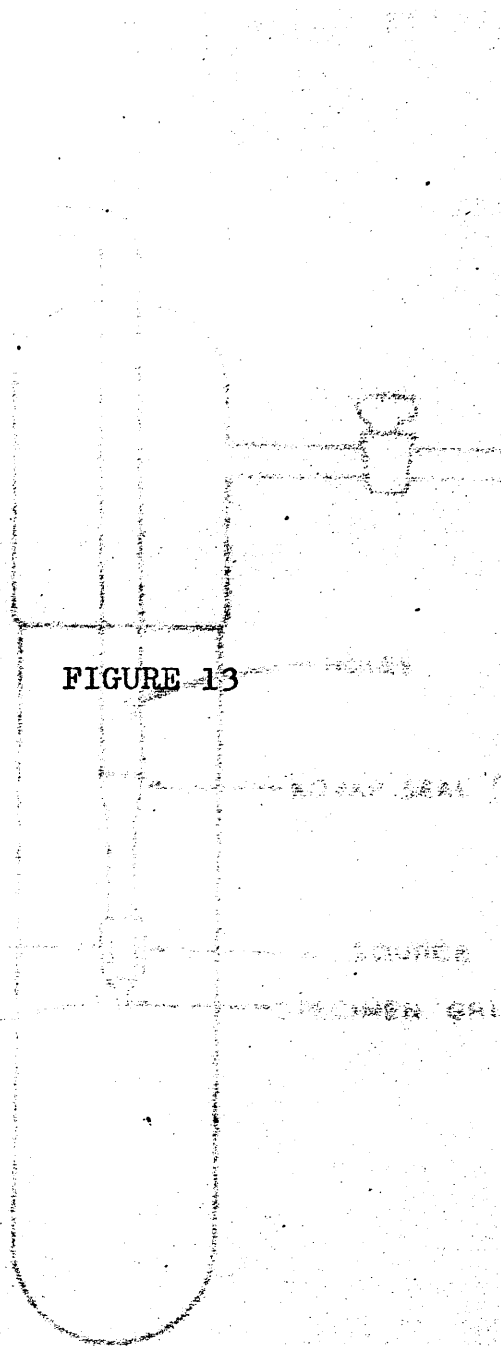


FIG 12 DIAGRAM OF RIG.



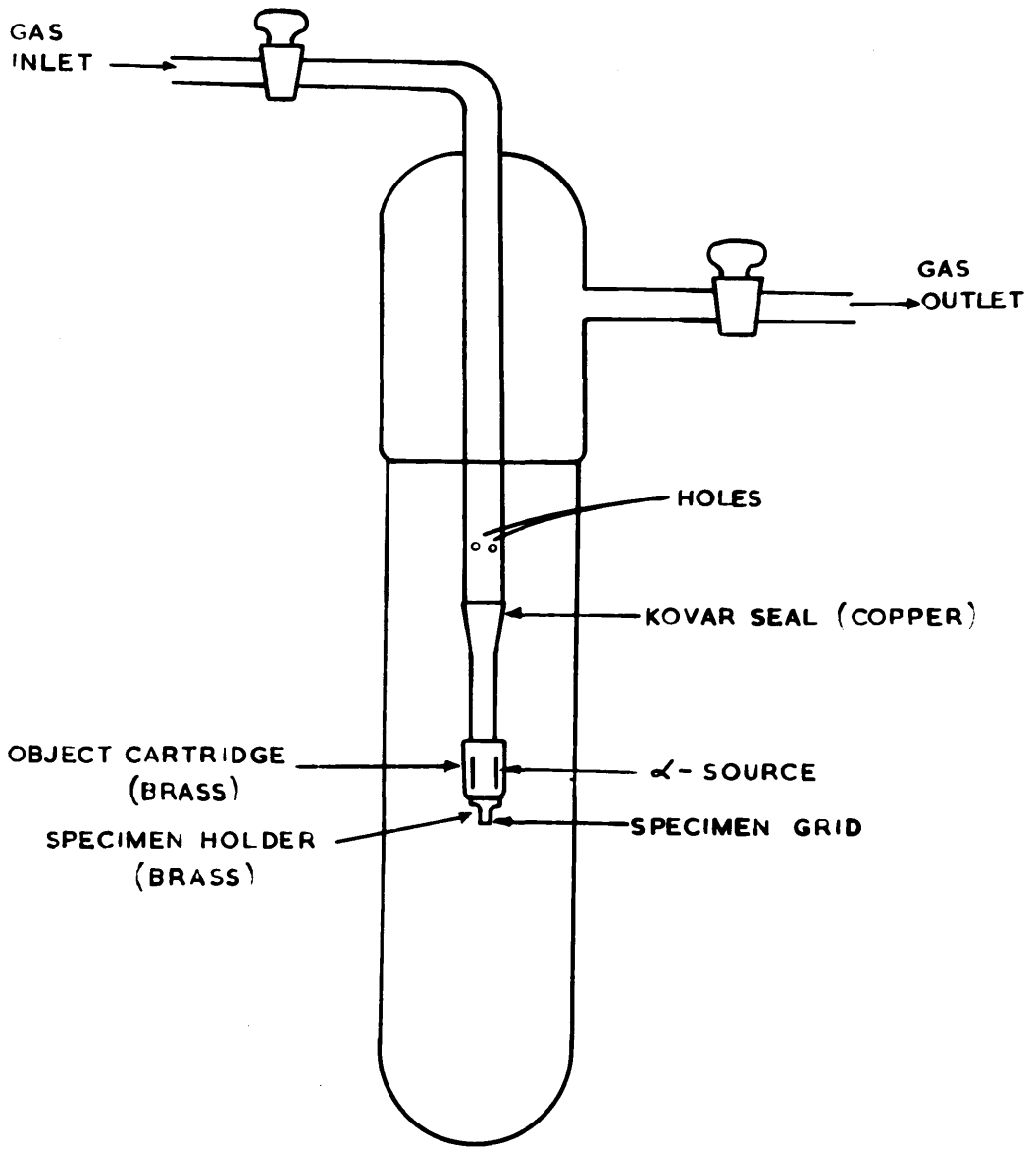


FIG.13 THE REACTION VESSEL.

adjacent to the α -source failed to produce visible deposits which were probably swept away by convection currents to other parts of the system.

The system was evacuated to a pressure of about 10^{-3} - 10^{-4} torr by means of a rotary pump and an air-cooled diffusion pump (not shown in the diagram) mounted on a mobile trolley. The system was flushed out with CO prior to filling and the required gas or gas mixture was radiolysed in the reaction vessel.

11. Proton Van de Graaff Experiments

The knowledge gained from the α -radiolytic work enabled a set of experiments to be designed in an attempt to reveal, by infrared analysis, the various functional groups in deposits formed by radiolysing CO both in the presence and in the absence of metallic carbonyl impurity. The high dose rates available with the proton Van de Graaff accelerator at Harwell, allowed sufficient deposit to be collected for the infrared work. The cell used for irradiation purposes is shown in Fig. 14. The cell was evacuated, then filled to a pressure of 40 cm Hg with the required gas, and was subjected to a 1.75 MeV proton beam for two hours at a beam current of 0.2 μ A. The total energy absorbed by the CO (\sim 34.5 ml at N.T.P.) was about 1.25×10^{22} eV taking into account the energy



FIGURE 14



CELL USED IN PROTON
EXCHANGE EXPERIMENTS

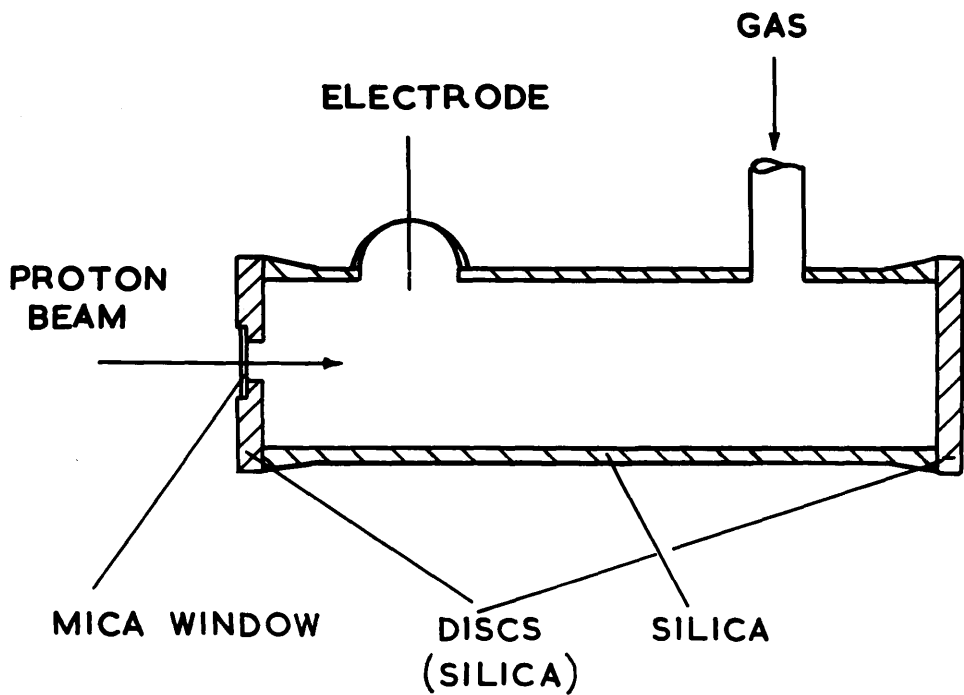


FIG.14. CELL USED IN PROTON VAN DE GRAAFF EXPERIMENTS.

loss in the mica window (Best, 1968). The solid which settled around the cell walls was scraped into a glass tube for subsequent examination.

12. Electron Microscopy

The Siemens Elmiskop I was operated at an accelerating voltage of 80 kV. The rate of contamination of the specimens was found always to be greater with the double condenser illuminating system ($1-3 \text{ \AA sec}^{-1}$) than with the single condenser system ($\sim 0.1 \text{ \AA sec}^{-1}$). This finding, together with the observed nature of the deposited material from the radiolyses favoured using the single condenser system. Images were recorded on plates at magnifications ranging from 6,000 to 80,000 times.

13. Microanalytical Techniques

Three techniques, electron diffraction, electron probe microanalysis and infrared spectroscopy, were used for the qualitative analysis of deposited material from the CO radiolyses.

(a) Electron Diffraction

By using the selected area diffraction technique described in the introduction it was possible to study the diffraction characteristics of single particles or clusters of particles since areas of about $0.5 \mu^2$ could be selected for study. Information was thus obtained about the nature

of the particles and in particular cases identification of constituent elements was achieved.

Diffraction studies were made using an accelerating voltage of 80 kV or 100 kV and from the known d-spacings of an evaporated thallic chloride standard, the camera constant and d-values for the specimen under study were calculated.

(b) Electron Probe Microanalysis

This method of analysis can detect concentrations of about 0.1 per cent of most elements in a selected one square micron area of a specimen (Birks, 1960) and was employed in the present work in an effort to gain some knowledge about the composition of the deposits from CO radiolyses. Two types of microprobe were used.

(i) Siemens X-ray Spectrometer Attachment

The attachment is shown schematically in Fig.15. A special specimen cartridge is used which necessitates operation of the microscope at an increased objective lens focal length of 7 mm (normal operation ~2 mm) and results in a deterioration of the resolution to about 100 $\overset{\circ}{\text{A}}$. This value of ~100 $\overset{\circ}{\text{A}}$ was, however, more than sufficient for viewing individual deposit particles and clusters, and areas were selected and their X-ray emission

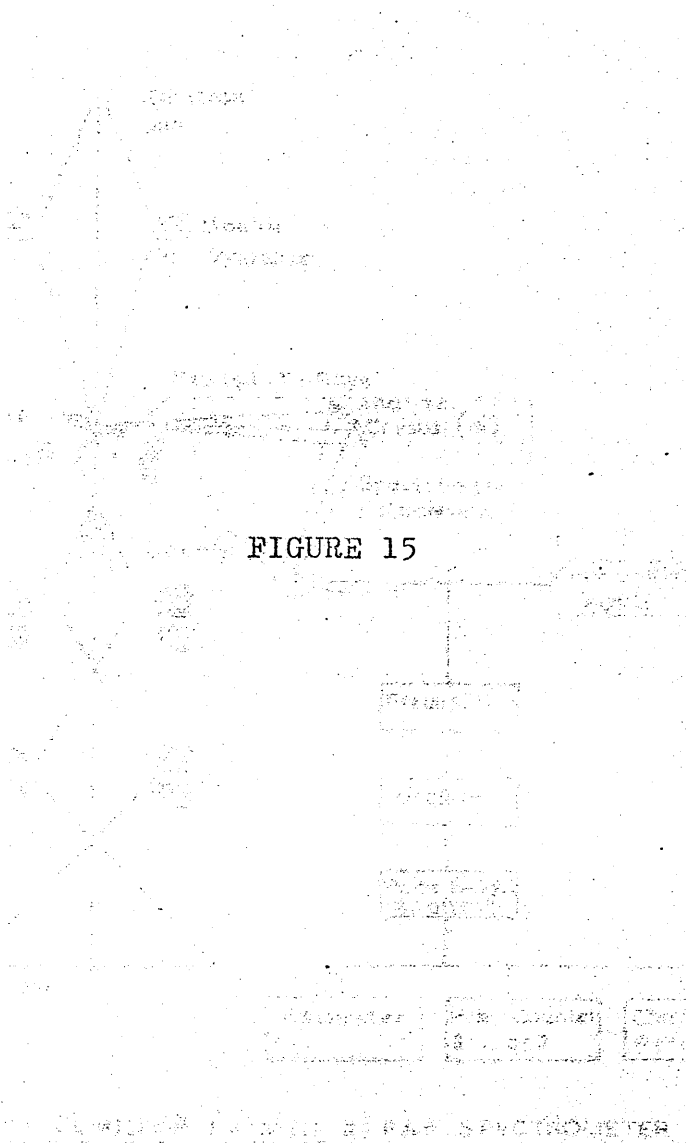


FIGURE 15

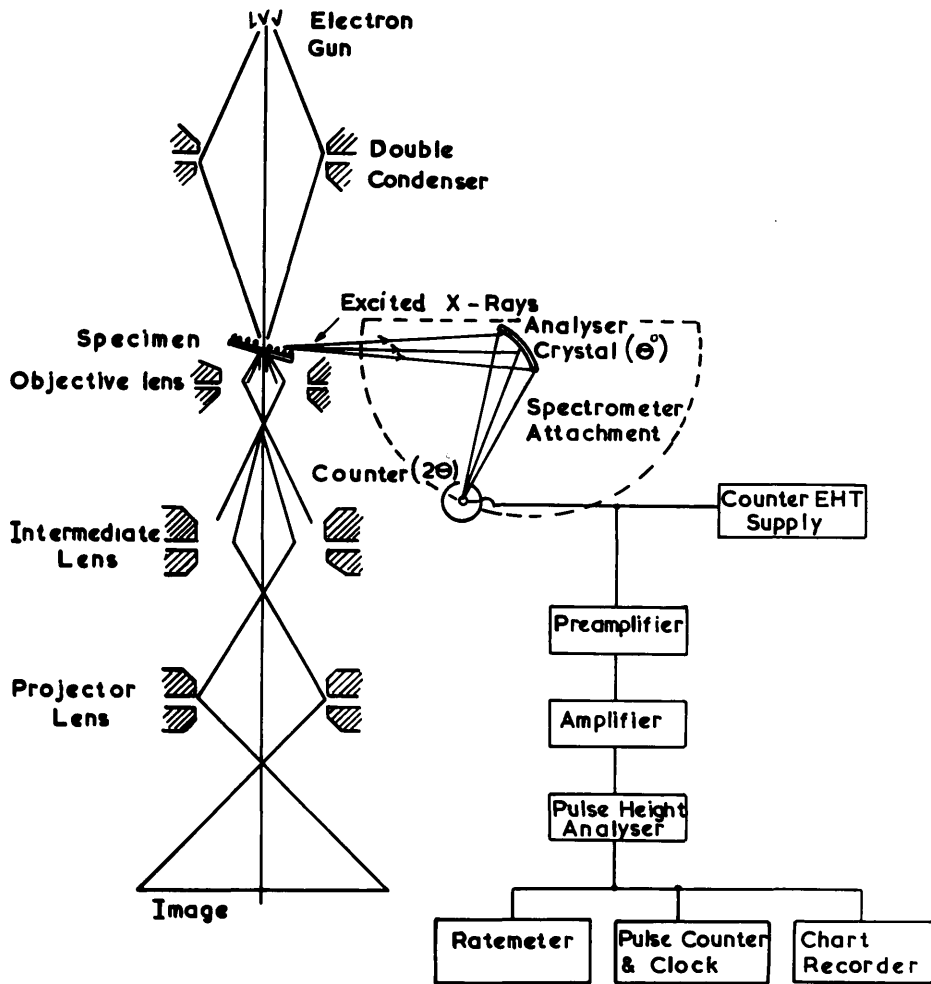


FIG. 15. SIEMENS ELMISKOP I A WITH X-RAY SPECTROMETER ATTACHMENT.

spectrum recorded on chart paper. The electrons which were transmitted through the specimen formed the normal bright field image which could be photographed as usual. The instrument is capable of detecting elements down to atomic number 12.

(ii) G.E.C. - A.E.I. S.E.M. 2

The resolving power of this instrument is about one micron ($10,000 \overset{0}{\text{Å}}$) which is not good enough to observe single particles or small clusters of deposit. The specimens were therefore examined by scanning "blind" over their surface until an emission was detected at a pre-set angle for a particular element. It is possible with this instrument to scan the electron beam probe over an area of about 250 square microns. Electron pictures can be obtained by amplifying the current induced in the specimen by the capture of electrons from the electron beam. The different currents from different elements in a specimen of mixed composition are used to modulate the brightness of a cathode ray tube and the resulting image can be recorded on film. Alternatively, the probe can be scanned across the specimen and the resulting X-ray emissions corresponding to a particular element can be shown on the cathode ray tube and recorded on film. It is also possible to scan linearly through a particular

area of the specimen, the X-ray output being continuously recorded on a chart. A high concentration of the particular element chosen for examination will result in a peak in the recorded trace through that area.

The specimens were mounted on $\frac{1}{4}$ " brass cubes using Durofix cement and were then streaked with silver paint (Degussa, g Leitsilber) or were coated with a conducting material (carbon or aluminium) to prevent charging up in the electron beam.

A special feature of this instrument is the ability to detect elements of low atomic number and this was utilised in the detection of carbon in deposits.

(c) Infrared Analysis

(i) Solids from Van de Graaff Experiments

These solids were mixed with potassium bromide and compressed into micro-discs (3 mm diameter) and were examined in a Perkin Elmer 257 Grating Infrared Spectrophotometer.

(ii) Solids from α -radiolysis of CO

Over a period of 30 days sufficient deposit was collected to allow an infrared spectrum to be run. Fig.16 shows the apparatus used to collect deposit.

Impure CO (I.C.I.) at approximately atmospheric pressure was passed through the α -source (B) and then bubbled

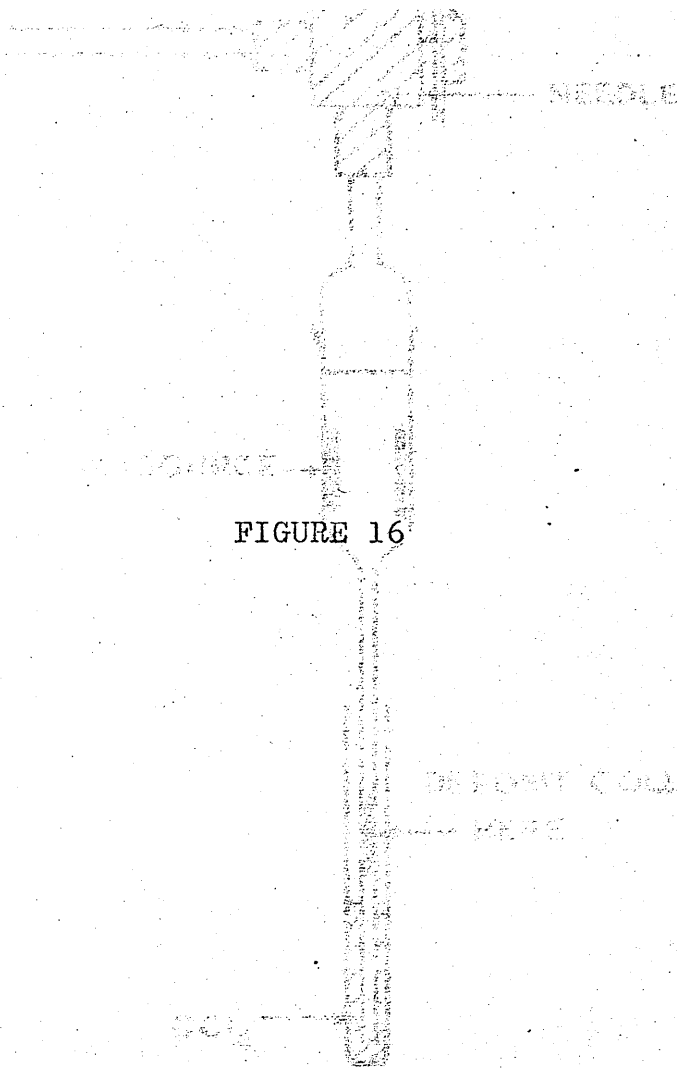


FIGURE 16

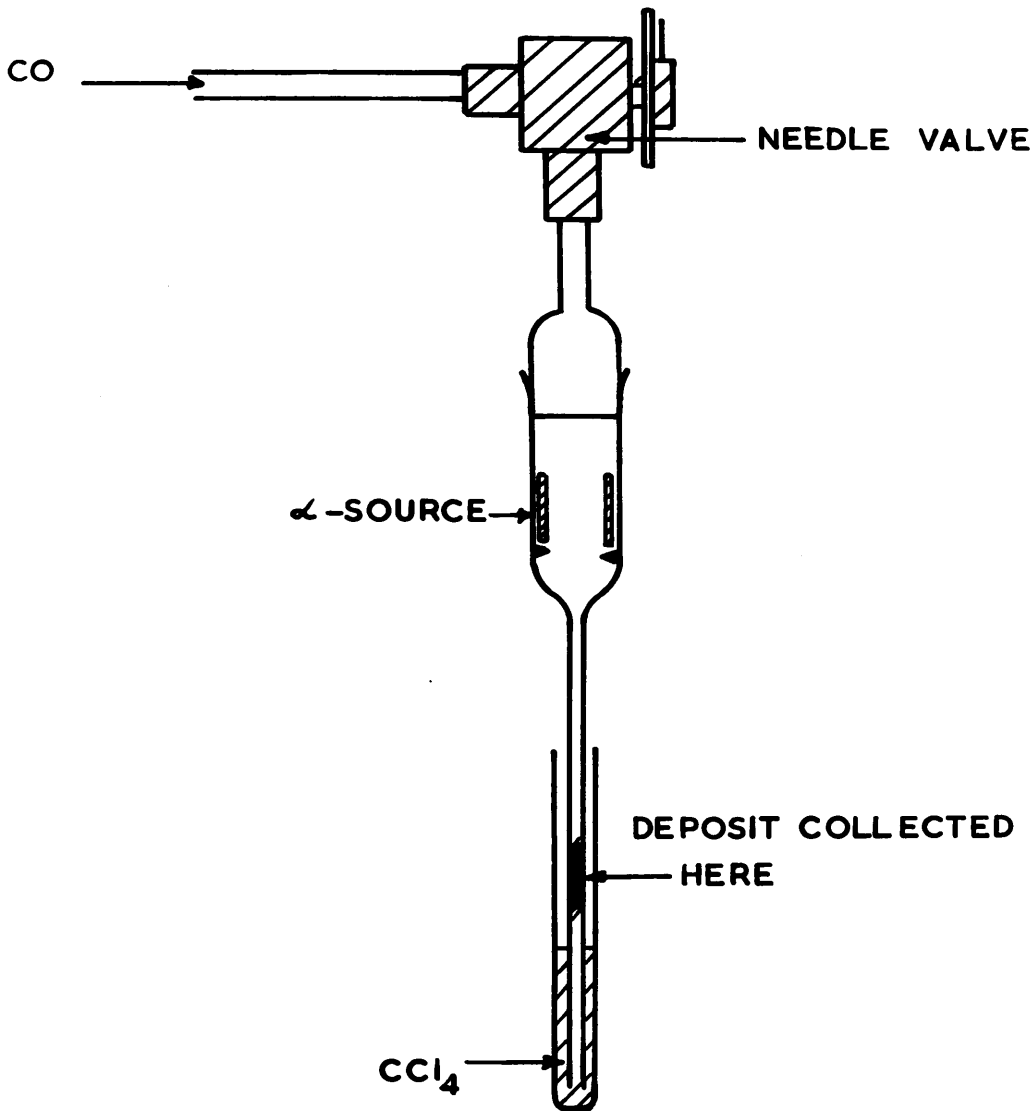


FIG. 16 GAS FLOW-BUBBLER.

into carbon tetrachloride at an arbitrary rate of about one bubble every 30 seconds. The intention was to suspend particles in CCl_4 and to use the suspension for the infrared determination. However, a solid product (~ 2 mg) collected in the capillary tube just above the level of the CCl_4 . This was removed and ground with KBr and compressed into a micro-disc (slot type, 10 x 2 mm) and examined in a Unicam SP 100 prism grating spectrophotometer.

14. Dosimetry

Measurement of the dose rate to gas from source B was made by estimating the rate of production of nitrogen from irradiated nitrous oxide. The α -source was mounted in a tightly fitting glass vessel (Fig. 17) so designed that no grease or wax was directly irradiated. The volume of gas irradiated was about 0.25 ml. Triply distilled nitrous oxide was admitted to the cell and left to be irradiated for a given time. The resulting gas was then removed and the nitrogen content estimated by gas chromatography (molecular sieve column, Linde 5A, 120°C) in a non-commercial chromatograph employing a thermal conductivity detector.

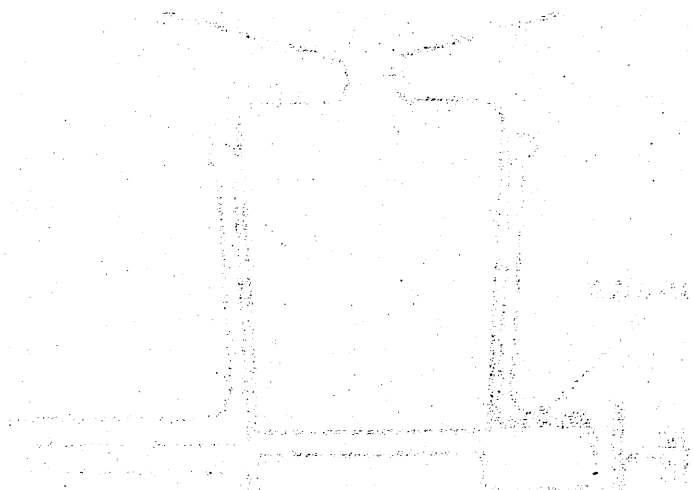


FIGURE 17

THE SCHEMATIC OF THE
 SYSTEM IS SHOWN IN
 FIGURE 17. THE
 SYSTEM IS A
 SIMPLE
 CIRCUIT
 WHICH
 IS
 USED
 TO
 MEASURE
 THE
 CHANGE
 IN
 THE
 SIGNAL
 DURING
 THE
 TEST.

THE SCHEMATIC OF THE
 SYSTEM IS SHOWN IN
 FIGURE 17. THE
 SYSTEM IS A
 SIMPLE
 CIRCUIT
 WHICH
 IS
 USED
 TO
 MEASURE
 THE
 CHANGE
 IN
 THE
 SIGNAL
 DURING
 THE
 TEST.

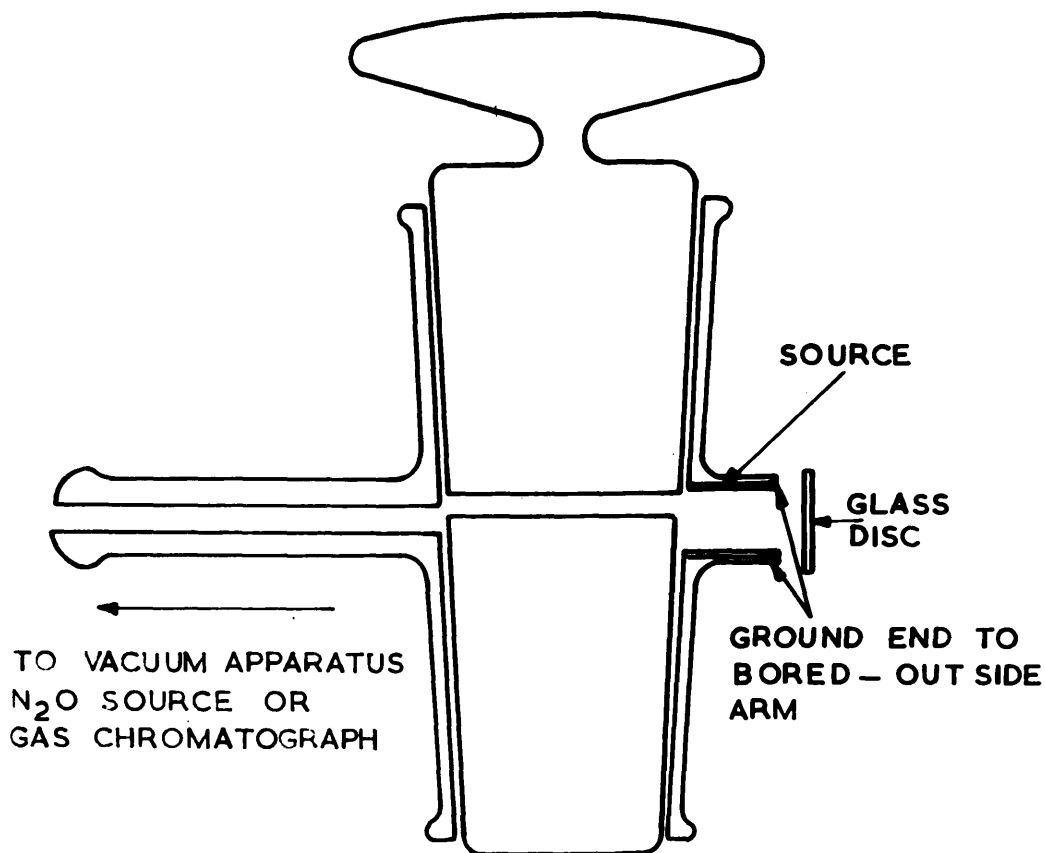


FIG.17. DIAGRAM OF CELL USED IN EXPERIMENTS
TO DETERMINE DOSE RATE TO GAS. THE DISC
WAS ATTACHED TO THE SMALL CHAMBER BY
MEANS OF VACUUM WAX AND HELD A GOOD
VACUUM OVER SEVERAL DAYS.

RESULTS

RESULTS

Contents.

	Page
1. <u>Dosimetry</u>	78
2. <u>Nature of Deposits from CO α-Radiolysis</u>	78
3. <u>Particle Size</u>	85
4. <u>Particle Density (per unit area) as a Function of Dose</u>	87
5. <u>Particle Density as a Function of Pressure</u>	89
6. <u>The Effect of Exposing Particles to the Atmosphere</u>	92
7. <u>The Effect on the Radiolysis of Varying the Gas Composition</u>	98
(a) The Effect of Methane	98
(b) The Effect of Oxygen	99
(c) The Effect of Water Vapour	110
(d) The Effect of Metallic Carbonyls	112
(i) Iron pentacarbonyl, Fe(CO) ₅	112
(ii) Nickel tetracarbonyl, Ni(CO) ₄	119
8. <u>External Deposition</u>	122
9. <u>Electron Diffraction Studies</u>	133
10. <u>Electron Probe Microanalysis</u>	159
11. <u>Experiments Within the Irradiation Zone of the α-Source</u>	165
12. <u>Proton Van de Graaff Experiments</u>	178
13. <u>Infrared Analysis</u>	180
14. <u>Electron Paramagnetic Resonance Spectra from Van de Graaff Solids</u>	187

1. Dosimetry

Nitrous oxide was irradiated by α -particles from source B for a duration of 72 hours in one experiment and 93 hours in another, at ambient temperature and a pressure of 67 cm Hg. This led to a dose rate of 1.6×10^{16} eV g⁻¹ sec⁻¹ in each case, which corresponds to 5×10^{12} eV sec⁻¹ to carbon monoxide at one atmosphere pressure within the volume (0.25 ml) of the source. It is assumed that the absorption of 100 eV by nitrous oxide leads to the production of 11.3 molecules of nitrogen, i.e. $G_{N_2} = 11.3$ (Flory, 1963).

In the present experiments then, an irradiation time of one hour is equivalent to a dose of 2.7×10^{-3} eV/molecule of CO with source B.

2. Nature of Deposits from CO α -Radiolysis

The first set of experiments was designed to find the irradiation time necessary to produce a visible deposit at a pressure of 0.2 atmospheres; no deposit was observed after 90 hours irradiation. This negative result, when considered with later positive results from 17 hours irradiation at atmospheric pressure, was useful in establishing that the deposit was in fact produced by irradiation of CO and did not arise from the source itself or from the action of α -particles on residual pump vapours and greases.

Table II gives details of experiments 1-20. In experiments 1-5, spectroscopically pure CO was used and deposits were obtained at the higher pressure of 0.4 atmospheres after 160 hours and 90 hours. In the remaining experiments cylinder CO was used at a pressure of one atmosphere thus allowing deposition times to be shortened to about 17 hours.

The physical appearance of the deposit particles on examination before exposure to the atmosphere was similar in all experiments irrespective of the grade of CO used, the irradiation time or gas pressure during radiolysis. Plates 1-3 show typical areas from experiments 5, 4 (Table II) and 24 (Table III) respectively. All particles are irregular in outline, have a loose open appearance and seem to be composed of smaller irregular sub-units. Plate 4, at a higher magnification, reveals the finer detail in the particles. In general, a fairly even distribution of single particles, aggregates and short chains of particles were observed over the entire area of the substrate (carbon film). In experiments of short duration, mainly single particles were observed, but with increase in irradiation time the number of chains appeared to increase and this was probably due to collision between particles already on the substrate and those settling out from the gas phase. The chains did not always lie flat on

the substrate and were often observed to wave about in the field of view, especially when the intensity of the electron beam was altered.

TABLE II
Details of Experiments 1-20

Gas	Expt. No.	α -source	Pressure of Gas (atm)	Time of Irradiation (hr)	Particle Density cm^{-2}	Particle size (\AA)
SPEC.-PURE CO	1	A	0.2	4	-	-
	2	"	0.2	23	-	-
	3	"	0.2	90	-	-
	4	"	0.4	160	3×10^8	$2,400 \pm 450$
	5	B	0.4	90	0.6×10^8	$2,200 \pm 500$
CYLINDER CO	7	"	1.0	17	1.5×10^8	$2,800 \pm 500$
	8	"	"	17	1.7×10^8	$2,800 \pm 600$
	9	"	"	17	1.7×10^8	$2,400 \pm 450$
	10	"	"	17	1.5×10^8	$2,400 \pm 600$
	11	"	"	64	5.4×10^8	$2,800 \pm 650$
	12	"	"	64	5.6×10^8	$2,400 \pm 550$
	13	"	"	7	0.7×10^8	$2,400 \pm 650$
	16	"	"	$4\frac{1}{2}$	4.6×10^7	$2,400 \pm 600$
	17	"	"	2	2.0×10^7	$2,600 \pm 500$
	18	"	"	1	7.0×10^6	$2,500 \pm 450$
	19	"	"	45	3.9×10^8	$2,700 \pm 550$
	20	"	"	$\frac{1}{2}$	$10^5 - 10^6$..

PLATE 1

Deposit particles from experiment 5

Magnification 50,000 X.

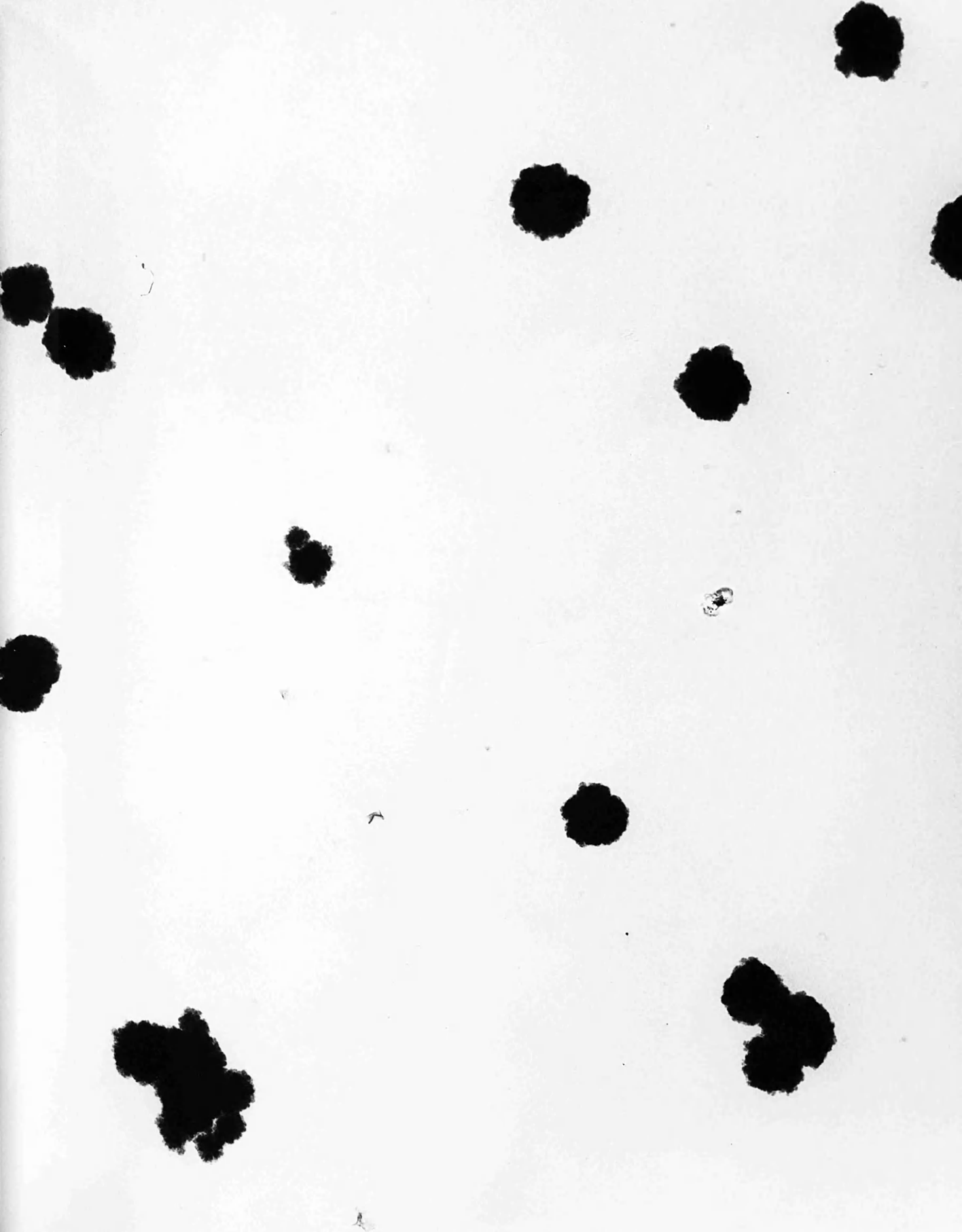


PLATE 2

Deposit particles from experiment 4.

Magnification 50,000 X.



PLATE 3

Deposit particles from experiment 24.

Magnification 50,000 X.



PLATE 4

Micrograph showing finer detail in deposit particles.

Magnification 200,000 X.



Measurements from specimens shadowed with platinum/carbon, e.g. Plate 5 (shadowed at an angle of 39°) show that the particles are not flattened in any way and that the average height corresponds to the diameter. The shape of the shadows varied from particle to particle indicating that the particles are irregular in all directions. At A in Plate 5, the parent particle has been detached from the substrate during evaporation of the shadowing material showing that the particles are rather loosely held by the film support. Care was taken in the manipulation of the electron microscope vacuum system so that particles were not swept away by violent gas currents. The best method found was to raise the specimen into the air-lock chamber immediately after radiolysis and then to pump away the radiolysed gas using the normal procedure. A two-way valve fitted to the air-lock allowed controllable pre-evacuation of the air-lock to about 1 mm Hg pressure after which the specimen was lowered back down into the microscope column for examination.

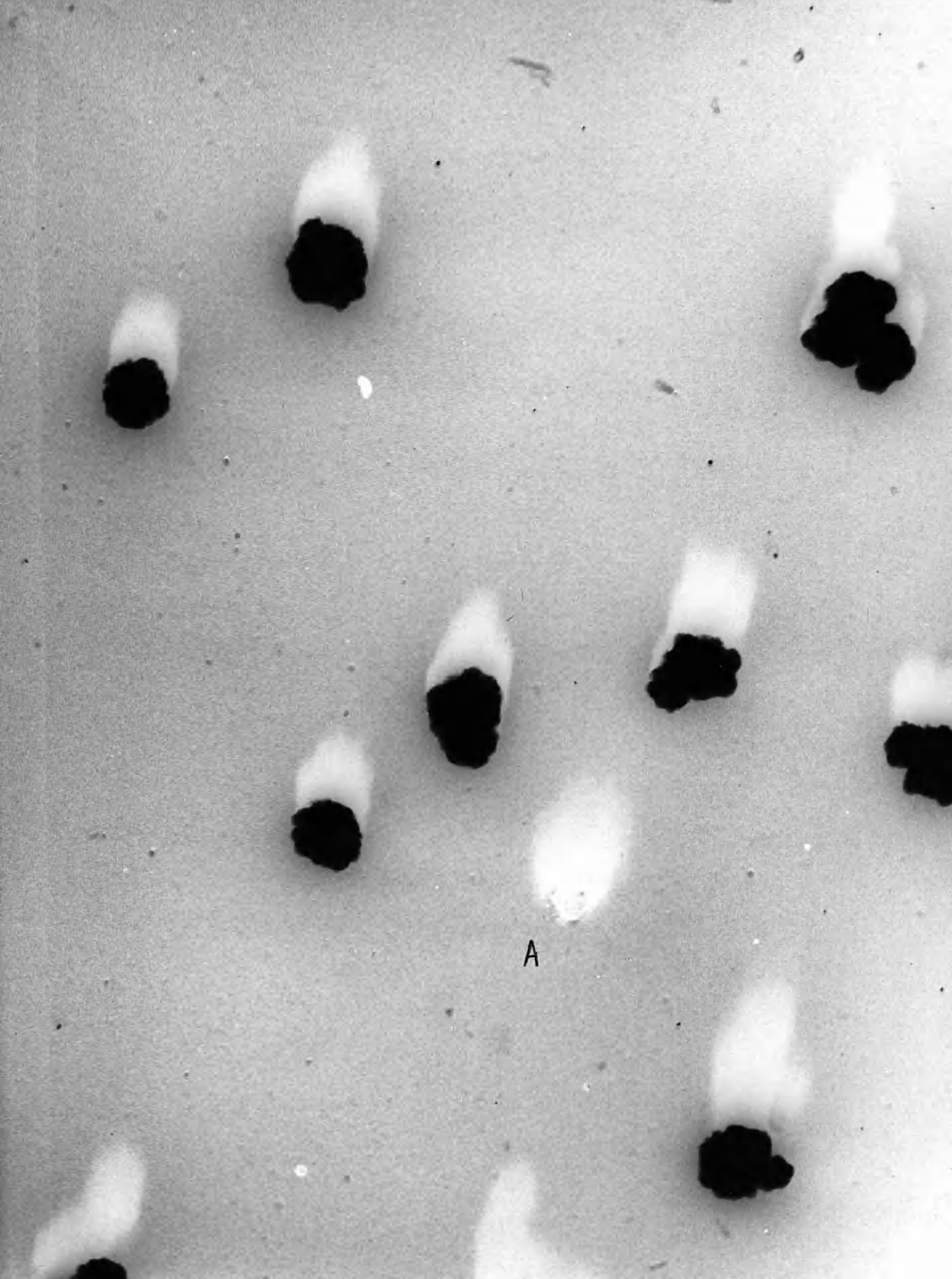
3. Particle Size

The diameter of about 150 particles was measured in each experiment from areas selected at random. The average particle diameter was found to be $2,500 \overset{\circ}{\text{A}}$ with an average deviation of $\pm 500 \overset{\circ}{\text{A}}$ and was remarkably constant throughout the series of experiments. Particle sizes

PLATE 5

Particles shadowed with platinum/carbon.

Magnification 50,000 X.



A

ranged from a lower limit of about 400 Å up to about 5,000 Å. The frequency distribution of particle diameters is shown in the histogram, Fig. 18, made from 280 measurements.

4. Particle Density (per unit area) as a Function of Dose

In order to establish a relationship between the quantities of solid material formed and the irradiation time or dose, the number of particles observed per unit area of the substrate was determined for each experiment and was used as a measure of the yield of solid. The particle density determinations were made by counting the number of particles on a given area of low magnification negative plates (x 6,000) and equating this to the density per unit area. The total area selected from a number of plates in each experiment usually contained 700-2,000 particles for counting, except in experiments of short duration when this number was fewer. The most suitable distributions for counting purposes were obtained with irradiation times between about 5 and 70 hours. Above 70 hours, counting became confused by the presence of chains and overlapping of particles whilst at the lower end of the scale the particle density determinations were less accurate because of the low numbers counted.

Experiments 7,8,9, and 11 and 12, were carried out under as near as possible identical conditions and establish

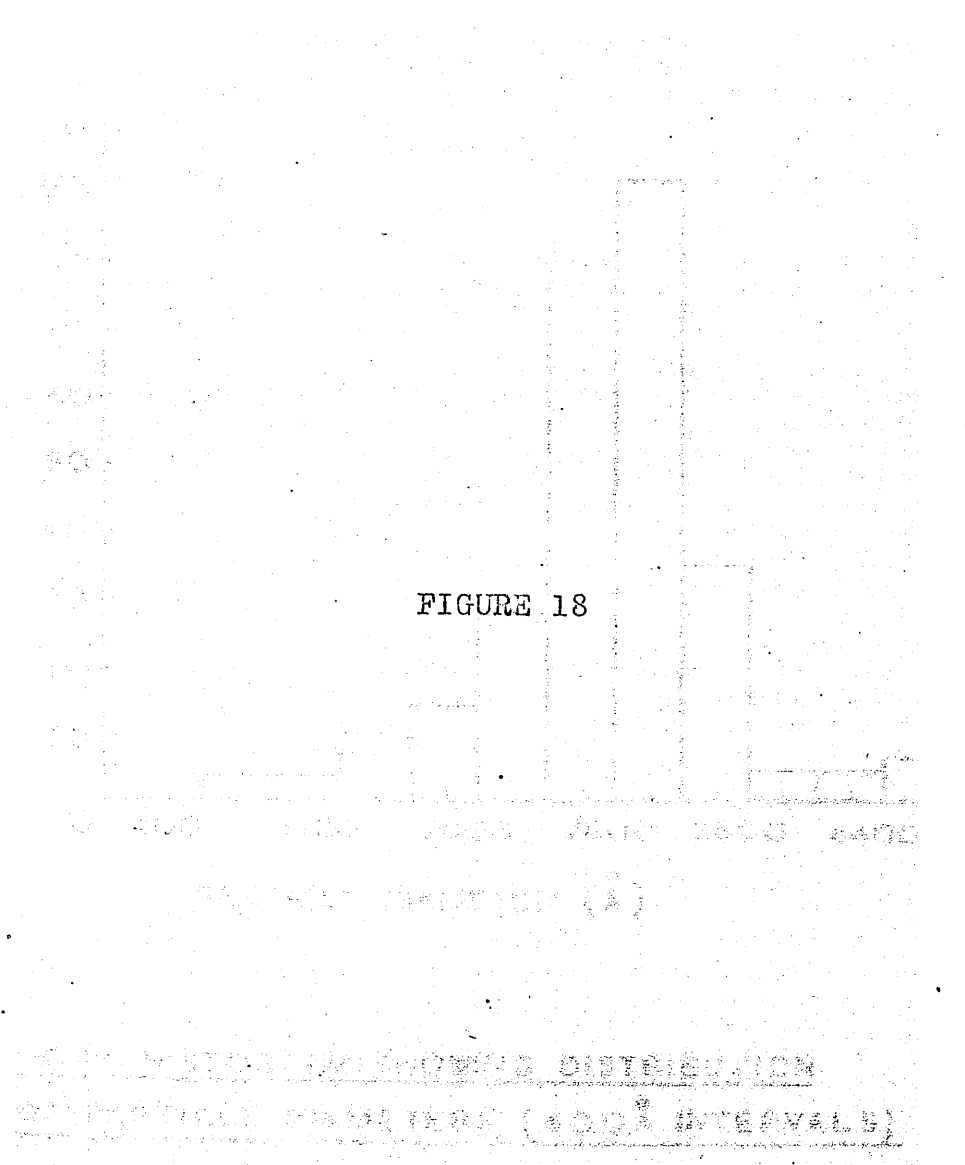


FIGURE 18

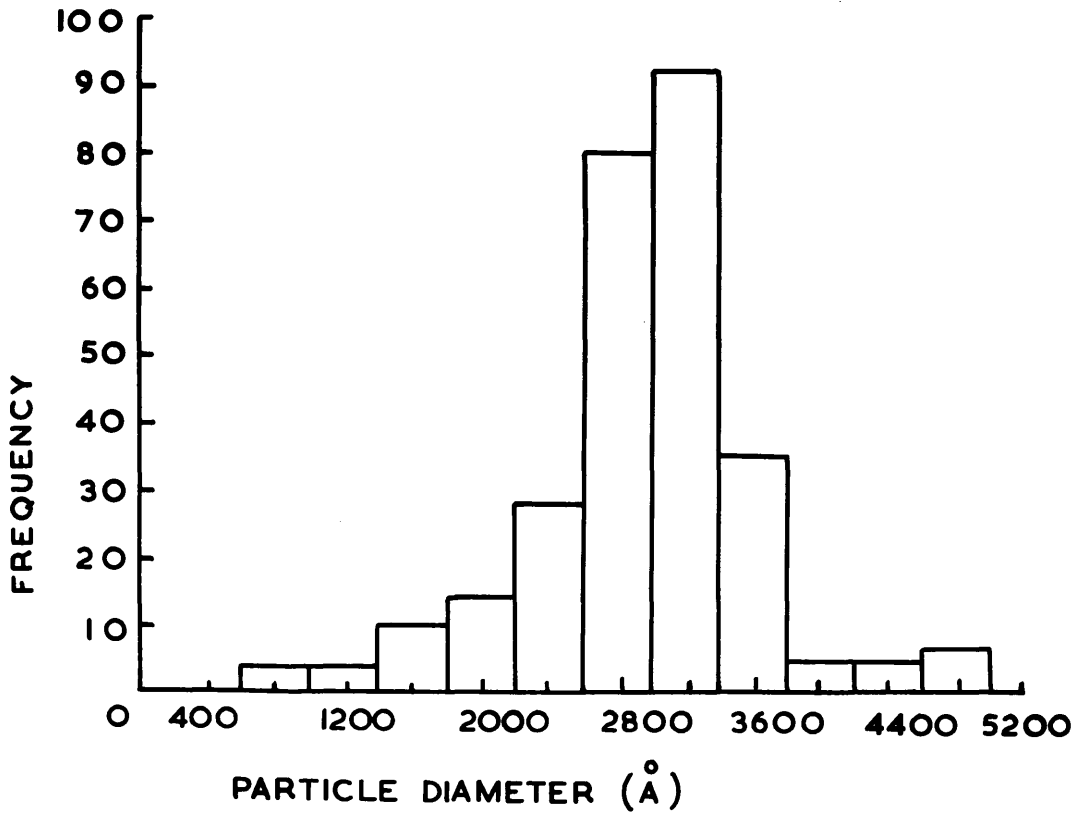


FIG. 18. HISTOGRAM SHOWING DISTRIBUTION
OF PARTICLE DIAMETERS (400 Å INTERVALS)

the reproducibility of the particle density and particle size measurements. Experiment 10 was performed with the mercury manometer removed from the vacuum line. An indication of the pressure within the microscope column was obtained by observing movement of the camera air-lock door at atmospheric pressure. From the results of experiments 7-20, a graph of particle density v. dose was drawn and is given in Fig. 19. A linear dependence is observed. With irradiation times less than one half hour no deposit particles at all were observed and it appears that this is the time necessary for particles to grow and settle out on to the specimen substrate with the particular geometry of the system. Fig. 20 shows an enlarged scale of part of the density v. dose curve from 0-7 hours.

5. Particle Density as a Function of Pressure

Table III lists results from a series of experiments conducted to investigate the dependence of particle density on pressure. Cylinder C0 was irradiated for 90 hours ($0.24 \text{ eV/molecule CO}$) in each experiment with α -source B.

FIGURE 19

.....

.....

.....

.....

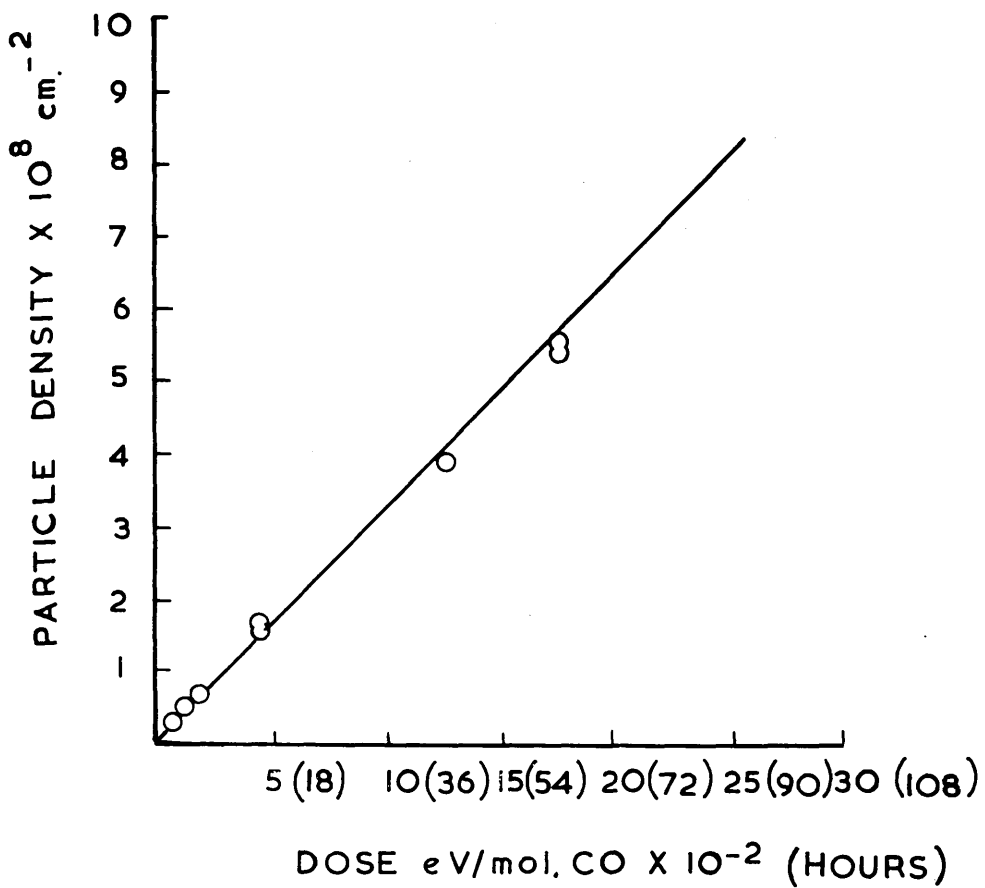


FIG. 19. GRAPH OF PARTICLE DENSITY v DOSE
FROM EXPERIMENTS (7-20) WITH CYLINDER CO

FIGURE 20

FOR SCALE (0-7 HRS) OF PAQ
DURING THE TIME SHOWN IN FIG. 18

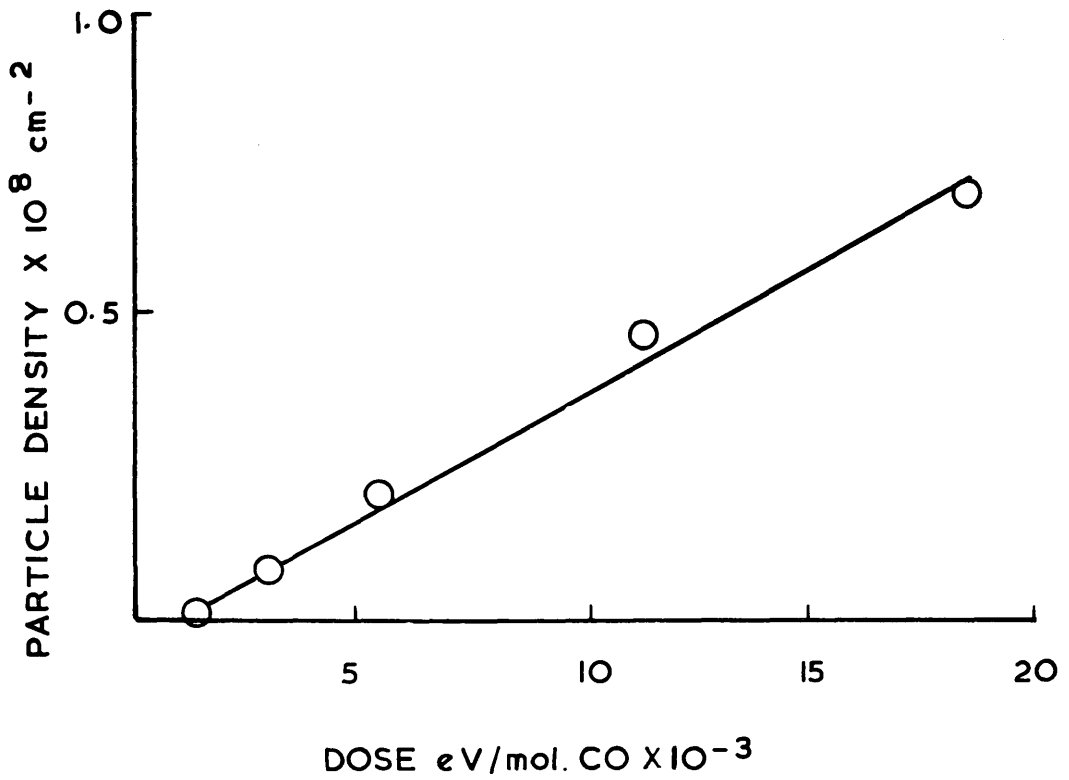


FIG. 20. LARGE SCALE (0 - 7 HRS) OF PARTICLE DENSITY v DOSE GRAPH SHOWN IN FIG. 19.

TABLE III

Data for particle density v. pressure curve

Expt. No.	Press. of CO (atm.)	Irradiation Time (hrs.)	Particle Density (cm ⁻²)	Particle Size (Å)
21	0.25	90	-	-
22	0.53	90	2.9 x 10 ⁸	2,400 ± 550
23	0.80	90	5.9 x 10 ⁸	2,500 ± 550
24	0.90	90	6.8 x 10 ⁸	2,500 ± 550
25	0.41	90	1.9 x 10 ⁸	2,500 ± 450

A graph of particle density v. pressure was drawn from the data in Table III and shows a linear relationship above a critical pressure of 0.25 atm (Fig. 21). A value of the particle density for a 90 hour exposure to radiation at 1.0 atmosphere pressure was obtained by extrapolation of the line in Fig. 19 and this point is consistent with the data of Fig. 21.

The physical appearance of deposit particles in this series of experiments was very similar to that observed in earlier experiments. The diameters were once again about 2,500 Å for all the pressures investigated.

6. The Effect of Exposing Particles to the Atmosphere

After completion of the initial electron microscope studies of the deposit particles from experiment 4, the

FIGURE 21

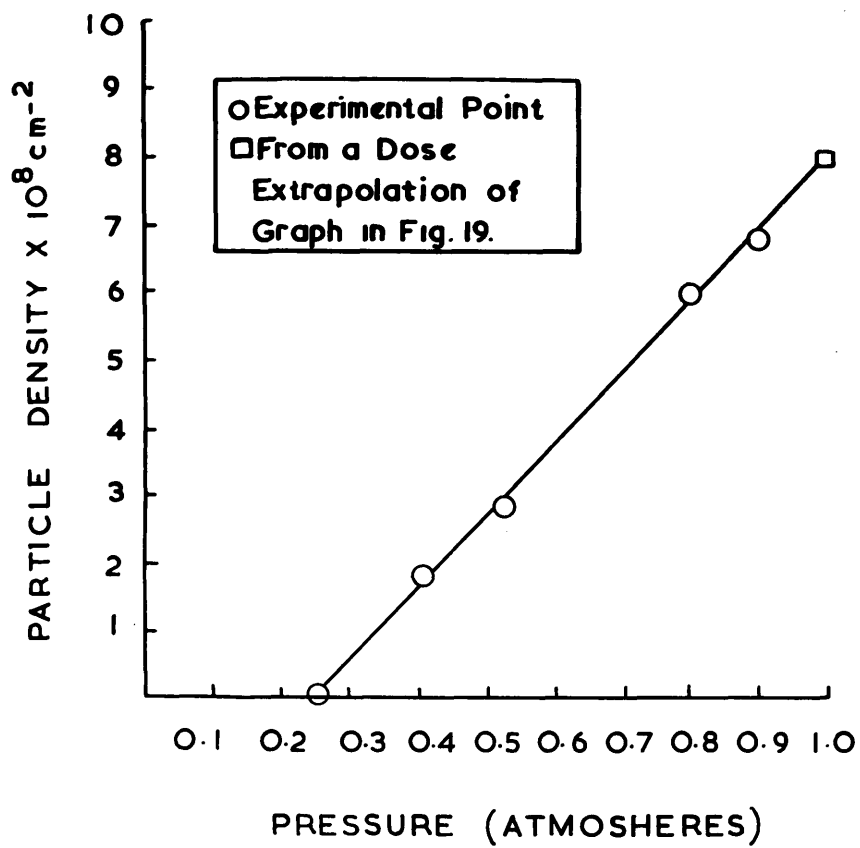


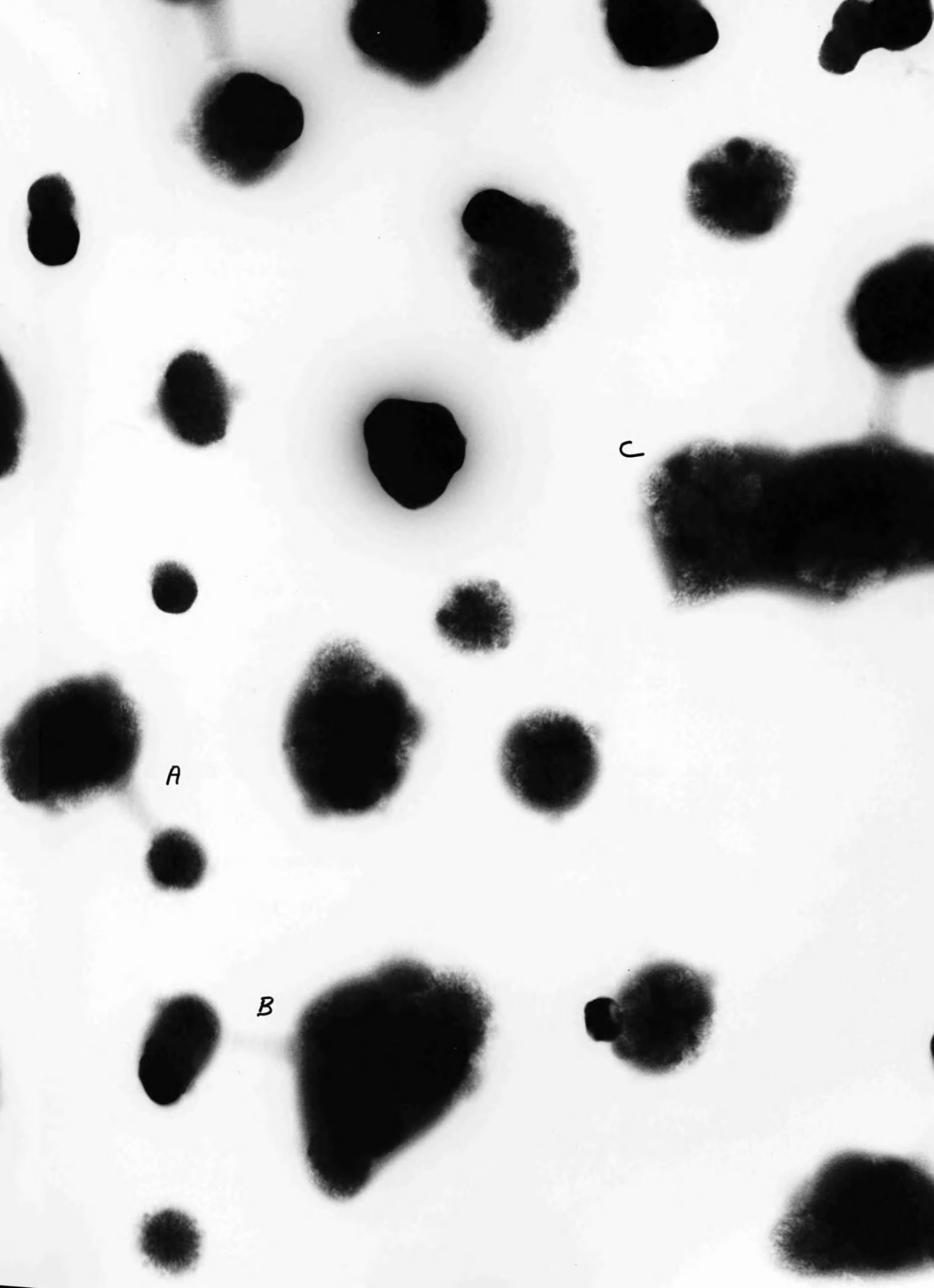
FIG. 21. GRAPH OF PARTICLE DENSITY v, GAS PRESSURE.

specimen was removed from the microscope and was exposed to the atmosphere then re-examined after two-day intervals. The appearance of some areas of the specimen after ten days exposure is shown in Plate 6. The particles which were originally irregular in outline are now much more rounded and are often joined by short necks of material such as at A and B. These new features suggest that the specimen has reacted with moisture in the atmosphere and has swollen up as a result. The bridging which has developed is obviously due to contact on swelling and subsequent shrinkage in the microscope vacuum system. Another characteristic effect observed is depicted at C, Plate 6. Here, and in many other areas, the image intensity of the particles is apparently reversed with the particle outlines appearing less dense than the surrounding material. This effect is very similar to that produced by the negative staining technique developed by Brenner and Horne (1959), in which an object of low density is embedded in a substance containing a high density element (lead acetate, for example) in order to increase the contrast between the object and the background film thus allowing the object to be distinguished more clearly. Results from later experiments do, in fact, reveal the presence of a heavy element (iron or nickel)

PLATE 6

Deposit from experiment 4 after
exposure to the atmosphere.

Magnification 50,000 X



A

B

C

in the deposits from CO α -radiolysis.. The contrast effect observed here is apparently a consequence of the drying down of the fluid material, formed on absorption of moisture, into a matrix which is more electron dense than the original "woolly" particles. Specimens from experiments 7-20 were similarly exposed to the atmosphere and re-examined at intervals. None of these specimens, however, was observed to have altered and the particles continued to have an irregular outline. Attempts to induce an effect were made by subjecting the specimens to steam for one minute or by spraying water directly on to the specimen grid but once again there was no change and the particles simply clustered together as illustrated in Plate 7 from experiment 9.

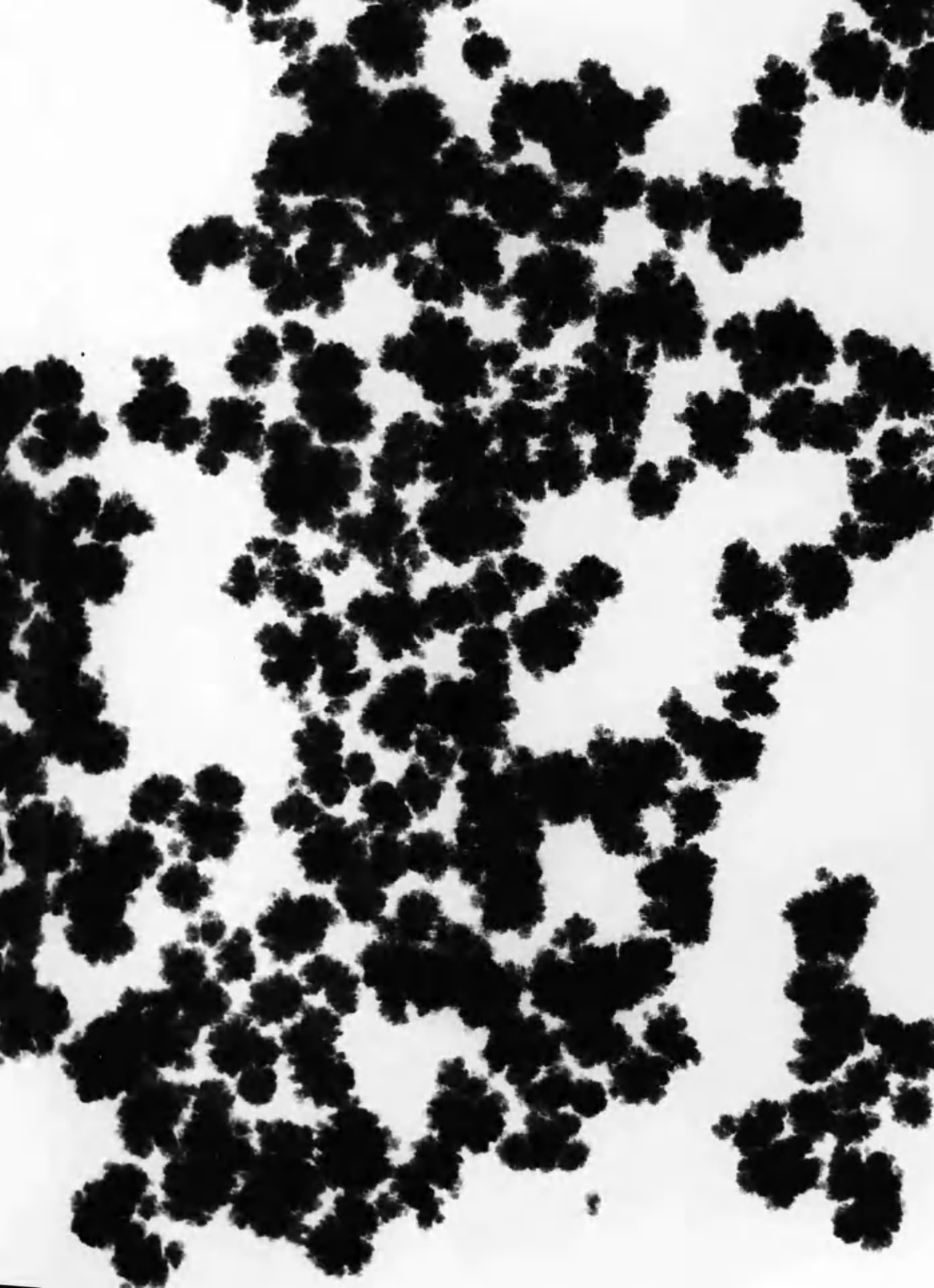
The anomalous behaviour of some areas of specimen 4 where there was no change in appearance after exposure to the atmosphere was later found to be a consequence of the effect of the electron beam on deposits and is discussed more fully later.

These initial experiments indicated that there was a difference in the fundamental behaviour of deposits towards moisture which appeared to depend on the grade of CO used during radiolysis. The use of cylinder CO (I.C.I.) seemed justified for three reasons; (a) it was less

PLATE 7

Deposit from experiment 9
after exposure to moisture.

Magnification 50,000 X



expensive; (b) it was necessary to produce deposits within a reasonable period of time (higher pressure available) and (c) the very nature of the electron microscope vacuum system where there are greased controls, numerous gaskets and vapours from photographic plates, did not allow a chemically clean system to be attained under normal working conditions. The reason for the variance in particle reactivity was obviously due to structural differences in the particles and it seemed likely that there was an impurity in the cylinder CO which was inducing a different growth mechanism from that obtained with spectroscopically pure gas. Experiments were therefore undertaken to investigate the effect of certain impurities on the α -radiolysis of CO.

7. The Effect on the Radiolysis of Varying Gas Composition

(a) The Effect of Methane

It was shown in the introductory section of this thesis that solids and liquids could be produced by the α -radiolysis of hydrocarbons. Additions of 10 % methane were therefore made to the CO in order to establish that the deposit did not arise purely from the decomposition of hydrocarbon impurities in the CO. Two experiments conducted for 18 hours and 65 hours gave particle densities of 1.5×10^8 particles cm^{-2} and 5.3×10^8 particles cm^{-2}

respectively. The good agreement between these figures and the corresponding figures for cylinder CO listed in Table III suggests that methane has little influence on the present radiolyses. The particles obtained in the presence of methane were inert towards water vapour and were similar in appearance and size to those produced from cylinder CO alone.

(b) The Effect of Oxygen

The work of Clay, Johnson and Warman (1963) and Anderson, Best and Willett (1966) showed that oxygen impurity influenced CO radiolysis and in the present work the effect of oxygen was examined. Leakage of air through the numerous joints and gaskets of the electron microscope would introduce a small amount of oxygen into the system during radiolysis so that even in experiments with spectroscopically pure gas some oxygen would be present (probably a few p.p.m.). The total amount, however, was undoubtedly much less than would be present in experiments with cylinder gas and experiments were designed to investigate the effect of varying the oxygen content. The investigation was conducted in three ways:

(1) The oxygen content of the cylinder gas was reduced by passing the CO through bright copper turnings at 450°C before admission to the microscope for radiolysis.

The procedure was to evacuate the microscope column plus the vacuum line with the tube containing the turnings, then to allow a small amount of CO into the system whilst pumping continuously. After the initial flushing out was completed the pumps were isolated and the gas was leaked slowly through the turnings into the microscope column.

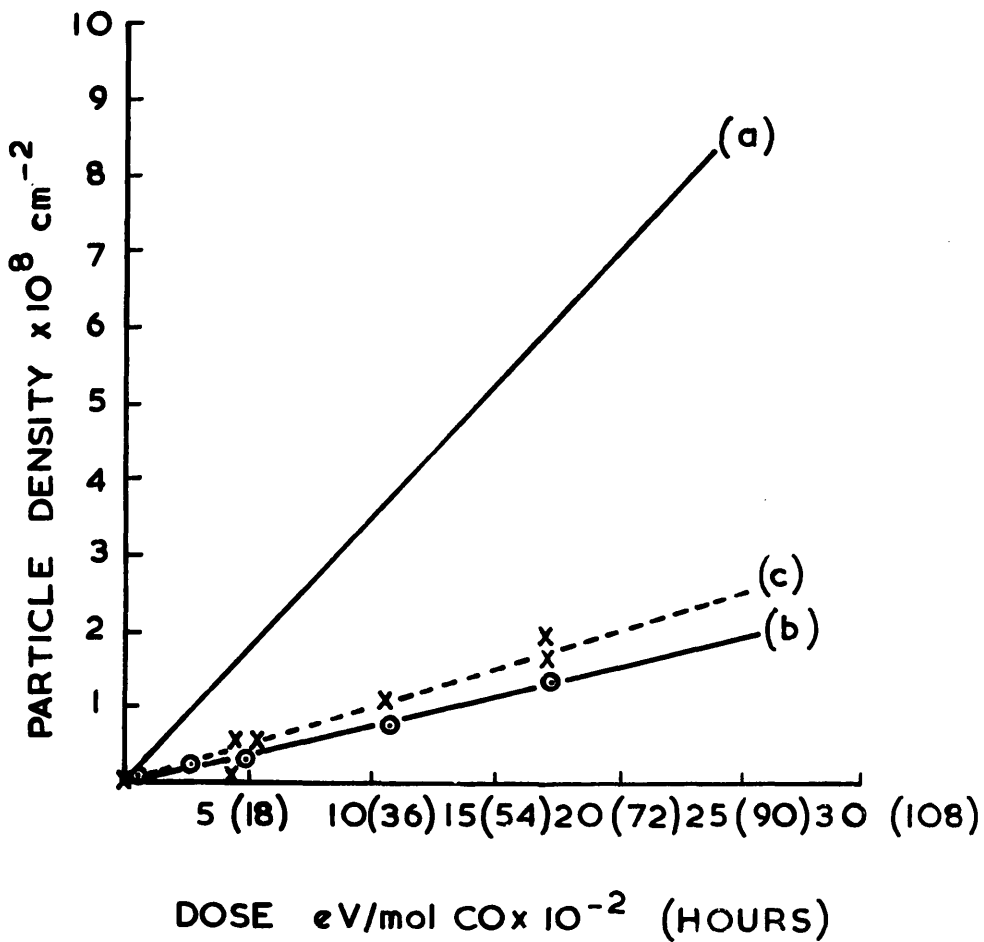
(2) Radiolyses were performed with cylinder CO to which oxygen was added from another cylinder connected to the vacuum line (Fig. 8).

(3) Any effect on the radiolysis caused by a reduction in oxygen content would be expected to be reversed if oxygen was added to purified gas. Since the purification process (1) was found to induce changes in deposit behaviour, additions of oxygen to purified CO were made in order to confirm or refute the influential role of oxygen impurity in these experiments.

Results of (1): The particle densities were determined (Table IV) for each experiment in which CO was purified by passage through hot copper turnings. The density v. dose graph from this data is shown in Fig. 22 (line (b)). The upper line (a) represents the results from the earlier experiments with cylinder CO and it is seen that about a four-fold reduction in yield of deposit is obtained after purification.

FIGURE 22

... (7.1) ... (10) ...
... (10) ...
... UNDER CO ...
... UNDER CO AFTER PASSING THRU ...
... PEAK ... AT 350°C ...
... UNDER CO FROM HANV ...



- (a) CYLINDER CO.
- (b) CYLINDER CO AFTER PASSING THROUGH COPPER TURNINGS AT 450°C
- (c) PURIFIED CYLINDER CO FROM HARWELL.

FIG. 22. PARTICLE DENSITY V. DOSE GRAPHS FOR VARIOUS GRADES OF CO.

TABLE IV

Experiments with purified cylinder CO (I.C.I.)

Expt. No.	Irradiation Time (hrs.)	Particle Density (cm ⁻²)	Particle Size (Å)
25	65	1.4 x 10 ⁸	2,100 ± 450
37	40	8 x 10 ⁷	-
38	10	2.5 x 10 ⁷	-
39	1½	0.8 x 10 ⁷	-
40	18	3 x 10 ⁷	-

Another set of experiments (Table V) with cylinder CO which had been purified at Harwell (oxygen content ~50 v.p.m.) gave particle counts close to line (b) - the density/dose relationship for this gas is given by line (c), Fig. 22.

TABLE V

Experiments with purified CO from Harwell

Expt. No.	Irradiation Time (hrs.)	Particle Density (cm ⁻²)
43	17	6 x 10 ⁷
44	65	1.6 x 10 ⁸
45	17	2 x 10 ⁷
46	20	6 x 10 ⁷
47	65	1.9 x 10 ⁸
52	40	1 x 10 ⁸
54	1	-

In addition to the drop in yield found in both sets of experiments with purified gas it was observed that the particles changed appearance after exposure to the atmosphere and in this way resembled the deposits obtained earlier from spectroscopically pure gas.

This method of producing reactive particles allowed more detailed studies to be made of the effect of water vapour. The reaction process was found to be a progressive one and it was possible to obtain an immediate change in particle appearance by spraying liquid water on to deposits or to obtain only partial reaction by leaving specimens in a closed vessel for several hours. Plate 8 shows an area where reaction with moisture has commenced and Plate 9 an area where reaction has progressed further. Several areas which were photographed and then relocated after exposure to moisture showed no change in appearance and it was then realised that electron beam irradiation of the deposit rendered it inactive. Re-examination of selected areas showed no reaction, but on moving across the specimen grid away from the irradiated spot ($\sim 50\mu$ diameter) a gradual increase in reactivity was observed. This effect of the electron beam explained the anomalous behaviour of deposits from experiment 4 where only certain areas had reacted. All areas of a specimen were found to react if they

PLATE 8

Particles which have absorbed moisture.

Magnification 50,000 X

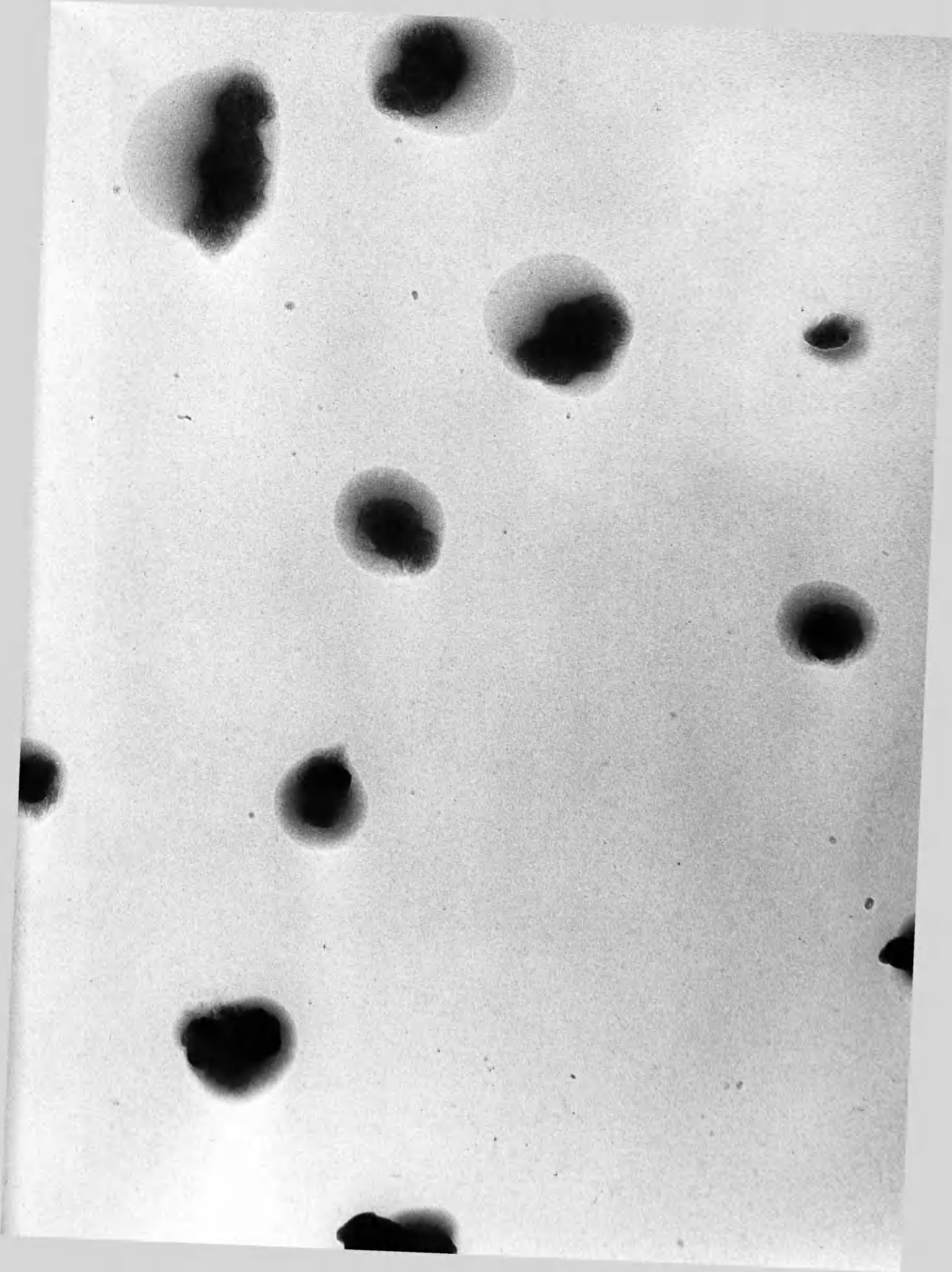
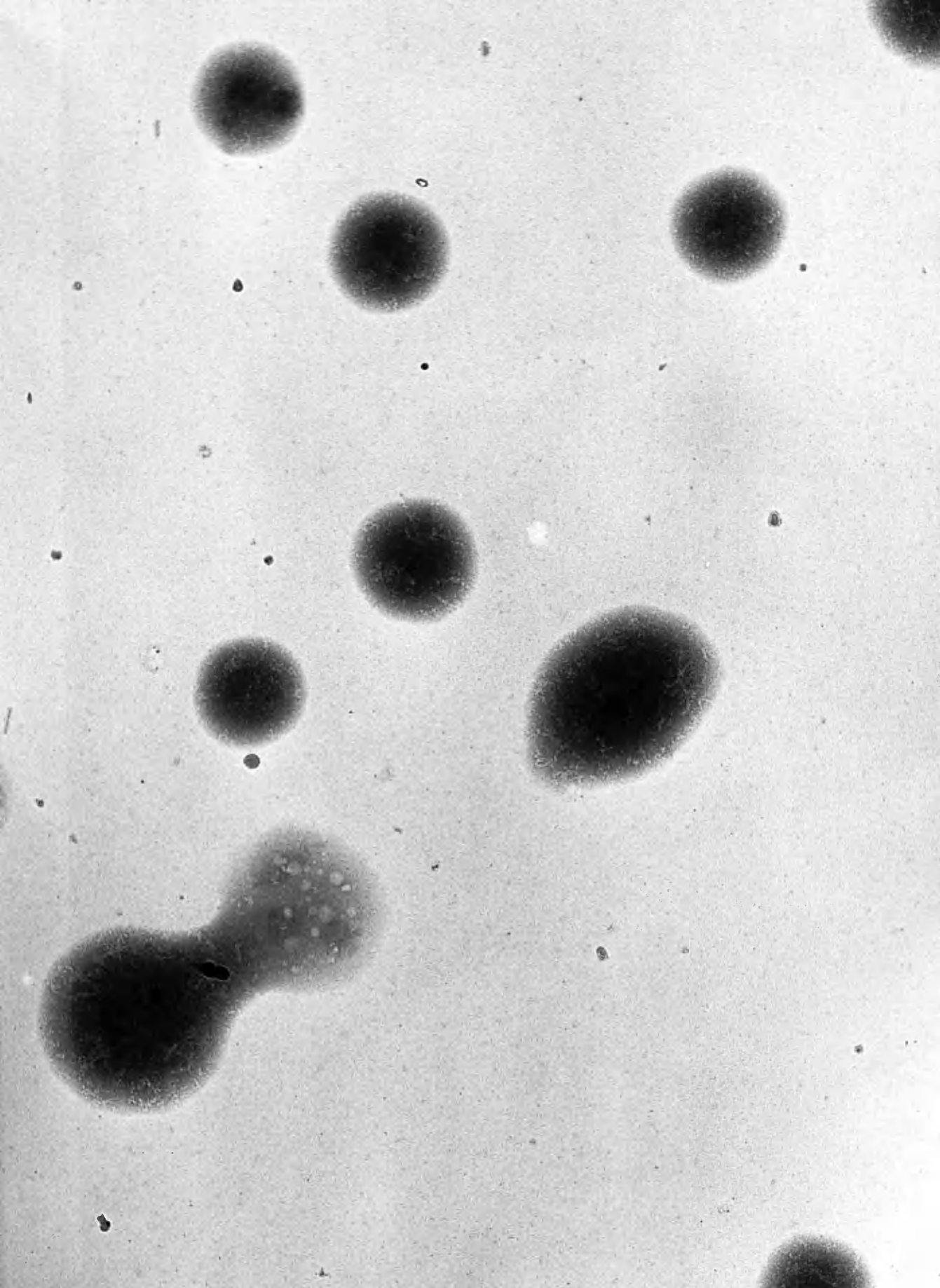


PLATE 9

Particles exhibiting a higher degree of moisture
absorption than depicted in Plate 8.

Magnification 50,000 X



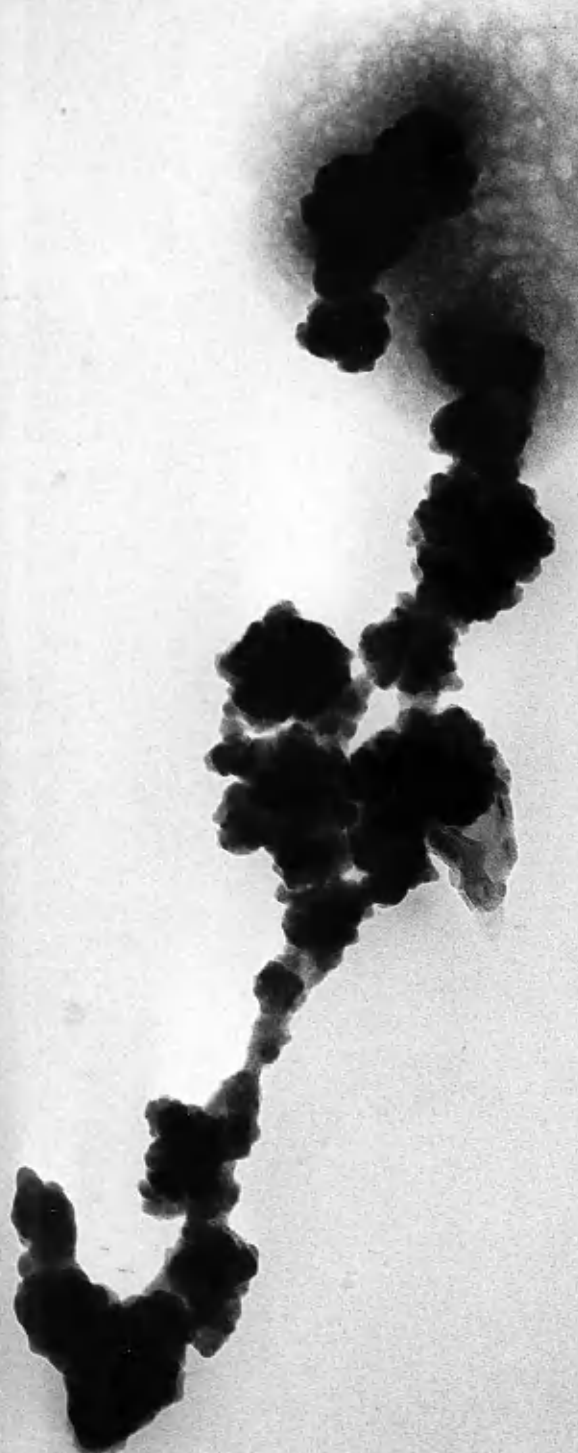
were not previously examined. The particles appear to absorb moisture and become liquid or semi-liquid and thereafter the fluid is apparently drawn down on to the substrate at points where the particles touch the film support. Plate 10 suggests that a surface tension action is operating at A where the chain of particles is pinned to the substrate, and similarly at B and C. In Plate 11 a fold in the carbon film support, caused by the drying out and shrinkage of the fluid, has resulted in movement of fluid along the length of the fold.

Results of (2). Two experiments were performed in which ~ 1 % of oxygen were added to the cylinder C0 prior to radiolysis. In both these experiments the deposits remained unchanged after exposure to the atmosphere and the particle densities were close to line (a), Fig. 22, i.e. excess oxygen did not appear to affect the radiolysis significantly. The experiment with 10 % oxygen (65 hours) gave a particle density of $4.8 \times 10^8 \text{ cm}^{-2}$ which is near the expected value of $5.1 \times 10^8 \text{ cm}^{-2}$ for untreated cylinder C0 at a pressure of 0.9 atmospheres. The yield from a 17 hour irradiation was 1.4×10^8 particles cm^{-2} and this is again close to the value of $1.6 \times 10^8 \text{ cm}^{-2}$ expected from cylinder C0 after an equivalent radiation dose.

PLATE 10

Electron micrograph showing bridging
between particles.

Magnification 100,000 X



A

B

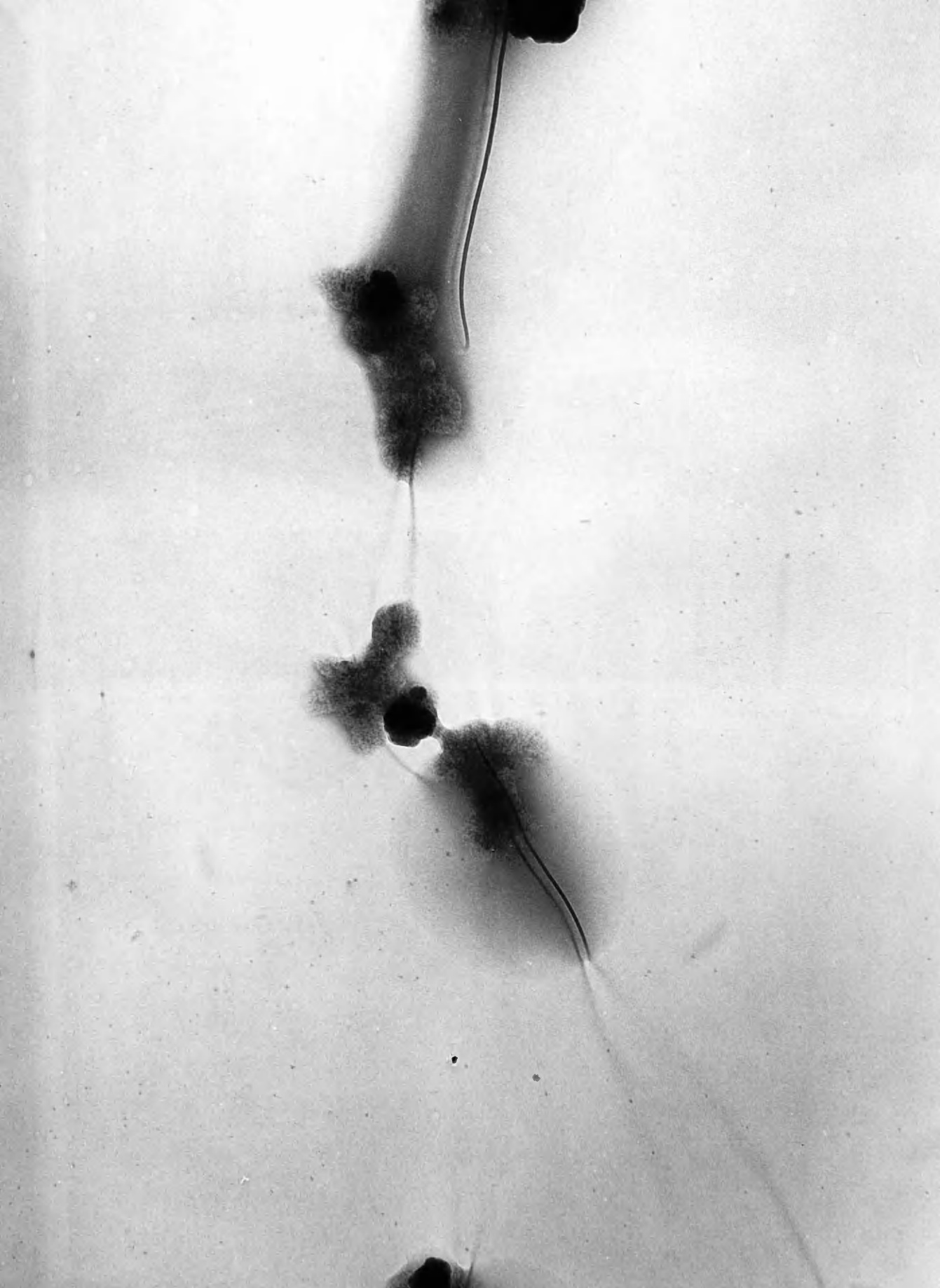
C



PLATE 11

This plate shows particles which have reacted with moisture. The resulting material has been drawn along folds in the support film.

Magnification 100,000 X



Results of (3). Table VI gives details of the experiments where oxygen was added to CO purified by passage through hot copper turnings and to the purified gas from Harwell.

TABLE VI
Purified CO/O₂ experiments

Experiment No.	49	50	53	65
Irradiation Time (hrs.)	65	17	65	65
Gas Mixture	CO(Harwell) +0.1 % O ₂	CO(Harwell) +0.8 % O ₂	CO(Harwell) +8 % O ₂	CO(over Cu) +0.8 % O ₂
Particle Density cm ⁻²	1.5 x 10 ⁸	0.4 x 10 ⁸	0.4 x 10 ⁸	0.5 x 10 ⁸
Particle Density with cyl. CO (I.C.I.)	5.5 x 10 ⁸	1.6 x 10 ⁸	5.5 x 10 ⁸	5.5 x 10 ⁸
Particle Density with purified CO	1.6 x 10 ⁸	0.5 x 10 ⁸	1.6 x 10 ⁸	1.6 x 10 ⁸

The results show that there is not an increase in the particle densities to values along line (a) in Fig. 22, as would be expected if oxygen was the impurity influencing these depositions, but show rather that the values are closer to those obtained with purified gas. In addition, all the deposits were found to be reactive from the CO/O₂ mixtures and thus resembled those from a pure gas. These results

therefore strongly indicate that oxygen is not the impurity effecting the significant changes in deposit reactivity and yield observed in the present experiments.

The particle densities in this set of experiments were generally even lower than those from equivalent experiments with purified gas; lowering of the yield is attributed to the oxygen additions and is discussed more fully later.

(c) The Effect of Water Vapour. Water vapour was added to purified CO (Harwell type) in order to observe any changes in the yields or deposit reactivity induced by radiolysing wet CO. Additions were made by allowing a known volume of liquid water to evaporate into the system from a flask connected to a side-arm in the vacuum line (at A, Fig. 8).

In the first experiment 0.1 ml of water was evaporated this being equivalent to about 1 v/o water vapour within the total volume of the system. The pressure was made up to one atmosphere with CO and the radiolysis was allowed to proceed for 18 hours. On examination, after pumping away the radiolysed gas mixture, the particles did not appear to differ in any way from those obtained with drier CO. Re-examination after exposure to the atmosphere for 24 hours showed that the particles in areas not previously viewed had reacted with or absorbed moisture whereas the particles in areas which had been previously irradiated by the electron

beam had not changed in appearance. The deposit from this experiment thus behaved in a similar manner to that from a drier gas. The particle density, determined by the usual method, was found to be 4×10^7 particles cm^{-2} which corresponds closely to the value of $5 \times 10^7 \text{ cm}^{-2}$ obtained with purified gases and inferring that the water vapour is not affecting the radiolysis.

In a second experiment 1.0 ml (~ 10 v/o) of water was evaporated into the system prior to radiolysis. The pressure registered in the manometer showed, however, that only 2-3 v/o of water remained as vapour after addition of the CO and it seemed likely that water was condensing on to the cold interior metallic surfaces of the microscope column. The long time found necessary to evacuate the microscope after deposition substantiated this suggestion. The CO in this experiment was therefore saturated with water vapour. Direct examination of the deposit which was produced showed that it had partially reacted with the water vapour in the CO after deposition or during deposition. Subsequent exposure to the atmosphere effected further reaction. It was not possible to obtain an accurate particle count due to the absorption effect but the yield was certainly not any greater than that expected from a dry purified gas.

The results of these two experiments indicate that water vapour does not significantly alter the deposition pattern

of the radiolysis in the present work except in causing premature absorption. No further experiments with wet CO were conducted since internal surfaces of the microscope, particularly the pole-piece systems, are readily damaged by water.

(d) The Effect of Metallic Carbonyls

(i) Iron pentacarbonyl, Fe(CO)₅

It is well known that iron pentacarbonyl is often present in steel cylinders of CO stored at room temperature and ~ 100 atmospheres (Newitt, 1940). The amount of carbonyl can vary from cylinder to cylinder. The cylinder of CO (I.C.I.) used in the present work was therefore a potential source of carbonyl and it became apparent that iron pentacarbonyl was possibly the impurity which effected the marked differences in yields and deposit reactivity in the present work, because (i) the de-oxygenation process could also effectively decompose the carbonyl and (ii) oxygen and water vapour had not been shown to affect the α -radiolysis significantly.

In order to test the probability of iron carbonyl decomposition in the existing apparatus, a silicon monoxide-coated platinum/iridium specimen mount was inserted into the tube containing the copper turnings and was examined in the electron microscope after the normal de-oxygenation

process had been completed. Plate 12 illustrates the nature of the crystalline material which was found to be deposited on to the specimen mount. The inset in Plate 12 shows the diffraction pattern given by the material. Measurements were made and are listed in Table VII. The derived d-values correspond with those of iron oxide, Fe_3O_4 , and show that it is highly probable that carbonyl is present in the cylinder of CO used and is decomposed in the purification process.

TABLE VII

Measurements from crystalline material

deposited on to specimen mount

(Camera constant from $\text{TiCl}_3 = 40.68$)

<u>Ring dia. (mm)</u>	<u>d-value (Å)</u>	<u>Literature values for Fe_3O_4 (A.S.T.M. Index)</u>
8.40	4.82	4.85
13.65	* 2.98	2.97
16.30	* 2.50	* 2.53
16.90	* 2.40	2.42
19.60	2.08	2.10
23.90	1.70	1.71
25.10	* 1.62	* 1.61
27.60	* 1.47	* 1.48

* Denotes strongest rings.

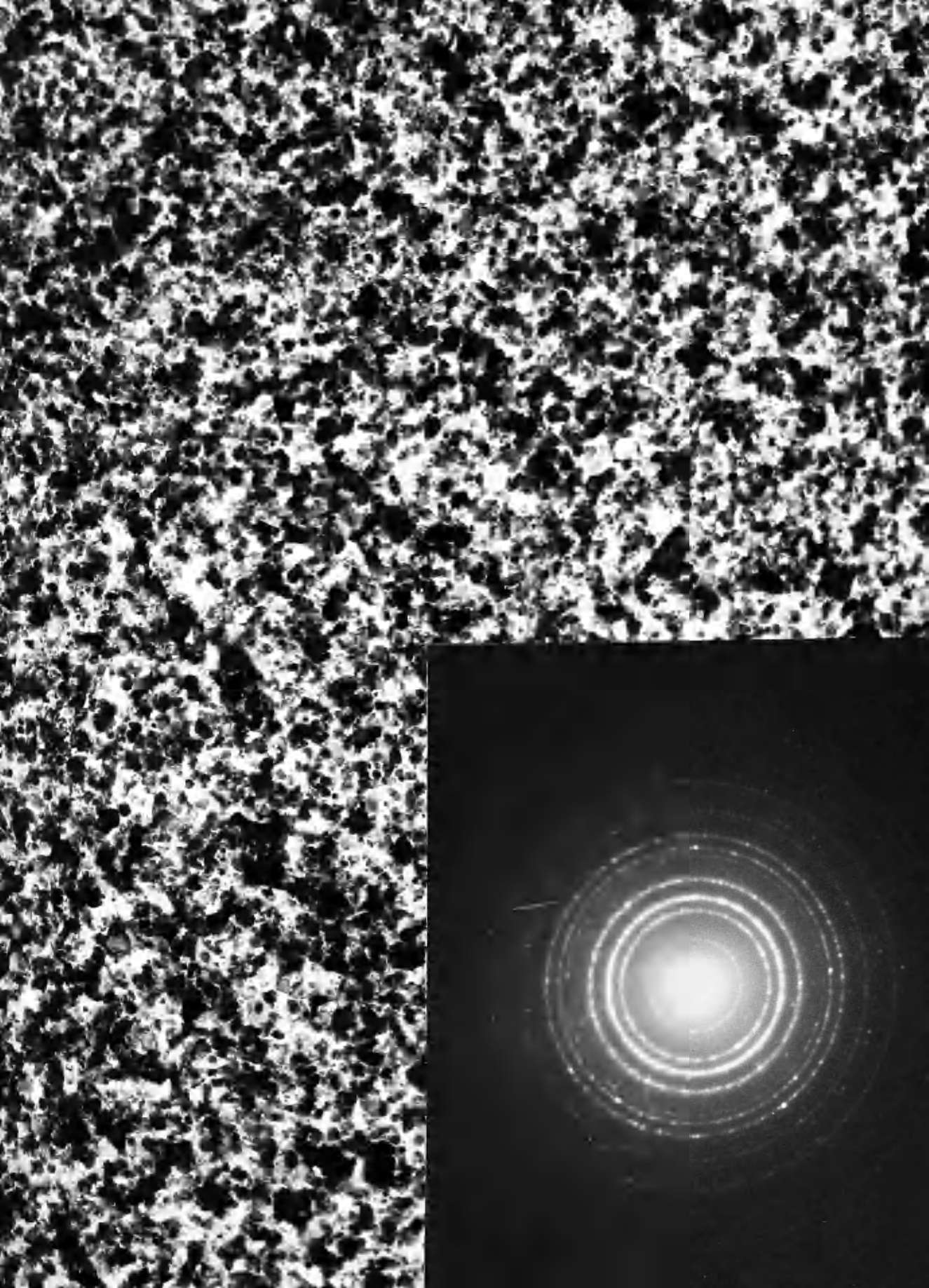
PLATE 12

Crystalline Fe_3O_4 obtained by passing
CO through a hot tube.

Magnification 100,000 X

Inset

Fe_3O_4 diffraction pattern from the
above crystalline material.



Several experiments were therefore conducted in a similar manner to those with the de-oxygenated gas except that the copper turnings were removed so that the hot tube only was used for purification purposes. Passage of CO through the tube resulted in the formation of a dark stain at the gas inlet end of the hot zone and this again was shown to be Fe_3O_4 from electron diffraction work. It was therefore possible to study any effects on the deposition pattern produced by removal of iron pentacarbonyl from the CO.

Three experiments were performed with CO when iron carbonyl had been removed by thermal decomposition (Table VIII). Particle density determinations show that the yield of deposit is reduced in these experiments to values close to these previously obtained with purified gases, thus strongly suggesting that it is in fact the iron carbonyl impurity in the gas which affects the radiolysis. Subsequent exposure of these deposits to the atmosphere caused absorption to occur and this again indicates that iron carbonyl is influencing deposit behaviour.

TABLE VIII

Experiments with CO after removal of iron pentacarbonyl

<u>Expt. No.</u>	<u>Irradiation Time (hrs.)</u>	<u>Pressure of Gas</u>	<u>Particle Density cm⁻²</u>	<u>Equivalent Particle Density from CO with Iron Present</u>
69	24	1.0 atm.	7×10^7	2.3×10^8
70	66	1.0 atm.	2.2×10^8	5.6×10^8
76	17	1.0 atm.	5×10^7	1.6×10^8

Confirmation of the influential role of iron pentacarbonyl was sought by making additions of $\text{Fe}(\text{CO})_5$ vapour to carbon monoxide which had been purified of carbonyls either at Harwell or by the thermal decomposition process. The details of these experiments are listed in Table IX.

TABLE IX

Experiments with Purified CO with $\text{Fe}(\text{CO})_5$ additions

<u>Expt. No.</u>	<u>Irradiation Time (hrs.)</u>	<u>Gas Mixture</u>	<u>Particle Density cm⁻²</u>
78	65	CO(over Cu) + 0.4 % $\text{Fe}(\text{CO})_5$	5.5×10^8
79	17	CO(Harwell) + 0.8 % $\text{Fe}(\text{CO})_5$	1.6×10^8
80	70	CO(Harwell) + 0.2 % $\text{Fe}(\text{CO})_5$	5.8×10^8

In all cases a high deposit yield was obtained and the deposits were found to be inert towards water vapour, i.e., both the yield and the reactivity of the deposit have been reversed by the addition of $\text{Fe}(\text{CO})_5$ vapour to the purified

CO, thus confirming the important role played by iron carbonyl.

In some initial experiments with the thermal decomposition process the particle densities were found to fall between lines (a) and (c), Fig. 22. These results were found to be due to the inefficient removal of iron pentacarbonyl and it was found necessary to pack the decomposition tube with glass beads in order to increase the surface area available for the thermal decomposition of the carbonyl. When this was done all further experiments gave yields close to line (c), Fig. 22.

A second cylinder of CO from Harwell gave yields of deposit intermediate between lines (a) and (c). On passing this gas through the hot tube the yields once again fell to lower values along line (c). A black stain was observed on the walls of the tube showing that this second (aluminium) cylinder of gas contained some iron pentacarbonyl. The first supply from Harwell which produced particle densities represented by line (c) did not leave a stain after passage through the tube and presumably was free from iron carbonyl.

Amount of $\text{Fe}(\text{CO})_5$ present in the cylinder gas (I.C.I.)

This was estimated by passing a measured volume of CO through the decomposition tube and analysing, colorimetrically, the deposit which formed as Fe_3O_4 on the surfaces of the glass beads.

The deposited film was dissolved in concentrated hydrochloric acid and the solution was evaporated down to about 1 ml. It was then oxidised with potassium permanganate (2 g / l) until a faint pink colour persisted and the volume was made up to 50 ml. 5 ml of potassium thiocyanate (~4N) and 2 ml hydrochloric acid (~4N) were added to a 10 ml aliquot and the volume was made up to 20 ml. A red colouration was produced. Two successive experiments required 5.3 and 5.7 ml of a standardised solution (1 ml \equiv 0.002 mg Fe) to match the colouration at the same volume. The volume of CO decomposed was 550 ml (at 1 atmosphere), therefore the gas (I.C.I.) contains about 80 p.p.m. by weight of iron present as the carbonyl $\text{Fe}(\text{CO})_5$, or 280 p.p.m. $\text{Fe}(\text{CO})_5$.

Addition of excess $\text{Fe}(\text{CO})_5$. Additions of 0.8 v/o of $\text{Fe}(\text{CO})_5$ were made to purified CO (Harwell) and to cylinder CO (I.C.I.). This 0.8 v/o is equivalent to about 200 times that originally present in the gas. The yields from both these experiments, however, remained close to values along line (a), Fig. 22 and indicate that the 80 p.p.m. Fe is sufficient to fulfil whatever role the iron is playing in the present experiments. Only when the iron is removed does a change in yield and reactivity occur. No difference in results have been observed in experiments with excess $\text{Fe}(\text{CO})_5$ present.

(ii) Nickel tetracarbonyl, Ni(CO)₄

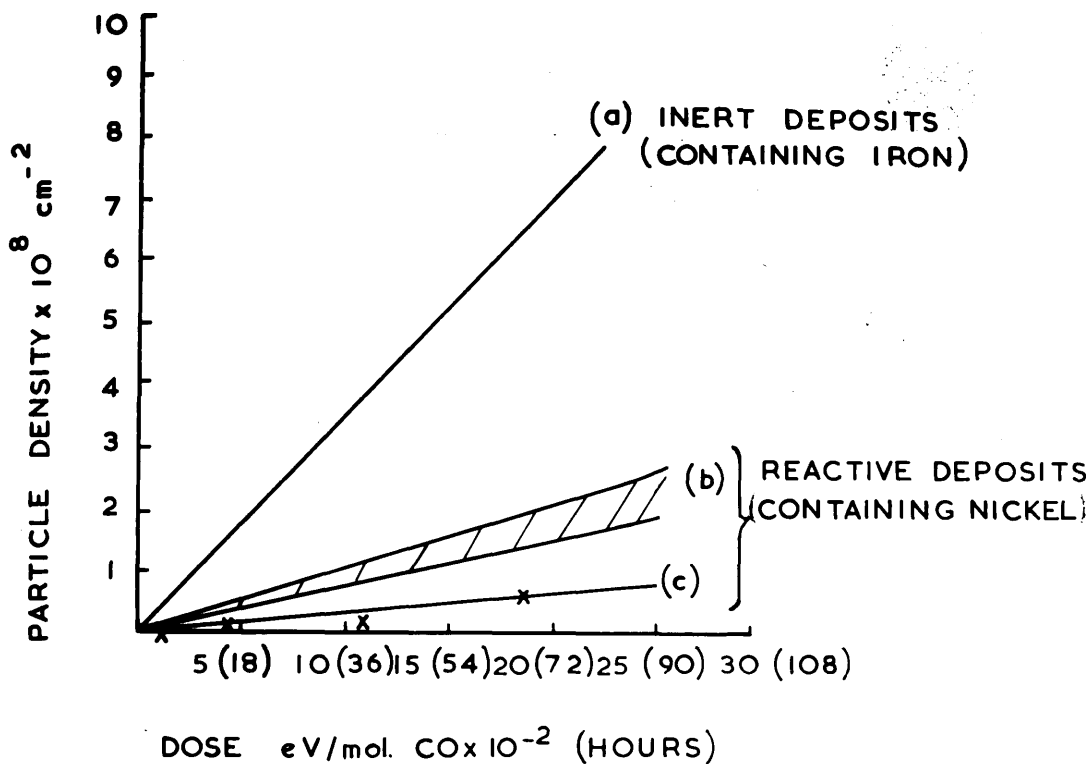
Electron diffraction work to be described later showed the presence of either iron or nickel in the deposits produced by α -radiolysis of CO; the iron can, of course, arise from the iron pentacarbonyl impurity in the gas. Nickel tetracarbonyl can be formed when CO is passed over nickel surfaces at room temperature and it was found that the needle valve in the vacuum line between the cylinder of gas and the microscope column was a potential source of nickel tetracarbonyl due to the nickel plating on the internal surfaces of the valve.

Since removal of iron from the CO had been shown to lead to a reduction in the amount of solid produced, a series of experiments were performed with the purified CO from Harwell with the needle valve removed from the vacuum line. A further reduction in yield was obtained (Table X), and is represented by line (c) in the dose v density graph (Fig. 23). Here line (a) represents the yields from cylinder CO containing iron carbonyl and the shaded region represents yields from gases purified of iron carbonyl as before.



FIGURE 23

The following text is extremely faint and largely illegible. It appears to be a descriptive paragraph or a list of items related to the figure. Some words are difficult to discern but may include terms like 'analysis', 'results', and 'conclusion'.



- (a) CYL. CO (I.C.I.) WITH IRON CARBONYL IMPURITY.
 (b) CYL. CO. WITH IRON REMOVED.
 (c) AS FOR (b) BUT WITH NEEDLE VALVE REMOVED.

FIG 23 PARTICLE DENSITY v DOSE GRAPHS
SHOWING INFLUENCE OF METAL CARBONYLS.

TABLE I

Experiments with purified CO (needle valve removed)

<u>Expt. No.</u>	<u>Irradiation Time (hrs.)</u>	<u>Particle Density cm⁻²</u>	<u>Particle Size (Å)</u>	<u>Remarks</u>
101	67	5×10^7	1600	-
102	40	2.5×10^7	1900	-
103	16	7×10^6	-	-
104	4	$1-3 \times 10^6$	-	-
105	40	3×10^7	-	CO ₂ /acetone cold trap inserted
106	65	1.7×10^8	-	Expt. with needle valve incorporated and 0.04 v/o Ni(CO) ₄ added

The particles from this latest series of experiments retained their characteristic features and reacted with or absorbed moisture on subsequent standing in the atmosphere. The average particle diameter, however, was now about 1600 Å compared with the higher value of 2,500 Å found in earlier experiments. Electron diffraction work showed that these deposits still contained nickel and therefore, either the CO (Harwell) contained some Ni(CO)₄ or there were nickel surfaces within the microscope column acting as sources of Ni(CO)₄. An experiment with a CO₂/acetone cold trap fitted between the source of gas and the column to remove Ni(CO)₄

from the gas failed to eliminate the nickel, i.e., nickel was still detected in the deposit. It was later learned that the pole-piece systems in the lenses of the microscope consisted of cobalt steel with a percentage of nickel present as an alloying constituent. (The manufacturers would not reveal the actual analysis figures for the steel). There does not appear to be any other source of $\text{Ni}(\text{CO})_4$ within the microscope column.

A single experiment in which 0.04 v/o of $\text{Ni}(\text{CO})_4$ vapour was added to purified CO (Harwell) produced results expected for the purified CO alone, i.e., the excess $\text{Ni}(\text{CO})_4$ did not appear to alter the yields significantly.

The results of these experiments involving iron and nickel carbonyls have shown that the yield of deposit decreases as the metal carbonyl impurity content is reduced. It was not possible to conduct in situ experiments with CO without some nickel carbonyl formation due to the presence of the nickel in the pole-pieces which therefore imposed a limitation on the ultimate purity obtainable in these experiments.

8. External Deposition

The vacuum system shown schematically in Fig. 12 was designed to allow the radiolysis of various gas mixtures to be performed in a system which would be free from metallic

carbonyls, provided that the iron in the CO gas could be efficiently removed by the thermal decomposition process. Neither in the reaction vessel itself (Fig. 13) nor in any other part of the vacuum system were there nickel components which could give rise to the formation of $\text{Ni}(\text{CO})_4$ vapour, thus making it theoretically possible to study the effect of the absence of carbonyls on the radiolysis.

A third α -source, C, was employed in these experiments, this being a direct replacement for source B which had become unsealed. It was first of all desirable to establish the relationship between the yield of deposit collected in the in situ experiments and that obtained with the different geometry of the external reaction vessel. Experiments in situ with source C resulted in yields of about one third of these obtained with source B, suggesting that the dose-rate to gas with this source (C) is lower (dosimetry has not yet been done on source C). The depositions were otherwise similar in every respect to those obtained with source B.

The design of the reaction vessel was important and was found to influence the rate of collection of particles on the specimen grid. Experiments with vessels with a large open volume above the α -source produced little or no deposit on the grid even after several days radiolysis. This lack of deposit is thought to be a consequence of convection

currents set up within the vessel; these could sweep away deposits before they had time to settle out on to the collecting substrate. The vessel which gave the highest yield of deposit and the most reproducible particle density results is shown in Fig. 13, where there is a more confined space above the α -source which to some extent simulates the geometry existing in the electron microscope experiments. Even with this design the yields of deposit tended to be lower than those obtained with an equivalent dose in situ. However, the apparatus was useful in confirming the importance of metal carbonyls in the deposition process and the following results were obtained.

(1) Radiolysis of CO containing iron carbonyl impurity gave deposits which were inert towards moisture and which were of similar appearance and size ($\sim 2,500 \overset{\circ}{\text{A}}$) to those produced in situ. There was, however, a greater tendency for the particles to aggregate in the experiments using the reaction vessel. The aggregation was probably due to induced convection currents which could cause particles to collide and stick together. This effect of clustering was less noticeable with the in situ experiments where there is greater insulation of the gas against changes in room temperature.

Electron diffraction work on the deposits revealed the presence of iron as was found with the deposits from in situ experiments.

(2) Radiolysis of CO freed from iron carbonyl but with excess ($\sim 10\%$) $\text{Ni}(\text{CO})_4$ vapour added from a cylinder (Fig. 12) gave deposits which resembled in every way those obtained in situ with iron-free gas, i.e., the deposits changed in appearance after standing in the atmosphere and were found to contain nickel. The yield was also lower than in (1) above and this reduction is consistent with the results reported for in situ radiolysis.

(3) Radiolysis of CO after attempting to remove all carbonyls.

CO was passed through a hot tube (at $\sim 500^\circ\text{C}$) packed with glass beads to decompose the iron carbonyl and was led directly into the reaction vessel for radiolysis. Since there are no nickel surfaces present the gas should now be free of metal carbonyls. After radiolysis (6 days) the specimen mount was removed from the vessel and examined in the electron microscope. An extremely small yield of deposit was observed on the surface of the mount. By counting the number of particles on each of the $7,70\mu$ holes in the mount the yield was estimated to be $\approx 1 \times 10^5$ particles cm^{-2} . The removal of carbonyls has therefore resulted in a reduction in the yield of solid by about three orders of magnitude. The few particles that were observed were smaller than those found with the impure CO. When examined by electron diffraction, after oxidation, the particles

gave four weak rings which corresponded to the four strongest lines of Fe_3O_4 showing that some iron was still present in the deposit, presumably from iron carbonyl which had not been completely removed by the purification process. The experiment was repeated after inserting three carbon dioxide/acctone cold traps into the vacuum system to condense out any carbonyl not removed by the thermal process but again a small yield of deposit was produced with iron as a constituent element. No further attempts were made to eliminate the iron completely as the results clearly showed that the deposit yield tended towards zero as the metallic carbonyl content was reduced.

(4) α -Radiolysis of nickel tetracarbonyl vapour

In order to try to clarify the role played by iron and nickel carbonyls in the α -radiolytic process it was decided to radiolyse the pure carbonyls and to look for deposition products. Since all previous radiolyses had been performed at one atmosphere pressure and since the maximum pressures obtainable with the carbonyls alone are much lower than this (~ 30 cm Hg for $\text{Ni}(\text{CO})_4$ and ~ 2 cm Hg for $\text{Fe}(\text{CO})_5$ at 20°C), the total pressure in each case was made up to one atmosphere by adding the inert gas helium to the system prior to radiolysis.

After evacuating the vacuum line and flushing out twice with helium, $\text{Ni}(\text{CO})_4$ vapour was introduced into the reaction vessel to a pressure of 10 cm Hg and the pressure brought up to one atmosphere with helium. Subsequent examination of the specimen grid showed that there was a very small yield of deposit from this mixture. It was not possible to obtain an accurate figure for the particle density since most of the particles were much smaller than any observed previously, ranging in size from about 200 \AA dia. down to 25 \AA . However, by counting the larger particles, a value of $\approx 1 \times 10^6$ particles cm^{-2} was obtained. Plate 13A shows an area with both large and small particles present. The behaviour of the particles after exposure to the atmosphere resembled that of all other deposits which contained nickel, i.e. some reaction had occurred. Plate 13B illustrates the appearance of the particles after standing in the atmosphere.

An equivalent experiment with $\text{Ni}(\text{CO})_4$ at a pressure of 10 cm made up to atmospheric pressure with iron-free CO gave a very much higher yield of solid, $\sim 5 \times 10^7$ particles cm^{-2} , and also much larger particles ($2000 \text{ \AA} - 2,500 \text{ \AA}$ dia.) as shown in Plate 14A (same magnification as 13A and 13B). Here, some reaction with moisture has occurred in the interval between formation and subsequent examination in the

PLATE 13A

Particles from He/Ni(CO)₄ radiolysis.

Magnification 50,000 X

PLATE 13B

Particles from the same experiment
as above after exposure to moisture.

Magnification 50,000 X

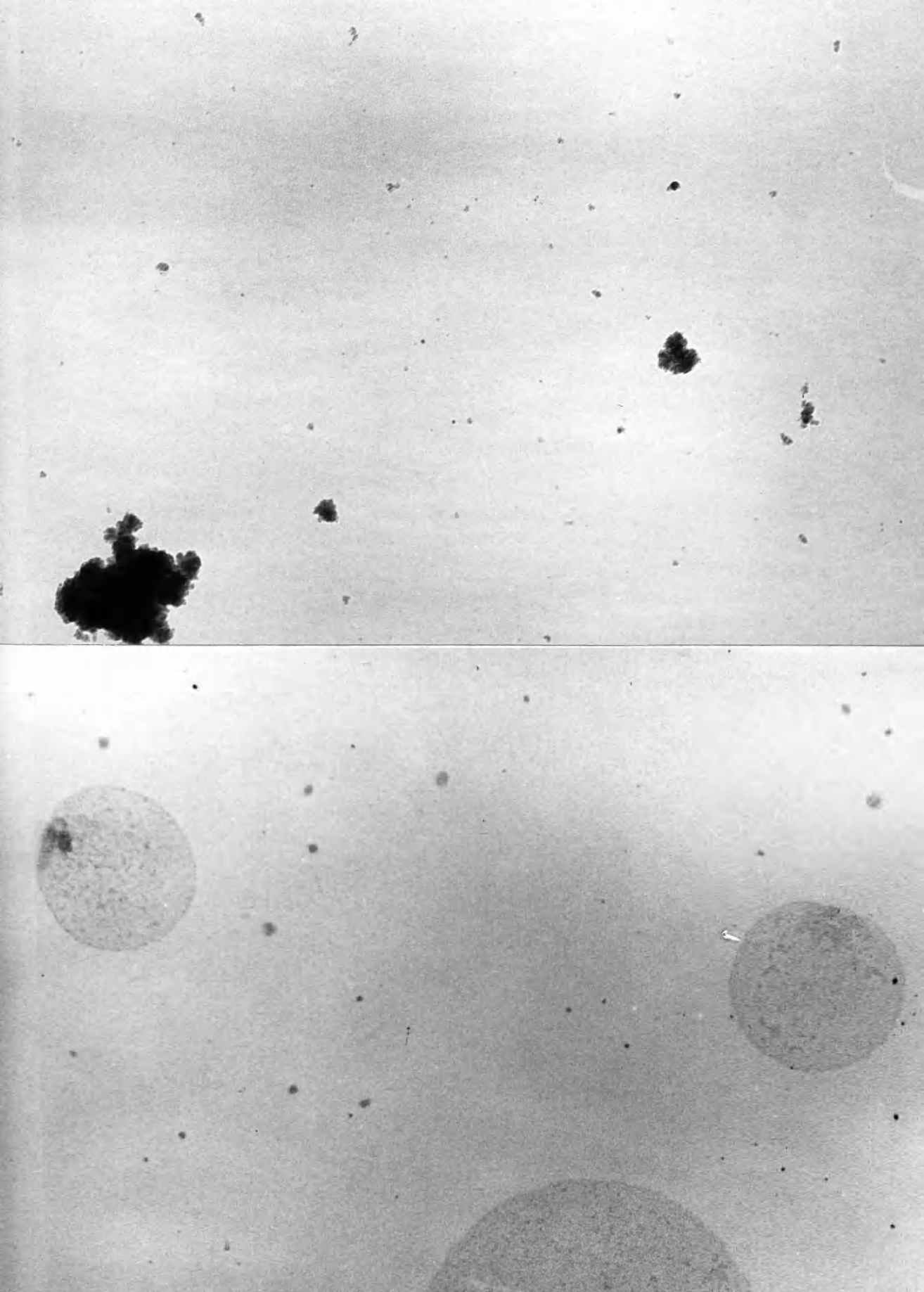


PLATE 14A

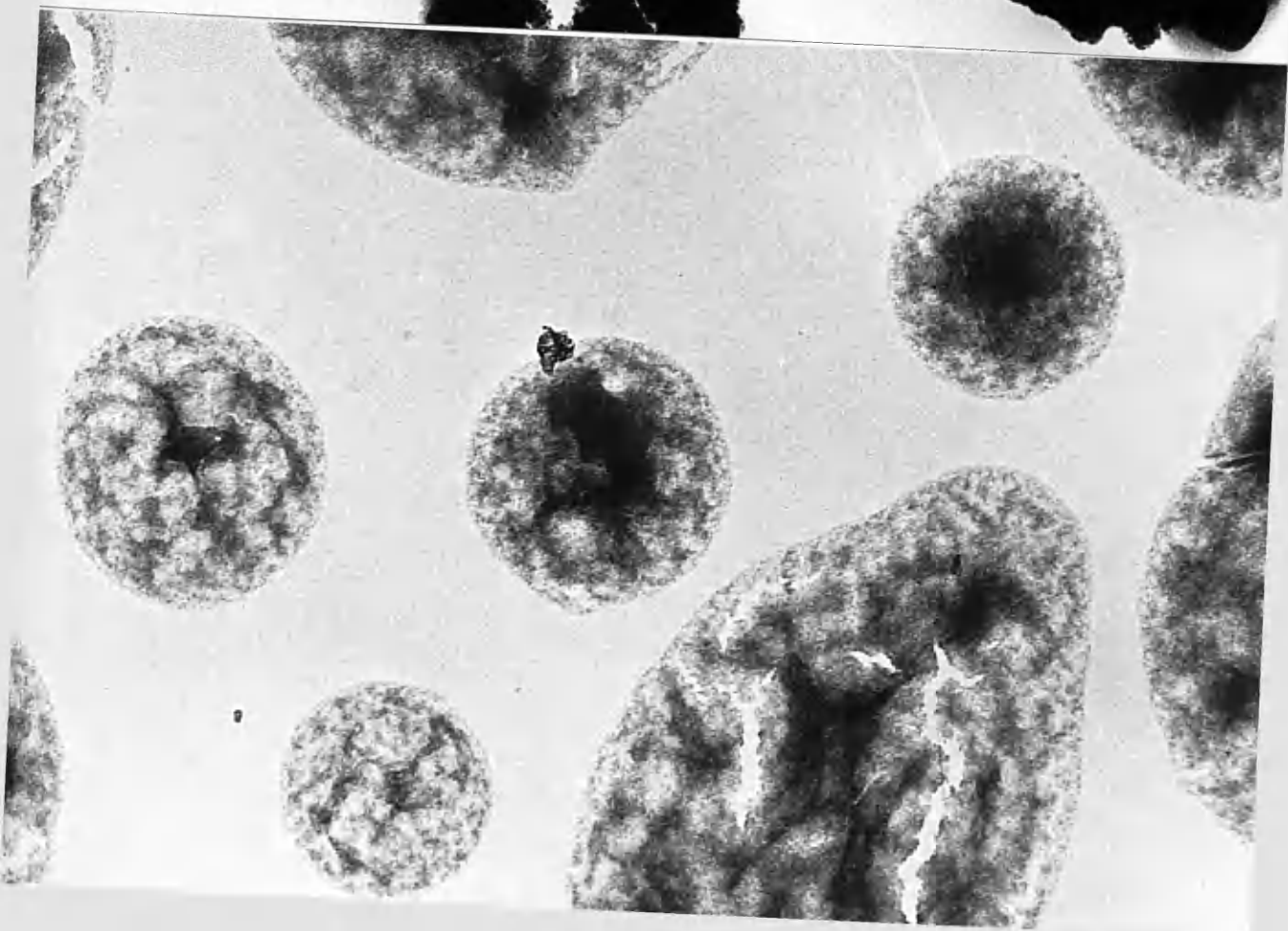
Particles from $\text{Ni}(\text{CO})_4/\text{CO}$ radiolysis.

Magnification 50,000 X

PLATE 14B

Particles from same experiment as
above after exposure to moisture.

Magnification 50,000 X



microscope and swelling is observed. Further exposure to the atmosphere enhanced swelling as illustrated in Plate 14B (same magnification as 13A, 13B and 14A).

(5) α -Radiolysis of Iron Pentacarbonyl

Liquid $\text{Fe}(\text{CO})_5$ contained in a flask (Fig. 12) was allowed to evaporate into the reaction vessel which had been previously flushed out and then filled to just under atmospheric pressure with helium. The manometer indicated the partial pressure of $\text{Fe}(\text{CO})_5$ to be about 2 cm Hg after equilibrium had been attained. The total pressure was then made up to one atmosphere with helium and the gas mixture was radiolysed for 20 days. Two effects were observed.

(a) A very small yield of solid, about $10^5 - 10^6$ particles cm^{-2} , was obtained on the specimen mount. An equivalent experiment with cylinder CO containing iron carbonyl impurity would have given approximately 4×10^8 particles cm^{-2} (as derived from dose v. particle density graphs). The low yield obtained with the $\text{Fe}(\text{CO})_5/\text{He}$ mixture strongly suggests that it is not in fact the iron carbonyl alone which has been giving the solid deposit throughout all of these experiments.

The solid obtained was similar in appearance to deposits from CO and did not change on subsequent exposure to moisture. There were insufficient particles for an accurate

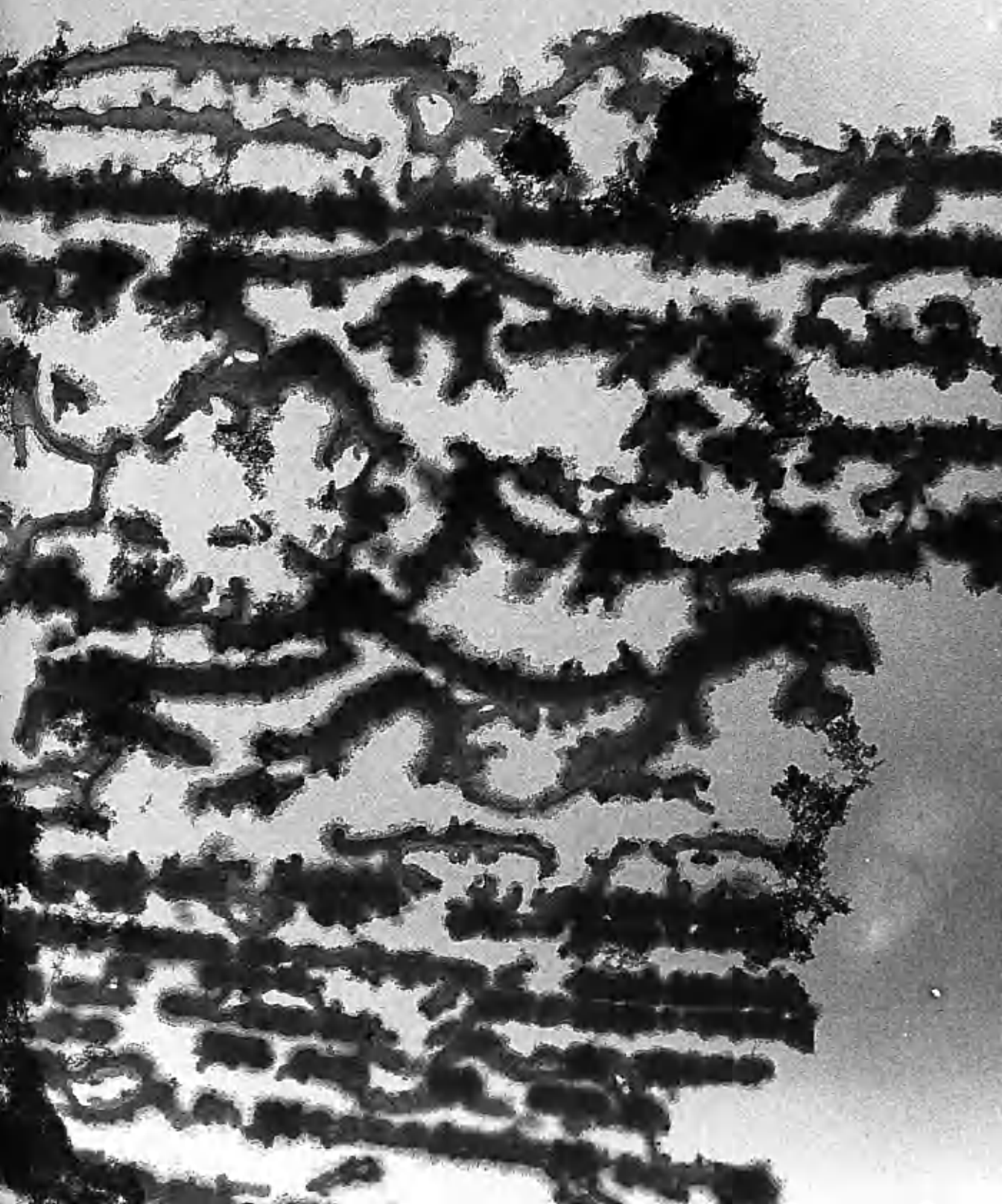
determination of particle size to be made; however, it was evident that the average size was much less than the 2,500 Å dia. value found for CO deposits, the particles being of the order of 1000 Å dia.. It is believed that the solid formed was produced from the secondary radiolysis of CO formed by the action of the α-particles on the iron pentacarbonyl. This is discussed later.

(b) A few small, flat, orange coloured crystals were found to have grown on the walls of the reaction vessel. These are almost certainly crystals of iron enneacarbonyl $\text{Fe}_2(\text{CO})_9$ which are known to be formed by the action of light on $\text{Fe}(\text{CO})_5$. These crystals were not observed on the specimen mount and were subsequently shown to behave differently in the electron microscope vacuum system from the normal deposit particles. Specimens suitable for microscopy were prepared by grinding the crystals between two glass slides and then picking up fragments with a specimen mount. The crystal fragments were found to be very unstable in the electron beam even at low beam intensities. At the normal operational intensity the crystals almost completely volatilised and in this way differed from the solids from CO radiolysis. Samples of solid known to be $\text{Fe}_2(\text{CO})_9$ behaved in a similar manner to the orange crystals found on the vessel walls and Plate 15 shows an area, photographed at a low beam intensity, where decomposition has already commenced.

PLATE 15

Electron micrograph of $\text{Fe}_2(\text{CO})_9$

Magnification 100,000 X



9. Electron Diffraction Studies

These studies were made as part of an attempt to gain information about the nature and composition of the solids produced by the α -radiolysis of carbon monoxide gas. As will be shown below, the diffraction characteristics from deposits examined immediately after their formation and collection on the substrate, yielded little information about deposit structure and the deposits were therefore heated under vacuum and in oxygen in order to induce a structural rearrangement which might give useful diffraction data. Previous results have strongly indicated that, in addition to the iron carbonyl impurity in the CO obtained from steel cylinders, there was probably some nickel carbonyl present in the system during radiolysis. The iron carbonyl has been shown to have the more pronounced influence on the deposition process and it evidently obscures any effect which nickel carbonyl has on the radiolysis. Only when the iron is removed does the influential role of the nickel become apparent. Electron diffraction studies were therefore made of solids from CO containing both iron and nickel carbonyl impurities and of solids from CO containing only nickel carbonyl impurity.

(a) Deposits from CO containing iron and nickel carbonyl impurity.

Electron diffraction studies of these deposits

revealed only very diffuse broad bands indicating that the deposits are of an amorphous nature. Deposits which were exposed to the atmosphere or to which water was deliberately added, and which had not been previously irradiated by the electron beam, gave similar diffuse bands on subsequent examination. Plate 16 illustrates the typical diffraction pattern obtained from this material. The pattern was the same whether taken from a single particle or from an aggregate and was in fact indistinguishable from the pattern given by the support film (carbon film).

The Effect of Heating Deposits in Vacuum

Deposits which were heated under vacuum for 15 minutes at 500°C in the Coating Unit were observed to shrink by about 10-20 per cent as shown in Plates 17A and 17B, which depict the same area before and after heating. The deposit, originally of a loose texture, has shrunk, forming dense cores of solid material surrounded by smaller irregularly-shaped particles. Areas which had not been previously irradiated by the electron beam showed a similar shrinkage effect but exhibited a higher degree of angularity in the dense regions which often were hexagonal in outline. Plate 18, for example, shows the presence of these hexagonal regions. Heating further to 650°C caused the support film (silicon monoxide) to crystallise out, thus confusing observations at

PLATE 16

Typical electron diffraction pattern from the
deposit from CO radiolysis.

PLATES 17A and 17B -

Deposit from CO (containing iron and nickel
carbonyls) before and after heating in
vacuum for 15 minutes at 500°C.

Magnification 200,000 X



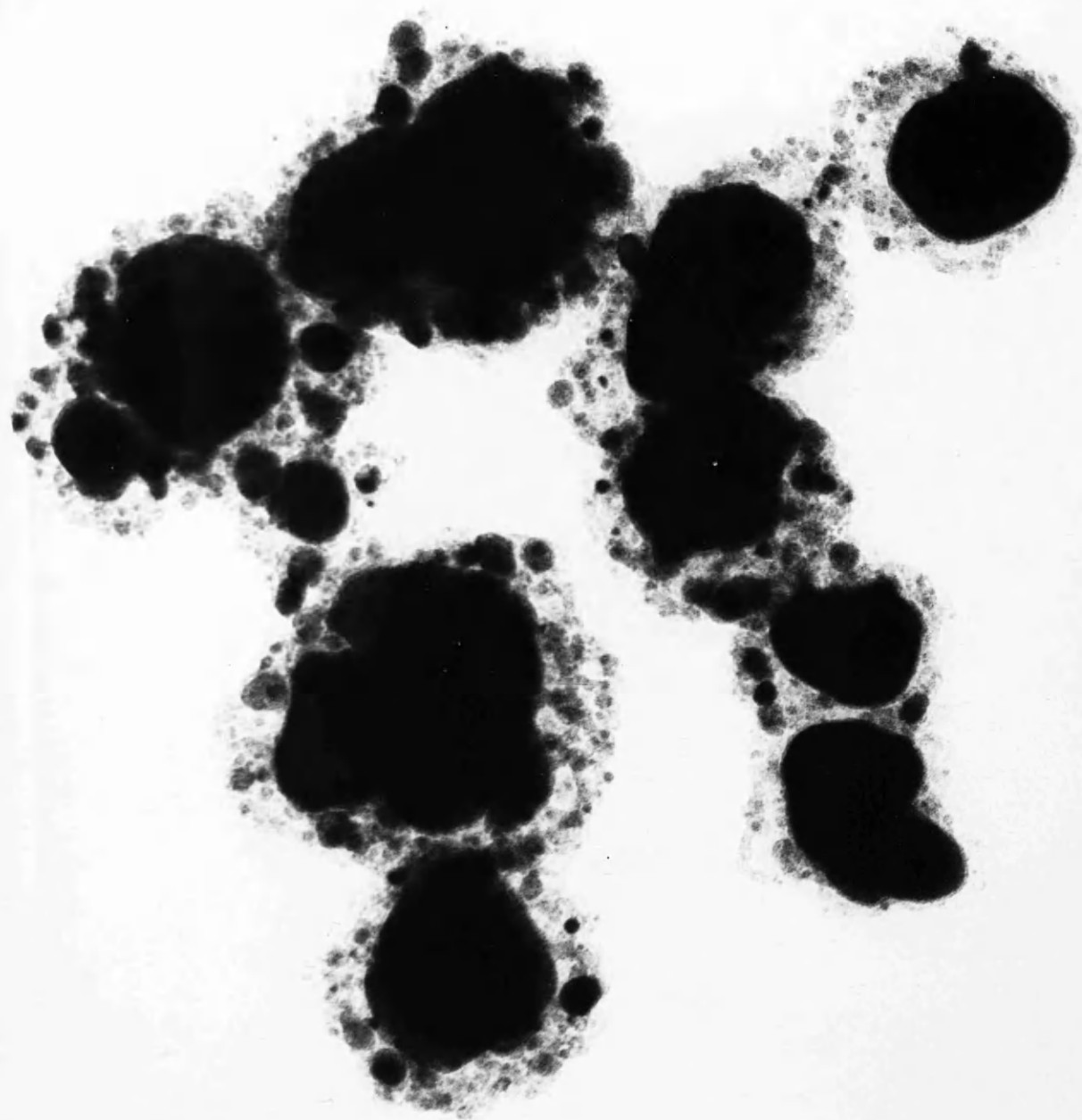
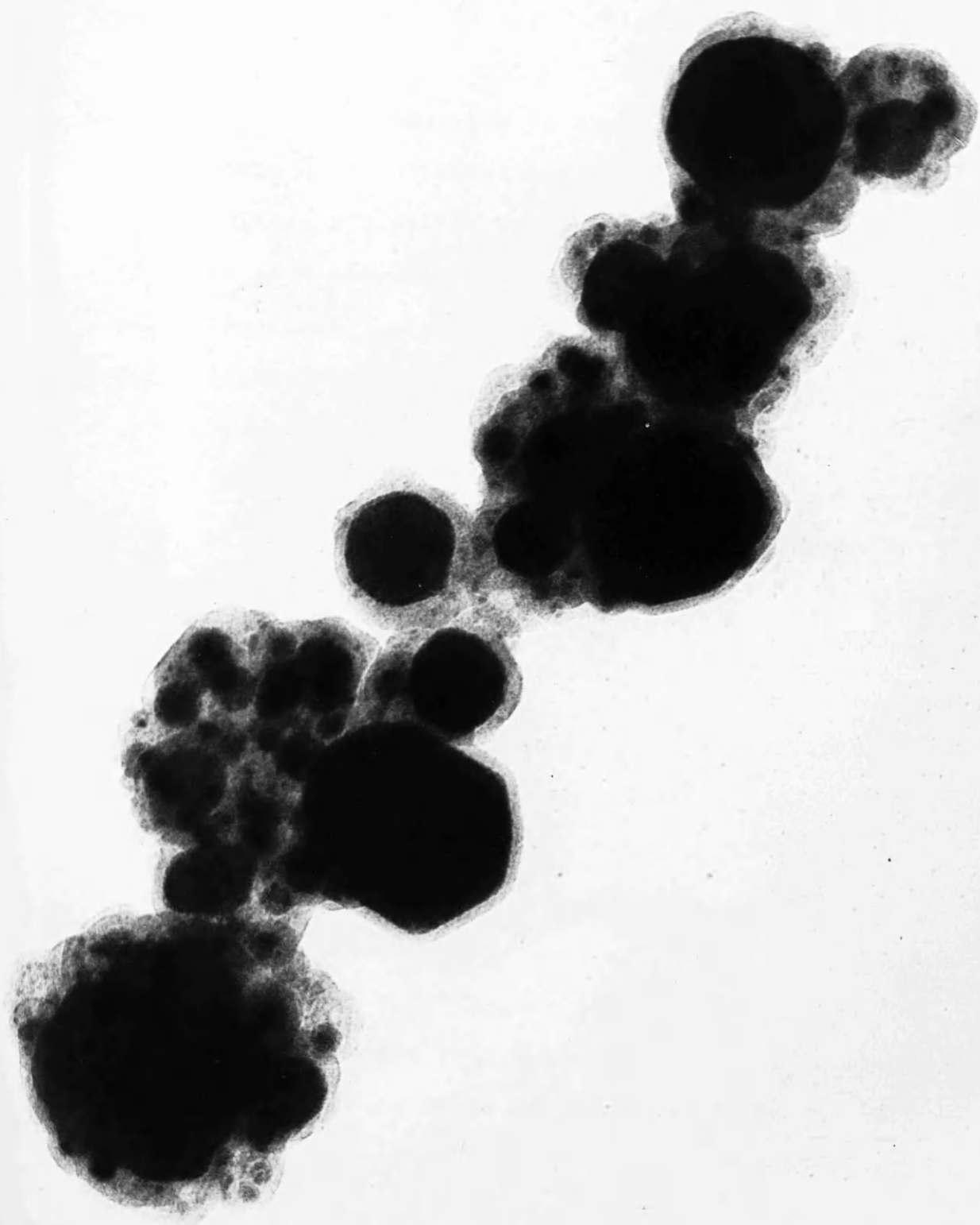


PLATE 18

Electron micrograph illustrating the angular material obtained after heating the deposit in a vacuum for 15 minutes at 500°C. This specimen had not been previously examined in the microscope.

Magnification 200,000 X



higher temperatures. The crystallisation process was presumably due to the formation of silicon dioxide from the monoxide and oxygen impurity in the system.

Electron diffraction patterns from areas such as those shown in Plates 17B and 18 were rather weak and consisted of diffuse rings - somewhat sharper than from unheated specimens - and a few spots, as illustrated in Plate 19. The patterns indicated that some ordering of the deposit structure had occurred on heating.

The shrinkage effect could be followed continuously by increasing the intensity of the electron beam during examination of the deposit, i.e. by using the beam as a source of heat, but with this method it was not possible to monitor the temperature. The Siemens Object Heating Device, however, was useful for observing the progressive behaviour of the particles during heating in situ, and Plates 20A - 20E show that most of the shrinkage occurs between 250°C and 500°C; beyond 500°C the shrinkage effect diminishes and some sintering of the material evidently occurs. At the highest temperature attained, 1000°C, some interaction between the deposit and the support film appears to have taken place, for example, at 'V' in Plate 20E. Other areas showed a similar interaction at 1000°C and in some regions it was possible to observe the deposit reacting with and breaking

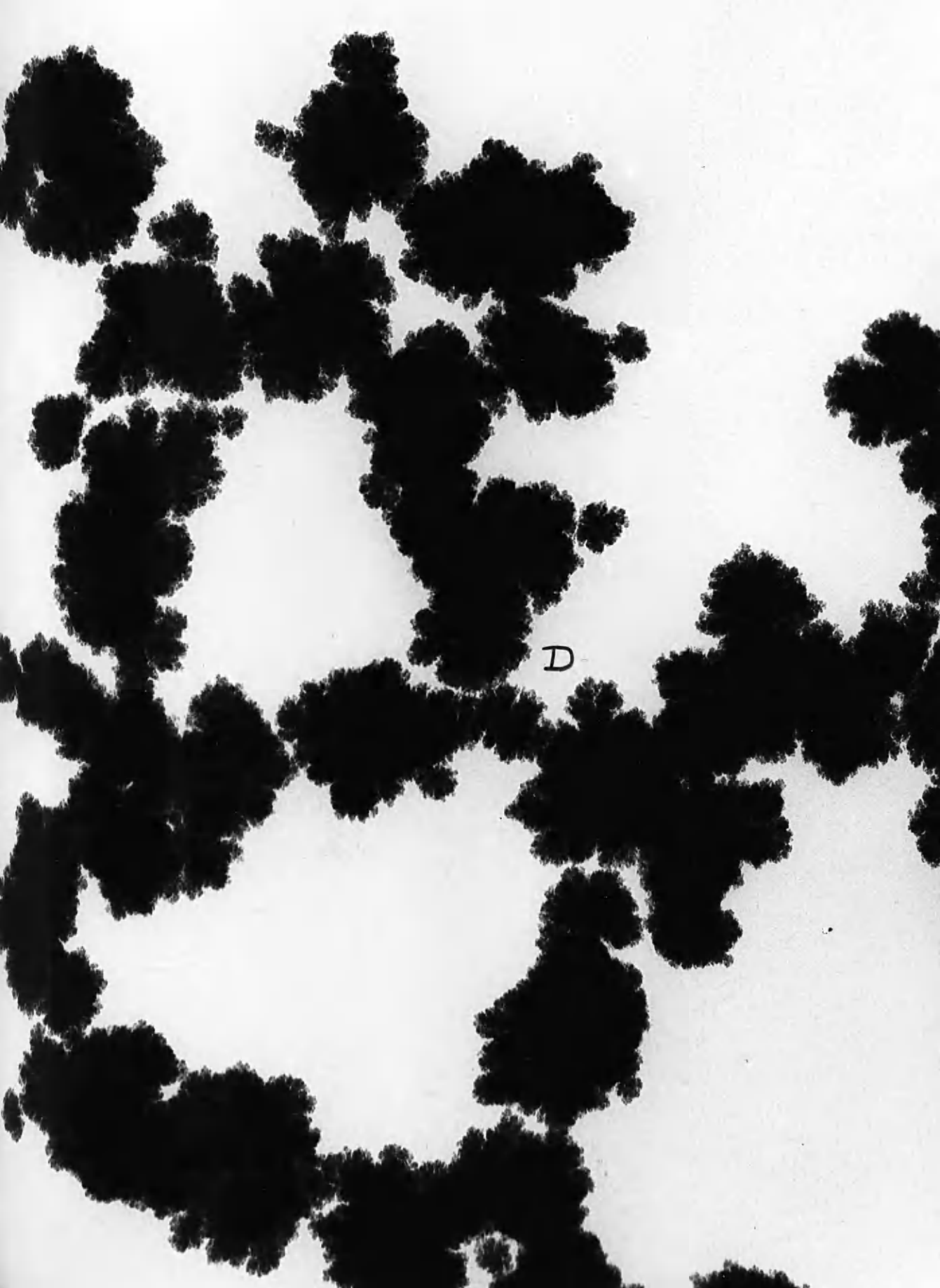
PLATE 19

Electron diffraction pattern from
vacuum-heated deposits.

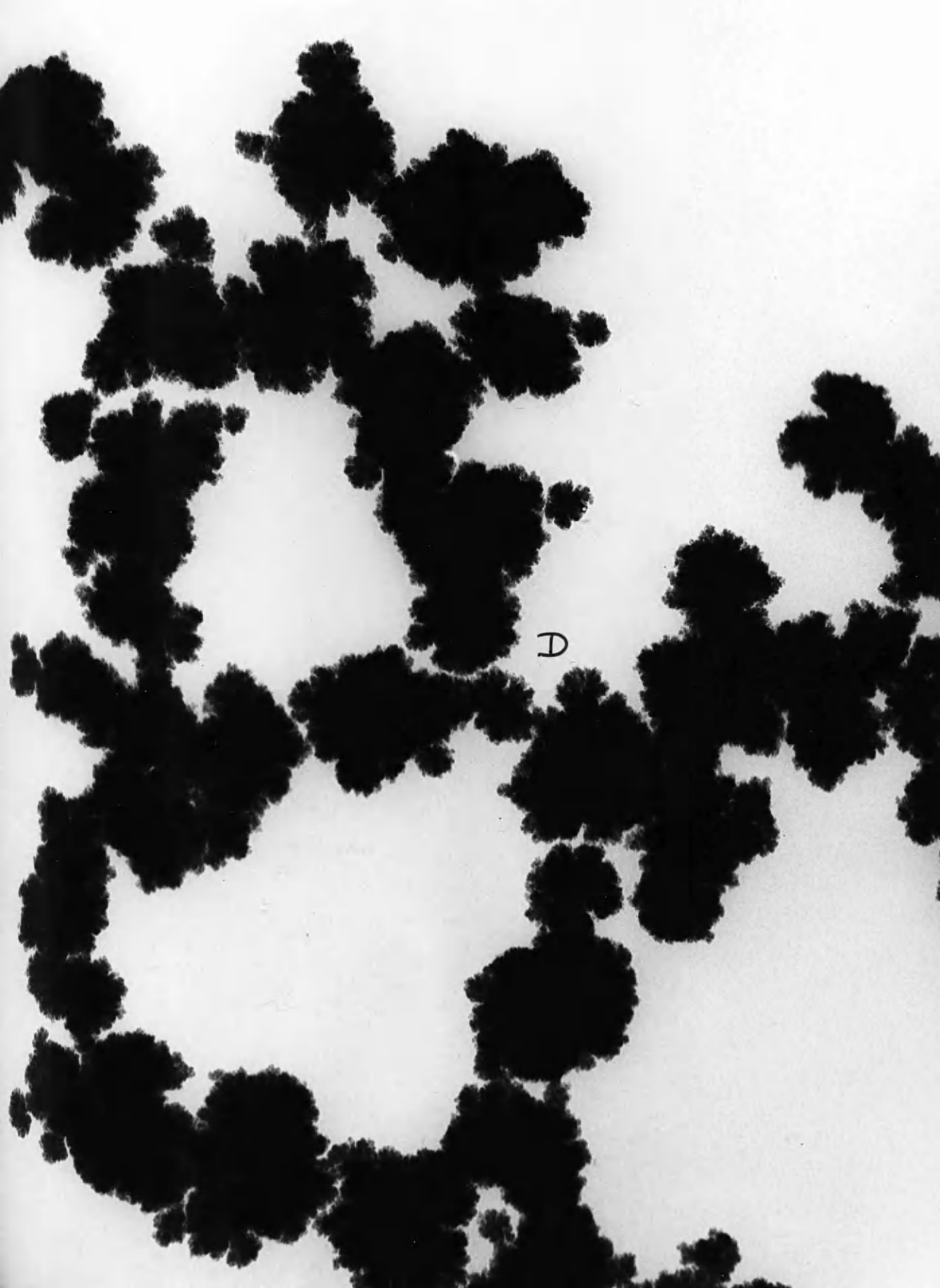
PLATES 20A to 20E -

Series of micrographs showing the same area of deposit before heating in vacuum and then after heating to 250°C, 500°C, 750°C and 1000°C respectively.

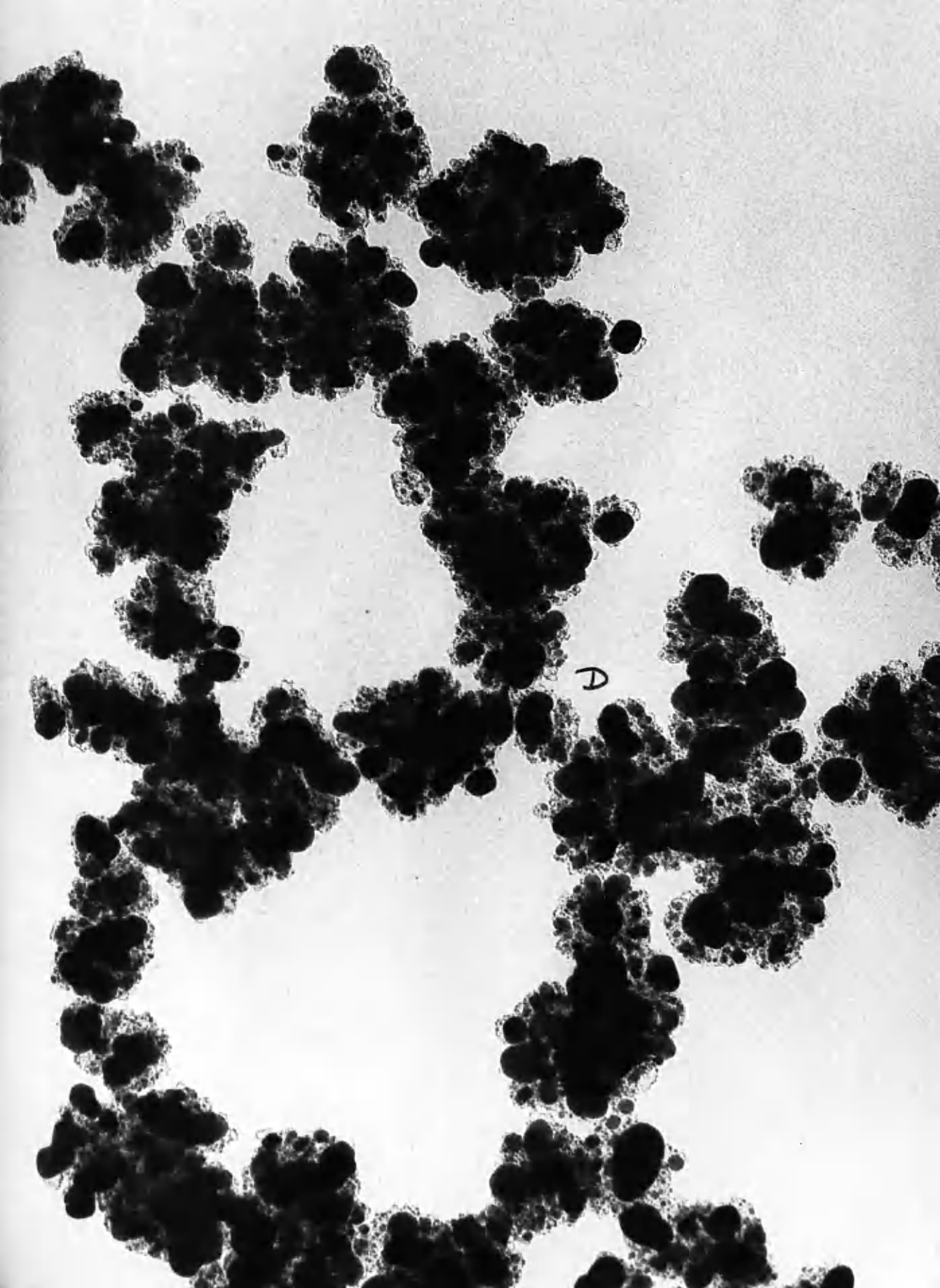
Magnification 100,000 X



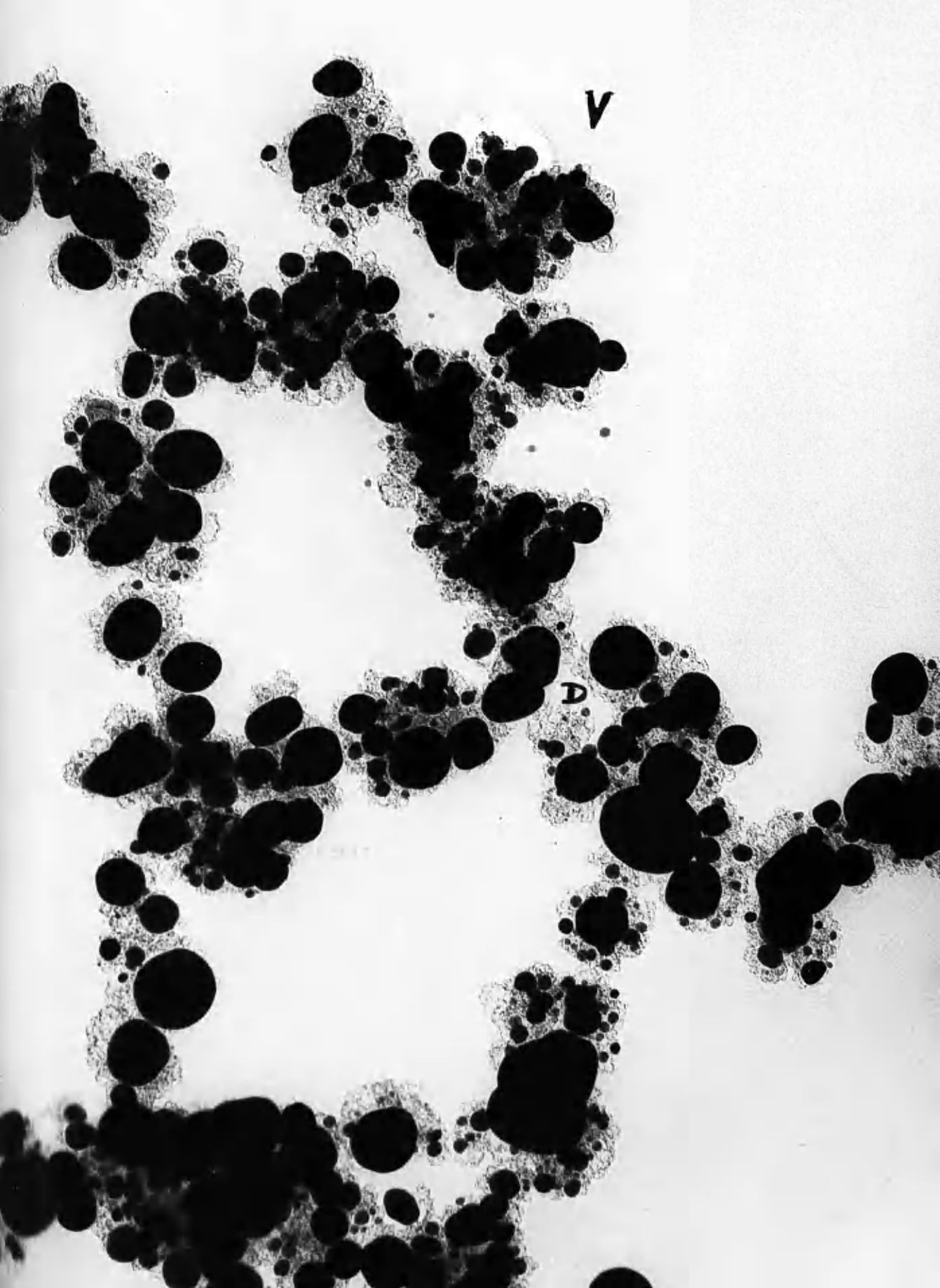
D



D







up the support film. Plate 21 shows an area where reaction between the background film and the deposit has been severe.

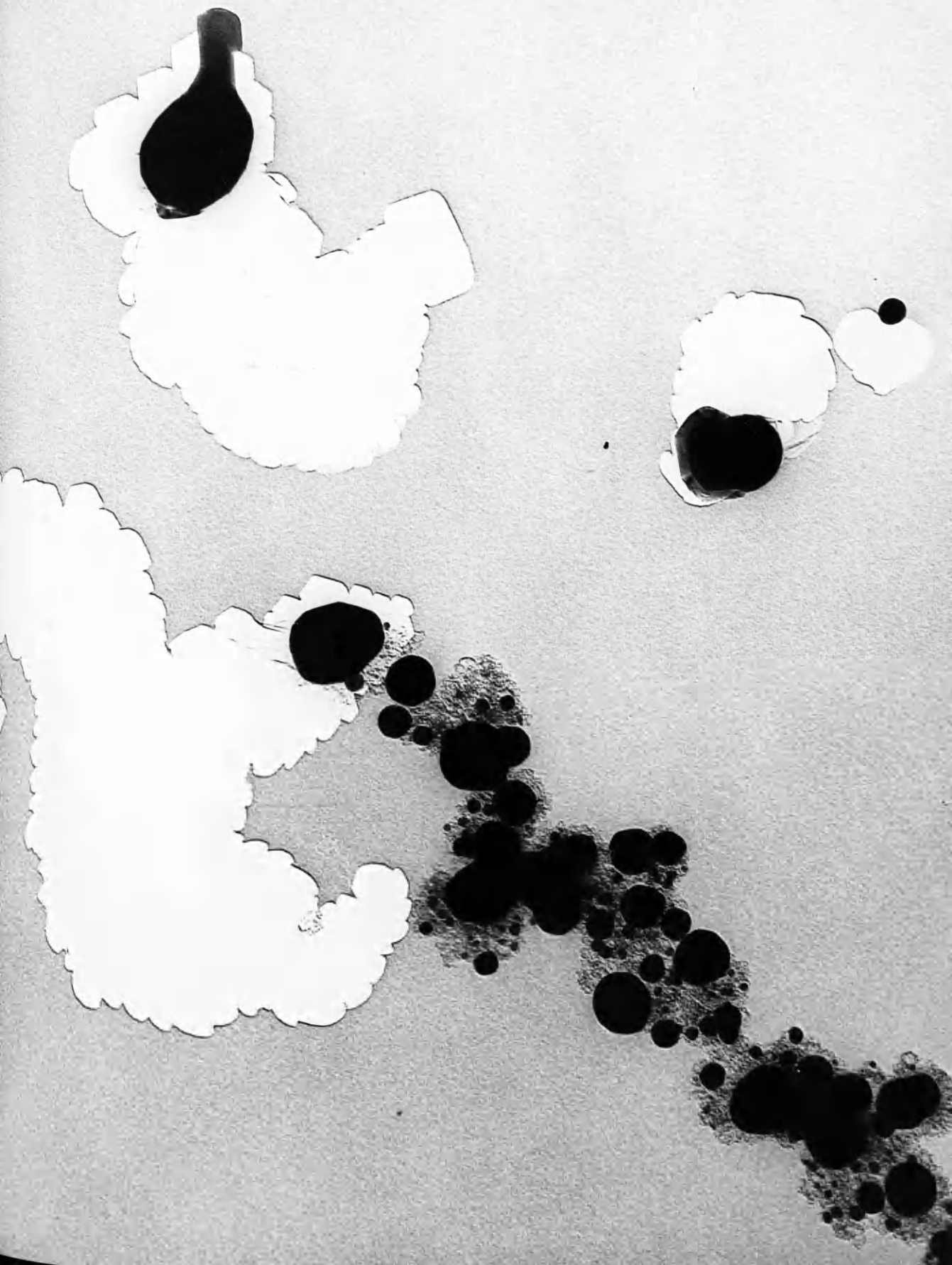
Plates 22A - 22E show respectively, the diffraction patterns from the deposit at room temperature, then after heating to 250°C, 500°C, 750°C and 1000°C. These patterns were obtained by centring the diffraction aperture around the area marked with a 'D' in each of the series of micrographs 20A - 20E. The series shows that the transformation from a random structure to a more ordered one occurs mainly between 250°C and 500°C, as illustrated by the increasing sharpness of the rings and the appearance of diffraction spots between these temperatures. Above 500°C there is little change in the diffraction patterns and this observation is consistent with the physical changes in appearance after heating.

The residue remaining after heating the deposits is likely to be either carbon, a carbide, an oxide or some other inorganic substance. The d -spacings obtained from measurements of the diffraction patterns of the residues are listed in Table XI, but insufficient data are available to characterise the material. At the higher temperatures there is probably some contribution to the diffraction patterns from the compound or compounds formed by the interaction between

PLATE 21

Electron micrograph showing severe
reaction between the deposit and
the support film (at 1,000°C).

Magnification 100,000 X



PLATES 22A to 22E

Electron diffraction patterns from deposit
heated to various temperatures.

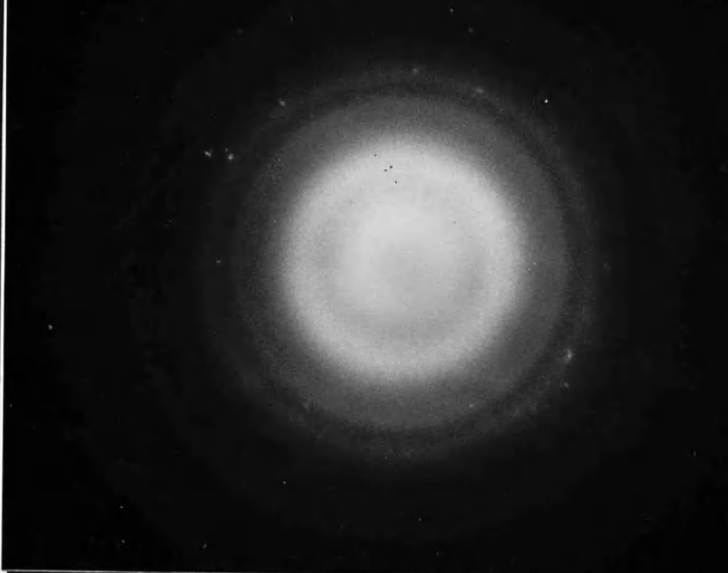
22A - Room temperature

22B - 250°C

22C - 500°C

22D - 750°C

22E - 1,000°C



the deposit and the silicon monoxide support film. It was noted that the monoxide film was more stable in the microscope vacuum system and did not crystallise out even at $\sim 1000^{\circ}\text{C}$.

TABLE XI

d-Spacings from vacuum heated deposits

Deposits heated in Coating Unit	Temp.	<u>d</u> -spacings
	500°C	2.09, 1.23
Deposits heated in situ	250°C	2.09, 1.73, 1.25
"	500°C	2.08, 1.83, 1.71, 1.56, 1.21, 1.11, 0.99
"	750°C	1.71, 1.21, 0.99
"	1000°C	1.82, 1.70, 1.56, 1.11, 0.99

The Effect of Heating Deposits in Oxygen

The appearance of deposits which had been heated in a stream of oxygen for 15 minutes at 500°C was found to be similar to that of vacuum heated deposits. The diffraction patterns were now, however, much stronger and consisted of a series of spotty rings as shown, for example, in Plate 23. The d-spacings derived from these rings are given in Table XII and are found to correspond with those of Fe_3O_4 , showing that iron, from iron carbonyl impurity, is a constituent element in deposits from the α -radiolysis of impure CO. Since nickel carbonyl is also present during radiolysis,

PLATE 23

Diffraction pattern from deposit which has
been heated in oxygen.

The pattern corresponds to Fe_3O_4 .



a search for nickel or nickel oxide spacings was made but none was found. If nickel is in fact present in the deposits it is possible that it is converted, on subsequent oxidation, to the isomorphous substituted oxide NiFe_2O_4 . The d -spacings and the intensities of the rings of this oxide are very close to those of Fe_3O_4 (see Table XII), and with the selected area diffraction technique where an accuracy of 1-2 per cent is to be expected, it was not possible to distinguish between these oxides. On one occasion, after heating further to 650°C for 30 minutes, a diffraction pattern was obtained which corresponded to $\alpha\text{-Fe}_2\text{O}_3$ and again no evidence for nickel was obtained. These results suggest that nickel is absent or perhaps present in undetectable amounts in the deposits from CO containing both iron and nickel carbonyl impurities.

TABLE XII

<u>d-spacings from oxidised deposit</u>	<u>Fe_3O_4 spacings (A.S.T.M. Index)</u>	<u>NiFe_2O_4 spacings (A.S.T.M. Index)</u>
4.82	4.85	4.82
* 2.98	2.97	* 2.95
* 2.50	* 2.53	* 2.51
* 2.40	2.42	2.41
2.08	2.10	2.09
1.70	1.71	1.70
* 1.62	* 1.61	* 1.61
* 1.47	* 1.48	* 1.48
	etc.	etc.

* denotes strongest spacings.

(b) Deposits from CO containing nickel carbonyl impurity
(iron carbonyl removed by thermal decomposition)

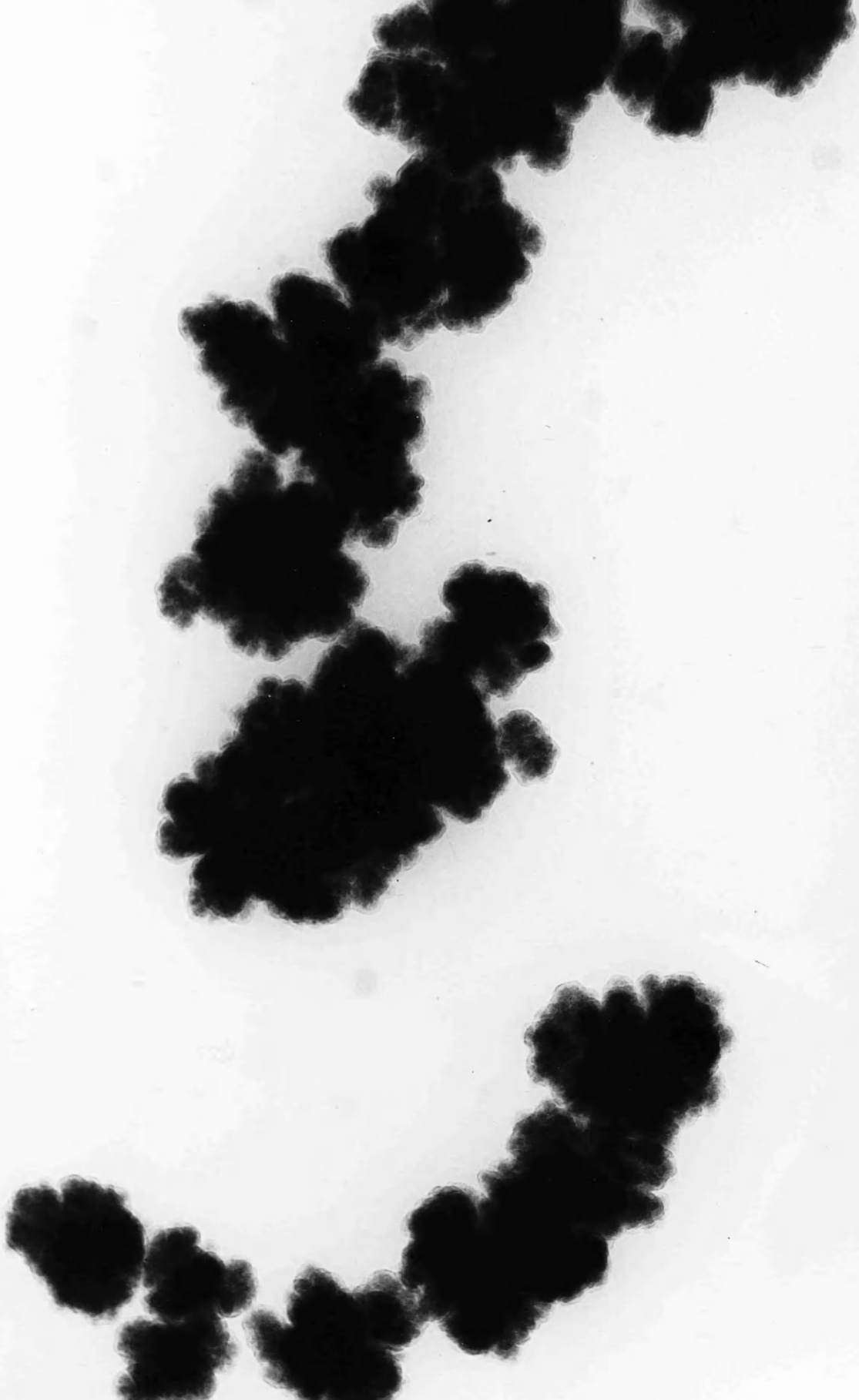
Earlier work has shown that deposits from CO purified of iron carbonyl react with moisture, unless rendered inactive by irradiation from the electron beam. Diffraction studies were therefore made of (i), inactive deposits and (ii) deposits which had subsequently reacted with water vapour.

(i) These deposits gave a similar diffraction pattern to deposits from CO containing both iron and nickel carbonyl impurity; this consisted of diffuse bands of no analytical significance. On heating in a vacuum (15 minutes at 500°C) a shrinkage of the particles was once again observed and is illustrated by micrographs of the same area before and after heating, Plates 24A and 24B respectively. The effect produced by heating was noted to be different from that of deposits from CO containing both iron and nickel as impurity (Plate 17B) and the dense regions were invariably smaller and more numberable than previously observed. This difference in appearance after heating suggests that the original deposits produced by the two grades of CO (i.e. CO of variable carbonyl content) are structurally different, as would be expected, since earlier observations of their behaviour towards water vapour revealed that one was reactive and the

PLATES 24A and 24B

Deposit from CO (containing nickel
carbonyl) before and after heating
in vacuum for 15 minutes at 500°C.

Magnification 100,000 X





other inert. The electron diffraction pattern (Plate 25) from areas such as in Plate 24B consisted of two fairly sharp bands only, which again contrasts with the spotty patterns from CO deposits containing iron.

(ii) Plate 26A shows a group of particles which have reacted with water vapour. After heating in a vacuum or in oxygen, the swollen regions shrink to form small dense particles as illustrated in Plate 26B. Now, by moving the electron microscope objective aperture to one side, it is possible to allow the diffracted beams from a crystalline specimen to form the image instead of the transmitted beams. The resulting picture is termed a dark field image and Plate 26C shows such an image from the particulate material in Plate 26B. Each bright streak represents a region of crystallinity and thus shows clearly that the particulate material is highly crystalline. There is no evidence of crystallinity in the background film. When the crystallites are heated further they grow in size as depicted in Plates 27A and 27B. Shadowing (Ni/Pd at 15°) establishes that the crystallites are small and flat having practically no visible shadow as can be seen from Plate 28. Folds in the background film are also revealed by the shadowing; these have formed during the drying out and decomposition of the swollen regions.

Specimens which were heated in oxygen (15 minutes at 500°C) gave strong diffraction patterns from the resulting

PLATE 25

Electron diffraction pattern from the
specimen depicted in Plate 24B.

PLATE 26A

A group of particles which have
reacted with water vapour.

Magnification 100,000 X

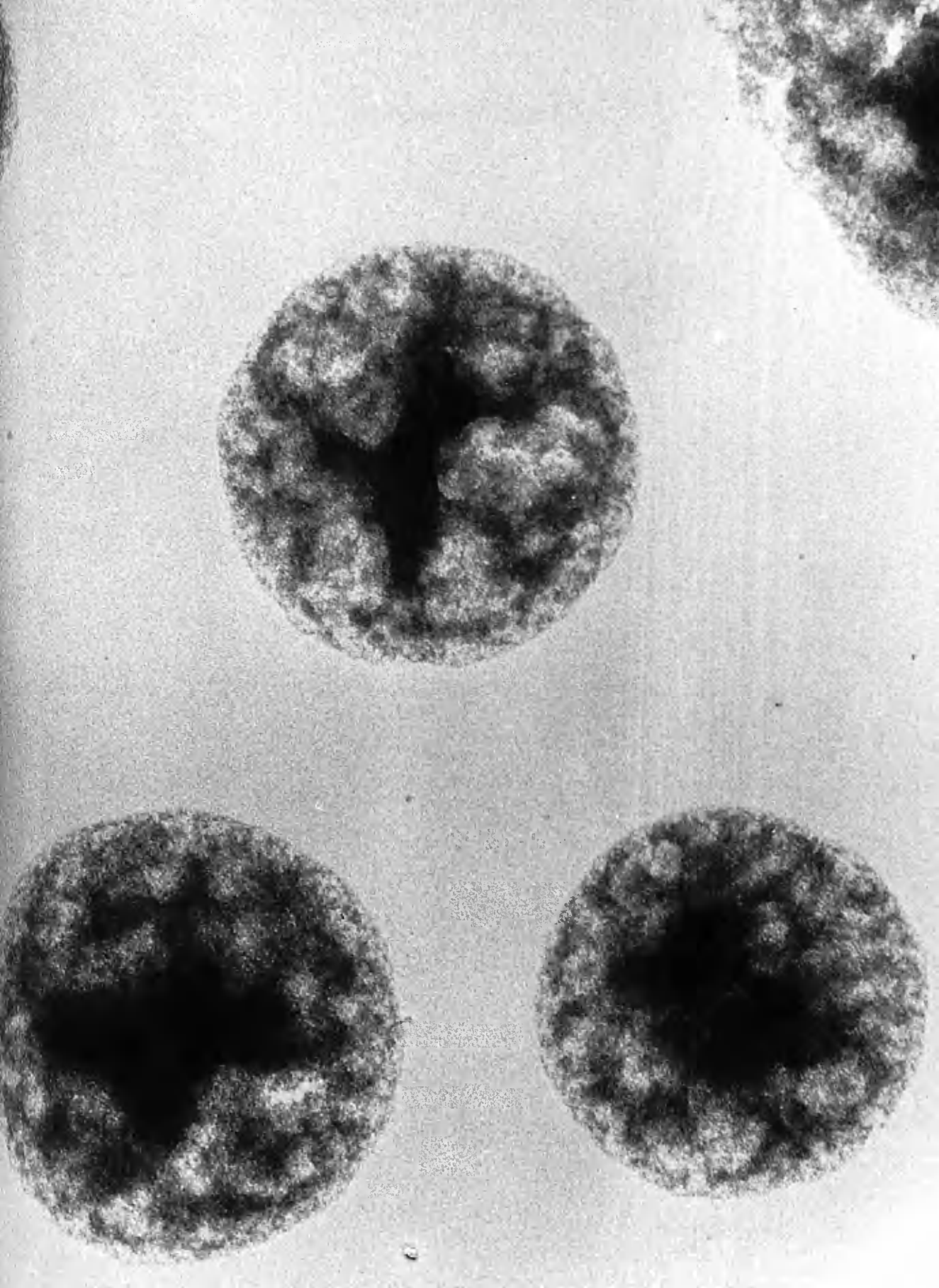


PLATE 26B

The same area as in Plate 26A after
heating in vacuum. Small
crystallites are now observed.
Magnification 100,000 X

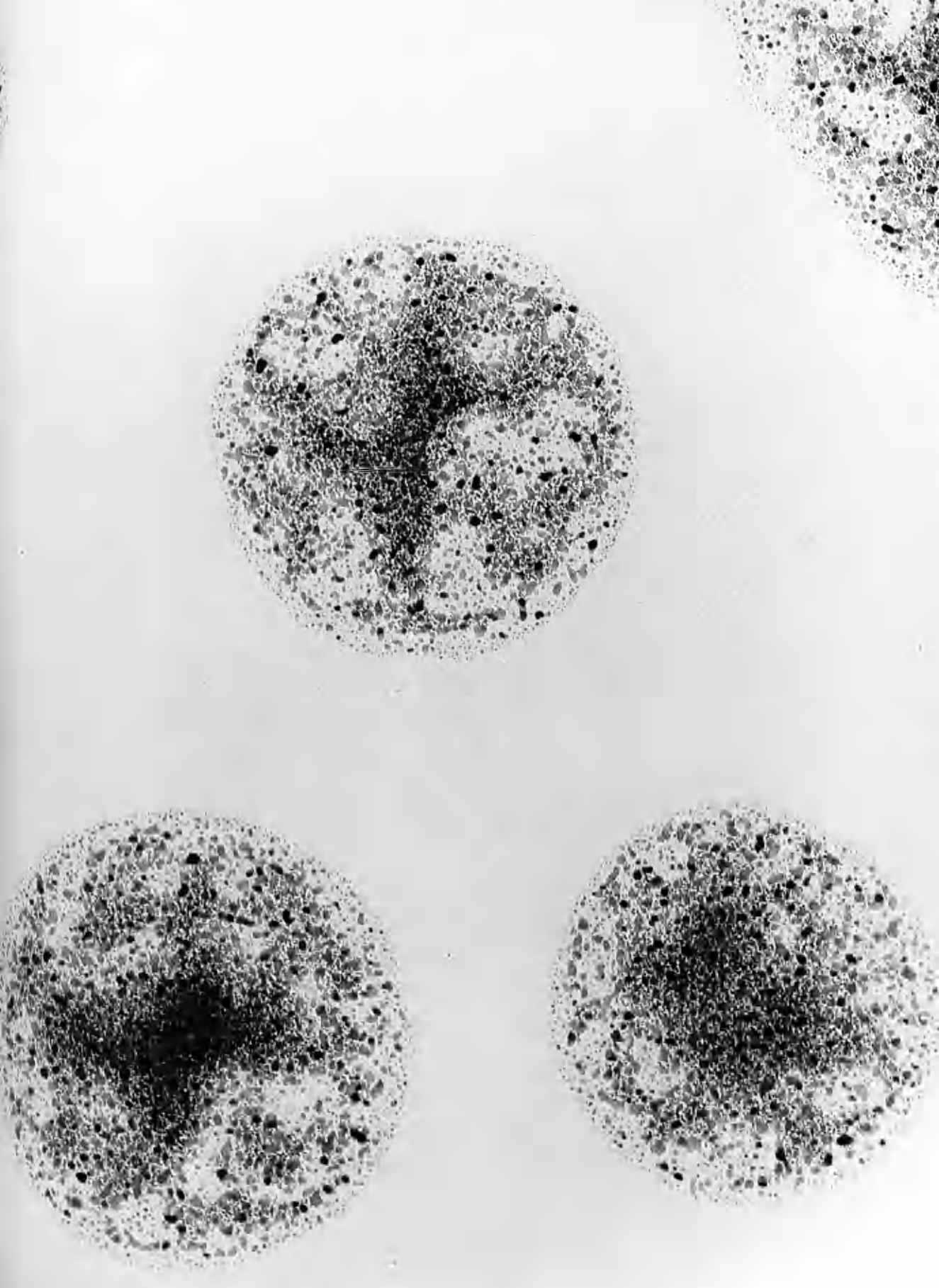


PLATE 26C

Dark field image from area in Plate 26B.

Magnification 100,000 X

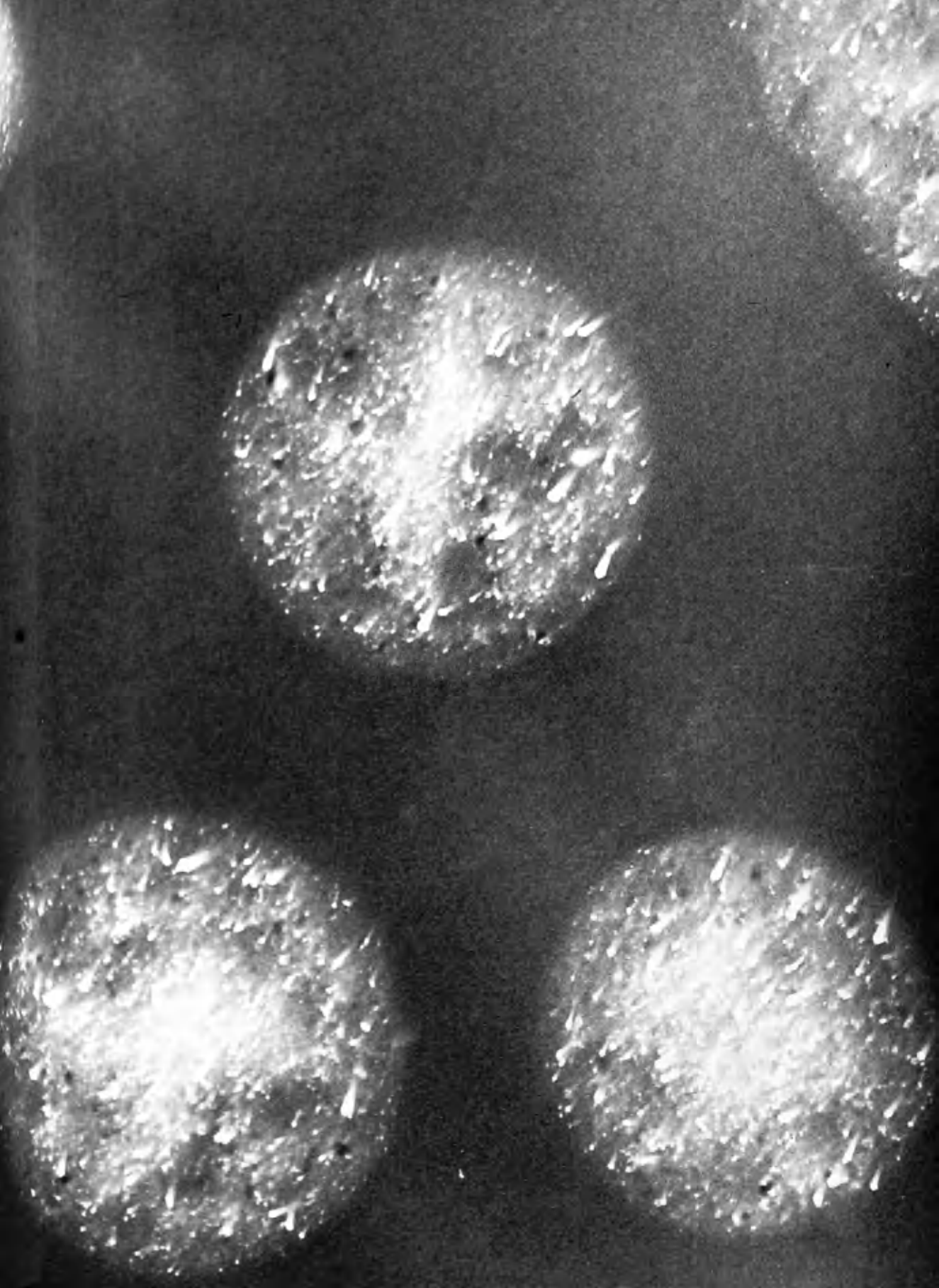


PLATE 27A

An area showing the crystallites in
vacuum-heated deposit.

Magnification 100,000 X

PLATE 27B

The same area after further heating.

The crystallites have grown in size.

Magnification 100,000 X

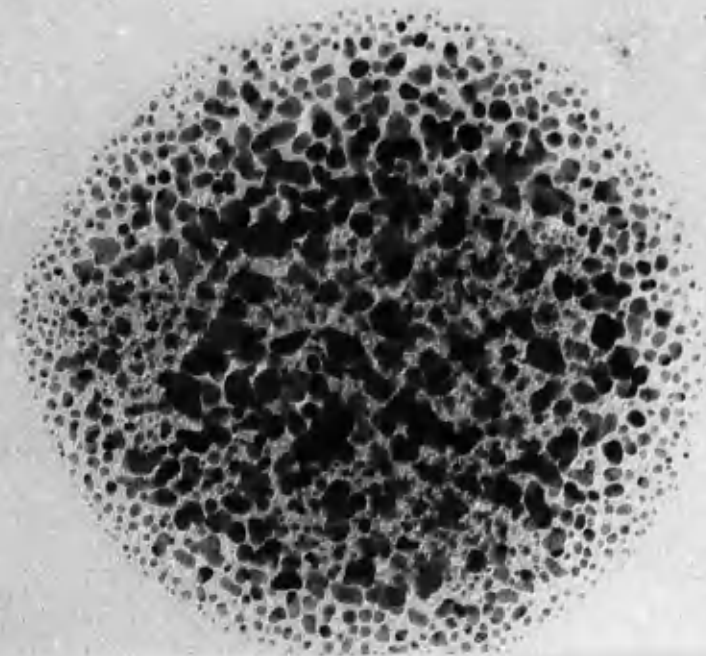
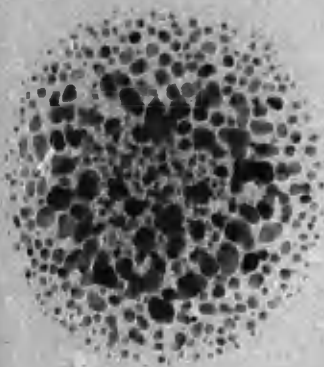
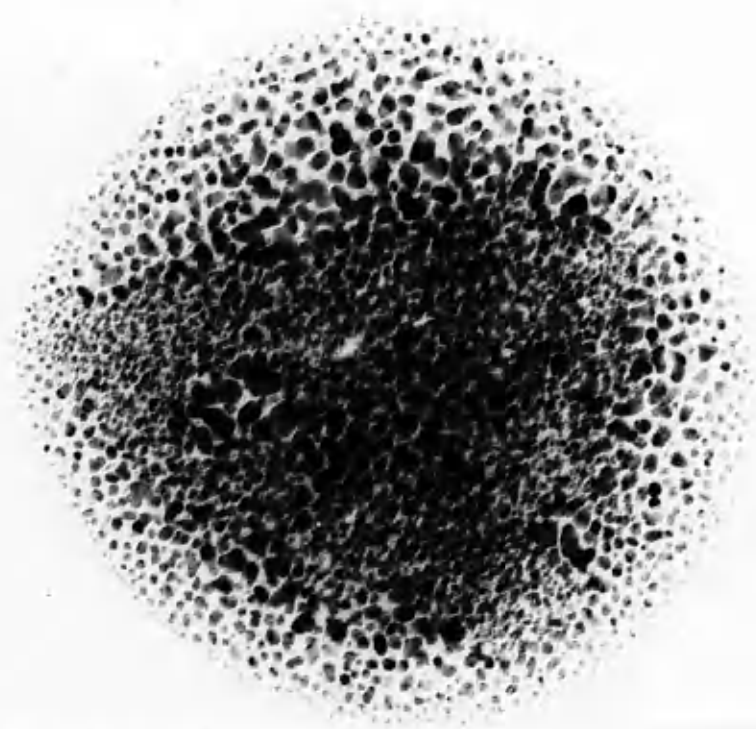
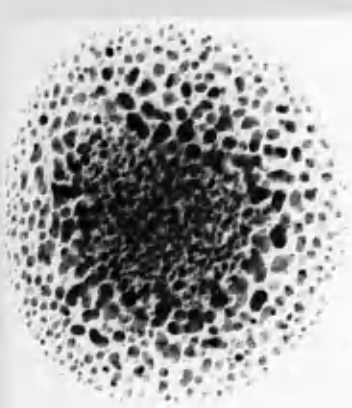
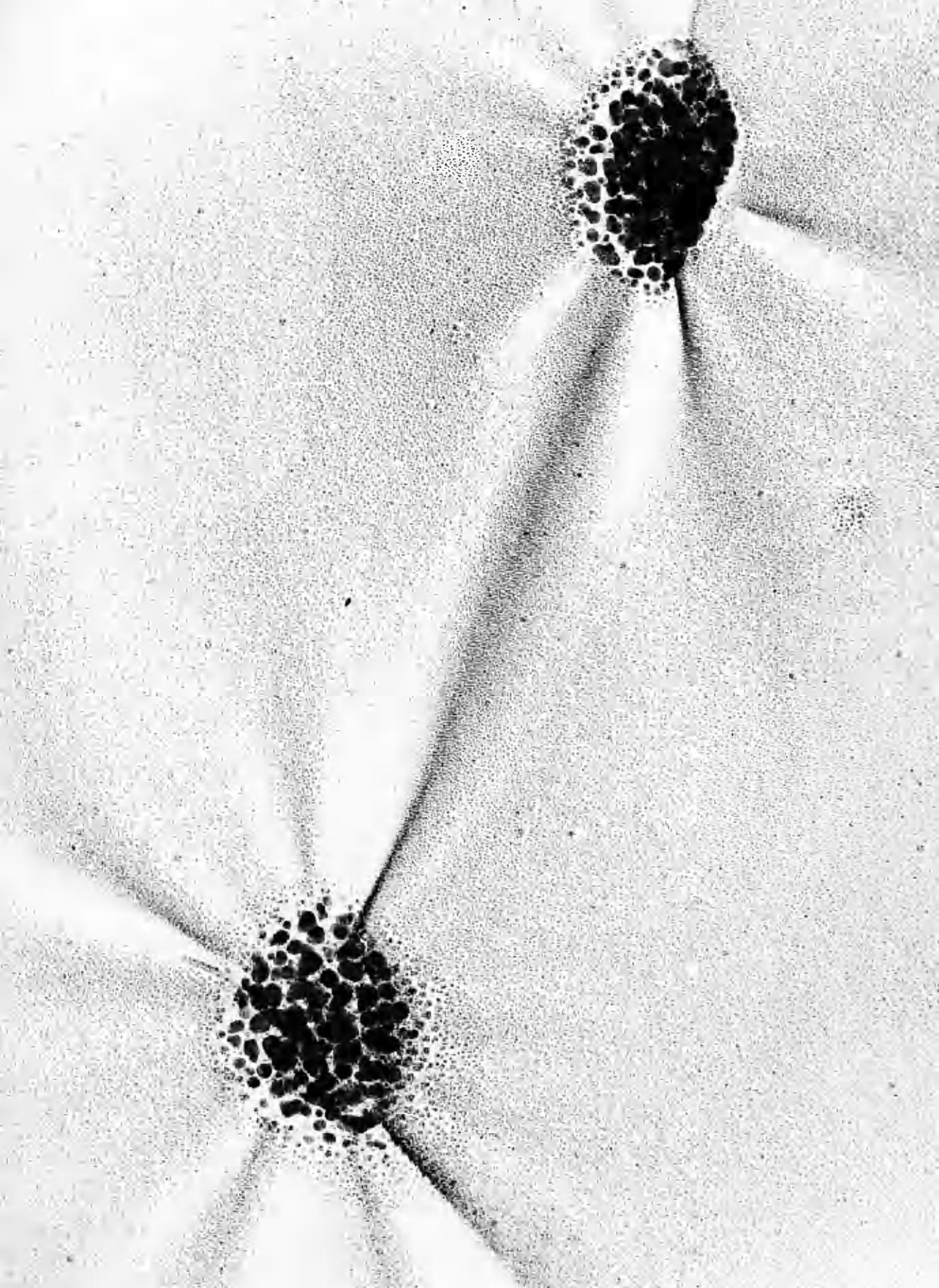


PLATE 28

Electron micrograph of shadowed
crystallites. Folds in the
background film are revealed.

Magnification 100,000 X



crystallites and consisted of spotty, concentric rings typical of a polycrystalline material. Measurements from the patterns showed that the crystallites were nickel oxide. The nickel in these deposits obviously arises from the nickel carbonyl impurity in the CO during radiolysis and its presence is analogous to that of iron from the iron carbonyl in the CO. The results from similar specimens on carbon support films which were heated under vacuum were initially confusing, since the diffraction patterns corresponded to nickel with one of the strong nickel oxide spacings also evident (Table XIII). On further heating the nickel oxide ring disappeared leaving only the nickel rings as illustrated in Plates 29A and 29B. The oxide ring at 'A' in Plate 29A is not observed after further heating (Plate 29B). The disappearance of the oxide ring was subsequently shown to be due to the chemical reduction of the oxide initially formed by the carbon support film and Plates 30A - 30D illustrate this effect.

TABLE XIII

Measurements from diffraction pattern shown in Plate 29A

<u>d-spacings (Å)</u>	<u>Ni spacings (A.S.P.H.)</u>	<u>Remarks</u>
2.00	2.034	
1.74	1.762	
1.45	-	NiO spacing (1.476 Å)
1.23	1.246	
1.05	1.062	
1.00	1.017	

PLATE 29A

Electron diffraction pattern from deposit heated under vacuum. The pattern corresponds to nickel with a nickel oxide ring also present at 'A'.

PLATE 29B

Electron diffraction pattern from the same specimen as above after further heating under vacuum. The nickel oxide ring has almost completely disappeared.

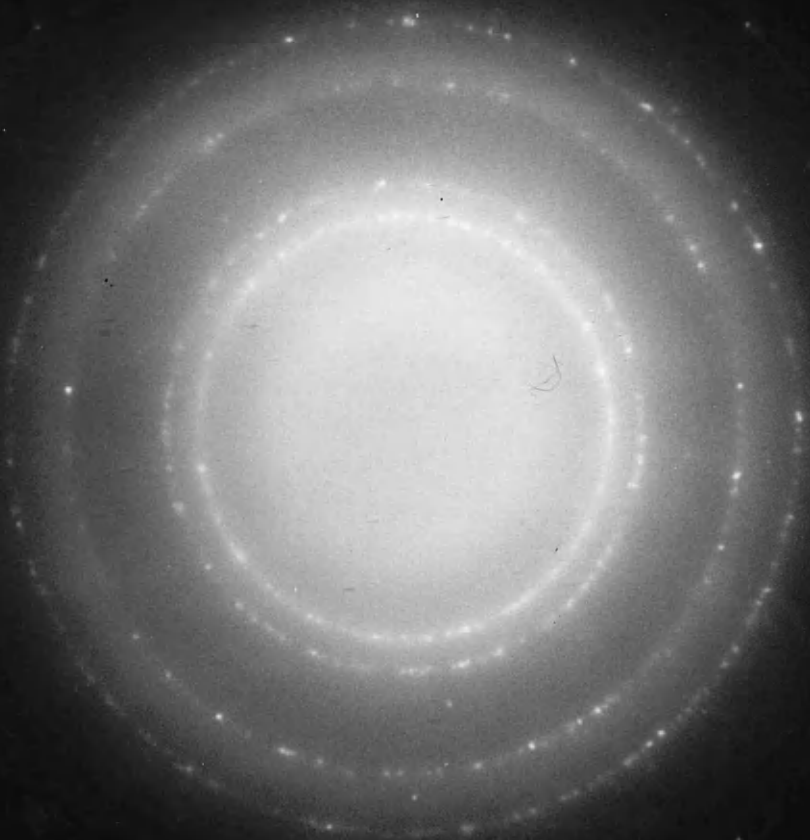
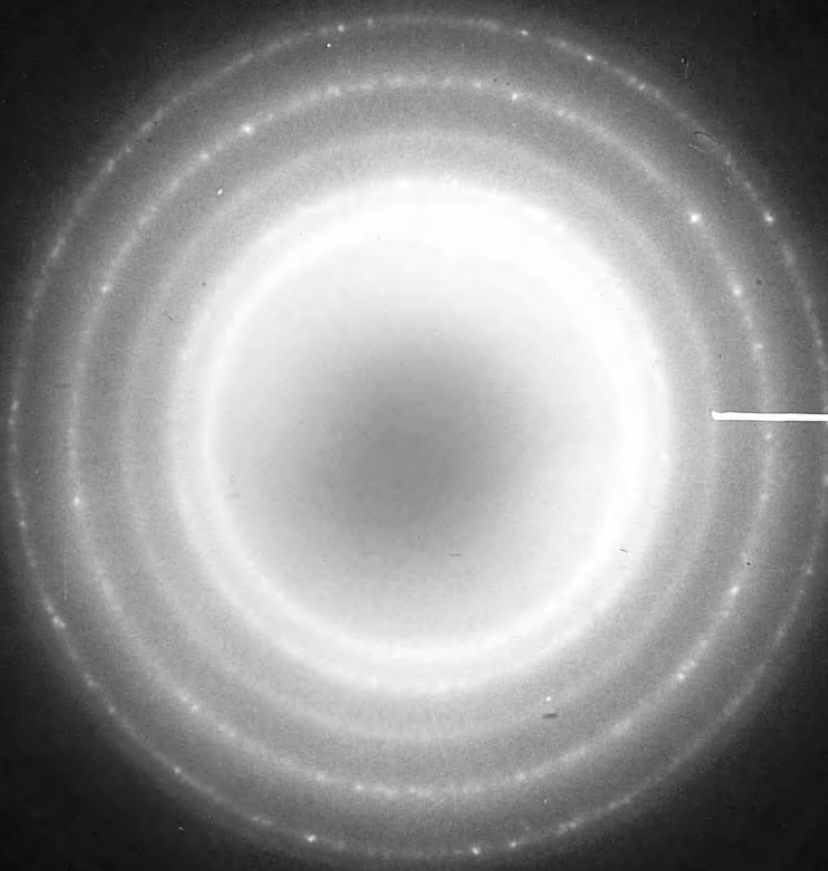


PLATE 30A

Crystallites of NiO
Magnification 100,000 X

PLATE 30B

Electron diffraction
pattern of NiO.

PLATE 30C

Crystallites after
heating in the
electron beam.
Magnification 100,000 X

PLATE 30D

Electron diffraction
pattern consisting of
NiO and Ni rings.

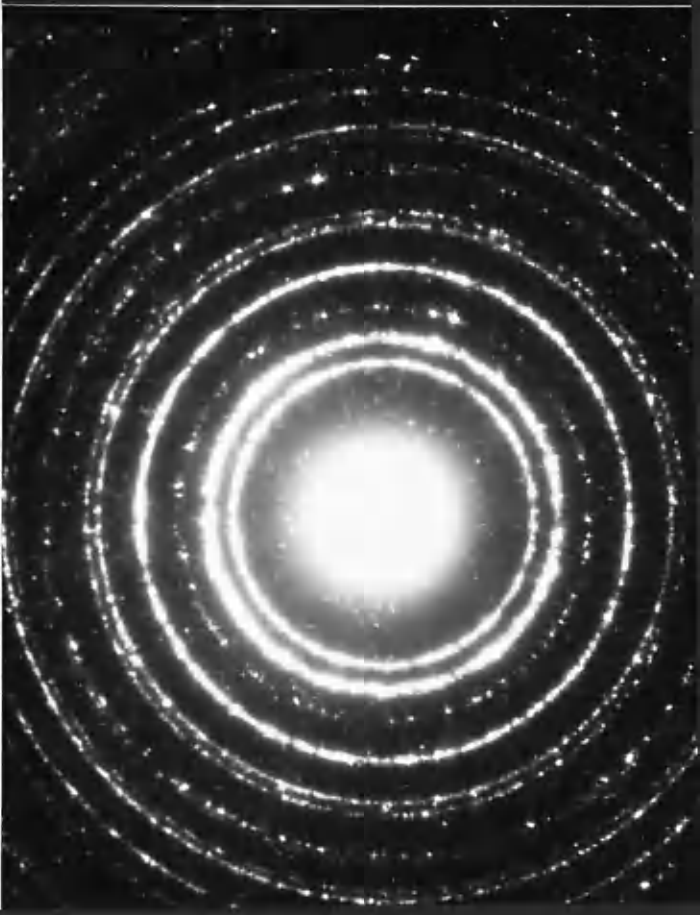
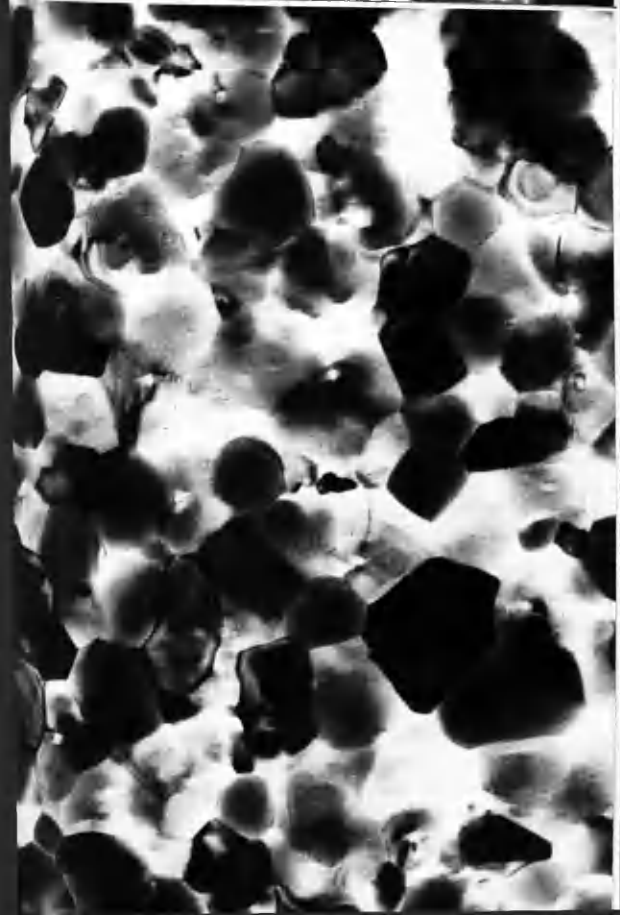
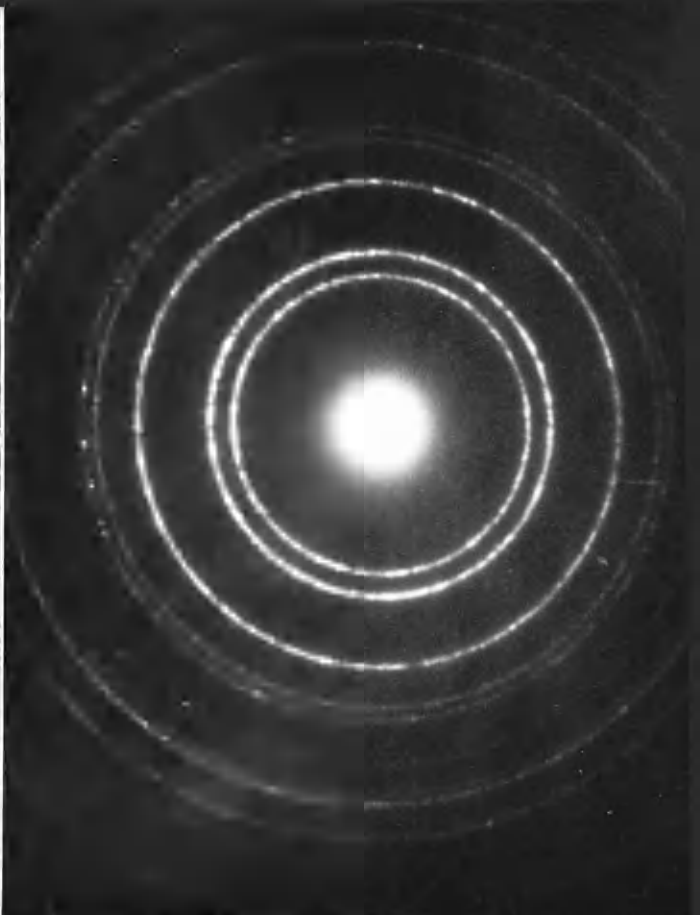
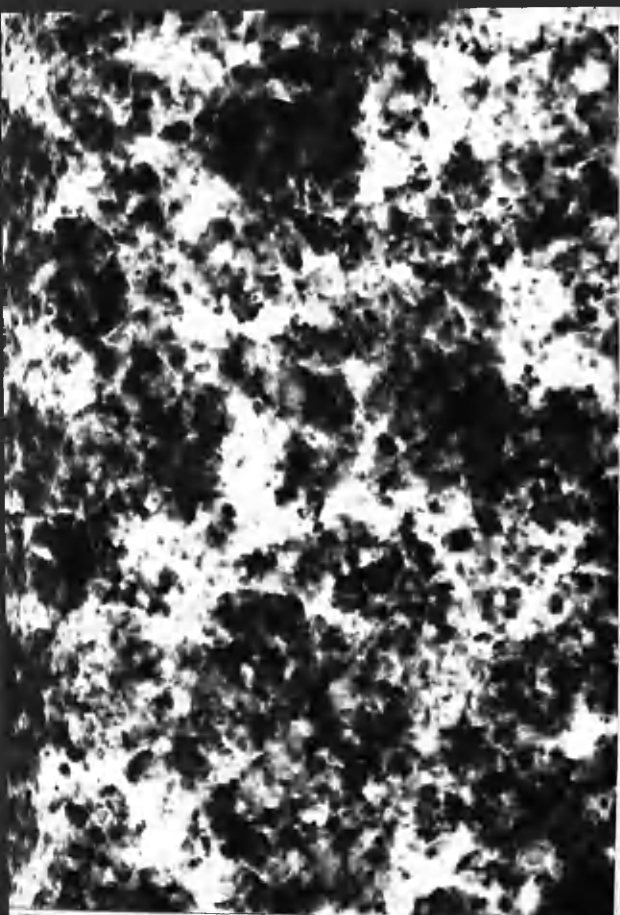


Plate 30A represents an area of nickel film which was evaporated on to a carbon support film and which was subsequently converted to the oxide by heating carefully in oxygen. The corresponding nickel oxide pattern is shown in Plate 30B. After inserting the specimen into the electron microscope and increasing the intensity of the electron beam, as was done to heat the deposit specimens, a sintering of the oxide was observed (Plate 30C). The corresponding electron diffraction pattern now consisted of nickel oxide rings together with four extra rings whose d -spacings corresponded to the four strongest values for nickel. This confirms the ability of the carbon film to act as a reducing agent in the electron beam.

10. Electron Probe Microanalysis

Investigations with the electron microprobe were undertaken with a view to gaining further information about the composition of the deposits from CO α -radiolyses. The main aim was to confirm the presence of iron and nickel in the deposits from CO which contained both these carbonyls as impurities. As mentioned in the last section, iron alone was detected by diffraction techniques when both carbonyls were present during radiolysis but it was possible that nickel escaped detection due to the formation of a complex oxide.

(a) Deposits from CO containing both iron and nickel carbonyls

Plate 31A is a comparatively low magnification micrograph showing the typical distribution of particles over the support film from an 18 hour radiolysis. When this specimen and others like it were examined with the Siemens spectrometer attachment, no signal for iron or nickel was obtained under any of the experimental conditions employed, showing that insufficient X-rays ($FeK\alpha$ and $NiK\alpha$) were being generated in the area irradiated by the electron beam ($\sim 2-10 \mu$ dia. beam probe) to allow detection. The particles were therefore concentrated into a smaller area by spraying water on to the specimen grid from a commercial atomiser. The coagulation which occurred is shown in Plate 31B. On subsequent examination, weak peaks for $FeK\alpha$ radiation appeared at the appropriate angle, the strength of the signal depending on the number of particles being irradiated by the probe. Fig. 24 shows two negative results (runs 1 and 2) from areas containing only a few particles whereas run 3 gives a positive result for Fe from the area shown in the attached micrograph ($\times 10,000$). No nickel was detected in this area nor in any of the other regions which gave a positive signal for iron. A scan through the appropriate angles was made for other elements, for example, chromium, manganese, tungsten, molybdenum, mercury and sulphur, but none was detected.

PLATE 31A

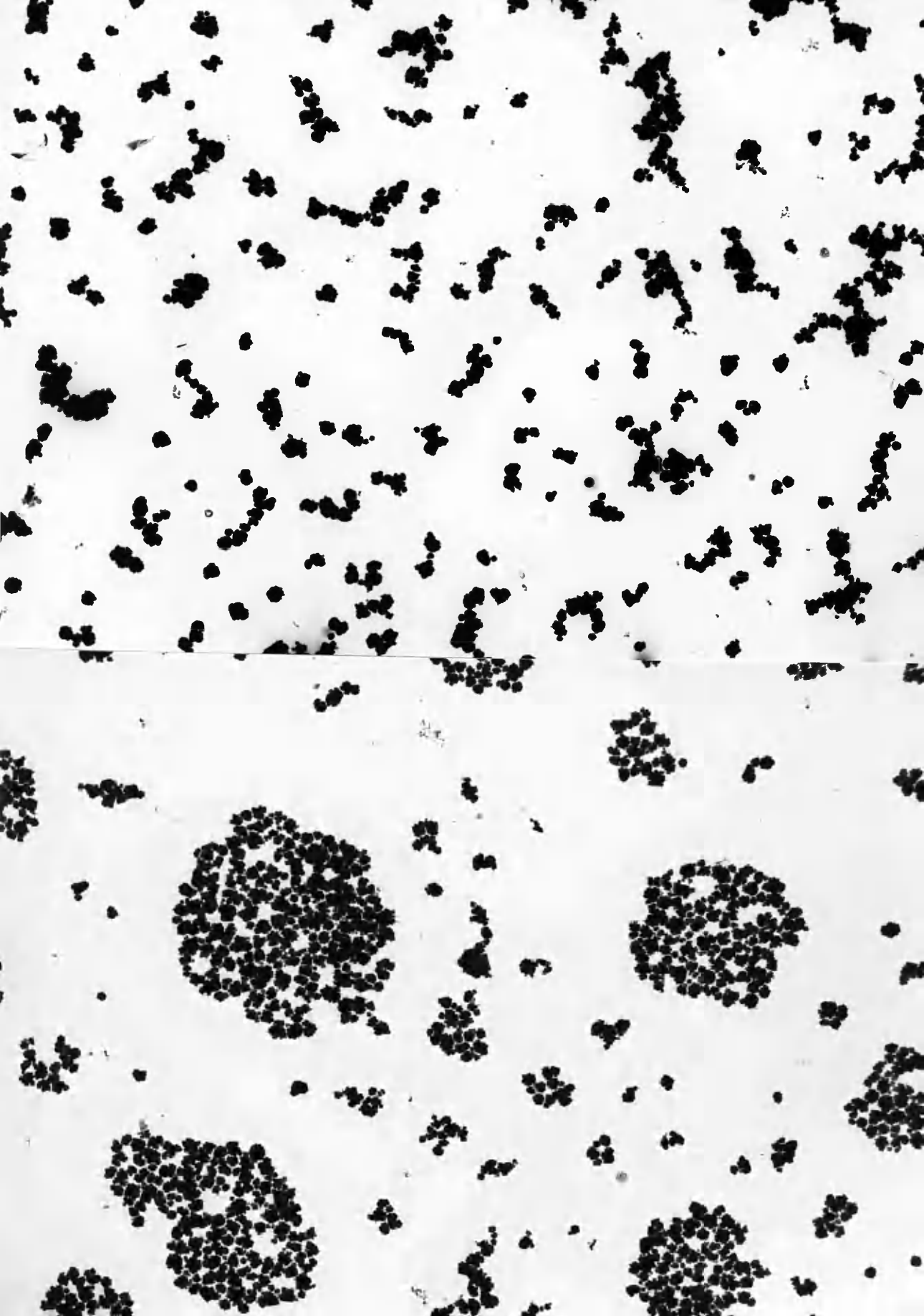
Low magnification micrograph showing the
distribution of particles over the support film.

Magnification 10,000 X

PLATE 31B

Particles which have been coagulated on
the support film.

Magnification 10,000 X



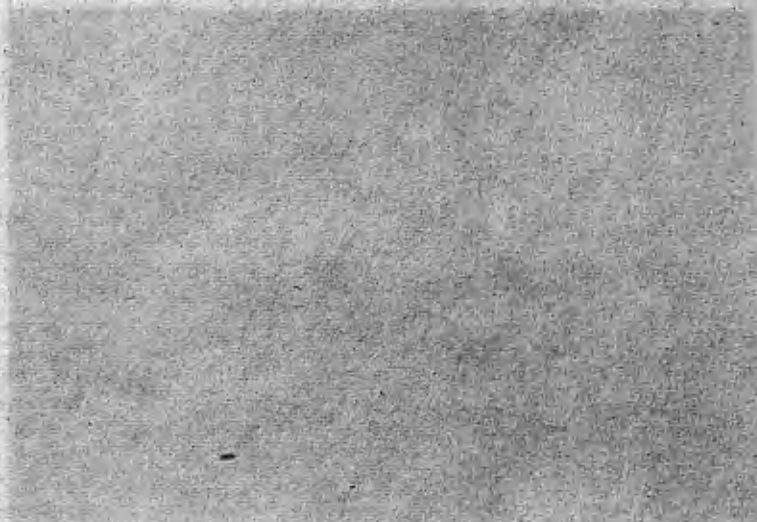


FIGURE 24

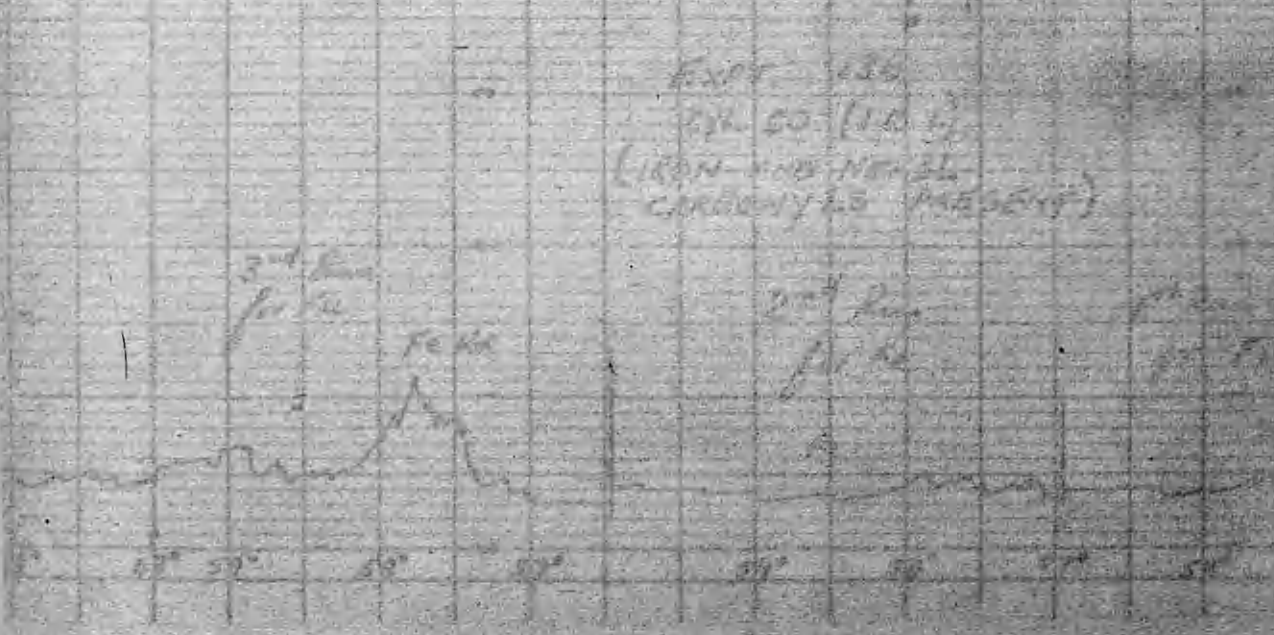


FIG. 24. ELECTRON MICROSCOPE SCAN OF DEBRIS FROM Fe-50 CONTAINING BOTH IRON AND ALKYL CARBOXYLS DEBRIS.

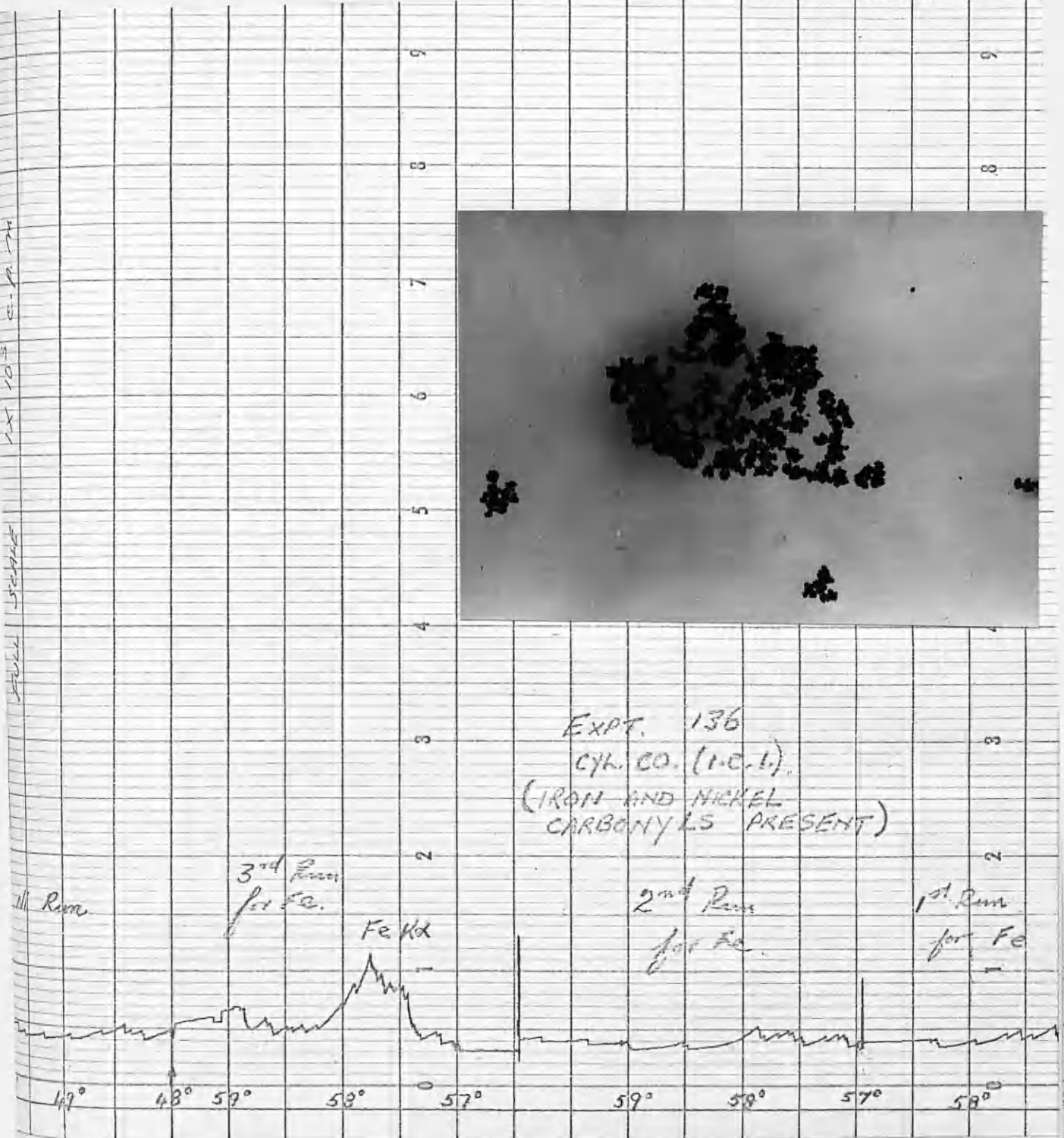


FIG. 24. ELECTRON MICROPROBE SCAN OF DEPOSITS FROM CO CONTAINING BOTH IRON AND NICKEL CARBONYL IMPURITY.

(b) Deposits from CO containing nickel carbonyl
(iron carbonyl removed).

These deposits were concentrated in the same way as before and as expected the particles reacted with the water during the coagulation process. Fig. 25 is the trace obtained from the area in the attached micrograph and a peak for nickel is observed. Other elements, including iron, were not detected.

S.E.M.2 Results

The results of the above investigations with the Siemens attachment were confirmed by S.E.M.2 studies, i.e., iron or nickel was found in deposits but not both together. In addition, carbon was detected in deposits which contained iron. The intensity of the signal for $CK\alpha$ radiation when compared with the corresponding peak for $FeK\alpha$ from the same area, suggested that there was a greater concentration of carbon in the deposit than iron (Wright, 1967). Again the signals were rather weak. A search for oxygen was made on a different specimen (on a carbon support film) but this was not detected.

Deposits in which nickel was found probably decomposed, when under examination with the probe, with the loss of volatiles and no carbon or oxygen was detected.

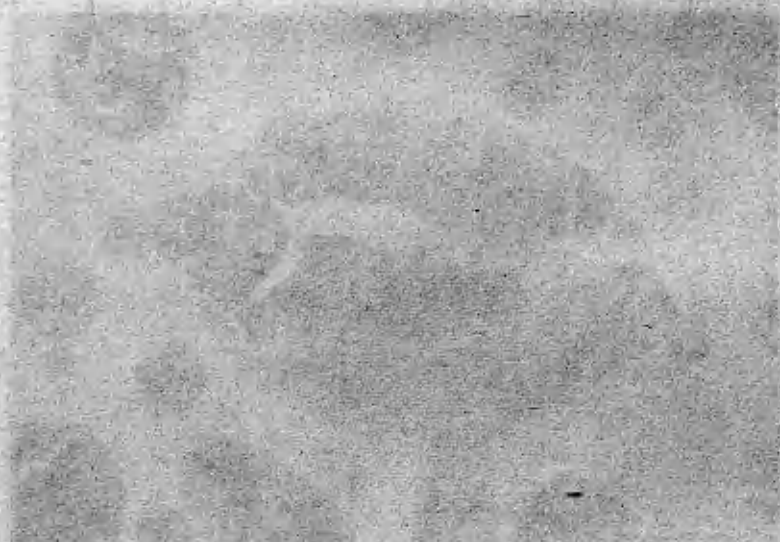


FIGURE 25

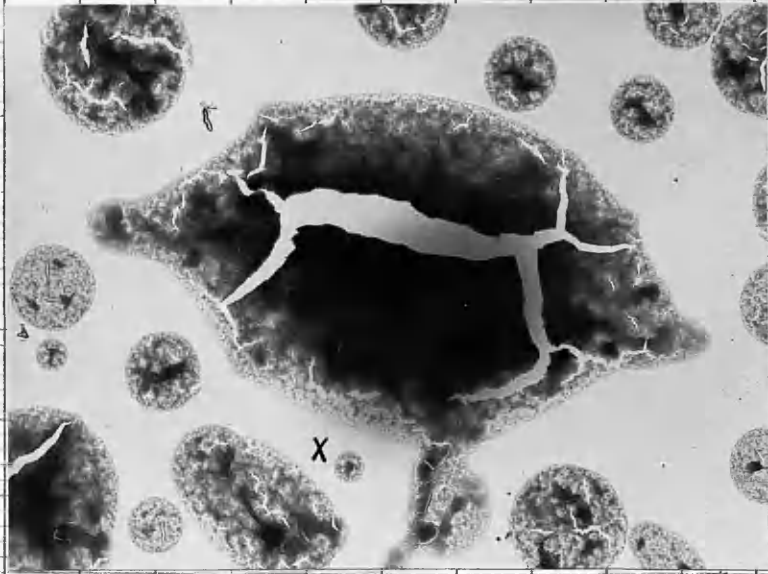
[Faint, illegible handwritten text]



FIG. 25. ELECTRON MICROSCOPE PHOTOGRAPH OF A PARTICLE
CONTAINING MERCURY SULFIDE SPHERULE.

FULL SCALE 1 X 10⁴ C.P.M.

5
8
7
6
5
4
3
2
1



EXPT. 161
(NICKEL CARBONYL
ONLY PRESENT)

P₂ Run

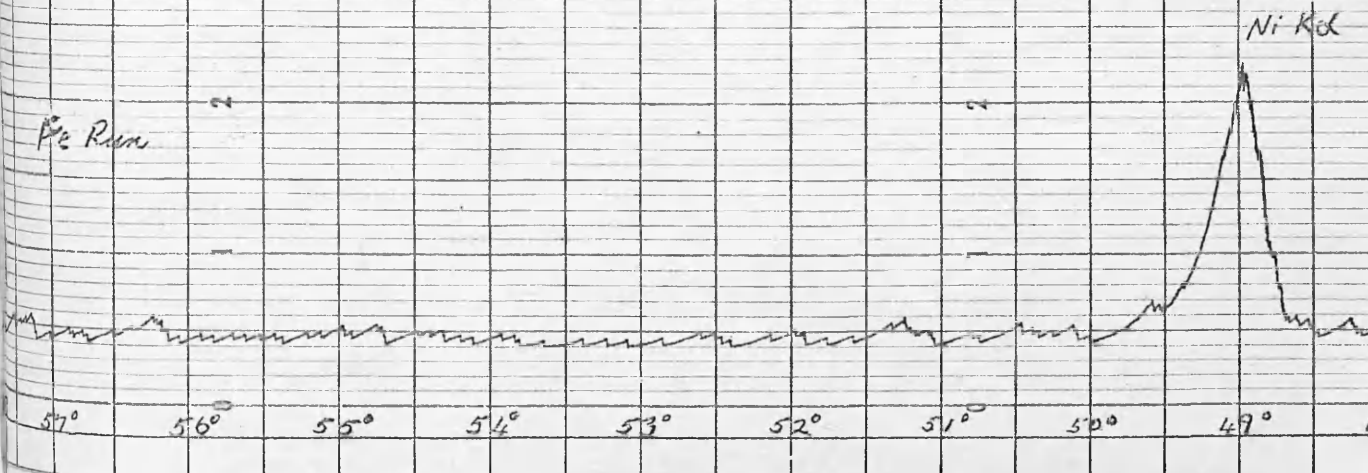


FIG. 25. ELECTRON MICROPROBE SCAN OF DEPOSITS FROM CO CONTAINING NICKEL CARBONYL IMPURITY.

Examination of Larger Sample

The results of the microprobe studies described so far were obtained from samples whose total weight spread over a 3 mm grid was probably about 1 μ g.

The 2 mg sample of deposit which was collected for infrared analysis, yet to be described, was subsequently subjected to microprobe analysis for iron and nickel. The sample in the form of a KCl micro-disc was coated with a thin layer of aluminium to prevent charging-up effects in the beam. The instrument used for this work was the S.E.M.2 (National Engineering Laboratories, East Kilbride).

Plate 32A is an electron optical picture (X 15,000) of the deposit (dark regions) embedded in the KCl. Plate 32B is an X-ray distribution picture for FeK α radiation from the same area and shows a concentration of emission centres in the dark regions. A line trace for iron was made across AB in Plate 32C and a fairly intense peak for iron is observed. No nickel was detected on tracing across AB.

11. Experiments Within the Irradiation Zone of the α -Source

All the experiments described so far were conducted with the specimen collecting grids placed outside the zone which is irradiated by the α -particles, and the deposit which was collected was shielded from further irradiation. These deposits were shown to be of an amorphous nature and the

PLATE 32A

Electron picture of deposit embedded in KC₂

Magnification 1,500 X

PLATE 32B

X-ray distribution picture of same area as above.

Magnification 1,500 X

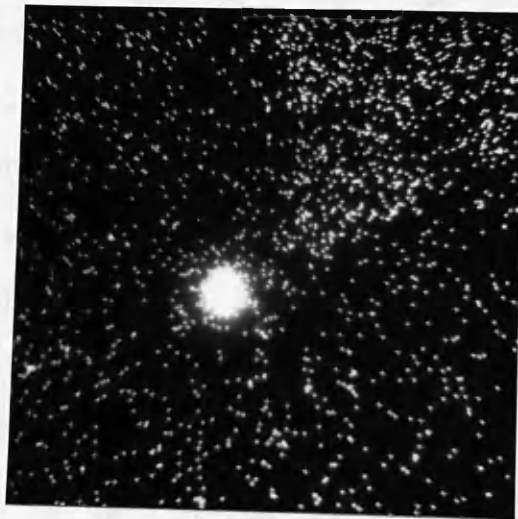
PLATE 32C

Line trace through AB.

Magnification 1,500 X



(a)



(b)



(c)

electron diffraction work revealed little information about their structure.

Experiments were subsequently made with the specimen grids placed inside the irradiated volume to observe any effect of secondary α -radiation on the solid deposit. It was hoped that the structure of the solid might rearrange - as did the solids from the α -radiolysis of hydrocarbons - to one which would give an electron diffraction pattern, or that the solid would grow on the surface of the support film rather than in the gas phase as normally occurred. The usual position of the specimen grid is 9 mm below the base of the α -source, outwith the irradiated volume. Specimen grids were subsequently placed 1 mm from the base of the source and also in the centre of the source and radiolysis of CO was allowed to proceed as before. In both cases the solid which was collected resembled in appearance the typical gas phase deposit obtained at 9 mm from the base and the average particle size remained at about 2,500 Å diameter. Variation in the metallic carbonyl content of the CO resulted in the formation of the two distinct types of deposit previously observed. The quantity of solid which was collected on the grid was found to decrease as the grid was placed higher into the α -source and was approximately proportional to the volume of gas being irradiated directly above the grid. Table XIV gives the relevant data.

TABLE XIV

Relationship between yield of solid and irradiated volume
(All yields quoted are for 18 hour experiments.)

<u>Specimen-source distance</u>	<u>Average particle density cm⁻²</u>	<u>Irradiated volume</u>
9 mm	1.7 x 10 ⁸	~ 90 mm ³
1 mm	1.0 x 10 ⁸	~ 60 mm ³
Centre	0.9 x 10 ⁸	~ 45 mm ³

The only different effect that was noted in these experiments was that the carbon support film was grainier than usual and appeared to be covered with minute ($\sim 30 \text{ \AA}$) particles. It was possible that these were a genuine product of the radiolysis and not an artefact and were perhaps a precursor to the formation of the large gas phase deposit particles. Adamson, Dawson, Feates and Sach (1966) who found fine particulate material on graphite specimens irradiated by ultraviolet light in the presence of various mixtures of CO₂, CO and CH₄, believed that gaseous species held at surface sites on the graphite were being decomposed by the radiation to give the observed solids. It was therefore decided to investigate the effect of α -radiation on CO in the presence of various graphite specimens held within the irradiation zone.

Plate 33A is a typical micrograph of a thin area of a graphite flake. This specimen was subjected to α -radiation

PLATE 33A

Electron micrograph of thin flake of graphite.

Magnification 100,000 X

PLATE 33B

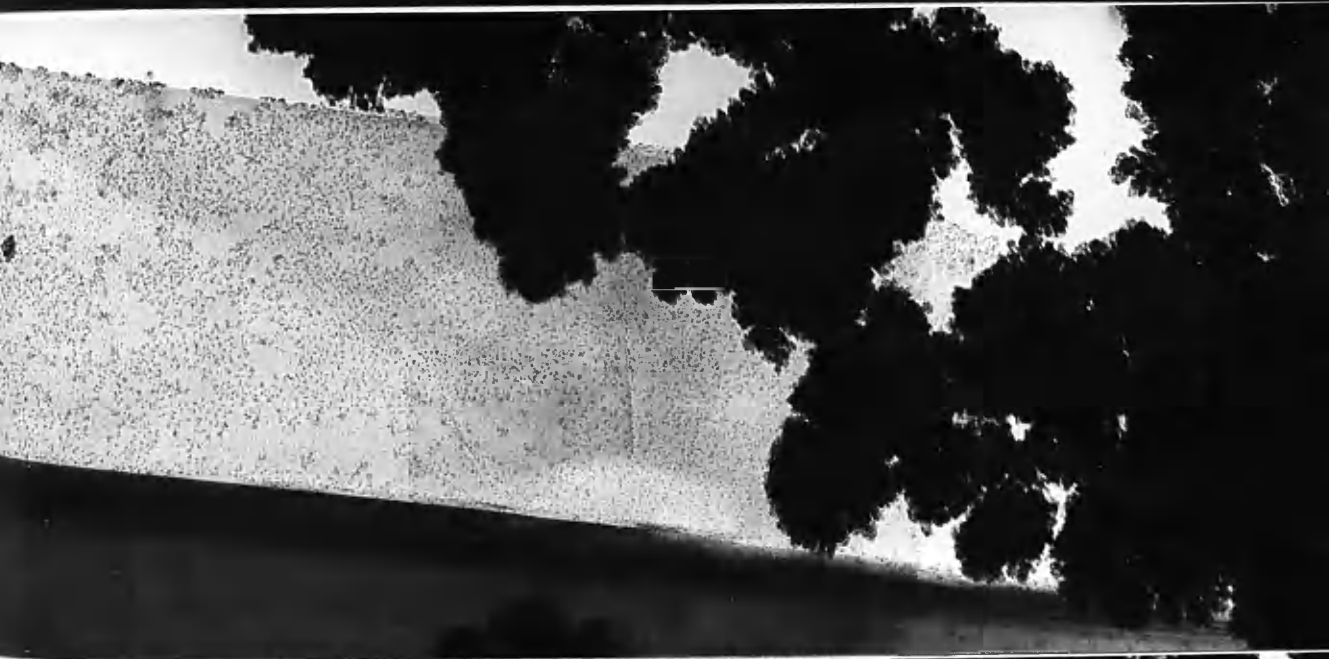
Same area of graphite after irradiating in CO
for 65 hours.

Magnification 100,000 X

PLATE 33C

Same area after exposure to the atmosphere for
48 hours.

Magnification 100,000 X



in one atmosphere pressure of CO for 65 hours. Re-examination of the same area (Plate 33B) showed that in addition to the usual gas phase deposit particles there were now very small ($\sim 30 \text{ \AA}$) particles on the graphite surface; these were also observed on the background film but do not show up well in this particular series of plates because the graphite is lying at an angle to the support film. The particles on the background were randomly distributed whereas on the graphite some arrangement appeared to have occurred. The specimen was then exposed to the atmosphere for 48 hours and then examined once more. Plate 33C illustrates that little has happened in the interval. However, areas which were not previously photographed were found to have changed in appearance. In Plate 34A, for example, it is observed that the particles have apparently reacted with moisture and have begun to crystallise out under the influence of the electron beam. The dark field image (Plate 34B) shows that some of the small dense particles are in fact crystalline. Electron diffraction patterns were taken from this crystalline material and measurements corresponded to nickel. Plate 35 is a typical pattern from the particles on the background film and the actual area giving these rings is shown. Patterns taken from graphite surfaces were confused by the contribution from the graphite itself but it was just possible to distinguish the nickel rings.

PLATE 34A

Surface deposits which have apparently
reacted with moisture.

Magnification 100,000 X

PLATE 34B

Dark field image from Plate 34B.

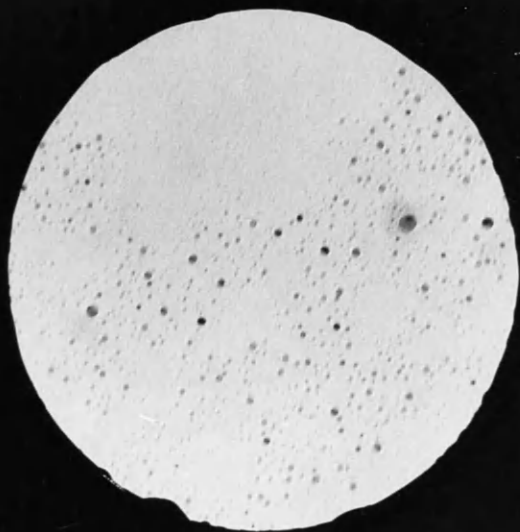
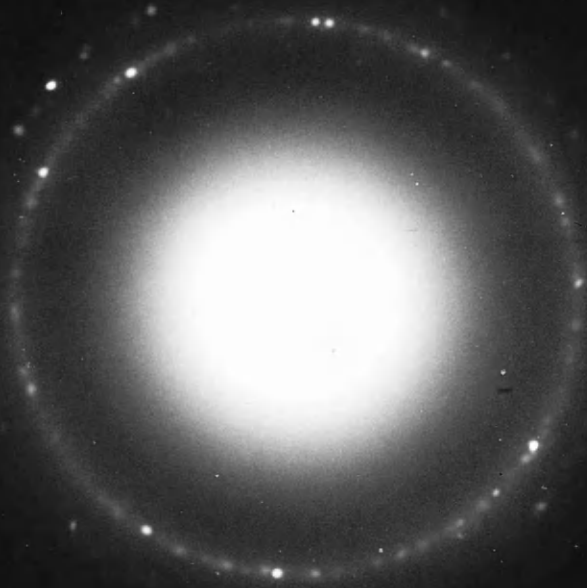
Magnification 100,000 X



PLATE 35

Electron diffraction pattern from the small
particulate material on the support film.

The pattern corresponds to nickel.



These surface deposits are therefore characteristic of the large gas phase deposits formed from iron-free CO inasmuch as they changed on exposure to the atmosphere and contained nickel. It was found that the surface deposits were hygroscopic even when depositions were performed with CO containing iron carbonyl impurity and this strongly suggests that they are formed by a surface reaction rather than in the gas phase, otherwise iron would surely have been incorporated into the solid which would consequently be inert. It appears that the CO is held at specific sites on the graphite surface and is subsequently decomposed to give the fine deposits. In order to substantiate the above suggestion radiolyses were performed using three types of graphite whose surface properties varied as a consequence of the 'defect' content inherent in the graphite. The 'defect' content constitutes step edges, vacancies, interstitials and dislocations and these can vary according to the treatment received by the graphite during its formation or from subsequent treatment. Plate 36A shows a flake of graphite (P.G.A.) which has been neutron irradiated (4×10^{20} n/cm²) and subsequently decorated with silver. The silver particles are distributed at random both on the background and to a lesser extent on the graphite surface. The vacancies on the surface produced by the neutron irradiation tend

to act as 'sinks' for the silver particles which are held at some of these sites and at other 'defects' on the surface. Similar specimens when subjected to α -radiation in the presence of CO give a similar distribution of particles on the surface, for example, Plate 37A.

P.G.A. and SP1 specimens when decorated with silver showed some lining-up of particles mainly along flake edges as shown in Plates 36B and 36C respectively. Similar specimens after α -irradiation in CO also showed a tendency for the particles to arrange on the surface (Plates 37B and 37C).

It was possible to count, approximately, the number of surface particles in a given area of a high magnification micrograph (X 200,000) which thus gives a measure of the surface particle density per unit area. Table XV lists the densities found on decorating and radiolysing the three types of graphite.

TABLE XV

Particle densities for radiolysed and decorated graphites

Graphite	Radiolysed		Decorated	
	Graphite surface density/cm ²	Background density/cm ²	Graphite surface density/cm ²	Background density/cm ²
Neutron irradiated	23 x 10 ¹¹	17 x 10 ¹¹	4.45 x 10 ¹¹	6.4 x 10 ¹¹
P.G.A.	19 x 10 ¹¹	17 x 10 ¹¹	2.6 x 10 ¹¹	6.2 x 10 ¹¹
SP1	8.7 x 10 ¹¹	15.6 x 10 ¹¹	1 x 10 ¹¹	4 x 10 ¹¹

PLATE 36A

Neutron irradiated graphite decorated with silver.

Magnification 100,000 X

PLATE 36B

P.G.A. graphite decorated with silver.

Magnification 100,000 X

PLATE 36C

SP1 decorated with silver.

Magnification 100,000 X

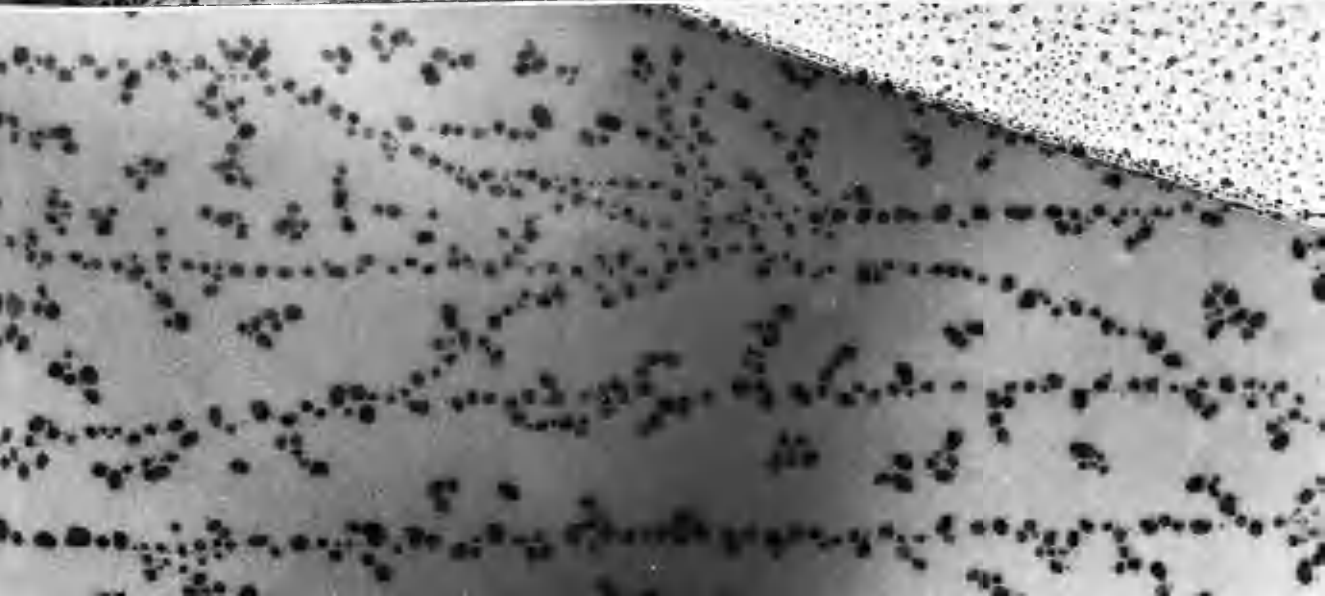
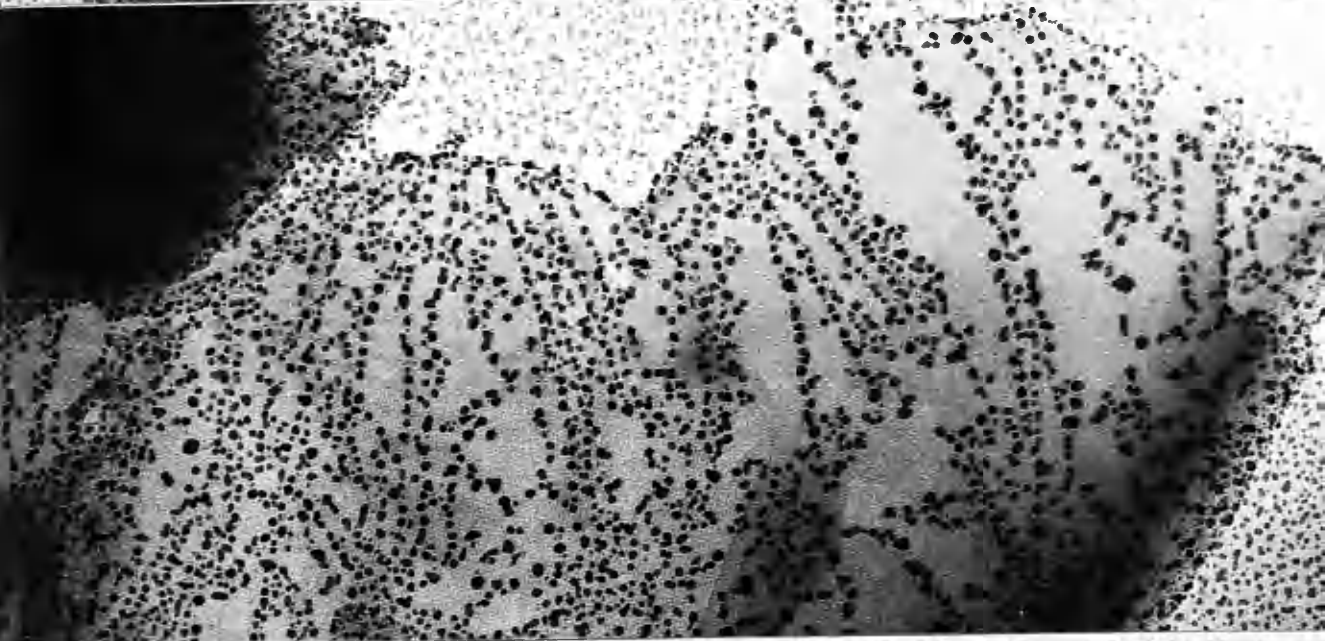
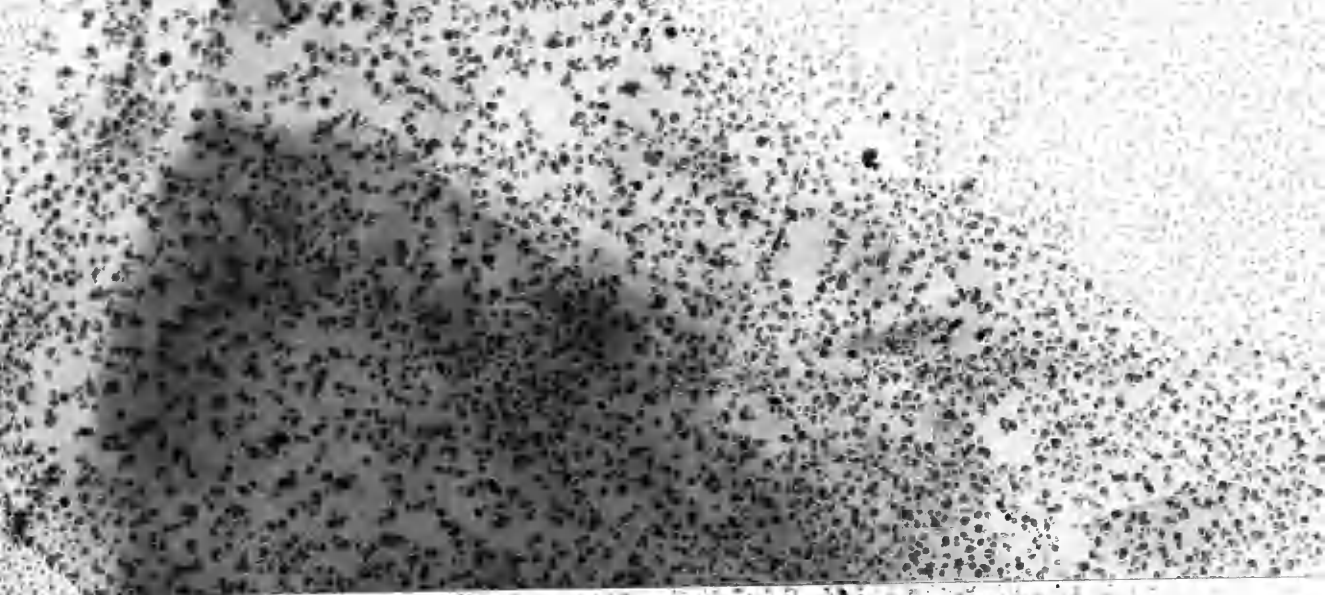


PLATE 37A

Neutron irradiated graphite exhibiting surface
deposits after radiolysing in CO.

Magnification 100,000 X

PLATE 37B

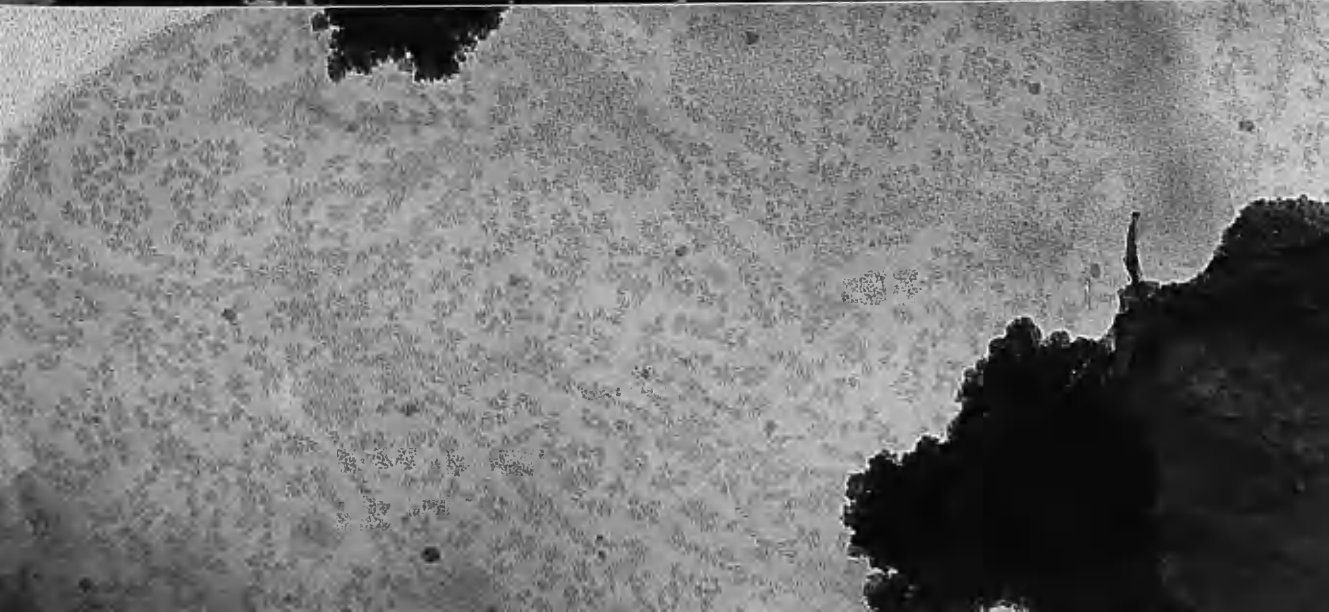
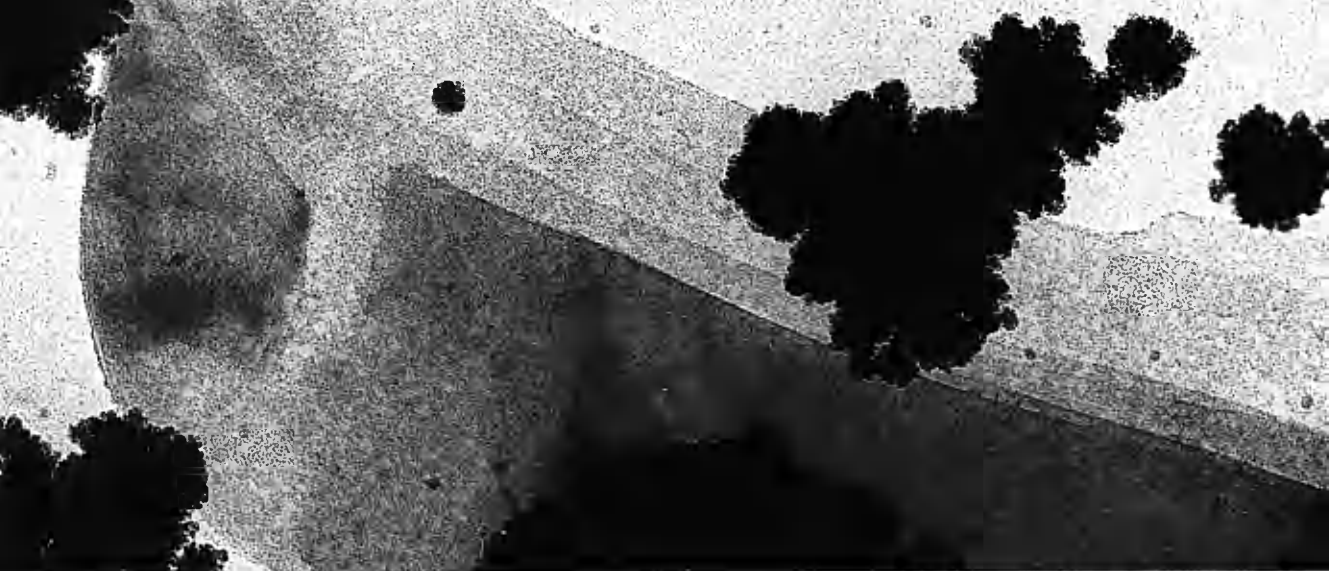
P.G.A. graphite showing some alignment
of the surface particles.

Magnification 100,000 X

PLATE 37C

SP1 graphite similarly radiolysed in CO.

Magnification 100,000 X



On dividing the number of particles found on the surface by the number found on the background, the ratios for the radiolysed samples work out at $1:2:2.8 \equiv \text{SP1:P.G.A.}:$ neutron irradiated P.G.A. and for the silver decorated specimens they are $1:2.16:2.77 \equiv \text{SP1:P.G.A.}:$ neutron irradiated P.G.A. This similarity in the particle distribution on the graphite surfaces strongly suggests that the surface deposits from the radiolysed samples are formed by a surface reaction rather than by a gas-phase process.

The ratio $1:2:2.8$ did not always strictly hold and the values given are the averages of a large number of measurements. The number of particles on the neutron irradiated graphite was, however, always greater than found in the other two graphites but sometimes there were more particles on the SP1 than on the P.G.A. samples and sometimes no surface deposit was observed in some areas of the radiolysed specimens. Graphite specimens prepared by a dry technique gave similar particle counts after radiolysis to those prepared by the wet ultrasonic method.

The size of the particles remained approximately the same in all three radiolysed samples whereas in the silver decorated samples the average size increased as the particle count decreased due to combination of the particles which are mobile at the temperature of decoration. Graphite

specimens placed in the usual position 9 mm from the base of the α -source, i.e., outwith the irradiation zone, did not show any surface deposits after CO radiolysis.

12. Proton Van de Graaff Experiments

The comparatively high dose rates available with the proton Van de Graaff apparatus at Harwell provided an opportunity to obtain sufficient solid for infrared analysis. Three main experiments were performed in which the iron carbonyl content of the CO was varied. All other conditions were as near as possible identical.

Experiment A. In this experiment cylinder CO was used without further purification. Small quantities (probably about 200 p.p.m.) of iron carbonyl would thus be present during proton radiolysis as in the α -radiolytic experiments. Now, since the dose rates available with this apparatus are very much greater than that from the α -source - about two thousand times greater - much larger amounts of solid can be obtained, and it was predicted that in this experiment all the iron carbonyl in the volume of CO being radiolysed would be used up before deposition had ceased and the solid would contain some iron but insufficient to render the solid completely inert towards moisture.

Experiment B. A similar experiment to A above was made, but with the iron carbonyl impurity removed from the CO by

the use of cold traps. The resulting solid was expected to be free from iron and consequently of an hygroscopic nature.

Experiment C. In this experiment excess iron pentacarbonyl (~3 v/o) was added to the CO prior to radiolysis and it was believed that the solid would contain sufficient iron to render it inert towards water vapour.

(a) Visual Observations

It was possible to observe the solid forming in the gas phase within the reaction cell during an experimental run. The time before a 'smoke' was observed in the cell decreased as the iron carbonyl content of the CO was increased in the three experiments. Towards the end of the run in experiment C, long, fine chains of particles built up around the electrode. These were subsequently found to be magnetic and evidently contained a high iron content. The solids from experiments A and B were partially soluble in water and gave a yellow acidic solution. Sample C was apparently insoluble in water but was partially soluble in 50% hydrochloric acid.

(b) Electron Microscopy of Deposits

The solids from the three experiments - several runs were necessary to obtain sufficient for microscopy and infrared analyses - were removed from the reaction vessel

and put into glass tubes for subsequent examination. Plates 38A, 39A and 40A are typical electron micrographs of the solids from experiments A, B and C respectively. The most interesting feature is that the solid from B consists of smaller particles (300-500 $\overset{\circ}{\text{A}}$) than A (1000 $\overset{\circ}{\text{A}}$) where the iron content in the CO was greater. The solid from C is composed of both large particles (up to 1000 $\overset{\circ}{\text{A}}$) and long chains of material.

Samples of the three solids were subsequently placed in a Petri-dish containing some water, for 48 hours, and were then examined in the electron microscope. Plates 38B and 39B show that these samples (A and B) have obviously reacted with water whereas the solid from experiment C does not appear to have changed in any way.

Qualitative analysis with the electron microprobe (S.E.M.2) revealed no iron in B, a small amount in A and larger quantities in sample C, as was predicted.

13. Infrared Analysis

The solids from experiments A, B and C were made into micro-discs for infrared analysis by compressing with potassium bromide. So also was the solid which deposited on the capillary tube in the 'bubbler' experiment (Fig. 16) where CO was passed through the α -source for 30 days into CCl_4 . The original intention here, was to suspend deposit particles in CCl_4 for subsequent infrared work but instead

PLATE 38A

Solid from the proton irradiation of CO
(experiment A).

Magnification 100,000 X

PLATE 38B

Same solid which has been exposed to
water vapour.

Magnification 100,000 X

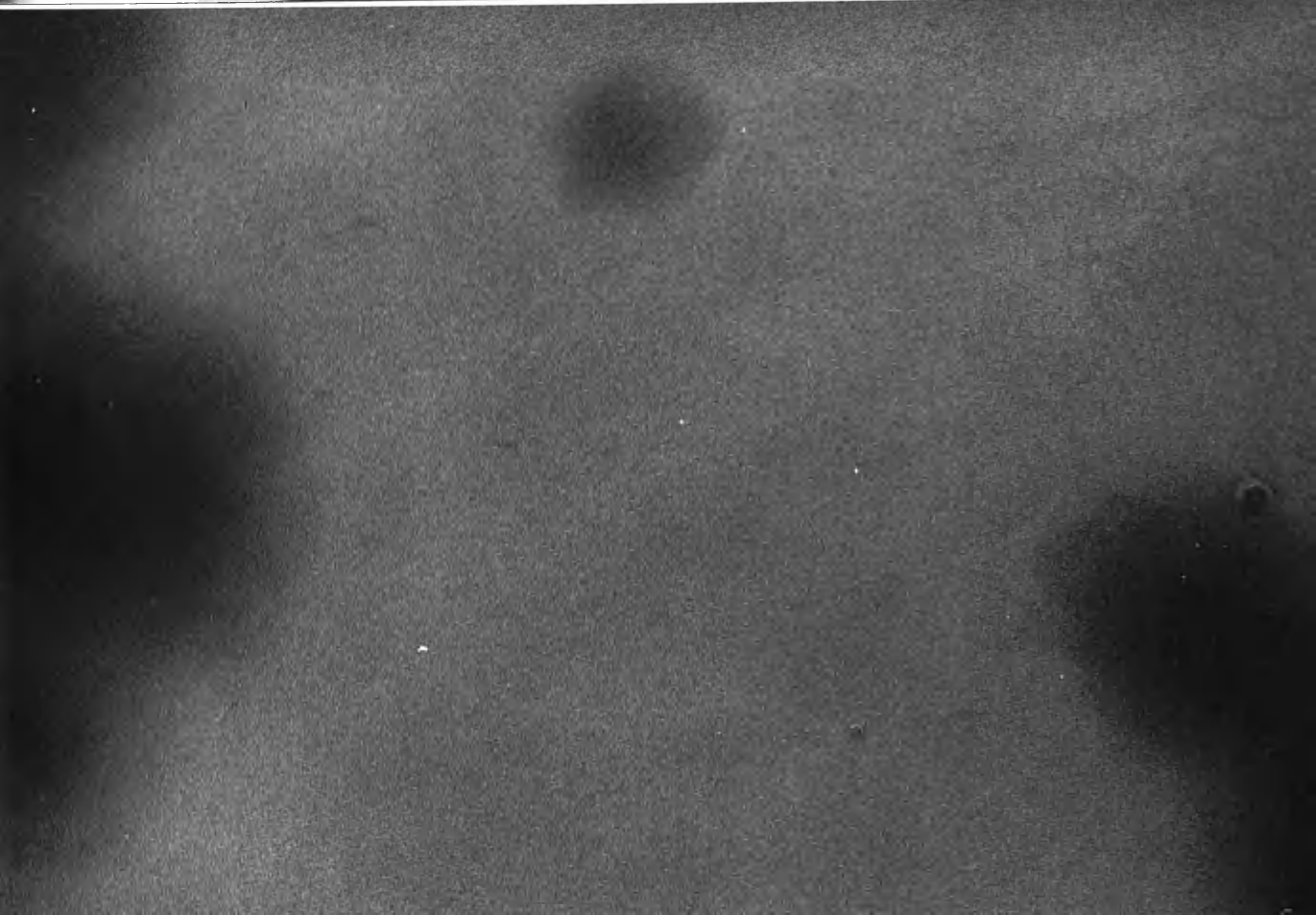
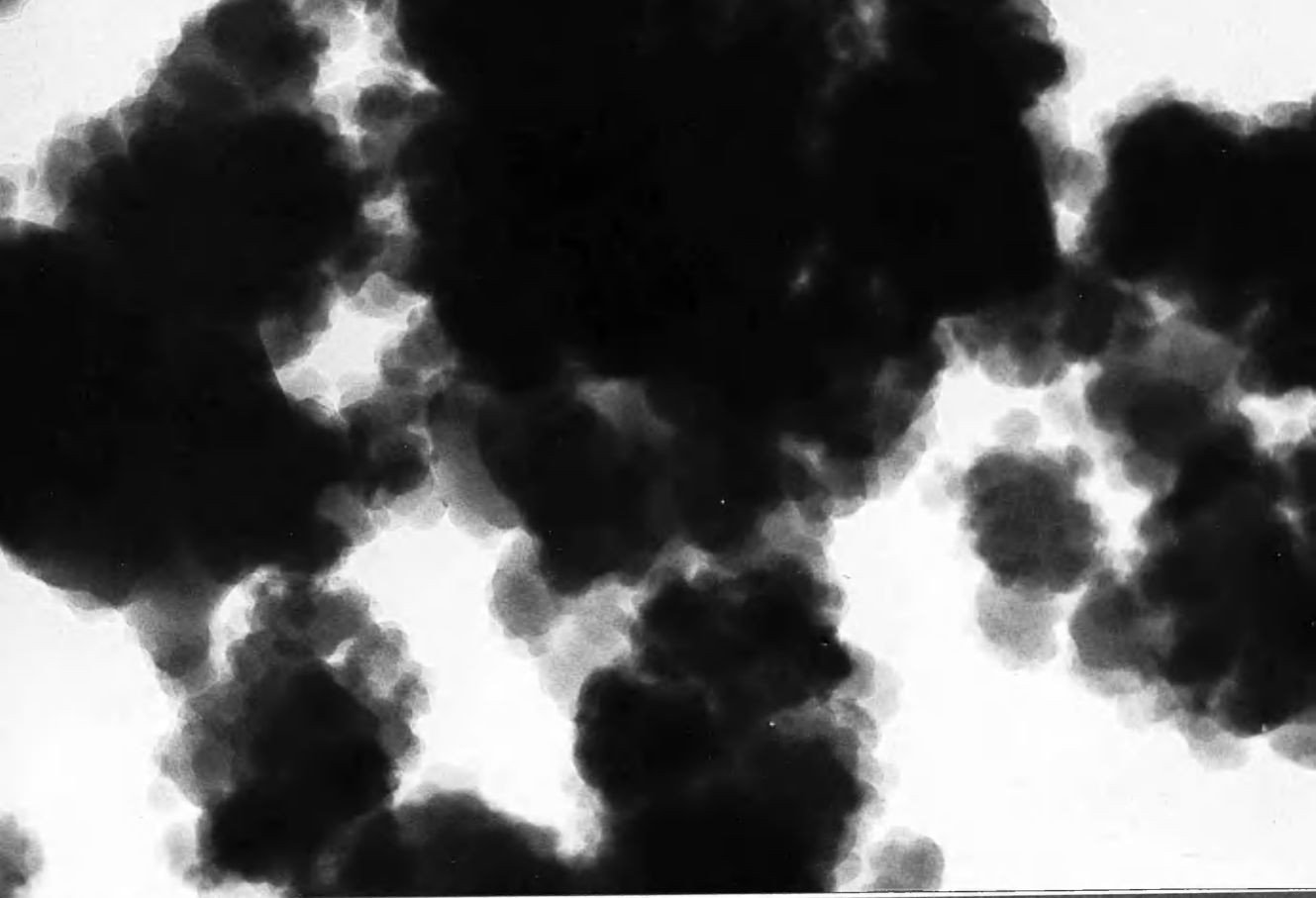


PLATE 39A

Solid from experiment B.

Magnification 100,000 X

PLATE 39B

Same solid after exposure to water vapour.

Magnification 100,000 X

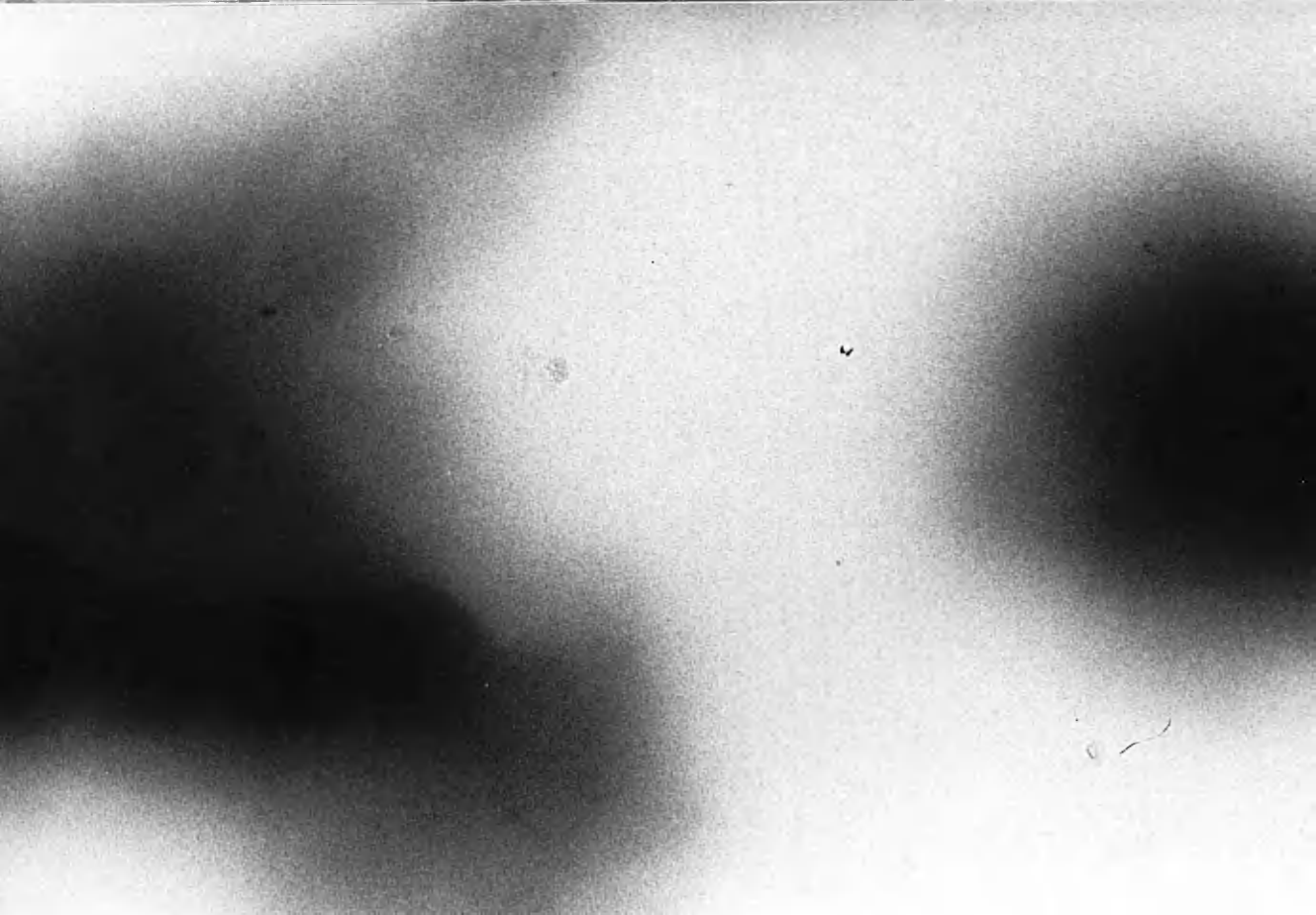
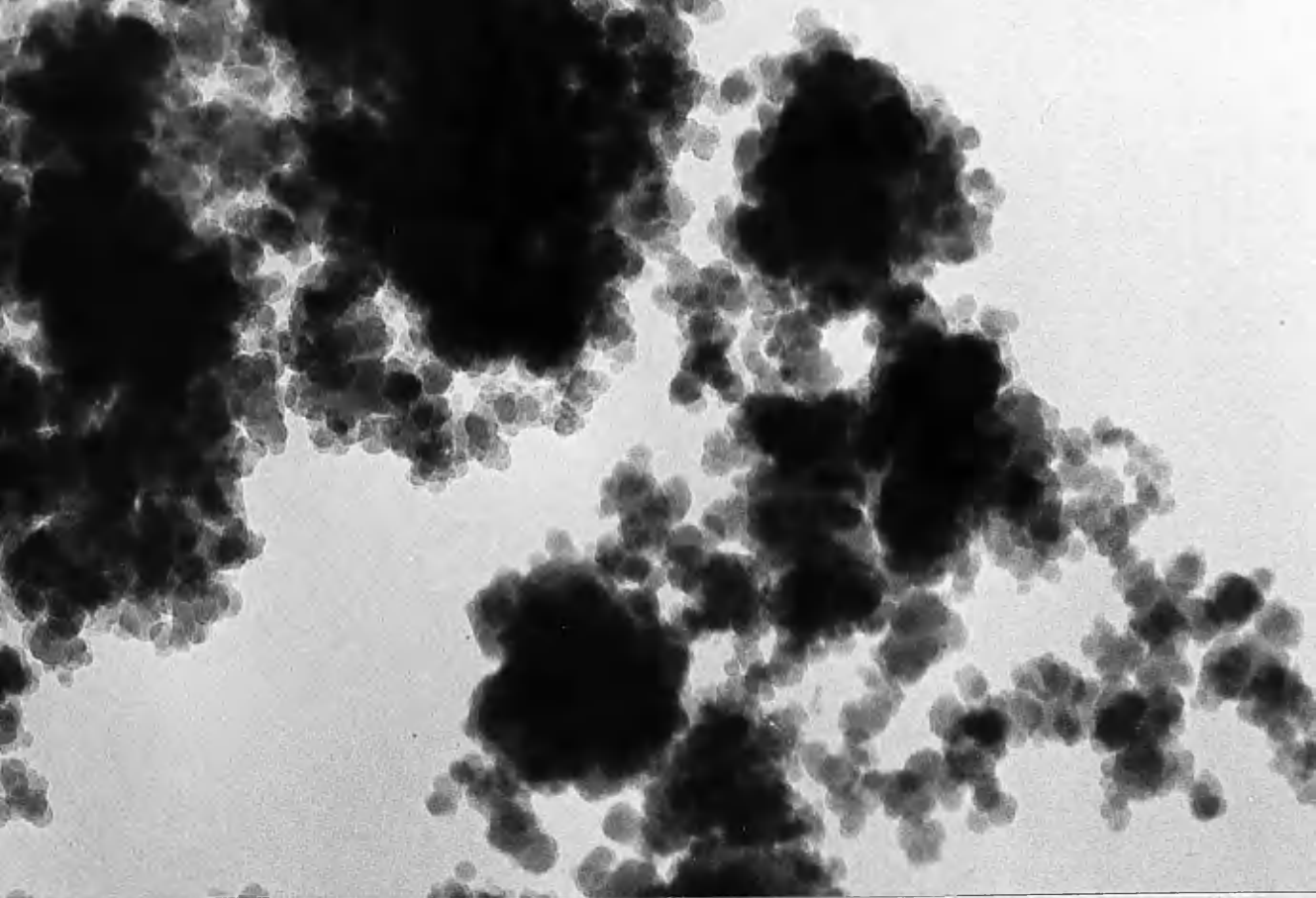


PLATE 40A

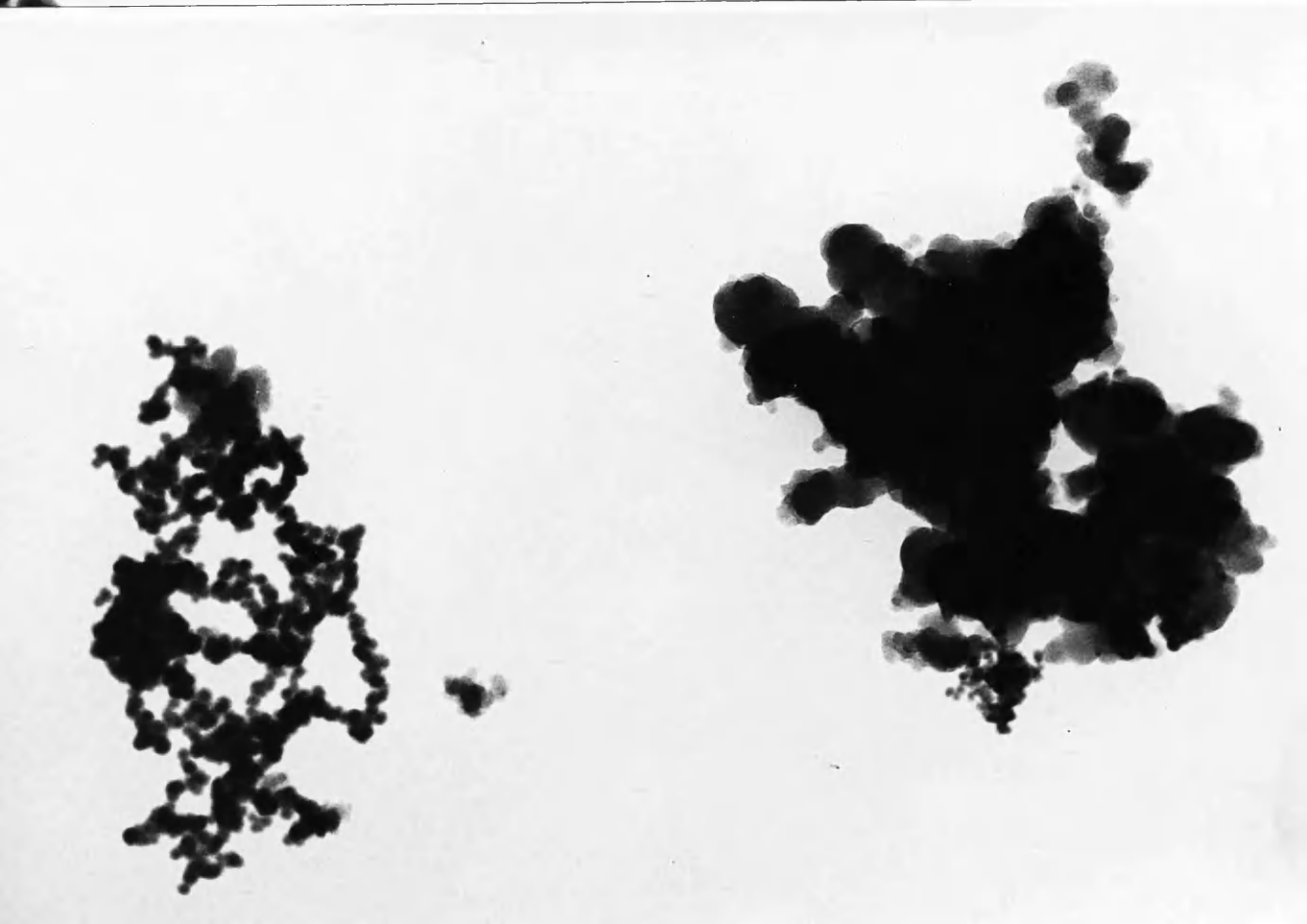
Solid from experiment C.

Magnification 100,000 X

PLATE 40B

Same solid after exposure to water vapour.

Magnification 100,000 X



the solid gathered on the walls of the capillary. Since cylinder CO (I.C.I.) was used in this experiment, iron carbonyl would be present during radiolysis and possibly also nickel carbonyl from reaction between the CO and the needle valve. The solid was partially soluble in hydrochloric acid and gave a yellow solution.

Fig. 26 shows the spectrum (4000-625 cm^{-1}) for each of the four solids; there are similarities and differences evident. A and B are almost identical and show absorptions for water ($\sim 3500 \text{ cm}^{-1}$), C-H ($2,900 \text{ cm}^{-1}$) and C=O (1725 cm^{-1}). The absorptions at 1620 cm^{-1} and 1400 cm^{-1} in A and B are attributed to the asymmetric and symmetric stretching frequencies of the carboxylate ion, COO^- , respectively. The greater intensity of the asymmetric frequency (1620 cm^{-1}) conforms with data presented in Infrared Structural Correlation Tables and both absorptions fall well within the ranges assigned to the carboxylate ion frequencies (asymmetric, $1625 \text{ cm}^{-1} - 1500 \text{ cm}^{-1}$; symmetric, $1410 \text{ cm}^{-1} - 1300 \text{ cm}^{-1}$). In sample C there is a fairly strong additional absorption at 2000 cm^{-1} which is most likely due to the allene group $\text{C}=\text{C}=\text{C}$. The absorptions at 1575 cm^{-1} and 1400 cm^{-1} are again attributed to the carboxylate ion. The dip in the curve at 1630 cm^{-1} possibly arises from conjugated $\text{C}=\text{C}$ bonds but this evidence is weak. However, the lowering of

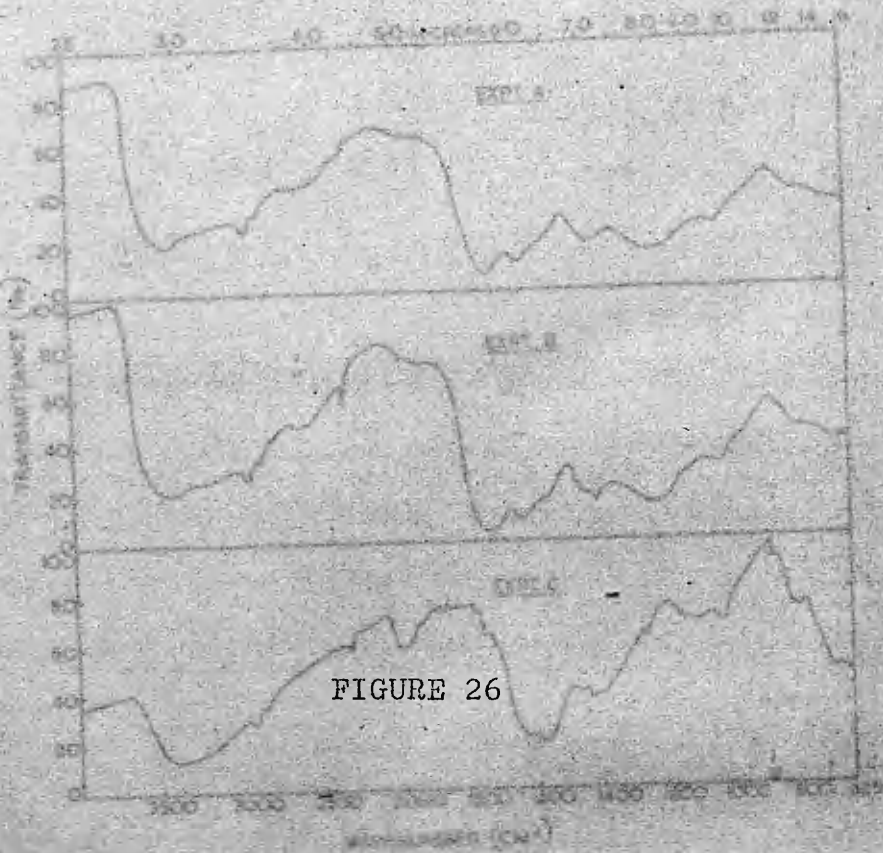


FIGURE 26

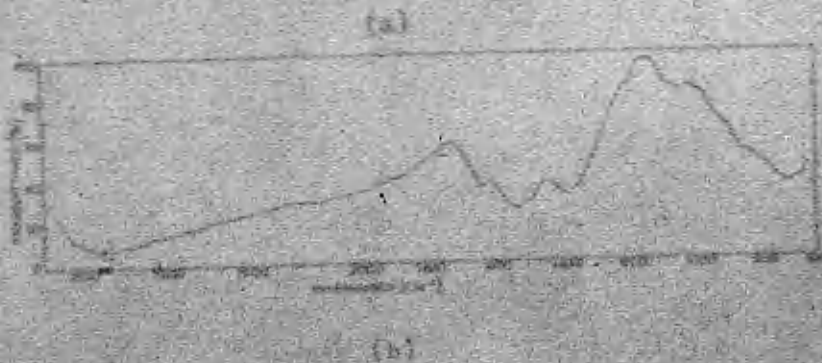
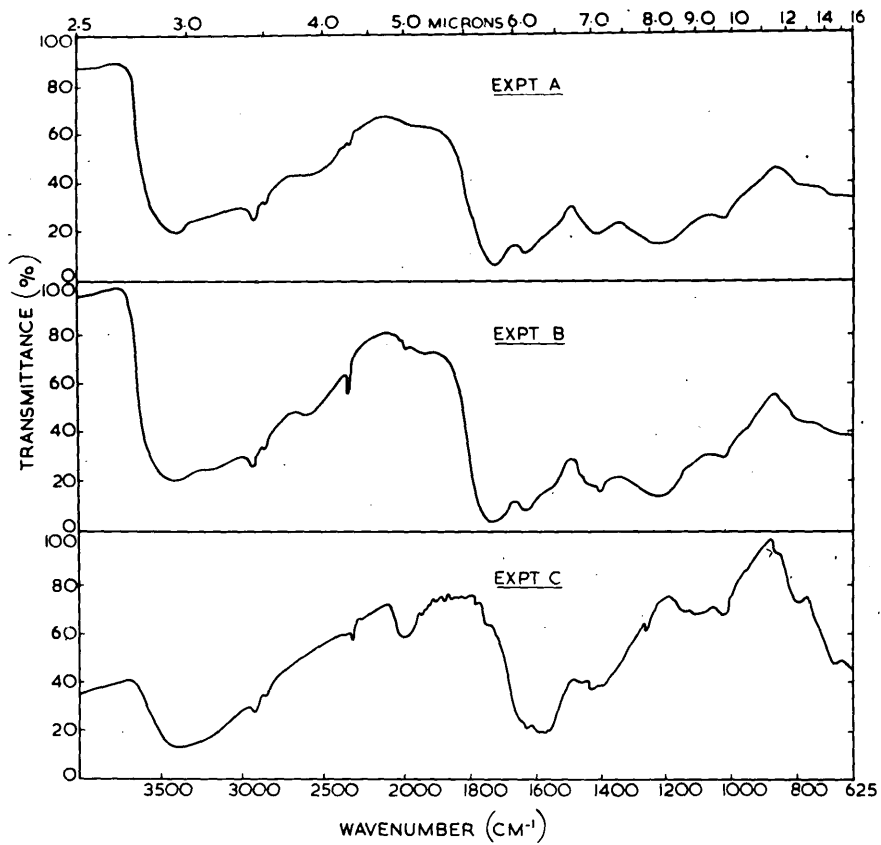


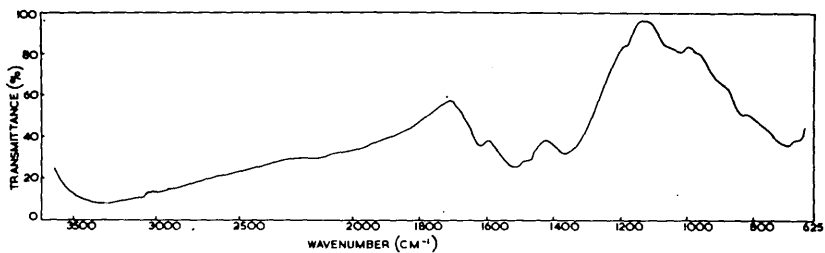
FIG. 25 INFRARED SPECTRA OF SOLIDS FROM

(a) THERMAL RADIOLYSIS OF CO

(b) ALPHA RADIOLYSIS OF CO



(a)



(b)

FIG. 26 INFRARED SPECTRA OF SOLIDS FROM
 (a) PROTON RADIOLYSIS OF CO
 (b) ALPHA RADIOLYSIS OF CO

the asymmetric frequency of the carboxylate ion to 1570 cm^{-1} is consistent with the introduction of conjugation. There is no evidence of an absorption for $\text{C}=\text{O}$ in this sample. In the alpha-radiolytic sample the absorptions at 1530 cm^{-1} and 1370 cm^{-1} are once more attributed to the carboxylate ion. The appearance of the well defined absorption at 1620 cm^{-1} provides stronger evidence of a conjugated $\text{C}=\text{C}$ system. This absorption can also arise from dissolved water in the micro-disc, but this frequency persisted on re-examination of the solid after drying under vacuum for 24 hours. Like sample C, the alpha-radiolytic solid does not exhibit an absorption for $\text{C}=\text{O}$.

Other frequencies in the spectra are unassigned but it is possible that the absorption at 1200 cm^{-1} is due to the presence of the lactone group, $\text{C}-\text{O}-\text{C}$. It is interesting to note that the samples with the lowest iron content, B (no iron) and A, exhibit an absorption indicative of the $\text{C}=\text{O}$ group, whereas sample C and the alpha-radiolytic solid do not exhibit an equivalent absorption for this group. Also noteworthy is the evidence of a higher degree of unsaturation in sample C and the alpha-radiolytic sample manifested by the absorptions for $\text{C}=\text{C}$ and $\text{C}=\text{C}=\text{C}$. A possible explanation for these differences is discussed later.

14. Electron Paramagnetic Resonance Spectra from Van de Graaff Solids.

After the microscopy and infrared studies had been completed, there was just sufficient solid available from experiments A and B for electron paramagnetic resonance spectroscopy measurements to be made. A Decca-Newport spectrometer was used for this purpose. The instrument had to be operated under the most sensitive detection conditions in order to obtain a signal. The spectra were run in duplicate and were apparently identical. Fig. 27 shows the typical signal obtained. A single, broad absorption (resonant field 3305.6 ± 0.2 gauss) is observed with no hyperfine structure. This result is very consistent with the radical $O=\overset{\cdot}{C}-\overset{\cdot}{C}-\overset{\cdot}{C}=O$ (A.L. Porte, 1969).



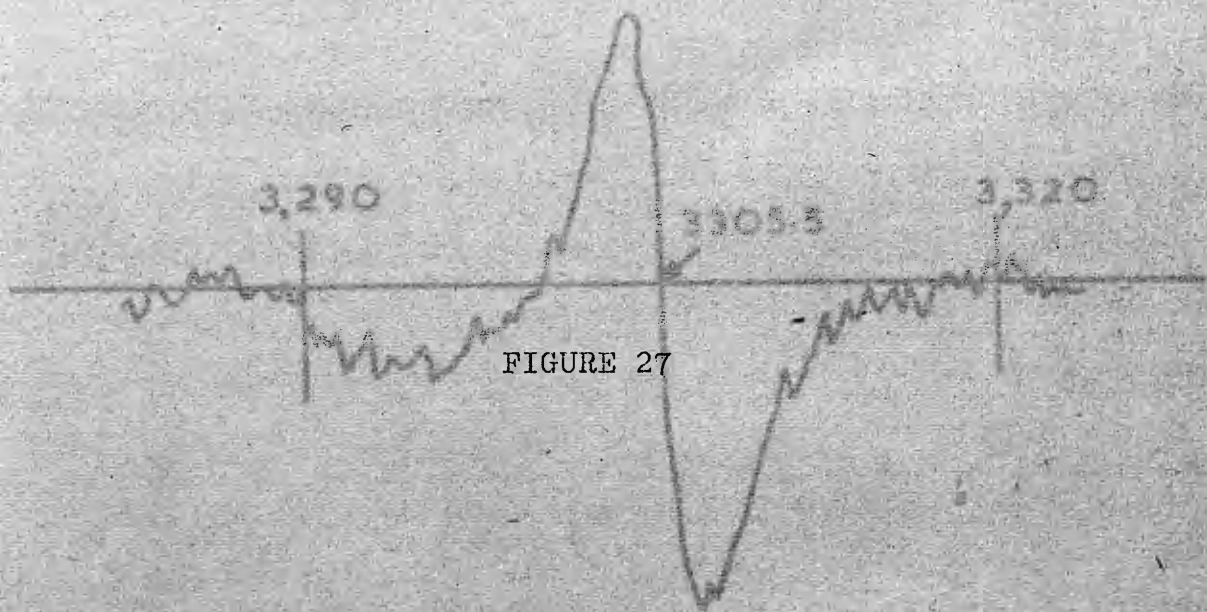


FIG 27 EPR SPECTRUM OF PROTON
VAN DE GRAEFF SOLIDS.

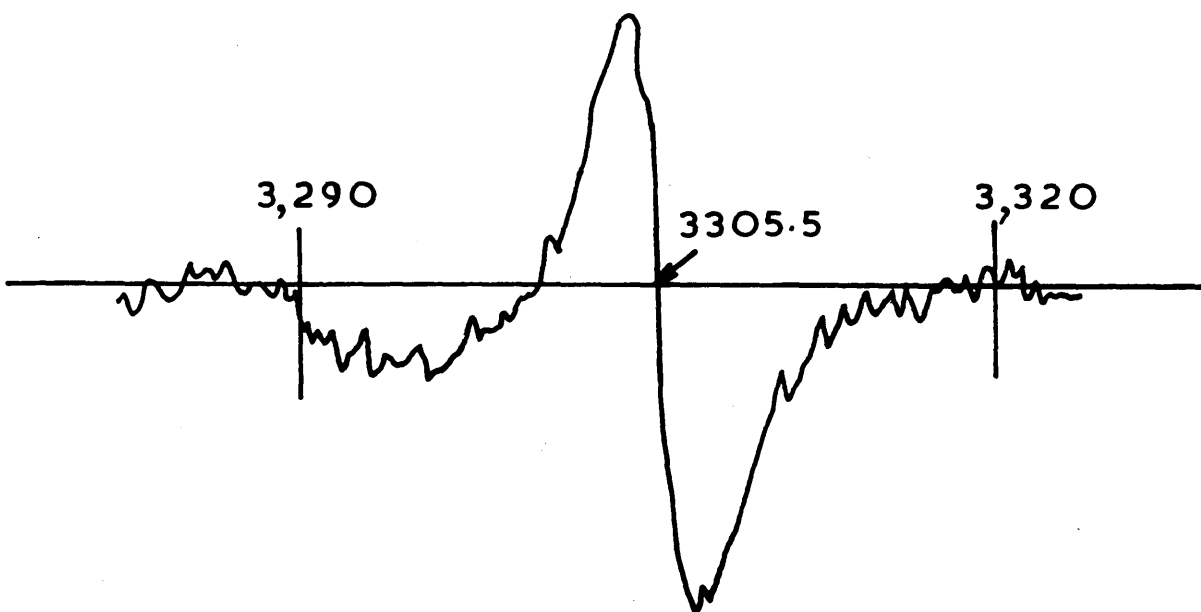


FIG. 27 EPR SPECTRUM OF PROTON
VAN DE GRAAFF SOLIDS.

DISCUSSION

Contents

	Page
1. <u>'Blank' Experiments</u>	190
2. <u>Evidence for Gas Phase Formation of Solid</u>	192
3. <u>Particle Size</u>	193
(a) General Considerations	193
(b) The Effect of Metallic Carbonyls on Particle Size	197
(c) Particle Sizes in the Proton Van de Graaff Experiments	198
4. <u>Particle Morphology</u>	199
(a) General Considerations	199
(b) The Effect of Water Vapour on Particle Morphology	202
5. <u>Composition and Chemical Nature of the Solids</u>	205
6. <u>Factors Affecting Deposit Yields</u>	213
(a) Effect of Metallic Carbonyls	213
(b) Effect of Oxygen	215
(c) G Value for Formation of Solid	219
7. <u>Deposition in the Presence of Graphite</u>	222
(a) General Considerations	222
(b) Surface Deposits	222
8. <u>Future Work</u>	223

DISCUSSION

1. 'Blank' Experiments

It was important to establish that the solid material which settled on to the electron microscope specimen grid after radiolysis was a genuine product from the carbon monoxide gas and was not an artefact. The initial experiments where no deposits were obtained with low pressures of CO show that the solid does not arise from the α -source itself or from the protective Araldite coating. The leakage of plutonium from source B provides evidence that the coating does decompose slowly under irradiation. The same experiments also eliminate the radiolytic decomposition of residual pump vapours in the microscope as the source of the solid material.

The early work of Cameron and Ramsay (1908) and of Wurtzel (1919) on the α -radiolysis of CO_2 showed that solid mercuric oxide could be formed if mercury was present as an impurity in the system during radiolysis. It was therefore possible that mercury could react in this way in the present experiments since a small amount would be present in the system from the mercury manometer in the gas line. It was also possible that mercury could affect the radiolyses by a charge transfer mechanism, $\text{CO}^+ + \text{Hg} \rightarrow \text{CO} + \text{Hg}^+$, in a similar manner to CO_2 (Rudolph and Lind, 1960a) since

mercury, like CO_2 , has a lower ionisation potential than CO . By this process the mercury could deactivate the CO and thus reduce the amount of reaction. However, the early experiments with the external apparatus where cold trapping was introduced, show that the yields of solid obtained do not appear to differ significantly from those when mercury is present. In addition, electron diffraction work and electron probe microanalysis do not reveal any evidence of mercury in the solid material, and it is concluded that mercury has little, if any, influence on the present radiolyses. In the introductory section of this thesis it is shown that liquids and solids can be produced by the action of α -radiation on hydrocarbons. Methane and other low molecular weight hydrocarbons tend to give a liquid polymer after α -radiolysis, but it is possible to obtain a solid by secondary irradiation of the liquid polymer (Lind and Bardwell, 1926). A few parts per million of hydrocarbons were believed to be present in the CO used throughout this work, methane being the most probable impurity. Although it seemed unlikely that such small amounts of hydrocarbons could account for all of the deposit collected, the methane additions to CO were made in order to ascertain the effect of increased hydrocarbon content. The addition of 10 % methane to the CO would not only increase the methane content by several

orders of magnitude but would also increase the ethane and propane content considerably since these are present as impurities in the methane. The particle density counts from these experiments do not show an increase in the yield of solid after radiolysis with increase in hydrocarbon content, and the shape and size of the particles appear to be identical with those from experiments where no methane was added. These results strongly suggest that the solid deposit formed in the present work is not a consequence of hydrocarbon decomposition. The results of subsequent experiments which are discussed later, show that the solid arises from the CO and that metallic carbonyls strongly influence the radiolytic processes occurring. The effect of oxygen on the radiolyses is also discussed.

2. Evidence for Gas Phase Formation of Solid

Sufficient evidence has been obtained to establish that the particles ($2,500 \overset{\circ}{\text{Å}}$ diameter) formed by the α -radiolysis of CO grow in the gas phase within the irradiation zone of the α -source and subsequently settle out on to the specimen grid. Evidence for this is revealed by the three-dimensional nature of the particles; they have approximately the same dimension in all directions, as illustrated by the shadowing experiments, and may be considered to be irregular spheres. The ease with which the particles can

be removed from the supporting film and the small area of attachment to the support, manifested after removal of a particle (Plate 5), indicate that the particles are loosely held on the surface and are therefore most likely to be formed in the gas phase since substances which grow on a surface are generally extended preferentially along one or two axes and have a much wider area of contact with the surface. Further evidence of a gas phase formation of solid is obtained from the results of the experiments where the collecting substrate was raised into the α -source. In these experiments it is found that the yield of solid decreases as the substrate is raised higher into the α -source, the yield obtained being approximately proportional to the irradiated volume above the substrate. Had the particles grown on the support film the yields would have been expected to remain constant since the same irradiation dose was given to all of these experiments.

3. Particle Size

(a) General Considerations

It has been established that the particles from the radiolyses form within the irradiation zone of the α -source and settle out on to the specimen grid. Using data given by Green and Lane (1957) it is calculated that the terminal velocity of the particles (2,500 \AA diameter) is

about 2.5×10^{-4} cm sec⁻¹. The particles would therefore take about six to seven minutes to fall from the lower regions of the irradiated volume of the α -source on to the support film. About 110 minutes would be required for them to reach the support from the upper regions of the α -source. The time necessary for a particle to fall from the irradiation zone on to the substrate is therefore short compared with the duration of an average experiment (17 to 65 hours). The average size of the particles produced within the electron microscope would not be expected to differ much from those obtained with the external reaction vessel since the geometry of the two systems is quite similar, and, indeed, this is borne out by the particle size measurements. Both systems are essentially static, there being no flow of gas other than that which arises from convection currents due to room temperature changes. The higher number of short chains observed in the reaction vessel experiments compared to the in situ work, is believed to be due to the greater ease with which thermal gradients can be set up within the reaction vessel which is less well insulated than the microscope column. The turbulence which results causes the particles to collide to form the chains.

The stopping power of a 5 MeV α -particle in carbon monoxide at atmospheric pressure is calculated to be

$0.01 \text{ eV } \text{Å}^{-1}$. Taking a value of 34 eV for ion pair formation (Lind, 1961), this means that the average distance between ion pairs is $3,400 \text{ Å}$. Although this might suggest that aggregation along an α -track is unlikely to be of prominence in the present experiments since the average particle diameter ($2,500 \text{ Å}$) is less than $3,400 \text{ Å}$, it is possible that aggregation could occur when the individual ionisation events are closer together than $2,500 \text{ Å}$. The present electron microscope studies have, however, shown that extensive chains of particles are not found, the particles existing mainly as single units, small aggregates and short chains.

The average particle diameter is found to be about $2,500 \text{ Å}$, this value remaining effectively constant over a range of experiments where the parameters of pressure, dose and gas composition are varied. The experiments with the collecting substrate placed into the irradiated volume of the α -source also result in the production of gas-phase particles of about the same size as these collected outwith the source. This indicates that the particles do not grow continuously within the irradiation zone of the α -source once they have settled out on to the substrate. The particle size distribution of an aerosol apparently depends mainly upon coagulation and sedimentation rates (Dunning, 1960; Junge, 1963). Junge states that

sedimentation controls the upper size limit of an aerosol particle and coagulation the lower size limit. The value of $2,500 \text{ \AA}$ for the average particle diameter is not peculiar to the present system but appears to occur rather frequently in a number of other aerosol systems. For example, Chamberlain (1968) describes the work of M.J. Heard, who obtained 2000 \AA diameter particles of ammonium sulphate by the action of α -radiation from thoron in a capacity box (1 cubic metre) containing atmospheric air. The aerosol took several hours to form in this large volume. An electron micrograph of the solid showed the presence of single particles, aggregates of three or four particles and short chains, and this was remarkably similar in appearance to micrographs of the solid from the present work where the particles are formed in a small volume (0.25 ml) and are visible after about 20 to 30 minutes. The fairly uniform particle size appears to be the result of the competing processes of coagulation, sedimentation and diffusion (Chamberlain, 1968). The intercept on the pressure variance curve, Figure 21, probably arises from the diffusion of small 'smokes' from the irradiation zone. As the pressure of CO gas is lowered the growth rate of the particles will decrease due to the collisions between activated species becoming less frequent, and it appears

that at the low pressure end of the scale the species giving rise to particle growth can diffuse from the irradiation zone before appreciable growth occurs. This diffusion process would also account for the absence of a visible deposit in some of the early experiments conducted at low pressures (Table II). In the present work then, particles formed at pressures between 0.25 and one atmosphere (for a constant irradiation time of 90 hours) have approximately the same size (Table III). Experiments conducted at one atmosphere pressure for various irradiation times up to 90 hours, also produce particles of about the same size (Table II).

(b) The Effect of Metallic Carbonyls on Particle Size

Significant changes in particle size are found when the metallic carbonyl content of the carbon monoxide is decreased. Concentrations of iron pentacarbonyl between 280 parts per million, the amount estimated to be present in the cylinder gas, and 0.8 v/o, achieved by deliberate addition of $\text{Fe}(\text{CO})_5$ vapour, gave particles of the standard size (2,500 Å). Also present in the gas in these experiments was an unknown quantity of nickel tetracarbonyl vapour formed by the reaction between the CO and the nickel in the needle valve in the gas line and the nickel in the microscope pole-pieces. Excess nickel tetracarbonyl, like iron

pentacarbonyl, failed to alter the particle size. However, when the iron carbonyl was removed (leaving the nickel carbonyl) the average particle size dropped to about 2,100 Å. This value is only slightly lower than that found when iron is present (2,500 Å) but it is thought to be outwith the errors of measurement. Furthermore, on removing the iron carbonyl and decreasing the nickel carbonyl content by taking the needle valve out of the gas line, that is leaving only the pole-pieces as the source of nickel carbonyl, then the average particle size value falls to about 1,600 Å, (Table X). These findings suggest that the metal carbonyls must in some way enhance the growth of solid in the present experiments. The external glass apparatus was useful in extending these experiments to the stage where only traces of iron carbonyl were present and in these cases particles below 100 Å were observed after long irradiation times, thus confirming the importance of metal carbonyls in the particle growth process.

(c) Particle Sizes in the Proton Van de Graaff Experiments

The results of the series of experiments performed with the Van de Graaff apparatus again reflect the important role of metallic carbonyls in the radiolysis of CO. In experiment B where the carbonyls were removed from the CO prior to radiolysis, the particles were found to be 300 - 500 Å in diameter whereas particles of up to about 1000 Å

were obtained in the other experiments (A and C) where iron carbonyl was present. These results, together with the visual observation that particles are formed more quickly when carbonyl is present, lend support to the belief that carbonyls enhance the growth rate of solid in the gas phase and are consistent with the results of the α -radiolytic work.

The particle sizes of the solid from the proton irradiation of CO in a flowing system, reported by Baird, Dawson and Wood (1964), were shown to vary between 300 \AA and 13,000 \AA , depending on the collecting position within the irradiation cell, the beam energy used, the temperature and the rate of flow of gas. It is difficult to correlate the particle size results of these experiments with the present ones owing to the wide variety of conditions used and the fact that the present Van de Graaff deposits were mechanically ground before viewing, unlike the former preparations where the solid was collected directly on the grid within the proton irradiation cell. In addition, the effect of metallic carbonyls on the radiolysis was not known then, and it is possible that some metal carbonyl impurity was present in these experiments.

4. Particle Morphology

(a) General Considerations

The solid particles produced in the gas phase by the α -radiolysis of CO consist of single units, aggregates

and short chains as depicted in Plates I to III. These specimens have not undergone any preparatory treatment subsequent to deposition and are thus a true representation of the morphological nature of the solid particles formed by the α -radiolysis of CO. The similarity between these micrographs and those of Watson, Vanpee and Lind (1950) and of Ryan (1963) where mechanical treatment had been given to the solids, suggests that the grinding treatment does not alter the structure significantly, assuming of course, that the particles from these experiments were initially like those of the present work. The physical appearance of the particles from the in situ experiments does not seem to differ from those produced in the external apparatus and there is no apparent difference between the particles produced with different α -sources. The yield of solid from source C, however, is about one third that obtained with source B for the irradiation time and presumably the dose rate to gas with this source is about one third that of B (measurements have not yet been made) since the deposit yields have been shown to depend linearly on the dose (Figure 19). In experiments of short duration, up to about 12 hours with source B, mainly single particles are observed evenly distributed over the entire area of the specimen grid. After longer irradiation times the number of chains observed

appears to increase. This effect is believed to result from collision between particles already on the substrate and those settling out on to the grid, which becomes progressively covered with particles. The chains are evidently pinned at one end on to the substrate and wave about, thus tending to pick up further particles from the gas phase. Furthermore, the geometry of the deposition systems and the dose rate to gas for a given α -source are the same for each experiment, and this should lead to a constant rate of formation and sedimentation of particles.

Details of the particle structure are revealed in Plate 4 at a magnification of 200,000 times (1 mm \equiv 50 $\overset{\circ}{\text{A}}$). This micrograph shows that the particles have a 'woolly' texture and are composed of small irregularly-shaped sub-units, which are often less than 100 $\overset{\circ}{\text{A}}$ diameter. Individual particles of this order of size have been found in other experiments in the present work, for example, as illustrated in Plate 13A, and it is possible that these small units are precursors in the formation of the larger particles. The molecules composing the particles do not form extensive crystalline arrays but come together in a random manner as revealed by the electron diffraction studies. This is in agreement with the work of Watson, Vanpee and Lind (1950) and Lind and Wright (1963) who found the deposits to be of an amorphous nature.

(b) The Effect of Water Vapour on Particle Morphology

The effect of water vapour on the hygroscopic particles, that is, the particles from experiments performed in the absence of iron pentacarbonyl, is to cause the particles to swell up and become fluid, as illustrated in Plates 8, 9, 10 and 11. An interesting feature which occurs is the bridging between particles. This effect is similar to the 'necking' observed by Watson, Vanpee and Lind (1950) who postulated the existence of two distinct phases, one solid and one liquid, in the solid from the α -radiolysis of CO. Baird, Dawson and Wood (1964) also reported evidence of small particulate material surrounded by a substance of a less dense nature when low proton beam currents were used. The appearance of the particles illustrated in Plate 10 is also quite similar to that observed in other proton irradiation experiments where a tenuous membrane is often found to link particles in a chain-like manner. In view of the knowledge gained in the present work it is suggested here that the less dense 'liquid' material formerly observed by these workers is a consequence of moisture absorption and is not a genuine second phase formed during radiolysis.

It has been shown that particles which contain iron do not react with water whereas those which contain nickel as

moisture were observed to shrink on heating in vacuo leaving a residue of nickel or nickel oxide, and it seems likely that volatile material is lost at this stage due to the decomposition of the solid. The volatile material may be CO, CO₂ or other organic gases.

The phenomenon of potentially reactive deposits being rendered inert by viewing in the microscope before exposure to the atmosphere caused some confusion in the initial stages of the work and accounts for the apparently anomalous results at that time. The difference in reactivity after viewing is almost certain to be the result of the irradiation damage induced in the specimen during examination in the microscope. According to Reimer (1965) a dose of about 6×10^9 rads per second is absorbed by an object viewed at a magnification of 10,000 times at an operating voltage of 60 KV. This high dose can give rise to modifications of the specimen and in particular can cause cross-linking between molecules, thus altering the nature of the solid and conferring quite different properties to it. Polymers are especially susceptible to irradiation damage and a high degree of cross-linking or chain scission can occur. Analytical evidence discussed later indicates that the radiolytic solids produced in this work are composed of polymeric units of a carbon suboxide and it is suggested that the effect of the electron beam on these is to

cause cross-linking, with the result that a higher molecular weight, insoluble material is formed.

5. Composition and Chemical Nature of the Solids

It has been established by previous work mentioned in the introductory section of this thesis, that the solid produced by the action of high energy radiation on carbon monoxide consists mainly of carbon and oxygen. Marsh and Wright (1964) reported that the solids from their reactor and proton irradiations were probably polymers of carbon suboxide but found them to be structurally unlike the thermal polymer of carbon suboxide which has a ring structure. They proposed on the basis of infrared data submitted to them by A.M. Deane, that the solids were similar to polymers which might be produced by pyrolysis of lactones. Anderson, Best and Willett (1966) suggested that the solid from their proton and gamma experiments was a linear polymer of carbon suboxide and showed that the empirical composition ($C_{1.5}O$) of the solid did not change significantly over a 200-fold variation in the dose-rate. It has been calculated, from dosimetry measurements, that the dose-rate to gas in the present proton experiments is about two thousand times greater than the dose-rate available with the plutonium α -source. The analytical data which have been acquired indicate that structurally similar solids are produced by these two different ionising radiations. The

Erratum - page 206

Between "Vilesov and Kurbatov (1961) give the values
of these as 8.28 eV for $\text{Ni}(\text{CO})_4$ and"

and "8.53 eV for $\text{Fe}(\text{CO})_5$ "

insert "7.95 eV for $\text{Fe}(\text{CO})_5$ whereas Winters and Kiser
(1964) give the values as 8.64 eV for
 $\text{Ni}(\text{CO})_4$ and"

deposits from the α -radiolyses and from the complementary proton experiments have been shown by electron diffraction, electron probe microanalysis and infrared spectroscopy techniques, to consist mainly of carbon, oxygen and either iron or nickel according to the metallic carbonyl impurities present in the carbon monoxide during radiolysis. Iron and nickel have not been detected to occur together in the solid material when both these carbonyls are present in the gas; under this condition (both carbonyls present) there is evidence for iron only. When the iron carbonyl is removed from the CO then nickel is found to be one of the constituents of the solid, provided, of course, there is nickel carbonyl in the gas during radiolysis. The preference for iron to be incorporated into the solid may well be due to the respective ionisation potentials of iron pentacarbonyl and nickel tetracarbonyl. Vilesov and Kurbatov (1961) give the values of these as 8.28 eV for $\text{Ni}(\text{CO})_4$ and 8.53 eV for $\text{Fe}(\text{CO})_5$. Nevertheless, in both cases the value for the iron carbonyl is lower than that for nickel carbonyl and it is possible that energy transfer occurs from the $\text{Ni}(\text{CO})_4$ to the $\text{Fe}(\text{CO})_5$ on absorption of radiation, so that the latter is preferentially decomposed. After the initial absorption process has occurred, the carbonyls may be degraded by the consecutive loss of CO molecules to give the metal ion, as was found by Winters and Kiser (1964)

in their mass spectrometric studies. However, the most abundant ions produced from $\text{Fe}(\text{CO})_5$ and $\text{Ni}(\text{CO})_4$ were respectively Fe^+ and NiCO^+ . Nickel tetracarbonyl is apparently more resistant to decomposition by radiation than iron pentacarbonyl. This was demonstrated by Garratt and Thomson (1934) who used ultraviolet light and Barzynski and Hummel (1963) who used ^{60}Co γ -radiation. The resistance to decomposition is attributed to the rapid recombination of the primary products, nickel tricarbonyl, $\text{Ni}(\text{CO})_3$ and carbon monoxide (Pearson, Basolo, Day, Kangas and Henry, 1968). On absorption of energy, iron pentacarbonyl tends to form iron enneacarbonyl $\text{Fe}_2(\text{CO})_9$. The present studies have shown, however, that the solid from the α -radiolysis of CO in the presence of iron pentacarbonyl is quite unlike iron enneacarbonyl. It is not known whether the metal ion or one of the many possible intermediate carbonyls formed during degradation, for example, NiCO^+ , $\text{Fe}(\text{CO})_4^+$, subsequently reacts with the CO decomposition products to produce the solid material which is observed in the present experiments. The reaction may occur via the metal ion in the experiments where $\text{Fe}(\text{CO})_5$ impurity is present and via an intermediate carbonyl when $\text{Ni}(\text{CO})_4$ impurity is present. This could account for the different behaviours of the resulting solids towards water vapour since different chemical structures would almost certainly be formed by the different reaction processes.

The results of the infrared studies help to elucidate the chemical structures of the radiolytic solids. The most prominent features of these studies as a whole, are the absorptions indicative of C=C=C, C=O, COO⁻ and, possibly, C=C. These groups could be readily accounted for by the formation of a polymer built up from carbon suboxide units, that is from units of O=C=C=C=O. The electron paramagnetic resonance spectrum of the solid (from the proton experiments) is very consistent with

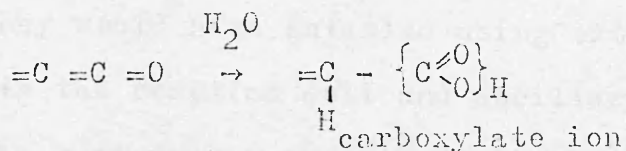


and tends to confirm that such a polymer is formed. However, it is difficult to write a definite structure for such a polymer, especially one which would account for the observed partial solubility of the solids in water and hydrochloric acid. Smith, Young, Smith and Carter (1963) state that there are at least sixteen different ways (excluding various resonance forms and random combinations) of drawing a regular repetitive polymeric structure based on C₃O₂ units. The partial solubilities of the solids in polar solvents would be difficult to account for if a regular repetitive structure was postulated for the solid material produced in the present work, and it is proposed here that the solids are composed of basically similar units of different molecular weight. The

absence of crystallinity in the solid tends to support this suggestion. The higher molecular weight material could account for the insoluble portion of the solid and the lower molecular weight material for the soluble component of the solid.

There is some evidence in the infrared spectra which indicates that the four solids examined by this technique have absorbed moisture. The absorption could occur either during radiolysis from water impurity in the gas, or on subsequent exposure of the solid to atmospheric conditions. Examination of the electron micrographs of the solids shows that when iron carbonyl is present in the gas as an impurity there must be a very limited amount of water absorbed after exposure to the atmosphere since their physical appearance is apparently unaltered. In the absence of iron carbonyl the particles have a quite different morphology after exposure to the atmosphere, and appear to have absorbed relatively large amounts of water. The results of the electron microscopy studies are consistent with the visual observations, made on the 'bulk' samples, which reveal that the iron-free solids are partially soluble in water yielding an acid solution and the iron-containing ones are apparently insoluble in water (partially soluble in hydrochloric acid). The greater insolubility of the iron-containing deposits is obviously due

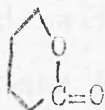
to some effect which the iron has upon the chemical structure of the solids. The most striking difference apparent in the infrared spectra of the solids is that the iron-free solid exhibits an absorption for the carbonyl group whereas the solids containing iron (from experiment C and the α -radiolytic experiment) do not have a corresponding absorption for C=O. This suggests that the iron bonds with the oxygen in the C=O group thus masking its characteristic absorption. More than one oxygen could bond to the iron and in this way neighbouring molecules could be linked together to give a solid of higher molecular weight and greater insolubility. Carbonyl groups which have not bonded to iron would remain free to add on water, possibly by the mechanism proposed by Schmidt, Boehm and Hofmann (1955, 1959) -



This would result in the formation of a carboxylic acid and would account for the acidity of the solution obtained with the soluble portion of the material and for the appearance of the carboxylate ion absorptions in the infrared spectra.

The general features of the spectra, when compared with those obtained by Smith, Young, Smith and Carter (1963) and Blake, Beles and Jennings (1964) for the thermal polymer of

carbon suboxide, indicate that, although there are some similarities between the polymers, the radiolytic polymer does not have the six-membered lactone ring structure of the thermal material. In particular, the intense absorption at 1775 cm^{-1} attributed to



by Blake, Eccles and Jennings,

does not appear in the present studies, and it is concluded that the radiolytic polymer has mainly a linear structure. Unfortunately it has not yet been possible to collect sufficient deposit with a nickel content for a comparative infrared study. This would have involved the utilisation of the α -source, for many months in the 'bubbler' apparatus and was impracticable. An alternative would have been to conduct further Van de Graaff experiments but these were deliberately avoided since they would have entailed using extremely toxic $\text{Ni}(\text{CO})_4$ vapour in the reaction cell and ancillary equipment, and there was the real danger that the cell window might be disrupted during radiolysis. An estimate of the quantity of iron in the α -radiolytic solid can be obtained from the intensity of the $\text{FeK}\alpha$ signal given by the solid with the Siemens X-ray spectrometer attachment. Fuchs (1966) who developed this instrument, gives a plot of the X-ray intensities of $\text{FeK}\alpha$ signals against the known masses of iron giving rise to these signals. The signal of 50 counts per

minute (above the background count) for the FeK α radiation obtained from Fig. 24 corresponds to a mass of approximately $10\bar{g}^{-13}$ of iron. The inserted micrograph shows that about 70 particles were irradiated by the electron beam to give this signal. If the particle density (g cm^{-3}) is taken as unity then the amount of iron in the solid is calculated to be about 18 per cent by weight or approximately 4 atomic per cent. The percentage of iron in the solid is inversely proportional to its density (g cm^{-3}) so any deviation from unity would affect this figure considerably. It is more difficult to make a good estimate of the nickel content of the solid since the number of particles contributing to the signal can not be counted directly, due to the hygroscopic nature of these particles. However, if the small area 'X' in Fig. 25 is taken as being formed from one particle, then it is estimated that 150-200 particles were irradiated to give the signal observed in Fig. 25. Since this signal is about three times greater than that for the iron, then, assuming that the detection efficiency for NiK α radiation is similar to that for FeK α radiation, the amount of nickel in the solid is calculated to be about 20 per cent. In view of the assumptions which have been made, these analyses must be regarded as semi-quantitative, but they show nevertheless that the iron and nickel have been concentrated from a few p.p.m. in the gas phase to several per cent in the solid.

6. Factors Affecting Deposit Yields

(a) Effect of Metallic Carbonyls

The results of the experiments made with various concentrations of metal carbonyls in the gas show clearly that as the carbonyl content is reduced the number of particles produced tends towards zero (Fig. 23). This implies a priori that the carbonyls are the source of the solid deposit. However, the results of other experiments show that this is not the case. Firstly, the addition of excess metal carbonyl does not produce the corresponding increase in yield which would be expected if carbonyl decomposition accounted for all of the solid obtained in these experiments. Secondly, the radiolysis of pure metal carbonyls in an inert gas (helium) produces yields about three orders of magnitude lower than similar irradiations with CO containing parts per million of carbonyls. It seems unlikely that the different energy absorption processes which will exist between these two sets of experiments could cause such a discrepancy in the yields of solids. The small yield that is obtained from the pure carbonyls is attributed to the secondary radiolysis of CO formed by the action of the α -particles on the carbonyls. Fairly strong evidence for degradation of iron carbonyl to the metal and CO is afforded by the results of experiment C, (3 v/o $\text{Fe}(\text{CO})_5$ added to CO), one of the proton

experiments, which showed strands of magnetic particles - presumably iron particles - were formed after the normal gas-phase deposition process had ceased. The iron can only have arisen from the excess $\text{Fe}(\text{CO})_5$ present in this experiment. In the α -radiolytic experiments there is a linear relationship between the deposit yield and the irradiation time (dose). There is no deviation from linearity even at the highest dose used (Fig. 19), indicating that there is still sufficient iron carbonyl present at this stage to maintain a steady yield of solid. Calculation, based on a 20 per cent iron content for the solid, reveals that several years irradiation would be required before the iron carbonyl content of the CO would be used up in the in situ experiments. The iron carbonyl obviously encourages the growth of deposit particles since a reduction in the iron carbonyl content of the CO - to values below 280 p.p.m. - results in a decrease in the yield of solid in the α -radiolytic experiments. The visual observations made during the proton experiments, that 'smokes' formed faster in the reaction cell when excess iron carbonyl was present, are consistent with this picture. The iron (or some other product formed by the action of ionising radiation on $\text{Fe}(\text{CO})_5$) apparently links the CO decomposition products together as they form in the gas phase. The infrared data acquired suggest that any such linkage occurs

between the iron and the carbonyl groups of the basic suboxide units. The iron would thus effectively cause cross-linkage between neighbouring molecules which would result in a faster rate of growth of particles; these would have a higher molecular weight, would have fewer terminal end groups and would be less soluble in water. This explanation fits the observed phenomena.

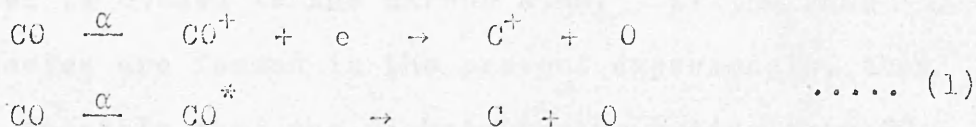
Nickel is evidently less effective as a 'nucleating' agent since the particle densities (per cm^2) from CO gas containing $\text{Ni}(\text{CO})_4$ only, drop by about 70 per cent (Fig. 22) and are accompanied by a slight decrease in the average particle size. The role of nickel has not been determined due to the inability to collect sufficient deposit for analyses. However, it would appear that either there are fewer of the same type of bonds formed or that the nickel is bonded to the organic part of the polymer in a different manner from the iron. The iron and nickel analysis figures, although semi-quantitative, do indicate that there is as much nickel incorporated into the solid as there is iron from respective experiments. This evidence favours the suggestion that the nickel is bonded to the molecule in a different way from iron.

(b) Effect of Oxygen

Fairly large amounts (~ 10 V/o) of oxygen have been shown to have little effect on the present α -radiolytic

experiments other than to cause a slight decrease in the deposit yields. However, in practically all of these experiments the effect of oxygen is masked by the presence of metal carbonyls in the gas. When the carbonyls are removed the yield of solid tends towards zero. This drastic reduction in yield is undoubtedly due to the effect of oxygen which becomes apparent in the absence of carbonyls. Anderson, Best and Willett (1966) showed that as little as 2 p.p.m. (V/v) of oxygen were sufficient to cause a reduction in the yield of solid in their proton and gamma irradiation experiments. Low dose-rate experiments were particularly sensitive to traces of oxygen. The present α -radiolytic experiments were conducted at a dose-rate of about 200 times less than their lowest dose-rate experiments and so would be expected to be very susceptible to traces of oxygen in the system. The hot copper turnings used to remove oxygen from the CO would not give gas of the required purity for oxygen to have a negligible effect and therefore all the experiments both in situ and in the external apparatus are potentially susceptible to the effect of oxygen. The presence of metal carbonyls in the gas apparently counteracts the reduction in the yields obtained with oxygen impurity. The combined effects of oxygen and metal carbonyls makes it difficult to write a reaction scheme for the formation of solid from CO

radiolysis. However, the following steps are suggested to be the main ones occurring in the experiments.



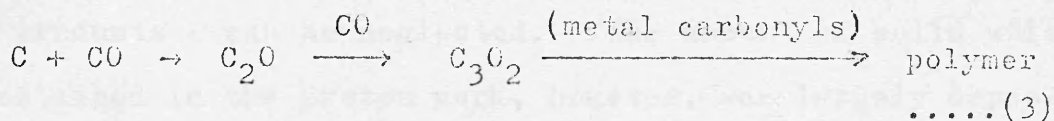
The initial act must be the formation of ion pairs and excited CO molecules which can dissociate into carbon and oxygen ions, or atoms. Unless there is a foreign molecule present to deactivate the CO^+ ion, reaction via CO^+ is about twice as frequent as that via CO^* (Stewart and Bowlden, 1960). If sufficient energy is transferred to the CO^+ ion and becomes associated with the C-O stretching vibration, then the ion may dissociate directly into carbon and oxygen. Alternatively the reaction, $\text{CO}^+ + \text{CO} \rightarrow \text{C}^+ + \text{CO}_2$ may occur if the CO^+ ion is sufficiently excited (Hirschfelder and Taylor, 1938).

Lorquet (1960) made a mass spectrometric study of CO and found that the principal ions formed are CO^+ , C^+ and O^+ , in the ratio 94:4:2. Briggs and Clay (1968) give chemical evidence for the formation of oxygen atoms in the gamma radiolysis of CO.

In the present experiments it is probable that the metal carbonyls are dissociated to the metal and CO on absorption of energy. It is noteworthy that Winters and Kiser (1964), in their mass spectrometric investigations, found the most

abundant ion formed from $\text{Fe}(\text{CO})_5$ is Fe^+ , whereas with $\text{Ni}(\text{CO})_4$ the most dominant ion produced is NiCO^+ in which the nickel is bonded to the carbon atom. If the same ionic species are formed in the present experiments, then it seems possible that the nickel, in the solids from CO containing $\text{Ni}(\text{CO})_4$ impurity, is bonded to the carbon atoms rather than to the oxygen atoms as is evidently the case with the iron-containing solids. Numerous substituted compounds of both nickel and iron carbonyl are known.

The carbon and oxygen atoms formed by (1) above may react as follows:



In the absence of oxygen impurity, CO_2 and polymer may be produced by reactions (2) and (3). The presence of oxygen impurity will favour the formation of CO_2 , probably by the chain mechanism suggested by Clay, Johnson and Warman (1963), and the yield of solid will fall. These authors did not detect any carbon-containing products other than CO_2 when the oxygen content exceeded 0.1 per cent in their experiments. Lind and Bardwell (1925) also found that the α -radiolysis of CO in the presence of oxygen failed to produce a solid product. Any solid particles which are formed in the present

experiments where oxygen is present and metal carbonyl is absent, do not apparently attain a sufficiently high growth rate which will allow them to settle out on to the specimen grid and they are lost to the system. The presence of metal carbonyls seems to enhance the growth rate by linking the polymer molecules together to such an extent that sedimentation occurs.

The low dose-rate ($\sim 5 \times 10^{12}$ eV sec⁻¹ within the volume of the α -source) and large volume (10 litres) of gas used in the α -irradiations results in a <0.01 per cent decomposition of CO and any effect which CO₂ might have on the radiolysis - for example, charge transfer or back reaction with products - can be neglected. The amount of solid which was obtained in the proton work, however, was largely dependent upon the oxygen content in the CO and the accumulation of CO₂ within the small volume of the reaction cell.

(c) G Value for Formation of Solid

Baird, Dawson and Peates (1965) obtained a value of G (solid atoms) = 10 from the early results of the present work. The effects of metal carbonyls on the α -radiolysis of CO were not known at that time and the solid was assumed to have the stoichiometric formula (C₃O₂)_n. Re-calculation, allowing for the 4 atomic per cent of iron estimated to be present in the solid, and making the same

assumptions as before (particles spherical with a density of 1 g cm^{-3}) indicates that about 3.3×10^{11} atoms (mean atomic weight = 15.2) are incorporated into the solid each second. The dosimetry measurements give the dose-rate as $5 \times 10^{12} \text{ eV sec}^{-1}$, thus about 7 atoms are incorporated into the solid for every 100 eV of energy absorbed by the gas, that is $G(\text{solid atoms}) = 7$ for solid produced in situ. This value is derived from line (a) in Fig. 22 (iron carbonyl and oxygen present in the system). Similar considerations applied to line (b) (nickel carbonyl and oxygen present in the gas) gives $G(\text{solid atoms}) = 2$. As the carbonyl content is further reduced the yields of solid fall due to the increasing effect of oxygen and the $G(\text{solid atom})$ values consequently tend to zero. Anderson, Best and Willett (1966) obtained a mean value of $G(-\text{CO}) = 8$ for the initial disappearance of CO in the absence of oxygen. Taking the stoichiometry as $4n\text{CO} \rightarrow n\text{CO}_2 + (\text{C}_3\text{O}_2)_n$ this gives $G(\text{solid atoms}) = 10$. The good agreement between this value and the present one of $G(\text{solid atoms}) = 7$ in the presence of oxygen impurity, might infer that iron carbonyl efficiently reduces the inhibiting effect of oxygen on the formation of solid. However, in view of the many assumptions made in deriving this value, the agreement may well be fortuitous, particularly since the dosimetry calculations

do not allow for any possible effects which iron carbonyl may have on the energy absorption processes. Barzynski (1968) and Barzynski, Hentz and Burton (1965) have indeed shown that iron and nickel carbonyls can act as effective energy acceptors in the gamma-radiolysis of certain hydrocarbons which have greater ionisation potentials than the metal carbonyls. Carbon monoxide has a higher ionisation potential (14 eV) than either iron or nickel carbonyl and yet it has been found that the effect of the presence of carbonyls is to enhance the decomposition of CO rather than to retard decomposition by charge transfer. To explain these results it was suggested earlier that iron carbonyl caused faster aggregation of growing particles by chemically combining with them. The role of iron carbonyl may be more complex. It is suggested here that iron carbonyl may deactivate, by charge transfer, one or more of the ionic species formed in the initiation or propagation steps in the chain mechanism postulated by Clay, Johnson and Warman (1963) for the formation of CO_2 by the radiolysis of CO in the presence of oxygen. In this way the inhibiting effect of oxygen on the formation of solid would be counteracted. These authors did in fact find that small amounts of impurities, such as mercury, carbon dioxide and certain inert gases, considerably reduced the $G(\text{CO}_2)$ values in their experiments.

7. Deposition in the Presence of Graphite

(a) General Considerations

In order to use the silver decoration counts as a reference it was found necessary to 'decorate' the three types of graphite simultaneously, as it was found that the counts varied with the experimental conditions used. The particle counts are particularly susceptible to variations in the weight of silver evaporated and to the time and temperature of heating allowed to induce mobility of the silver. The condition of the graphite surface is also of paramount importance and recent work (Baird, Fryer and Walker, 1969) shows that areas of graphite which have been previously examined in the electron microscope will not decorate under the conditions used in the present work, due to the thin contaminating layer which forms on the surface by interaction between the electron beam and residual oil vapours. This finding may account for some of the anomalous results in the present work; these were largely eliminated by making a large number of measurements. The 2:1 ratio of particle counts between the PGA and SPI graphite samples agrees well with the ratio found by Adamson (1966) and reflects the different surface properties of these graphites.

(b) Surface Deposits

The results of the experiments in which CO was irradiated in the presence of graphite within the irradiated

volume of the α -source show clearly that two distinct types of deposit are formed; there is the usual gas-phase deposit, the nature of which has already been discussed and a second material composed of particles of about 30 \AA diameter. Particle count measurements and other evidence described earlier indicate that the fine, particulate material is formed on the surface rather than in the gas phase and this supports the similar suggestion made by Adamson, Dawson, Feates and Sach (1966). This surface material has been shown to behave in a similar manner to the iron-free (nickel-containing) deposits produced in situ in the gas phase and nickel has been found to be a constituent of the surface material. It would appear then that the process which produces solid less favourably in the gas phase - nickel containing solids obtained only on removal of iron carbonyl - is the preferred one for the formation of a surface deposit.

8. Future Work

Iron and nickel carbonyls have been shown to exert a pronounced influence on the radiolysis of carbon monoxide. It is evident that more detailed information about the nature and composition of the solids produced can be obtained only if larger quantities of the deposits can be collected for subsequent analyses. Sufficient material could probably

be obtained using the high dose-rates available with the proton Van de Graaff accelerator. A continuous gas-flow system would probably be required in order to avoid accumulation of carbon dioxide which would inhibit the decomposition process. Alternatively a static system could be employed with a substance added to absorb any carbon dioxide produced during radiolysis. Increased yields of solid might also be obtained by using carbon monoxide of very low oxygen concentration. The nature of the bonding of the metals in the solid polymers might be further elucidated by studying the solids produced by the radiolysis of carbon monoxide in the presence of various other metal carbonyls, for example, cobalt octacarbonyl, $\text{Co}_2(\text{CO})_8$, molybdenum hexacarbonyl, $\text{Mo}(\text{CO})_6$. The suggestion that a charge transfer process was responsible for the apparent inactivity of nickel carbonyl when iron carbonyl was present could also be investigated further by performing a series of experiments on the radiolysis of carbon monoxide in the presence of metal carbonyls of different ionisation potentials. Further experiments within the electron microscope would be limited mainly to studies of the physical nature of the solids.

REFERENCES

- Adamson, I.Y.R., (1966), Ph.D. Thesis, Glasgow University.
- Adamson, I.Y.R., Dawson, I.M., Feates, F.S. and Sach, R.S.,
(1966), Carbon, 3, 393.
- American Society for Testing and Materials, (1963),
Symposium on X-ray and Electron Probe Microanalysis,
S.T.P. No. 349.
- Anderson, A.R., Best, J.V.F. and Willett, M.J., (1966),
Trans. Faraday Soc., 62, 595.
- Anderson, A.R., Davidson, H.W., Lind, R.; Stranks, D.R.,
Tyzack, C., and Wright, J., (1958), 2nd. Conf. on
Peaceful uses of Atomic Energy, 335.
- Back, R.A. and Miller, N., (1959), Trans. Faraday Soc.,
55, 911.
- Baird, T., and Dawson, I.M., (1963), unpublished work.
- Baird, T., Dawson, I.M., and Feates, F.S., (1965),
A.E.R.E. R-4837.
- Baird, T., Dawson, I.M., and Wood, C.A.,
Contribution to Libby/Cockroft Meeting, Hanford,
- Baird, T., Fryer, J.R., and Walker, D.I., (1969),
unpublished work.

- Barzynski, H.F., (1968), *Z. physik. Chem.*, 60, 185.
- Barzynski, H.F., Hentz, E.R., and Burton, M., (1965)
J. Phys. Chem., 69, 2034.
- Barzynski, H.F., and Hummel, D., (1963), *Z. physik. Chem.*,
38, 103.
- Bassett, G.A., (1958), *Phil. Mag.*, 33, 1042.
- Bassett, G.A., (1960), *Proc. Eur. Conf. Electron Microscopy*,
Delft, 1, 270.
- Bassett, G.A., Menter, J.W., and Pashley, D.W., (1959),
Disc. Faraday Soc., 28, 7.
- Best, J.V.F., (1968), Private communication.
- Bethe, H.A., and Ashkin, J., (1952), "Experimental Nuclear
Physics, (ed. Segre)", Wiley, New York, 167.
- Birks, L.S., (1960), *Anal. Chem.*, 32, No. 9, 19A.
- Birks, L.S., (1963), "Electron Probe Microanalysis",
Interscience, New York.
- Blake, A.E., Beles, W.T., and Jennings, P.P., (1964),
Trans. Faraday Soc., 60, 691.
- Bradley, D.E., (1954), *Brit. J. Appl. Phys.*, 5, 65.
- Brenner, S., and Horne, R.W., (1959), *Biochim. biophys.*
Acta., 23, 103.
- Briggs, J.P., and Clay, P.G., (1968), *Nature*, 217, 947.
- Brodie, B.C., (1873), *Proc. Roy. Soc.*, 21, 245.

- Cameron, A.T., and Ramsay, W., (1908), J. Chem. Soc.,
93, 966.
- Chamberlain, A.C., (1968), Private communication.
- Clark, T.J., (1960), Hanford Report, HW-63855.
- Clay, P.G., Johnson, G.R.A., and Warman, J.M., (1963),
Disc. Faraday Soc., 36, 46.
- Copestake, T.B., Davidson, H.W., and Tonge, B.L., (1959),
J. Appl. Chem., 9, 74.
- Corney, N.S., and Copestake, T.B., (1962), G.E.C. Report
No. 14,157C.
- Cosslett, V.E., (1951), "Practical Electron Microscopy",
Butterworths, London.
- Crespi, M., and Lunt, R.W., (1925), J. Chem. Soc., 127, 2
- Davidge, P.C., and Marsh, W.R., (1955), AERE R-1374.
- Dondes, S., Harteck, P., and von Weyssenhoff, H., (1964),
Z. Naturforsch., 19a, 13.
- Dorfman, L.M., and Wahl, A.C., (1959), Radiation Research
10, 680.
- Dunning, W.J., (1960), Disc. Faraday Soc., 30, 9.
- Faltings, K., Groth, W., and Harteck, P., (1938), Z. phys
Chem., 41B, 15.
- Feates, F.S., and Sach, B.S., (1965), Carbon, 3, 261.
- Flory, D.A., (1963), Nucleonics, 21, No. 12, 50.

- Forchioni, A., and Willis, C., (1968), J. Phys. Chem.,
72, 3105.
- Fuchs, E., (1966), Rev. Sci. Instr., 37, 623.
- Garratt, A.P., and Thompson, H.W., (1934), J. Chem. Soc.,
2, 1817.
- General Electric Co. Ltd., (1962), Div. Report No. 8363/C.
- General Electric Co. Ltd., (1963), Div. Report No. 8526/C.
- Green, M.L., and Lane, W.R., (1957), "Particulate Clouds;
Dusts, Smokes and Mists", Spon, London.
- Groth, W., Passara, W., and Rommel, H.J., (1962), Z. physik.
Chem., 32, 192.
- Hall, C.E., (1953), "Introduction to Electron Microscopy",
McGraw-Hill, New York.
- Harteck, P., and Dondes, S., (1955), J. Chem. Phys., 23, 902.
- Harteck, P., and Dondes, S., (1957), J. Chem. Phys., 26, 1727.
- Heidenreich, R.D., (1964), "Fundamentals of Transmission
Electron Microscopy", Interscience, New York.
- Heisig, G.B., (1931), J. Amer. Chem. Soc., 53, 3245, 4460.
- Heisig, G.B., (1932a), J. Amer. Chem. Soc., 54, 2328.
- Heisig, G.B., (1932b), J. Phys. Chem., 36, 1000.
- Heisig, G.B., (1933), J. Amer. Chem. Soc., 55, 2304.
- Heisig, G.B., (1935), J. Phys. Chem., 39, 1067.
- Heisig, G.B., (1939), J. Phys. Chem., 43, 1207.

- Hennig, G.R., (1964), Appl. Phys. Letters, 4, 52.
- Hennig, G.R., (1965), 2nd Ind. Conf. Carbon and Graphite.
- Hennig, G.R., (1966), Chem. and Phys. of Carbon, 2, 1.
- Henri, V.P., Maxwell, C.R., White, W.C., and Peterson, D.C.,
(1952), J. Phys. Chem., 56, 153.
- Hirsch, P.B., Howie, A., Nicholson, R.B., Pashley, D.W.,
and Whelan, M.J., (1965), "Electron Microscopy of
Thin Crystals", Butterworths, London.
- Hirschfelder, J.O., and Taylor, H.S., (1938), J. Chem.
Phys., 6, 783.
- Holliday, B., (1963), Private communication.
- Honig, R.E., and Sheppard, C.W., (1946), J. Phys. Chem.,
50, 119.
- Hudswell, F., (1961), A.E.R.E. R-3663.
- Junge, C.E., (1963), "Air Chemistry and Reactivity",
Academic Press, New York.
- Kay, D.H., (1965), "Techniques for Electron Microscopy",
2nd Ed., Blackwell Scientific Publications Ltd.,
Oxford.
- Klemenc, A., and Wagner, G., (1938), Z. Anorg. und Allgem.
Chem., 239, 1.
- Labaton, V.Y., (1965), Private communication.
- Lind, R., (1966), Private communication.

- Lind, S.C., (1961), "Radiation Chemistry of Gases",
A.C.S. Monograph No. 151, Reinhold, New York.
- Lind, S.C., and Bardwell, D.C., (1924), Science, 60, 364.
- Lind, S.C., and Bardwell, D.C., (1925), J. Amer. Chem. Soc.,
47, 2675.
- Lind, S.C., and Bardwell, D.C., (1926), J. Amer. Chem. Soc.,
48, 2335.
- Lind, S.C., Bardwell, D.C., and Perry, J.H., (1926),
J. Amer. Chem. Soc., 48, 1556.
- Lind, E., and Wright, J., (1963), J. Brit. Nucl. En. Soc.,
2, 287.
- Lorquet, J.C., (1960), J. Chim. Phys., 57, 1078.
- Marsh, W.R., and Wright, J., (1964), A.E.R.E. R-4198.
- Moseley, H.G., (1913), Phil. Mag., 26, 1024.
- Mund, W., and Koch, W., (1925), Bull. Soc. chim. Belg.,
34, 121.
- Mund, W., and Koch, W., (1926), J. Phys. Chem., 30, 289.
- Mund, W., and Rosenblum, C., (1937), J. Phys. Chem., 41, 469.
- Newitt, D.M., (1940), "The Design of High Pressure Plant
and the Properties of Fluids at High Pressures",
Clarendon Press, Oxford, 20.
- Ott, E., (1925), Ber., 58, 772.

- Pearson, R.G., Basolo, F., Day, J.P., Kangas, L.F., and Henry, P.M.; (1968), J. Amer. Chem. Soc., 90, 1925.
- Porte, A.L., (1969), Private communication.
- Reimer, L., (1965), Proc. Symp. on "Quantitative Electron Microscopy", (ed. Bahr and Zeitler), 1082.
- Reyerson, L.H., and Kobe, K., (1930), Chem. Revs., 7, 479.
- Rosenblum, C., (1937), J. Phys. Chem., 41, 651.
- Rosenblum, C., (1948), J. Phys. Chem., 52, 474.
- Rudolph, P.S., and Lind, S.C., (1960a), J. Chem. Phys., 33, 705.
- Rudolph, P.S., and Lind, S.C., (1960b), J. Chem. Phys., 32, 1572.
- Ryan, B.A., (1963), Hanford Report, HW-67241.
- Schmidt, L., Boehm, H.P., and Hofmann, U., (1955), Z. Anorg. und Allgem. Chem., 282, 241.
- Schmidt, L., Boehm, H.P., and Hofmann, U., (1959), Proc. 3rd. Carbon Conf., Pergamon, London, 235.
- Smith, N.R., Young, D.A., Smith, E.N., and Carter, C.C., (1963), Inorg. Chem., 2(4), 829.
- Stewart, A.C., and Bowlden, H.J., (1960), J. Phys. Chem., 64, 212.
- Tingey, G.L., quoted by Ryan (1963).
- Vilesov, F.I., and Kurbatov, B.L., (1961), Dokl. Akad. Nauk SSSR, 140, 1364.

- Waber, J.T., and Wright, E.S., (1961), "The Metal Plutonium", (ed. Coffinberry and Miner), Univ. of Chicago Press, 196.
- Watson, J.H.L., Vanpee, M., and Lind, S.C., (1950), J. Phys. Coll. Chem., 54, 391.
- Winters, R.E., and Kiser, R.W., (1964), Inorg. Chem., 3, 699.
- Woodley, R.E., (1954), Hanford Report, HW-31929.
- Woodley, R.E., (1955), Hanford Report, HW-40142.
- Wourtzal, E.E., (1919), Le Radium, 11, 346.
- Wright, P., (1967), Private communication.